Ion-sensitive microelectrode studies of insect muscle

by

CATHERINE JILL DAWSON

Thesis submitted for the Degree of Doctor of Philosophy

1984

UNIVERSITY OF LONDON

Imperial College of Science and Technology,
Department of Pure and Applied Biology,
Neurobiology Section

ABSTRACT

Double-barrelled ion-sensitive microelectrodes were used to obtain simultaneous measurements of membrane potential and intracellular ionic activity in body-wall muscle fibres of the larvae of two insects: *Calliphora erythrocephala*, the blowfly (Diptera) and *Chilo partellus*, the rice stem borer (Lepidoptera). Ionic substitution experiments were performed on both preparations in order to assess the quantitative contributions of K^+, Na^+ and Cl^- to resting membrane electrogenesis in each insect.

In *Calliphora*, the muscle membrane potential was found to be explicable in terms of weighted contributions by the potassium and sodium ionic gradients across the cell membrane. (Cl^- was passively distributed in this preparation, playing no part in membrane electrogenesis). A model for resting membrane electrogenesis based on the Goldman-Hodgkin-Katz equation was proposed, and its predictions tested by a variety of modified ionic substitution experiments. It was thus proved to be correct.

Measurements of intracellular K^+ and Na^+ activities in two distinct developmental stages of this insect, larvae and prepupae, indicated that the activity of K^+ increased, whilst that of Na^+ decreased, with age. This suggests that there may be maturation of a Na^+/K^+ pumping mechanism during development.

In *Chilo*, the relationship between the membrane potential and the K^+ gradient across the cell membrane was found to differ markedly from the situation in *Calliphora*.

The contributions to membrane electrogenesis of a number of mechanisms (K^+, Na^+, Cl^-, Mg^{2+}, metabolic pump) were investigated and quantified. The most surprising finding from these experiments was that in *Chilo*, Cl^- is <u>not</u> passively distributed across the cell membrane, but is involved in resting membrane electrogenesis. This situation is unlike that in the majority of vertebrate and invertebrate muscles that have been studied.

CONTENTS

		Page
Abstract		2
Chapter I:	Introduction	6
Chapter II:	Materials and methods	49
Chapter III:	Intracellular ionic activity measurements in *Calliphora*	98
Chapter IV:	Ionic substitution experiments on *Calliphora*: a model of resting membrane electrogenesis	142
Chapter V:	Intracellular ionic activity measurements in *Chilo* larvae	176
Chapter VI:	Ionic substitution experiments on *Chilo* larvae	198
Chapter VII:	Discussion	219
Appendices	1-16	258
References		295
Acknowledgements		306

Table number	Title
1.	Summary of the liquid ion sensors available for the major inorganic ions.
2.	Osmotic and ionic properties of the haemolymph of some representative insects.
3.	Ions in the haemolymph of a number of insects from different orders.
4.	Effect of external K on intracellular K and resting potentials.
5.	Intracellular K concentration and resting potentials.
6.	Resting and action potentials, intracellular sodium concentration and theoretical overshoot of muscle fibres.
7.	Compounds used to fill the reference barrels of ISMs.
8.	Compounds used to back-fill the active barrels of ISMs.
9.	Ranges of resistances of active and reference barrels of ISMs.
10.	Intracellular K^+ activity data from *Calliphora* larvae.
11.	Intracellular K^+ activity data from *Calliphora* prepupa.
12.	Comparison of intracellular K^+ data from *Calliphora* larvae and prepupae.
13.	Intracellular Na^+ activity data from *Calliphora* larvae.
14.	Intracellular Na^+ activity data from *Calliphora* prepupae.
15.	Comparison of intracellular Na^+ data from *Calliphora* larvae and prepupae.
16.	Intracellular Cl^- activity data for *Calliphora* larvae, measured using ISMs with KCl/K_2SO_4-filled reference barrels.
17.	Intracellular Cl^- activity data for *Calliphora* larvae, measuring ISMs with RLIE-filled reference barrels.
18.	Intracellular Cl^- activity data for *Calliphora* prepupae.
19.	Comparison of the intracellular Cl^- data from *Calliphora* larvae and prepupae.
20.	Data from Cl^- depletion experiments on *Calliphora* prepupae.
21.	Data from K^+ substitution experiments on *Calliphora* prepupae.
22.	α values for *Calliphora* prepupae, calculated from E_m data obtained in Ringer solutions of various compositions.
23.	The effect of low a^o_{Na} on membrane resistance in *Calliphora*

prepupae.

24. Data from K^+ pulsation experiments on *Calliphora* prepupae.

25. Comparison between E_m values predicted using α values of 0.086, 0.169 and 0.036, and the measured E_m values.

26. Summary of the results obtained from substitution experiments on *Calliphora* in which (a^o_K + 0.036 a^o_{Na}) was varied whilst keeping (a^o_K + 0.036 a^o_{Na}) x a^o_{Cl} constant.

27. Intracellular K^+ activity data from *Chilo* larvae.

28. Intracellular Na^+ activity data from *Chilo* larvae.

29. Intracellular Cl^- activity data from *Chilo* larvae.

30. Data from K^+ substitution experiments on *Chilo*.

31. The effect of varying a^o_K and a^o_{Na} on membrane resistance in *Chilo*.

32. Data from Na^+ substitution experiments on *Chilo*.

33. Data from Cl^- substitution experiments on *Chilo*.

34. Data from K^+ substitution experiments on *Chilo* in the presence and absence of ouabain.

35. Relation between $[Na^+]_o$ and the resting potential in *Drosophila* larvae.

36. Effect of Na^+ substitution on E_m in leech anterior neuropile glial cells.

37. A comparison between $[K^+]_i$ data available for five species of Lepidoptera.

38. A comparison between $[Na^+]_i$ data available for five species of Lepidoptera.

39. $[Cl^-]_i$ data from five Lepidoptera species.

40. Membrane potentials recorded in *Calliphora* and *Chilo* preparations.

41. Intracellular K^+ activity data from *Calliphora* and *Chilo*, measured using NIC-type K^+ ISM's.

42. Intracellular K^+ activity data from larvae of *Calliphora* and *Chilo* measured using LIX- and NIC-type K^+ ISM's.

43. Intracellular Na^+ activity data in *Calliphora* and *Chilo*.

44. Summary of intracellular Cl^- activity data for *Calliphora* and *Chilo*.

45. Summary of changes in membrane resistance in *Calliphora* prepupae and *Chilo* larvae during a low-Na^+/high K^+ substitution experiment.

46. The contributions of various mechanisms to E_m in *Chilo*.

CHAPTER I

I.1 Ionic Properties and Excitability of Nerve and Muscle Cells

The signalling ability and general excitability of nerve and muscle cells depends on the uneven distribution of a number of inorganic ions (eg. K^+, Na^+, Cl^-, Ca^{2+}) on the two sides of the cell membrane. Each ion, 'x', has a characteristic equilibrium potential given by the Nernst equation which states that:-

$$E_x = \frac{RT}{Z_x F} \ln \frac{a_x^o}{a_x^i}$$

where E_x is the equilibrium potential for the ion 'x';

R is the Universal gas constant;

T is the Absolute temperature;

F is the Faraday constant;

Z is the valency of the ion 'x';

a_x^o is the extracellular activity of the ion 'x';

a_x^i is the intracellular activity of the ion 'x'.

The activity of an ion, 'x', is an "effective concentration" being the concentration of ions in the solution that are freely mobile (active) and can therefore contribute to the generation of an electrochemical potential. The activity, a_x, is related to the total ion concentration, C_x, by the activity coefficient, γ_x, as follows:

$$a_x = \gamma_x C_x$$

where $\gamma \leq 1$ and is dependent upon the ionic strength of the solution.

1.i. Goldman-Hodgkin-Katz Equation

If a given cell membrane is selectively permeable to an ion, the resulting membrane potential will closely resemble the equilibrium potential of that ion. The Constant-Field Theory (Goldman, 1943) is used as an approximation for the case when the membrane is permeable to a number of ions, but the permeability differs for the different ion species. According to this theory, if the cell membrane is permeable to K^+, Na^+ and Cl^-, then the membrane potential, E_m, is given by:-

$$E_m = \frac{RT}{F} \ln \frac{p_K a^o_K + p_{Na} a^o_{Na} + p_{Cl} a^i_{Cl}}{p_K a^i_K + p_{Na} a^i_{Na} + p_{Cl} a^o_{Cl}}$$

where a^o_K, a^o_{Na} and a^o_{Cl} are the extracellular activities of these ions: a^i_K, a^i_{Na} and a^i_{Cl} are their intracellular activities; and p_K, p_{Na} and p_{Cl} are the partial permeabilities of the membrane for each ion. This is known as the Goldman-Hodgkin-Katz equation and was first applied to the squid giant axon by Hodgkin and Katz (1949). It accounts well for the behaviour of membranes bathed in solutions of several electrolytes, but applies only to one state of the membrane (resting or active).

The Parallel Conductance Model described by Hodgkin and Huxley (1952) and elaborated by Hodgkin and Horowicz (1959) provides a more representative description of the change from inactive to active membrane. According to this model, the membrane is thought to contain a number of parallel channels eg. one for K^+, one for Na^+ and one for Cl^- (fig. 1). Each channel is associated with an electrochemical battery, 'E', in series with a variable conductance, 'g'.

1.ii. Ionic Pumps

Various ionic pumping mechanisms contribute to the maintenance of the membrane potential in excitable cells. At rest there is a tendency for ions to 'leak' across the cell membrane along their concentration gradients, and during excitation, permeability changes lead to influx and efflux of ions. In order to restore and maintain the concentration gradients of sodium and potassium ions across the cell membrane, a Na^+/K^+ pumping mechanism exists which expels three sodium ions from the cell and allows two potassium ions to enter (fig. 2a). Since the ions are moved against their respective concentration gradients, metabolic energy is expelled in the process such that for every three Na^+ and two K^+ pumped, one molecule of ATP is hydrdolysed. The Na^+/K^+ pump transfers a net amount of positive charge in the outward direction and the pump is said to be 'electrogenic'. This hyperpolarising current driven by the pump generates a proportion of the overall membrane potential, the magnitude of the contribution depending on other membrane properties such as its resistance. Thus, the Na^+/K^+ pump contributes about 2mV to the membrane potential of the squid giant axon (Hodgkin & Keynes, 1956) and up to -20mV to that of snail neurones (Thomas, 1969).

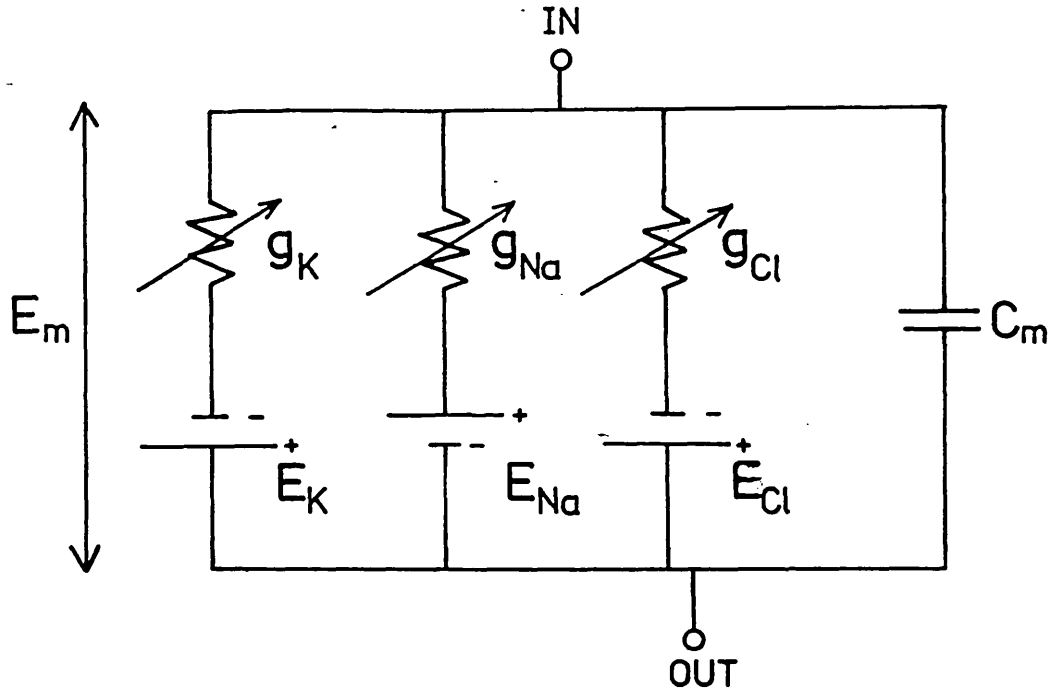


Fig. 1 Parallel conductance model for membrane electrogenesis. g_K, g_{Na} & g_{Cl} are the membrane conductances for K^+, Na^+ and Cl^- respectively; E_K, E_{Na} & E_{Cl} are the equilibrium potentials for each ion; C_m represents the membrane capacitance and E_m the membrane potential. (Modified from Hodgkin & Huxley, 1952.)

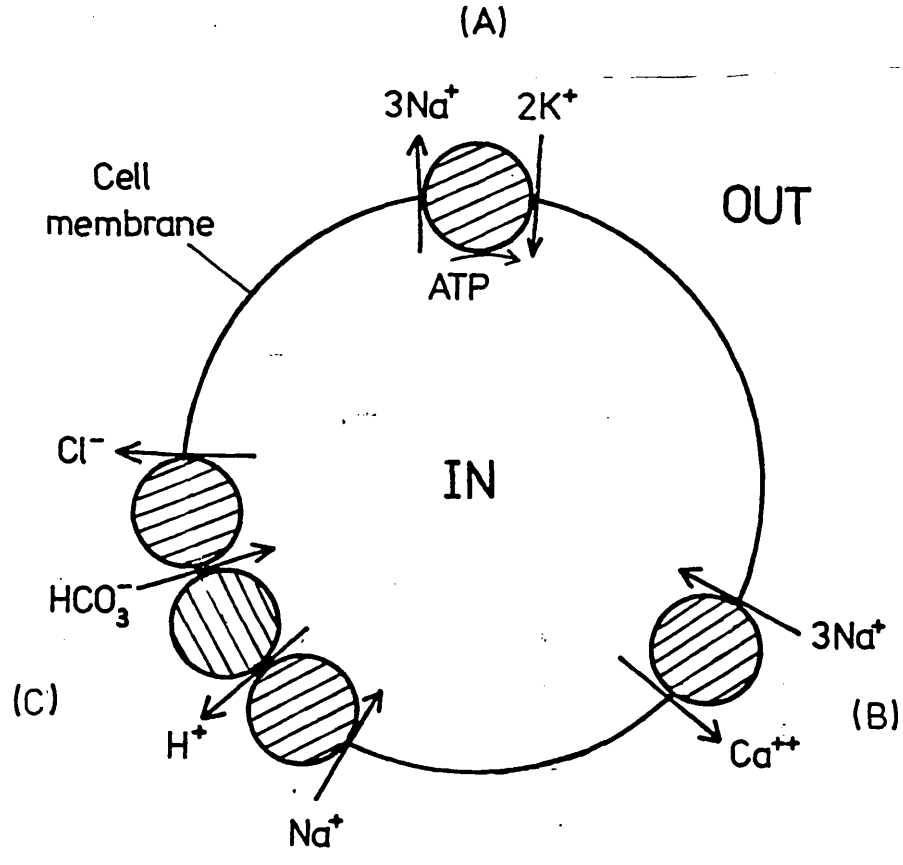


Fig. 2 Summary diagram showing the various mechanisms for transport of ions across an excitable cell membrane (A) Na^+ - K^+ pump; (B) Na^+/Ca^{2+} exchange; (C) a proposed scheme for regulation of intracellular pH.

A number of specific blockers of the Na^+/K^+ pump are known, including the cardiac glycoside, ouabain, although the latter has been suggested to have limited effectiveness in insect preparations (Anstee & Bowler, 1979).

The chloride equilibrium potential, E_{Cl}, is more negative or positive than the membrane potential, E_m, depending on whether the cell generates Cl^- dependent electrical activity. For example, inhibitory post-synaptic potentials are commonly Cl^- dependent, and in such units, E_{Cl} is more negative than E_m. Correspondingly, an outwardly directed Cl^- "pump" is present to maintain the intracellular Cl^- level lower than 'passive'. The exact nature of the Cl^- pump is not very clear at present. In snail neurones (Thomas, 1977), squid giant axon (Russell & Boron, 1979) and barnacle muscle (Boron *et al*, 1981), however, Cl^- transport has been found to be a part of an elaborate membrane mechanism regulating intracellular pH (fig. 2c).

Regulation of ionic gradients across cell membranes also depends on 'exchange' mechanisms. The main process maintaining intracellular Ca^{2+} activities at very low levels is the $Na^+ - Ca^{2+}$ exchange mechanism whereby the energy necessary for extrusion of Ca^{2+} from the cell (against its concentration gradient) is provided by an influx (down the concentration gradient) of Na^+ (fig. 2b). It has recently been suggested that the Na-Ca exchange in heart muscle is electrogenic with one Ca^{2+} moved out for three Na^+ flowing in (Horackova & Vassort, 1979).

I.2. Ion-Sensitive Microelectrodes

Thus, the gradients of the major inorganic ions, K^+, Na^+ and Cl^- across the cell membrane are important parameters in determining the electrophysiological properties of the cell. In the case of a cell bathed in a physiological saline, the extracellular activities of all ions are known. Using intracellular ion-sensitive microelectrodes (ISM's), their intracellular activities can also be measured, and hence the equilibrium potential for each ion calculated from the Nernst equation. The latter can then be compared directly with the membrane potential, E_m, to provide an indication of the role of each ion in generating E_m.

Theory of the ISM Potential

An ISM is essentially an ordinary glass microelectrode fitted at its tip with an ion-sensitive membrane which makes contact with the intracellular medium on the outside, and an appropriate back-filling solution on the inside. The electrical potential generated across the ion-sensitive membrane at the tip of an ISM, V_{ISM}, comprises the sum of two parts:-

$$V_{ISM} = V_{ION} + V_{LOC}$$

where V_{ION} is a potential which depends on the activity of the ion to which the ISM is sensitive and V_{LOC} is a local potential which would be recorded by an ordinary microelectrode. To obtain V_{ION} alone, a second, ion-insensitive reference microelectrode is used, and its potential (V_{LOC}) is subtracted from V_{ISM} using a differential measuring device. This is best achieved by means of a double-barrelled microelectrode comprising an 'active' (ion-sensitive) barrel and a 'reference' barrel.

The theory of the ion-sensitive electrode (ISE) was first formulated by Nikolsky (1937) and Eisenman *et al* (1966). For the perfect ISE, the ion-sensitive membrane is completely selectively permeable, ie: it is permeable only to one ionic species, 'x'. Ions 'x' can pass freely across the membrane, meeting no resistance whatsoever, whereas all other ions meet an infinite resistance to movement across the membrane, which then constitutes an impenetrable barrier. If there are two solutions, one on either side of the membrane, containing different concentrations of 'x', then an electrical potential develops across the membrane due to the diffusion of 'x' towards the side on which the concentration is less, until an equilibrium is reached. This results from the balance between the forces on 'x' due to the concentration gradient which gives rise to the diffusion and the electrical potential which is a consequence of this diffusion.

In practice, all ion-sensitive electrodes are 'imperfect' and respond also to a number of interfering ions with varying selectivities. The potential generated by such an electrode is described by the Nikolsky equation (Eisenman, 1969):-

$$E_m = E_o + RT \ln (a_x + k_{xy}.a_y^{Z_x/Z_y})$$

where Z_x and Z_y are the valencies of the ions 'x' and 'y';

a_x is the activity of the ion 'x';

K_{xy} is the selectivity coefficient of the 'membrane' for the ion 'x' over the interfering ion 'y'.

I.3 Types of ISM

Two types of ion-sensitive tip component may be used to make ISMs: liquid state (including ion-exchangers, LIX, and neutral ion carriers, NIC, figure 3a) and solid state (including glass membranes and metal surfaces, figure 3 b,c). The most fundamental difference between the liquid membranes and the glass membranes arises from the greater mobility of the ionic species and the larger quantity of active material present in liquid membranes. This has advantages eg. the action of the membrane is faster than that of a glass membrane with fixed ion-exchange sites, but one disadvantage is that interfering ions also tend to get carried into the sensor and take a long time to diffuse out, whilst with glass membranes, interferents tend to stay near the surface and are easily washed away. For this reason glass electrodes can be used for a much longer time than liquid membrane ones before their response starts to deteriorate, as the membrane is destroyed more slowly by interferents.

A LIX-type ISM has as its tip component a charged ion-exchanger consisting of large organic molecules. The ion-exchanger is dissolved in an inert organic solvent to form a liquid membrane which is insoluble in the aqueous ISM back-filling solution, and the aqueous medium outside the ISM tip. The ion-exchange sites are thus freely mobile within the membrane.

Organic solvents which have a lone pair of electrons on oxygen atoms but no exchangeable protons are well-known to solvate cations much better than anions. Thus, all the solvents commonly used for cation LIXs are aprotic donor solvents. Anions are better solvated by solvents with hydrogen-bonded protons such a decanol (Tsien, 1980). The ion exchanger itself is basically a salt which influences the preference of the liquid membrane for one particular ion. Firstly, there is a pronounced preference for either anions or cations depending upon the nature of the salt. If the salt consists of a very hydrophobic (organic) cation and a rather hydrophilic anion, then anions will tend to leave the sensor and this, together with the condition of no net current, encourages anions and not cations to enter the sensor in exchange. A salt of a hydrophilic cation (eg. alkali metal ion) with a hydrophobic anion analogously favours cation selectivity. Secondly, the selectivity for one

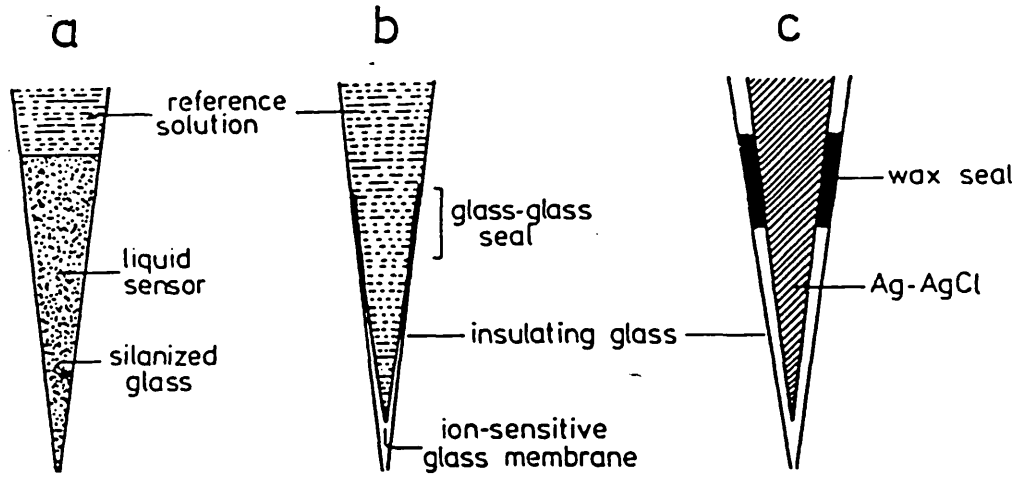


Fig. 3. *The tip assembly of three different types of ISM (not drawn to scale). (a) Liquid-state ISM. The length of the liquid sensor column can be 200 μm to several millimetres; the inside wall of the micropipette must be silanized. (b) Solid-state, glass membrane, recessed-tip type ISM; the recess volume is critical and determines the response time of the electrode. (c) Solid-state, metallic surface type ISM.* **(From Djamgoz & Laming, 1981)**

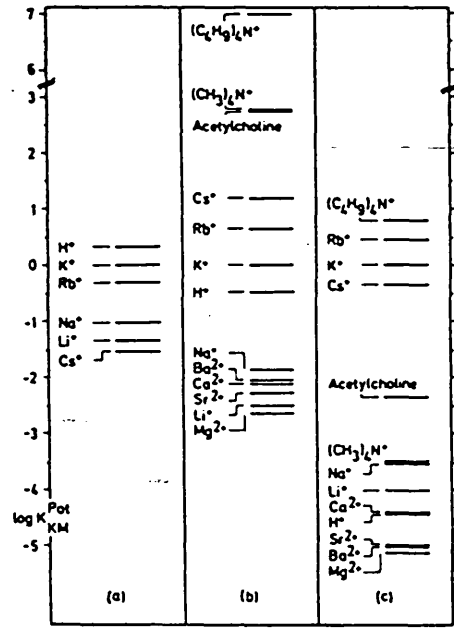


Fig. 4 Comparison of the selectivity coefficients obtained by the separate solution technique with 0.1 M solutions of the chlorides (except for a 10^{-1} M solution of tetrabutylammonium iodide). (a) Potassium sensitive glass NAS_{17-4}; (b) K^+ microelectrode with classical ion exchanger; (c) K^+ microelectrode based on neutral carrier.

(From Oehme & Simon, 1976)

particular anion or cation occurs because of the order of hydrophobicity of the ions. The membrane will naturally be most selective for the most hydrophobic ion in significant concentration in the aqueous solution. This is the principle behind the Corning K^+ and Cl^- LIXs. For example, the K^+ LIX has a solvent of the aprotic donor type, and a salt with a very large and hydrophobic anion and a smaller and more hydrophilic cation. The cation used is K^+ so that this ion both leaves and enters the sensor causing no long term changes in sensor composition. The sensor then responds to cations in order of their hydrophobicity so that it discriminates for K^+ against Na^+ by about 60:1, but K^+ is superceded by Cs^{2+} and quaternary ammonium ions. The Cl^- LIX behaves analogously to the K^+ LIX but favours anions according to their hydrophobicity. If any large monovalent anions are present they can cause significant interference.

Neutral ion carrier membranes contain ionophores (macrocyclic compounds) dissolved in a suitable inert organic solvent. The structure of the ionophore is such that it forms a polar cavity in which one specific ion can be enclosed because of ion-dipole interactions. Thus, one particular species of ion is enveloped in a hydrophobic shell and this promotes its entry into the organic membrane phase. Preference for divalent ions over monovalent ions is enhanced by ligands which form thin rather than thick shells around the ion, by solvents of high dielectric constant, and by an abundance of counterions (organic ions of opposite charge to that of the determinand) in the sensor (Morf *et al*, 1979).

Solid state ISMs are complex in structure (fig. 3c) with protruding tips of ion-sensitive glass (Hinke, 1959), recessed tips (Thomas, 1976) or 'reversed' tips (Thomas, 1969). Their response times are long (up to one minute), but they are generally highly selective and may be used for several weeks before this selectivity is lost. All liquid state ISMs have the same basic structure (fig. 3a). LIX-based ISMs tend to be poorly selective compared with the glass type, but are relatively simple to construct and have faster response times. NIC-based ISMs have rather high resistances, but have selectivities more comparable to those of solid state ISMs. Their useful lifetime is similar to that of LIX-based ISMs (a maximum of around two days). Thus, in cases where both a solid-state and a liquid-state sensor are available for a particular ion, the liquid-state one is usually preferred (provided its selectivity characteristics are satisfactory) because of the relative ease with which the latter can be incorporated into an ISM, and

because of the faster response times of the resulting ISM. The following section reviews the ion-sensors currently available for a range of ions, and compares their selectivities. The compositions of several sensors are described in table 1.

I.3.i. K^+ ISMs

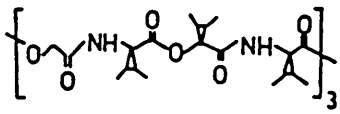
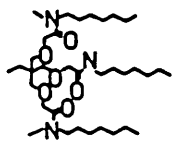
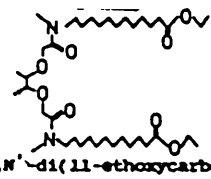
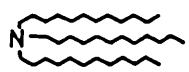
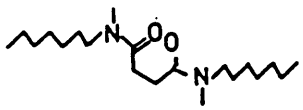
K^+-sensitive glass (NAS_{27-4}; Eisenman, 1967) is now little used because of the disadvantages outlined above. Two types of liquid ion exchanger exist: Orion and Corning 477317. The Corning LIX is around ten times more selective for K^+ over Na^+ than the Orion (Laming & Djamgoz, 1983). However, known interferents of the Corning LIX include a range of physiologically important compounds eg. acetyl choline and some other quaternary ammonium ions, biogenic amines and glutamic acid (Oehme & Simon, 1976; Kuramoto & Haber, 1981) (fig. 4). A highly selective neutral ion carrier for K^+ has recently been introduced (Oehme & Simon, 1976), since when it has been possible to construct K^+-ISMs with characteristics highly suitable for intracellular recording. It is based on the K^+ ionophore valinomycin, to which an organic salt (potassium tetra-p-chlorophenylborate, KTCPB) is added to reduce resistance. This also reduces selectivity to some extent, but the ISM still performs well (Oehme & Simon, 1976; Steiner *et al*, 1979; Coles and Tsacopoulos, 1979). Figure 4 provides a comparison between the selectivity coefficients for K^+ over various interferents for K^+-sensitive glass, K^+-LIX- and K^+-NIC-type ISMs.

I.3.ii. Cl^--ISMs

The solid-state Cl^--ISM consists of a silver wire coated with silver chloride, and sharpened to a point. This behaves as a perfect Cl^- electrode in response to pure Cl^- solutions, but there is some doubt about its performance intracellularly, possibly because of difficulties in construction and the large size of the tips (eg. Neild & Thomas, 1973; Saunders & Brown, 1977; compare Armstrong *et al*, 1977 with Bolton & Vaughan-Jones, 1977).

There is at present no NIC for Cl^-, and the most widely used LIX is that made by Corning (code 477315) (Walker, 1971; Ascher *et al*, 1976; Bolton & Vaughan-Jones, 1977; Saunders & Brown, 1977). This is relatively poorly selective for Cl^-, responding to a wide variety of anions eg. HCO_3^-. The selectivity characteristics and resistance of this LIX have recently been

Table 1. Summary of the liquid ion sensors available for the major inorganic ions

Type of ISM	Structure of active component	Cocktail composition	Code number	References
K^+	LIX	K^+ tetra (p-chlorophenyl) borate in 1-nitro -2,3-dimethylbenzene	Corning 477137	
K^+	Valinomycin-based 	5 wt % valinomycin 25 wt % 1,2-dimethyl -3-nitrobenzene 68 wt % dibutyl sebacate 2 wt % K^+ tetrakis (4-chlorophenyl) borate		Wuhrmann *et al* (1979)
Cl^-	LIX	Probably chloride salts of very large hydrophobic cations, dissolved in decanol	Corning 477315/ 477913 Orion 92-17-02	Baumgarten (1981)
Na^+	NIC 	10 wt % sodium ionophore (ETH 227) 89.5 wt % 2-nitrophenyl octyl ether 0.5 wt % sodium tetraphenyl borate	ETH 227	Steiner *et al* (1979)
Ca^{2+}	NIC 	10% calcium ionophore 1 % sodium tetraphenyl borate 89 % 2-nitrophenyl octyl ether		Oehme *et al* (1976)
	N,N'-di(11-ethoxycarbonyl) undecyl-N, N', 4, 5-tetramethyl 3,6-dioxaoctane diacid diamide			
H^+	NIC 	10 % tri-n-dodecylamine 0.7 % sodium tetraphenyl borate 89.3 % 2-nitrophenyl octyl ether		Ammann *et al* (1981)
	Tri-n-dodecylamine			
Mg^{2+}	NIC 	20 % ligand 1 % sodium tetraphenyl borate in propylene carbonate	ETH 1117	Lanter *et al* (1980)
	N,N' - diheptyl - N, N' - dimethyl succinic acid diamide			

improved by increasing the concentration of organophilic ligand fivefold (Corning 477913, Baumgarten, 1981). Figure 5 compares the selectivity coefficients of the two LIXs for a variety of anions.

I.3.iii. Na^+ ISMs

Na^+ LIX-ISMs have in general been found to have poor Na:K selectivity characteristics compared with those of Na^+-sensitive glass ISMs (NAS_{11-18}) (O'Doherty *et al*, 1979; Kotera *et al*, 1979). Recently, Na^+-sensitive neutral carriers have been developed which induce a K^+ discrimination in PVC liquid membrane electrodes and give ISMs with better selectivity and good response times (Guggi *et al*, 1976; Steiner *et al*, 1979). The resistance of the NIC is reduced by adding sodium tetraphenylborate, leading to some loss of selectivity with respect to divalent cations, particularly Ca^{2+}. Thus, under conditions where Ca^{2+} is present in significant quantities, the glass Na^+-ISM is still the best electrode. Figure 6 gives a comparison between the selectivities of Na^+ glass electrodes and Na^+ NIC electrodes.

I.3.iv. Ca^{2+}-ISMs

For Ca^{2+}, there is no glass ISM and the LIX available is highly resistive and poorly selective (Brown & Owen, 1979; Tsien, 1980). This leads to problems in measuring intracellular a_{Ca} because Ca^{2+} occurs at extremely low activities in cells (probably 10^{-7} to 10^{-8} M; Dipolo *et al*, 1976). The intracellular activities of Mg^{2+}, K^+ and Na^+ are 10^3 to 10^6 times higher, and thus interference by any of these ions would have a significant effect on the estimate of a_{Ca}^i. A synthetic NIC for Ca^{2+} exists which has high ion-selectivites with respect to Na^+ and Mg^{2+} (Oehme *et al*, 1976) and a second NIC has been developed more recently in which the liquid sensor is gelled into the tip with PVC. The latter is both selective and fine enough to measure a_{Ca}^i in cells with diameters of only 12-15μm (Marban *et al*, 1980; Rink & Tsien, 1980). (See figure 7).

I.3.v. H^+-ISMs

For the measurements of pH, the glass ISM appears to be more reliable than the antimony-based electrode, and the former shows excellent selectivity (Green & Giebisch, 1974; Brown & Owen, 1979). A neutral carrier-based H^+-selective microelectrode has recently been described which is suitable for

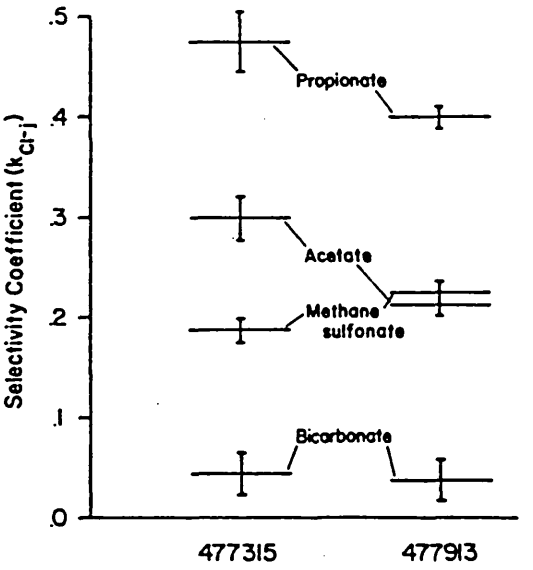


Fig. 5 Selectivity coefficients for ion-selective electrodes (ISE) made from Corning 477315 and 477913. Means ± SE are shown. Selectivity for some anions was altered by modification of sensor.

(From Baumgarten, 1981)

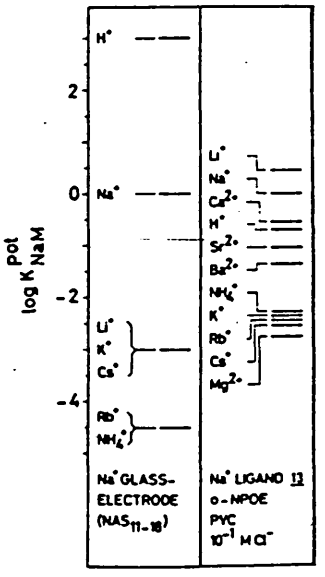


Fig. 6

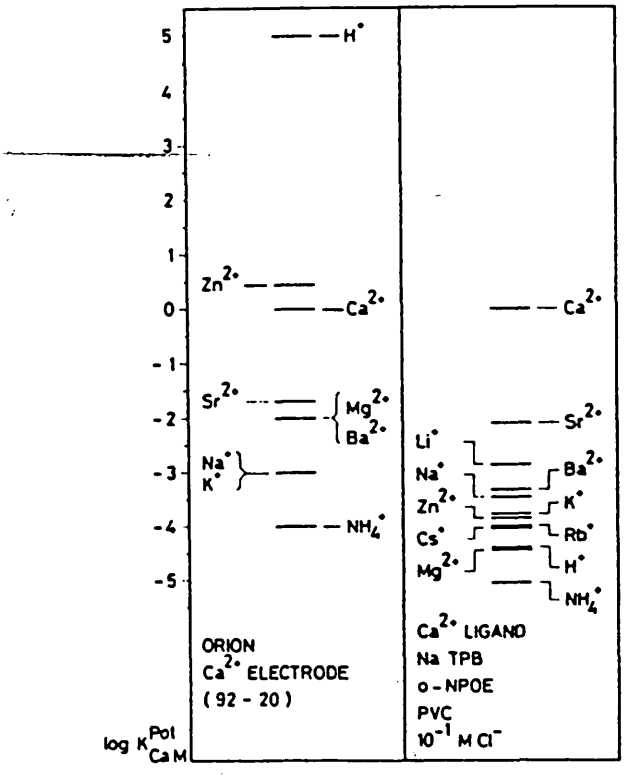


Fig. 7

Fig. 6. Comparison of the selectivities of a neutral Na^+ carrier with those of a sodium glass electrode (NAS_{11-18}). Na^+ ligand 13 is ETH 227. (From Morf & Simon, 1978).

Fig. 7. Comparison of the selectivities of a neutral Ca^{2+} carrier with those of the Orion 92-20 Ca^{2+} electrode. (From Morf & Simon, 1978).

intracellular studies (Ammann *et al*, 1981). This NIC belongs to the class of lipophilic amines and its selectivities in respect to Na^+, K^+, Mg^{2+} and Ca^{2+} are sufficient for intracellular measurements of H^+ ion activities 3.2×10^{-6} M (pH 5.5) at the typical ionic backgrounds encountered.

I.3.vi. HCO_3^-, Mg^{2+} and Li^+-ISMs

Bicarbonate-sensitive liquid membrane electrodes based on neutral carriers for hydrogen ions have recently been introduced (Funck *et al*, 1982). The membrane incorporates ethanolamines and related model compounds as the active components. Its mechanism of response involves the proton carrier properties of these compounds on one hand and the permeability for carbon dioxide of the PVC membrane phase on the other. This type of ISM has not yet been used for intracellular recordings.

A neutral carrier-based ISM is also available for Mg^{2+} (Lanter *et al*, 1980) with selectivities in respect to Na^+, K^+ and Ca^{2+} sufficient to allow a restricted range of intracellular Mg^{2+} assays.

A Li^+-selective neutral ligand developed by Guggi *et al* (1976) has been used successfully to measure intracellular Li^+ activities (Thomas *et al*, 1975). The microelectrode's behaviour was found to be stable intracellularly but it tended to give variable potentials in solutions containing divalent cations.

I.4 Electrochemistry of Insect Muscle

I.4.i Haemolymph

Insect muscles are bathed in haemolymph. The ionic and osmotic properties of insect haemolymph have been reviewed on several occasions (eg. Buck, 1953; Wyatt, 1961; Sutcliffe, 1963; Stobbart & Shaw, 1964; Florkin & Jeuniaux, 1974). Data on the ionic composition of the haemolymph of Diptera and Lepidoptera are summarized in tables 2 and 3. It should be noted, however, that the absolute values given for each parameter are of limited value since they were measured by flame photometry and similar techniques, and as such represent the total concentration of the ion present and not its activity.

Table 2. Osmotic and ionic properties of the haemolymph of some representative insects. (From Usherwood, 1969a)

Order	Species	Δ°C	m.Osm	Inorganic constituents (mM)							m.Osm Inorganic cations	m.Osm Inorganic anions	Organic constituents (mM)	
				Na^+	K^+	Ca^{++}	Mg^{++}	Cl^-	SO_4^{--}	HCO_3^-			Amino acids	Organic acids
Ephemeroptera	*Ephemera danica* (L)	0.504	271	103	18	–	–	77	–	–	121	–	–	–
Odonata	*Aeschna grandis* (L)	0.735	395	145	9	7.5	7.5	110	4	15	169	129	39	–
Dictyoptera	*Periplaneta americana* (A)	0.897(1)	482	157	7.6	4.2	5.4	144	–	–	174.2	–	163	–
Isoptera	*Cryptotermes havilandi* (L)	0.730	392	103	28	8.6(2)	17.6(2)	82	–	–	–	–	–	–
Plecoptera	*Dinocras cephalotes* (L)	0.583	313	117	10	–	–	111	4.1	–	–	–	39	–
Coleoptera	*Carausius morosus* (A)	0.570(3)	306(3)	15	18	15	106	101	16	5	–	35(5)	–	–
Orthoptera	*Locusta migratoria* (A)	0.841(6)	452(6)	60	12	17.2	24.8	97.6	–	–	114	–	53(4)	–
Dermaptera	*Forficula auricularia* (A)	0.736	396	96	13	32.9(5)	–	90	–	–	–	–	–	–
Heteroptera	*Notonecta oblique* (A)	0.756	406	155	21	15(7)	9.3(7)	122	–	–	203.3	–	–	–
Megaloptera	*Sialis lutaria* (A)	–	339	109	5	15	38	31	5(5)	15	167	51	85	–
Neuroptera	*Myrmeleon formicarius* (L)	–	–	143.5	8.7	12.1	31.3	–	–	–	196.5	–	–	–
Trichoptera	*Phryganea* sp. (L)	0.455	245	69	7	14.4(8)	51(8)	37	–	–	–	–	58	–
Diptera	*Gastrophilus intestinalis* (L)	0.872	469	206	13	7	38	14.8	4	14.5	26.4	33.3	62	–
Lepidoptera	*Bombyx mori* (L)	0.480	258	13.9	38.7	18.1	50.3	21	4.9	–	120	–	96(9)	–
Coleoptera	*Popillia japonica* (L)	1.03	554	20.2	9.5	7.9	19.4	19	4.9	–	80.9	–	170	–
Hymenoptera	*Apis mellifera* (L)	0.860	462	5.1	24	4.2	7.9	33	10.3	–	84.5	–	207	–

Order	Na^+	K^+	Ca^{2+}	Mg^{2+}	Cl^-	Phosphate	HCO_3^-	Citrate	Amino acids
EXOPTERYGOTA									
Odonata	149 [13] (104–179)	10 [12] (4–28)	7 [7] (2–6)	4 [5] (2–6)	110 [1]	4 [1]	15 [1]	1 [1]	23
Dictyoptera	129 [2] (100–157)	12 [2] (8–15)	6 [6] (2–10)	7 [5] (3–11)	126 [2] (107–144)	1 [1]		1 [1]	14
Cheleutoptera	14 [5] (9–21)	21 [5] (16–28)	6 [3] (4–8)	60 [3] (53–73)	98 [1]				20
Orthoptera	91 [14] (22–234)	20 [14] (3–62)	7 [7] (1–14)	11 [7] (1–17)	97 [2] (93–101)	28 [2] (16–40)			35
Heteroptera	106 [10]	15 [10]	10 [8]	6 [7]				2 [1]	
ENDOPTERYGOTA									
Diptera	106 [5] (40–206)	16 [15] (2–58)	6 [8] (4–10)	11 [6] (7–9)	26 [2] (15–36)	4 [1]	15 [1]	4 [10] (0–13)	26
Lepidoptera	11 [58] (1–40)	41 [69] (10–96)	13 [66] (3–65)	31 [58] (7–52)	42 [9] (10–86)	4 [3] (3–6)		19 [9] (5–49)	76
Coleoptera	77 [25] (2–165)	28 [28] (4–65)	19 [18] (5–78)	48 [17] (5–99)	32 [2] (19–44)	4 [2] (3–5)		4 [4] (2–7)	71
Hymenoptera	34 [13] (2–154)	39 [13] (19–61)	6 [10] (1–9)	8 [10] (1–12)	33 [1]			4 [3] (2–6)	70

Table 3. Ions in the haemolymph of a number of insects from different orders. The concentrations are expressed in mmol l^{-1}, the extreme values between round brackets, the number of observations between square brackets. (From Piek, 1975)

In Diptera, Na^+ is the main cation, with smaller amounts of K^+, Ca^{2+} and Mg^{2+} being present. Lepidoptera, however, are characterised by a low concentration of Na^+, and relatively high concentrations of K^+, Ca^{2+} and Mg^{2+}.

The dominant anion in all insect haemolymph is chloride. Phosphate is present in small quantities, and bicarbonate has been found in a few insects (including Diptera). Organic anions are also found in insect haemolymph at relatively high levels, particularly as free amino acids. In adult *Calliphora*, more than half of the amino acid content is accounted for by proline (Collett, 1976). Citrate occurs in all insects, and is found at particularly high levels in Lepidoptera (Levenbook & Hollis, 1961).

In addition to amino acids, the haemolymph of a number of orders, including Lepidoptera and, to some extent, Diptera, contains phosphorylcholine. Its exact function is unknown (Bridges, 1972).

Thus, whilst the anion contents of the haemolymph of Diptera and Lepidoptera are similar, there are marked differences in their cation contents. The muscle electrochemistries of the two orders might therefore be expected to differ.

In addition to these interspecies variations in haemolymph composition however, there may also be rhythmic changes in the concentration of certain ions during a 24 hour period, eg. K^+ in cockroach, Lettau *et al*, (1977) (Fig. 8), and more random changes depending on how recently the animal has eaten.

I.4.ii. Resting membrane electrogenesis in insect muscle: Diptera

The only published work on resting muscle membrane electrogenesis in Diptera was carried out on *Drosophila melanogaster* larvae (Jan & Jan, 1976). This concluded that the dependence of E_m in this insect on the extracellular K^+ and Na^+ follows the Goldman-Hodgkin-Katz equation, assuming that $P_{Na}/P_K = 0.23$ and that Cl^- is distributed passively (fig. 9). Thus, in *Drosophila* it was concluded that:-

$$E_m = \frac{RT}{F} \ln \left[\frac{[K^+]o + 0.23\ [Na^+]o}{[K^+]i + 0.23\ [Na^+]i}\right] = \frac{RT}{F} \ln \left[\frac{[Cl^-]i}{[Cl^-]o}\right]$$

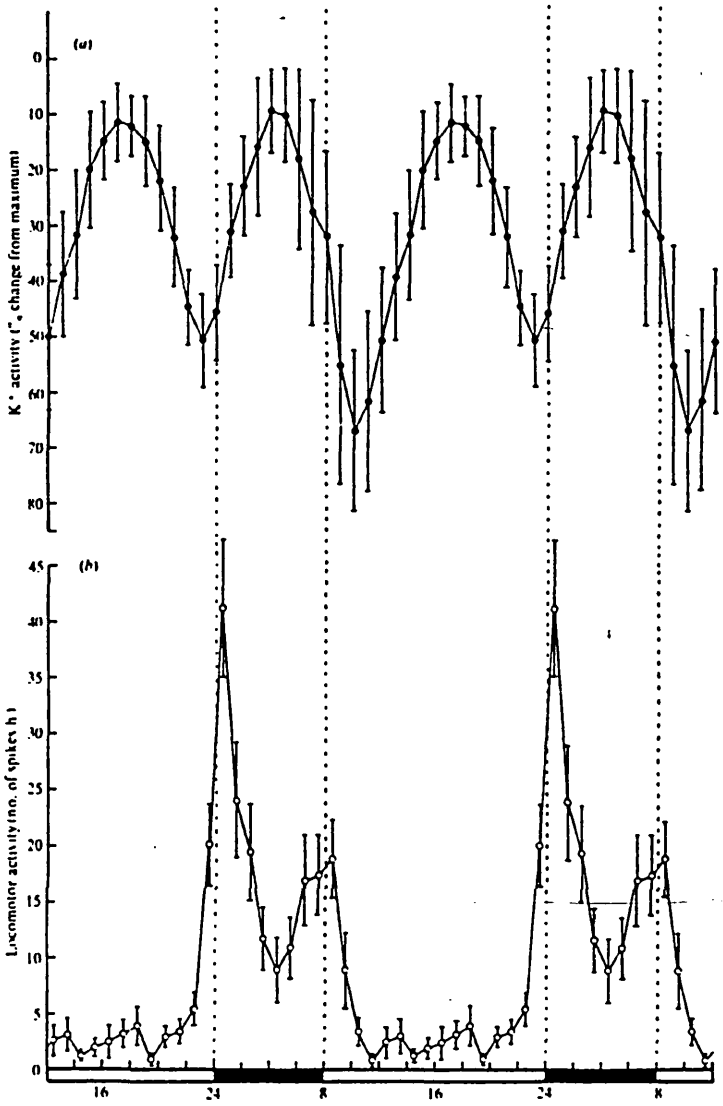


Fig. 8 (*a*) Composite curve of diel changes in K^+ activity from 14 cockroaches, expressed as a % change from the maximum for each individual. Bars mark the extent of the 95 % confidence limits of the mean. (*b*) Composite curve of locomotor activity from 15 cockroaches. In 6 of these, K^+ activity was measured simultaneously (records included in *a*). Bars are $\pm 1 \times$ S.E. of the mean. LD 16:8. 24 h cycle is doubled to show rhythms more clearly.

(From Lettau *et al*, 1977)

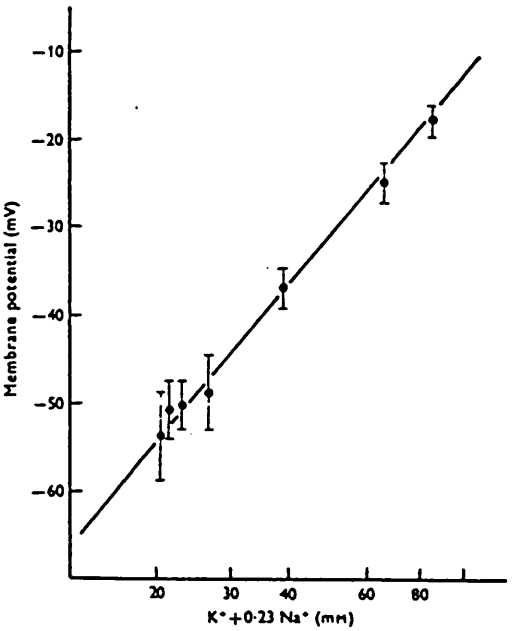


Fig. 9 Relation between muscle resting potential and log ($[K^+]_o$ + 0·23 $[Na^+]_o$). Chloride-free solutions containing 8 mM calcium sulphate (1 mM ionized calcium) were used. Each point is the average resting potential of about twenty ventral lateral longitudinal fibres, first and second from the ventral mid line, of a larva, which was dissected and equilibrated for 30–50 min in a chloride-free solution. Error bars represent standard deviations. (From Jan & Jan, 1976)

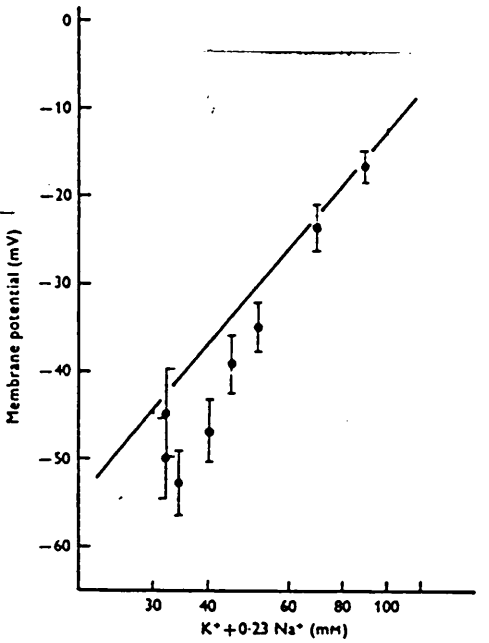


Fig. 10 Relation between muscle membrane potential and log ($[K^+]_o$ + 0·23 $[Na^+]_o$) when using solutions with constant product $[Cl^-]_o \cdot ([K^+]_o$ + 0·23 $[Na^+]_o$) (about 4450 mM²). Each point represents the average potential of about twenty ventral lateral longitudinal fibres in the abdominal segments of a larva. (From Jan & Jan, 1976)

The effect of changes in $[Cl^-]_o$ and $\{[K^+]_o + 0.23\ [Na^+]_o\}$ at constant product was also tested. If Cl^- is passively distributed across the muscle membrane, and if E_m depends on the extracellular K^+ and Na^+ according to the Goldman-Hodgkin-Katz equation there should be no movement of Cl^- across the cell membrane when $[Cl^-]o \times \{[K^+]_o + 0.23\ [Na^+]_o\}$ is kept constant. Changes in E_m should therefore be quick and reversible under these conditions.

The results obtained are shown in figure 10. The fit to the line predicted by the Goldman-Hodgkin-Katz equation does not appear to be very good, but the data was nevertheless taken to confirm that E_m depends only on $\{[K^+]_o + 0.23\ [Na^+]_o\}$ with chloride being passively distributed. No direct measurement of intracellular Cl^- activity and hence no values for the chloride equilibrium potential, E_{Cl}, were made in this (or any other insect) preparation.

The effects of high concentrations of di-valent cations on E_m were investigated by substituting them for Na^+. An average hyperpolarisation of 5mV was recorded when Mg^{2+} was increased from 4 to 47mM. Increased Ca^{2+} levels, however, led to large hyperpolarisations (up to 40mV when Ca^{2+} was increased from 1.8 to 45mM). This was attributed to a membrane stabilizing effect of Ca^{2+}, leading to more effective sealing of the cell membrane around the microelectrode at high extracellular Ca^{2+} levels, and hence to a more hyperpolarised E_m being recorded under these conditions (Stefani & Steinbach, 1969).

The major shortcoming of the work of Jan & Jan (1976) is the fact that the reversibility of changes in E_m was not tested during each experiment.

I.4.iii. Resting membrane electrogenesis in insect muscle: Lepidoptera

The most complete study of resting electrogenesis in a species of Lepidoptera is probably that of Rheuben (1972), working on subalar muscles of the moth, *Antherea polyphemus*. K^+-sensitive ISMs (based on the Corning LIX, 477317) were used to measure intracellular K^+ activities in adult preparations. The mean value obtained was 109.8mM, giving a potassium equilibrium potential of -28.5mV, which was considerably more positive than the average E_m of -60mV. Thus, it was concluded that K^+ was not the only ion involved in generating E_m.

Since Mg^{2+}, Na^{+}, and Cl^{-} are all known to be present in insect haemolymph, their effects on E_m were investigated by a series of substitution experiments. The concentration of a given ion in the extracellular medium was varied by changing the medium rapidly and the subsequent (within 5 minutes) changes in E_m monitored.

The extracellular Mg^{2+} concentration was found to have little effect on E_m when it was varied between 1 and 100mM (Tris methane-sulphonate was used as substitute) (fig. 11A). This was taken to imply that the membrane had a negligible resting permeability to Mg^{2+}.

A tenfold increase in extracellular Na^{+} led to a depolarisation of 4.6mV in E_m (fig. 11B), from which it was concluded that the muscle membrane was only slightly permeable to Na^{+}.

Changes in extracellular Cl^{-} (using SO_4^{2-} as a substitute) resulted in transient changes in E_m, whose peak amplitudes are shown in Figure 11C. Increasing extracellular Cl^{-} made E_m more negative, but it then slowly returned to its original value. Changing to a Cl^{-}-free solution caused a transient depolarising shift in E_m, followed by a return to the original value within 10 minutes. This was taken to suggest that Cl^{-} was passively distributed and played no part in generating E_m.

The effect of extracellular K^{+}, a_K^{+}, on E_m was determined using solutions containing zero Na^{+} and Cl^{-}, since the cell membrane was known to be significantly permeable to these ions. The maximum slope of the relationship between mean E_m and the logarithm of a_K^{+} was 35mV for a tenfold increase in K^{+}, (fig. 12A). This differs significantly from the 58mV predicted by the Nernst equation for a membrane which is permeable only to K^{+}, which was consistent with E_K not being equal to E_m. It was concluded that, whilst K^{+} is involved in generating E_m, other mechanisms were likely to exist.

In an attempt to assess the contribution of a metabolic mechanism to E_m three types of experiment were carried out. Firstly a number of metabolic inhibitors were applied to the preparation. Dinitrophenol (DNP, 0.5-1mM) which inhibits oxidative metabolism, produced a 30-35mV depolarisation in E_m within 15 minutes of application. However, ouabain (10^{-3}M) and ethacrynic acid (10^{-3}M), which are both known to specifically inhibit Na^{+} transport, had no effect on E_m. Diamox (10^{-4}M), a carbonic anhydrase inhibitor which

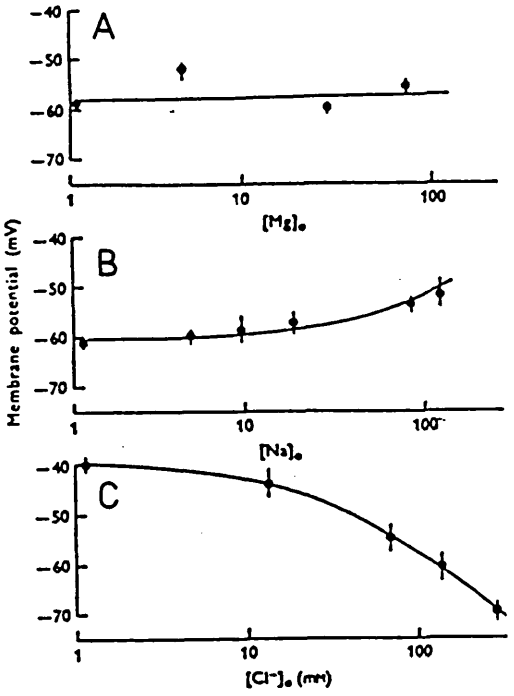


Fig. 11 The effect of Mg^{2+}, Na^+, and Cl^- on the resting potential. Error bars indicate ± 1 S.E. The data points for Mg^{2+} and Na^+ are the changes of potential (from that in reference Ringer to that in test Ringer) of groups of ten or more fibres normalized to the mean resting potential of 60 mV in reference Ringer. Since changes in external Cl^- produce only transient changes in membrane potential, the data points for Cl^- represent the average maximum change in single muscle fibres produced by changes from the reference solution to a test solution. (From Rheuben, 1972)

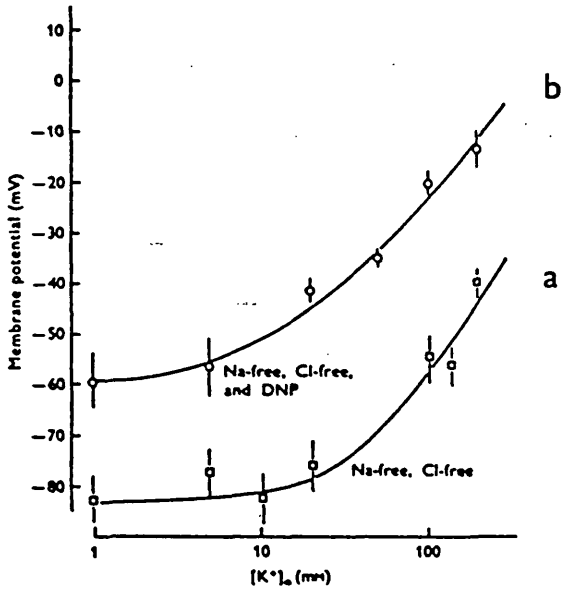


Fig. 12 The effect of changing external K^+ on the resting potential. Error bars indicate ± 1 S.E. The data was pooled and normalized as for Fig. 2A. Na-free, Cl-free and DNP: the effect of changing external K^+ in the absence of Na^+ and Cl^-, 1 mM-DNP present. Na-free, Cl-free: same as the preceding but without DNP. (From Rheuben, 1972)

might have been expected to interfere with Cl^- transport, also had no noticeable effect.

Secondly, the effect on E_m of depriving the tissue of oxygen was investigated and the introduction of nitrogen into the tracheae surrounding the muscles being studied resulted in a depolarisation of up to 35mV in E_m (fig. 13). This was approximately the same as that produced by DNP. The decrease in E_m was reversible if oxygen was returned to the tracheoles of the muscle fibre. DNP prevented this reversal if applied before oxygen was re-introduced (fig. 13).

Thirdly, the effect of temperature on E_m was also investigated. Membrane conductance was found to be directly related to temperature, increasing at high temperature and decreasing at low temperatures. E_m depolarised on cooling, and on warming, either depolarised or did not change.

From these experiments, it was concluded that part of the E_m in *Antherea* muscle fibres was generated by a mechanism dependent directly upon oxidative metabolism. This metabolically-maintained potential appeared to differ from previously investigated electrogenic transport systems eg. the ouabain-sensitive Na^+-K^+ pump, but its exact nature was not clarified further.

The resting E_m was found to be very sensitive to changes in external pH. For an increase in pH from 7 to 8, E_m hyperpolarised by up to 30mV (fig. 14). If H^+ were behaving as a permeable cation with a concentration gradient across the cell membrane, the above hyperpolarisation in E_m would imply that E_H needs to be at least 20 mV more negative than E_m. This would require that the internal pH be less than 5.6, which would be an unlikely internal milieu for a cell. The significance of this effect was not discussed further.

Several other studies have been carried out concerning resting membrane electrogenesis in Lepidoptera. It should be noted, however, that in all cases, estimates of intracellular K^+ levels were obtained using flame photometry. This technique measures the total K^+ concentration present in the cell, including that which is bound. It does not therefore provide a true measure of the"activity" of K^+ present ie. the number of ions present which are free to cross the cell membrane and play a part in electrogenesis (see section I.1.).

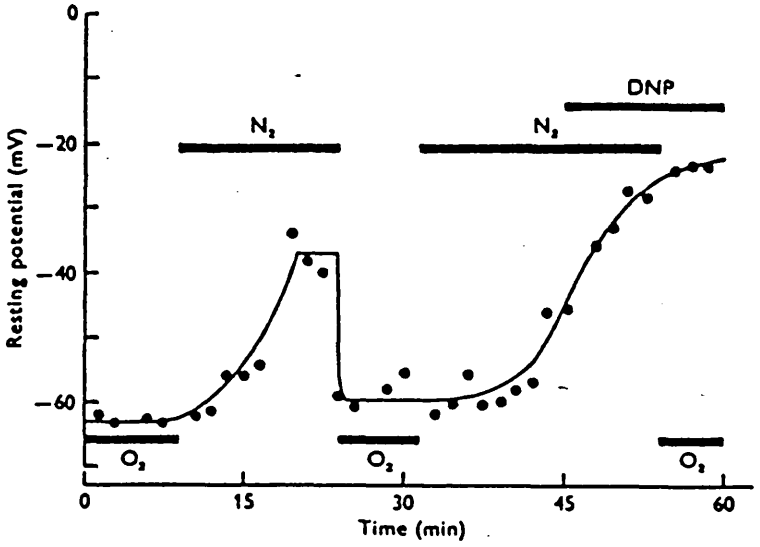


Fig. 13 The effect of anoxia on the membrane potential. The effect on the resting potential of N_2 or O_2 and DNP is shown. The bars indicate whether O_2 or N_2 was being supplied to the spiracle, and whether or not DNP was present in the Ringer. Each point represents the mean resting potential of a sample of fibres measured at that time. Although the depolarization associated with N_2 substitution in the cannula was slow (15–20 min), the repolarization when O_2 was returned was almost immediate. DNP blocks this repolarization. (From Rheuben, 1972)

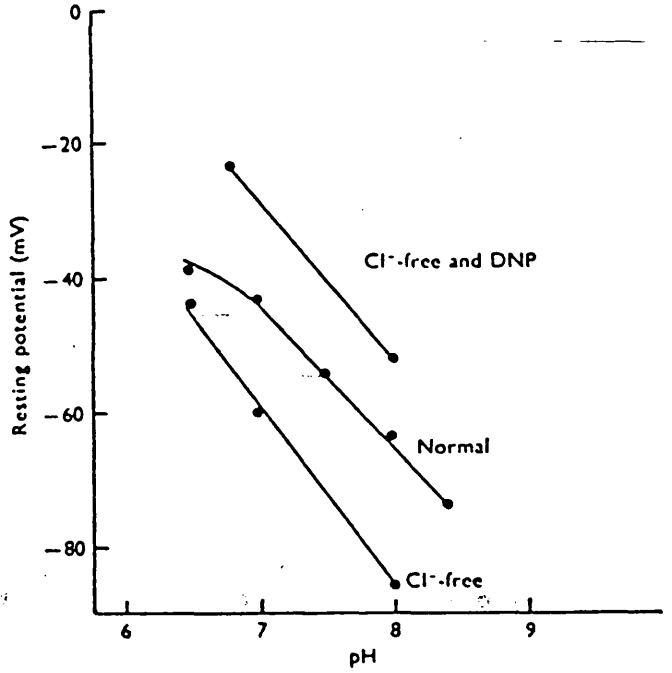


Fig. 14 The effect of pH on the resting potential. Each curve shown is the result obtained by changing the external pH and observing the potential change in a single fibre. The Cl^- free results were both obtained from the same fibre, the upper curve being obtained after DNP had decreased the membrane potential. The middle curve is from a fibre in another preparation. (From Rheuben, 1972)

Huddart (1966) studied the effect of K^+ on E_m in several species of Lepidoptera: *Bombyx mori* (fig. 15 A), *Sphinx ligustri* (Fig. 15 B) and *Actias selene*. In all cases. the relationship between the E_m and the logarithm of the concentration of extracellular K^+ ions appeared to be hyperbolic in shape. This is in agreement with data obtained by Rheuben (1972) for *Antherea*. Such hyperbolic graphs bear no resemblance to the straight line predicted by the Nernst equation for a membrane which is permeable only to K^+. Huddart found no correlation between E_m and the K^+ equilibrium potential, E_K, calculated from the measured K^+ distribution in the muscle (table 4, fig.15,B,C). Increasing extracellular K^+ led to a corresponding but smaller increase in intracellular K^+ concentration, so that in high K^+ salines, the ratio of intracellular K^+ to extracellular K^+ fell below one. It was concluded from this evidence that the E_m in these three insects is not generated solely by K^+, and that other mechanisms must also be involved.

In *Sphinx*, Huddart (1967) found that a 200-fold increase in extracellular Cl^- caused a 30% (14mV) sustained hyperpolarisation in E_m (fig. 15 D). No consistent correlation was found between E_m and E_{Cl}.

The resting E_m (-60mV average) of *Sphinx ligustri* was further investigated by Wareham *et al* (1975). Cooling the preparation from 20°C to 5°C and application of 0.5mM ouabain were found to depolarize the membrane potential by a maximum of 19mV, over 30 and 150 minutes, respectively. An active component was, therefore, thought to contribute some -19mV to E_m. The rest of the E_m (-41mV) was suggested to be generated by an "ionic electrode" mechanism. Wareham *et al* (1975) used an atomic absorption spectrophotometer to measure the K^+ content of the haemolymph and myoplasm in three insects and found these to be 23 and 110mM, rspectively. The mean value of E_K was calculated as -40mV, and this was taken as evidence for the "ionic electrode" being dominated by K^+, although no clear reasoning for this was provided. Wareham *et al* (1975) also found that replacement of Cl^- by propionate in the Ringer, caused a membrane depolarisation of around 19mV, but this was proposed to be an effect on the "active" component. Again, no clear reasoning was given!

The suggestion that an electrogenic metabolic pump generates a part of the E_m in *Sphinx* muscle is in agreement with conclusions of Huddart & Wood (1966) from experiments in which DNP (0.5mM) was applied to muscle fibres.

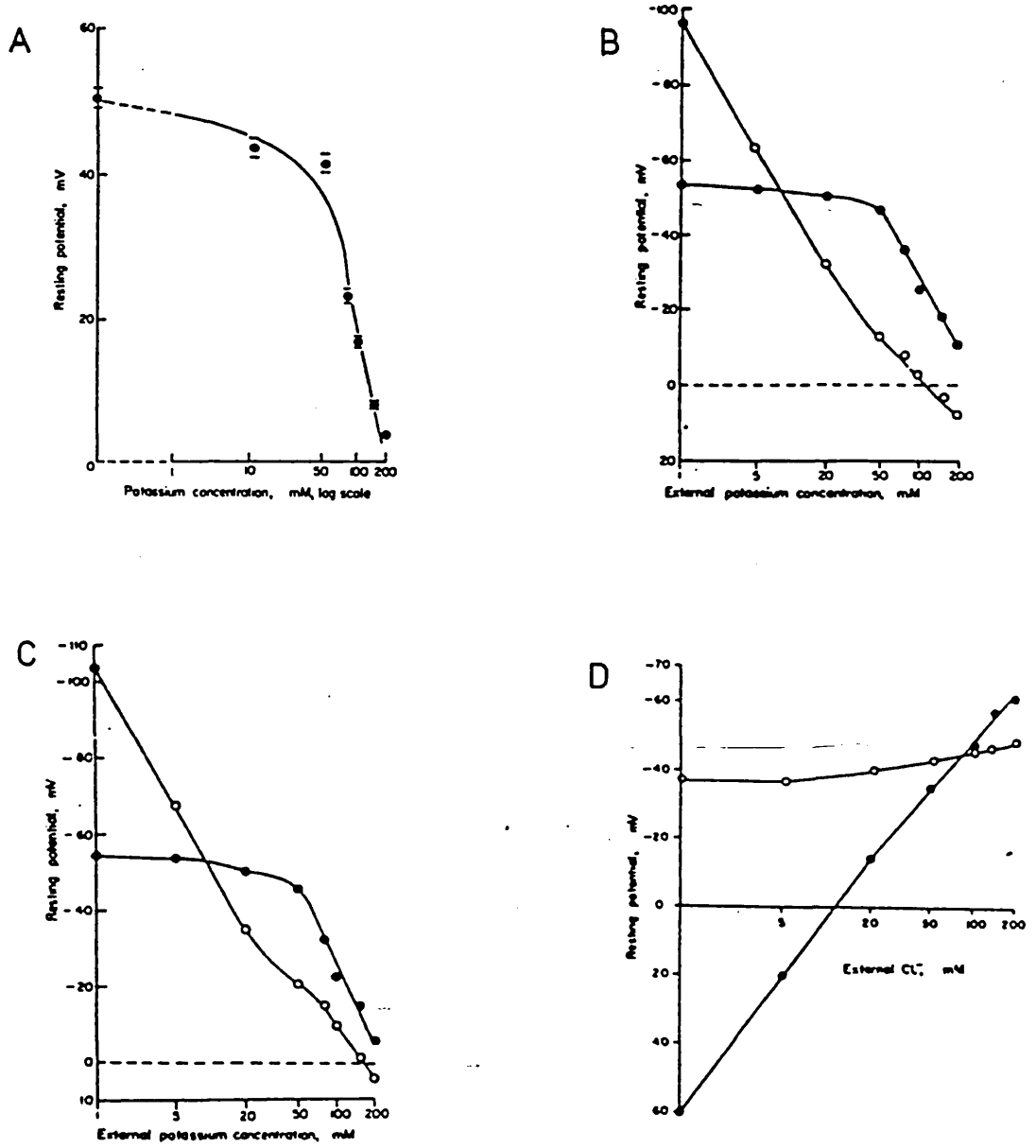


Fig. 15A The relationship between resting potential and the logarithm of the external K^+ concentration in *Bombyx mori* muscle fibres. (From Huddart, 1966b)

B-C The relationship between resting potential (full circles) and E_K (hollow circles) (predicted from data on intra- and extra-cellular K^+ concentrations) and $[K^+]_o$ for skeletal muscle fibres of (b) *Sphinx ligustri* and (c) *Actias selene* (From Huddart 1966b)

D Relationship between resting potential (hollow circles) of *Sphinx ligustri* skeletal muscle fibres. E_{Cl} predicted from data on the concentrations of chloride in the intra- and extra-cellular phases (From Huddart, 1967)

External Potassium (mM/l)	Intracellular Potassium (mM/Kg tissue water. Mean ± S.E.	Theoretical E_k (mV)	Observed resting potential, (mV). Mean ± S.E.
	Sphinx ligustri		
1	45·4 ± 3·0	−96·1	−53·6 ± 1·2
5	61·4 ± 3·2	−63·2	−52·0 ± 1·0
20	71·0 ± 4·2	−31·9	−49·9 ± 1·5
50	84·4 ± 7·0	−13·4	−47·4 ± 1·0
70	96·0 ± 3·3	− 7·9	−34·7 ± 0·8
100	111·2 ± 3·0	− 2·7	−25·4 ± 1·2
150	130·1 ± 4·6	+ 3·6	−18·2 ± 0·7
200	145·6 ± 8·3	+ 8·0	−10·7 ± 0·6
	Actias selene		
1	61·9 ± 5·5	−103·9	−54·4 ± 1·1
5	74·6 ± 4·6	− 68·0	−54·1 ± 1·0
20	80·6 ± 6·4	− 34·9	−51·5 ± 1·4
50	115·6 ± 5·2	− 21·0	−46·4 ± 1·3
70	131·4 ± 4·2	− 15·9	−32·9 ± 1·6
100	149·7 ± 7·1	− 10·2	−21·9 ± 1·1
150	157·1 ± 2·2	− 1·2	−15·2 ± 0·7
200	171·1 ± 5·0	+ 3·9	−12·0 ± 0·9

Table 4. The effect of external potassium on intracellular potassium and resting potentials. (From Huddart, 1966b).

	Muscle K mM/kg fibre water	Blood or equivalent saline K mM/l.	E_K at 18°C (see text) mV	Observed resting potential mV	Author
Carausius morosus	103·3 ± 6·4	18·0	44·1	41·0	Wood (1957)
Periplaneta americana	110·4 ± 7·3	13·3 ± 1·2 (saline 10·0)	53·1	*ca.* 57	Hoyle (1955a)
Locusta migratoria	124·0 ± 4·4	11·0 (saline 10·0)	63·2	*ca.* 62	Hoyle (1955a)

Table 5. Intracellular potassium concentration and resting potentials. (From Wood, 1963).

The resulting triphasic decline in E_m (fig.16) was attributed to changes in the permeability of the membrane to K^+, Na^+ and Cl^-. It was concluded that the most likely explanation for these changes was that the permeability of the membrane to the various ions was due to structural and physicochemical properties of the membrane which were dependent directly upon oxidative metabolism. In this case, the increasingly permanent nature of the changes caused by DNP would be due to irreparable damage caused to the membrane by depriving it of its metabolic support.

A summary of the data obtained from K^+ substitution experiments on various muscles of *Philosamia cynthia*, skeletal muscles of *Bombyx mori* and *Sphinx ligustri* is given in figure 17 (from Piek, 1975). All the graphs are similar in shape, showing a rather sharp change in the E_m curve at the $[K^+]o$ value which roughly corresponds to that in the haemolymph.

I.4.iv. Resting membrane electrogenesis in insect muscle: some other species

A few insect species have been studied in addition to those previously described, and these include representatives of omnivorous and herbivorous groups: the cockroach, *Periplaneta americana* (Wood, 1963; Wareham *et al*, 1974); several *Orthoptera*, including the locusts *Schistocerca gregaria* (Lea & Usherwood, 1973 b) and *Locusta migratoria* (Hoyle, 1952; Wood, 1963) and the grasshopper *Romalea microptera* (Usherwood, 1969); and the stick insect *Carausius morosus* (Wood, 1957, 1963) (table 5.)

The effect of extracellular K^+ on the membrane potential of several of these species is summarised in figure 18 (from Piek, 1975).

In cockroach muscles (from the coxae of the 3rd thoracic segment), E_m appears to be generated in a similar manner to that of the moth (Wareham *et al*, 1975) ie: it has two components, a set of ionic conductance mechanisms dominated by K^+, which is responsible for around 42mV and an active component which accounts for the remaining 18mV (Wareham *et al*, 1974).

The relationship between E_m and the logarithm of the extracellular K^+ is linear, with a slope of 43mV per tenfold change in K^+ (fig. 19). These experiments involved soaking the preparation for 2 hours in each of 6

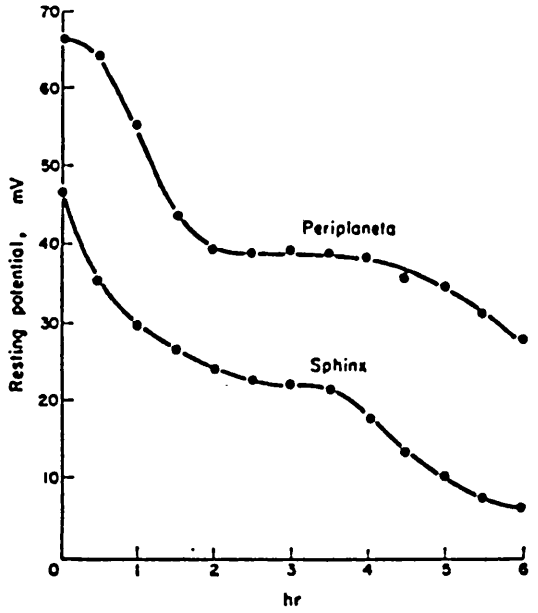


Fig. 16 Changes in the resting potential of *Periplaneta* and *Sphinx* under the influence of DNP (From Huddart & Wood, 1966)

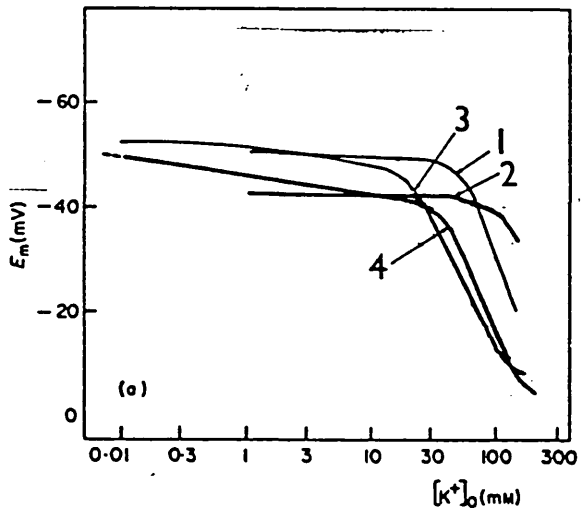


Fig. 17 Relation between the resting membrane potential and the external K concentration of some Lepidopteran skeletal muscle fibres equilibrated for a short time (maximum 2h) in a saline solution; 1. longitudinal flight muscle from *Philosamia cynthia*; 2. sternopedal muscle from *P.cynthia*; 3. Ventral longitudinal muscle of *P. cynthia* larva; 4. skeletal muscle from *Bombyx mori* (Huddart, 1966a) (Modified from Piek, 1975)

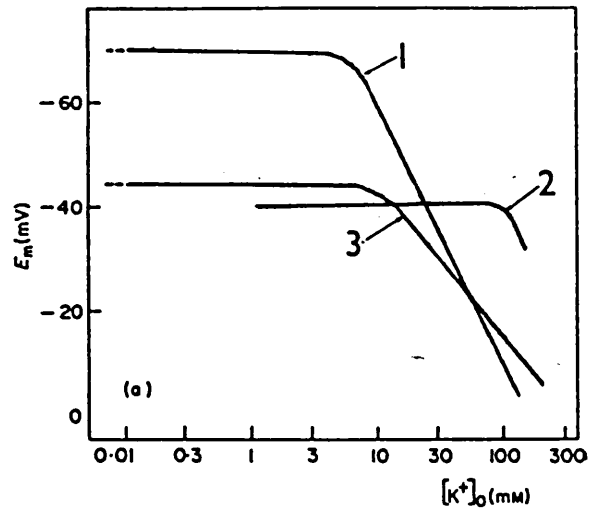


Fig. 18 Relation between the resting membrane potential and the external K concentration of some insect skeletal muscle fibres, equilibrated for a short time (maximum 2h) in a saline solution; 1. Flexor tibialis from *Schistocerca gregaria* (Orthoptera) (Hoyle, 1953); 2. Skeletal muscle from *Tenebrio molitor* larva (Coleoptera) (Belton and Grundfest, 1962); 3. flexor tibialis muscle from *Carausius morosus* (Cheleutoptera) (Wood, 1957). (Modified from Piek, 1975)

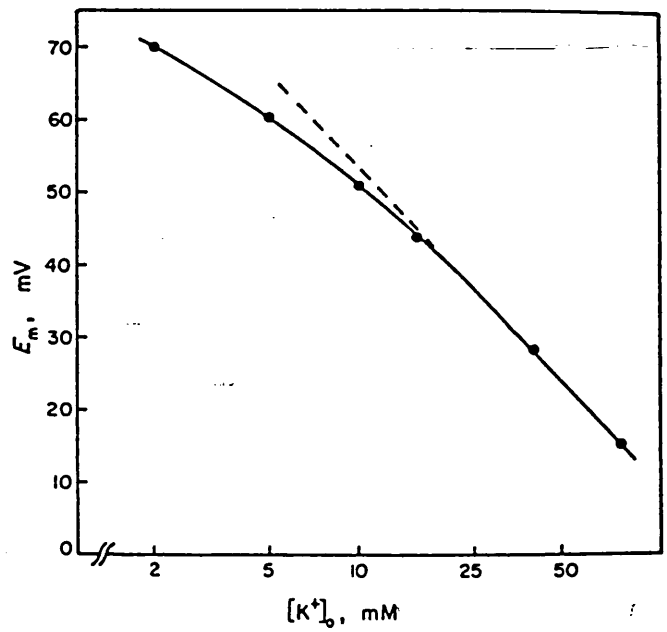


Fig. 19 Effect of variation of $[K^+]_o$ on E_m at room temperature, when $[Cl^-]_o$ = zero. Muscles were equilibrated with the salines for 2 hr at room temperature before recordings were made. Bicarbonate saline; chloride was replaced by propionate; K^+ was present as sulphate. Standard errors for the mean values of the resting potentials did not exceed the diameter of the points. Semi-log plot.

(From Wareham *et al*, 1974)

solutions. The reversibility of the E_m changes observed was not, however, tested. The effect of extracellular Na^+ on E_m was apparently not investigated by Wareham *et al* (1974). Wood (1963), however, found that increasing extracellular Na^+ led to a hyperpolarisation in E_m (table 6).

The major properties of the E_m of cockroach muscle are summarised in figure 20. Line A shows the straight line relationship (slope around 42mV per decade) between E_m and the logarithm of the extracellular K^+ concentration when $[K^+]o \times [Cl^-]o$ kept constant. When Cl^- was removed from the saline, a sustained depolarisation in E_m was observed (line B) whilst the slope of the E_m against the logarithm of $[K^+]o$ was unaffected. It was suggested that Cl^- was involved in generating E_m to some extent. Cl^- substitution experiments gave a sustained change in E_m of around 18mV per tenfold change in $[Cl^-]o$ (fig. 21).

The potassium equilibrium potential, E_K, in cockroach muscle was calculated using the intracellular K^+ concentrations reported by several workers (eg. 110mM, Hoyle, 1955; 110.4mM, Wood, 1963 (table 3); 112mV, Tobias, 1948) and the measured haemolymph K^+ content of around 17mM. The values of E_K were in the range -41 to -47mV, and were clearly more positive than the average E_m of -60mV.

Evidence for the involvement of a metabolic pump was obtained from three experiments: cooling (fig. 22 A), application of DNP (10^{-4}M) (fig. 22 B) and application of sodium cyanide (10^{-3}M) (fig. 22 C). All these treatments led to depolarisation of E_m by 15-20mV. Ouabain (5×10^{-4}) however, had little effect on E_m.

In locust extensor tibiae muscles, E_m has been found to be determined almost exclusively by K^+, obeying the Nernst equation for a K^+ electrode (Hoyle, 1953, fig. 23; Wood, 1963, table 5; Usherwood, 1967 a,b). There is, however, a small deviation from the predicted value for a K^+ electrode in low K^+ salines (fig. 24) which may be due to a small permeability to other ions. The contribution of these other ions to E_m becomes larger at low extracellular K^+ levels, when the potential would be better fitted by the constant field equation.

The rate at which the cell membrane depolarised in response to high K^+ (100mM K^+) was found to be much greater than the rate of repolarisation

External medium mM/l.	Mean resting potential ± S.E. (mV)	Mean action potential ± S.E. (mV)	Action potential *minus* resting potential (mV)	Mean intracellular sodium concentration ± S.E. mM/kg fibre water	Ratio Na_o/Na_i	Calculated E_{Na} (mV) at 18 C
Carausius morosus						
Zero Na	37·5 ± 1·4	34·4 ± 2·0	−3·1	2·9 ± 0·8	—	—
25 Na	39·5 ± 1·3	37·0 ± 1·2	−2·5	12·5 ± 1·5	2·0	17·4
50 Na	41·0 ± 1·6	42·4 ± 3·0	1·4	12·4 ± 1·4	4·0	34·8
100 Na	42·4 ± 1·7	43·5 ± 2·4	1·1	14·2 ± 1·9	7·0	48·9
150 Na	43·1 ± 1·4	47·5 ± 1·7	4·5	9·0 ± 1·8	16·7	70·3
Locusta migratoria						
Zero Na	28·0 ± 1·4	9·0 ± 0·9	−19·0	7·0 ± 2·6	—	—
25 Na	36·5 ± 2·6	18·0 ± 2·1	−18·5	9·4 ± 2·9	2·7	24·9
50 Na	39·5 ± 1·5	35·0 ± 2·8	−4·5	20·5 ± 1·6	2·4	21·9
100 Na	51·0 ± 2·1	58·0 ± 3·2	7·0	15·6 ± 1·8	6·4	46·6
150 Na	53·5 ± 4·4	59·0 ± 3·8	5·5	20·2 ± 2·4	7·4	50·2
Periplaneta americana						
Zero Na	26·7 ± 1·8	11·0 ± 1·1	−15·7	19·6 ± 2·1	—	—
25 Na	36·0 ± 2·1	22·4 ± 2·2	−13·6	32·4 ± 3·4	0·77	−6·5
50 Na	36·8 ± 2·0	37·0 ± 2·9	0·2	26·0 ± 1·9	1·9	16·1
100 Na	47·6 ± 3·3	49·0 ± 2·1	1·4	29·9 ± 2·9	3·3	30·0
150 Na	53·0 ± 2·2	55·0 ± 2·3	2·0	29·0 ± 2·8	5·2	41·4

Table 6. Resting and action potentials, intracellular sodium concentration and theoretical overshoot of the muscle fibres. (From Wood, 1963).

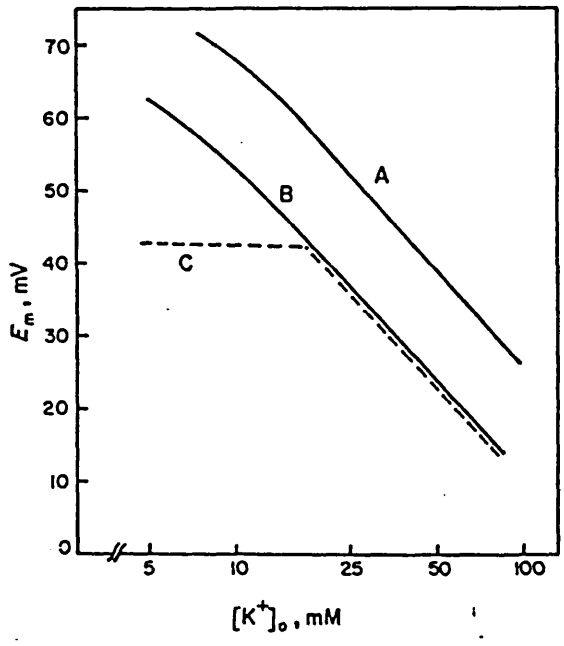


Fig. 20 Diagram summarizing major properties of E_m of cockroach muscle. Line A: behaviour when $[K^+]_o \times [Cl^-]_o$ maintained constant. Line B: behaviour in the absence of $[Cl^-]_o$. Line C: behaviour at 5°C, showing both the 18 mV depolarization below line A and the apparent insensitivity to reductions in $[K^+]_o$.

(From Wareham *et al*, 1974)

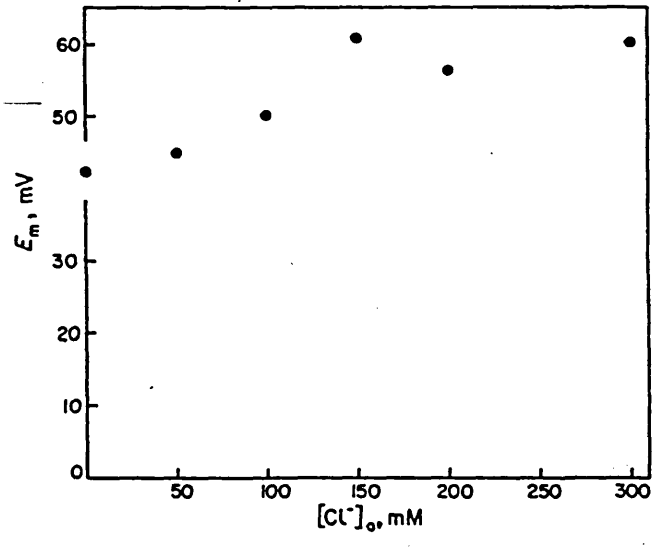


Fig. 21 Effect of variation of $[Cl^-]_o$ on E_m at a fixed value of $[K^+]_o$ of 16 mM at room temperature. E_m (ordinate) is plotted against $[Cl^-]_o$ (abscissa). S.E. did not exceed the diameter of the points. $KHCO_3$ = 16 mM; Cl^- varied by the addition of choline chloride; isosmocity maintained by the addition of glucose; equilibration for 2 hr, pH = 7·0. There is no evidence for hyperpolarization above the −60 mV seen with a normal $[Cl^-]_o$ of 150 mM.

(From Wareham *et al*, 1974)

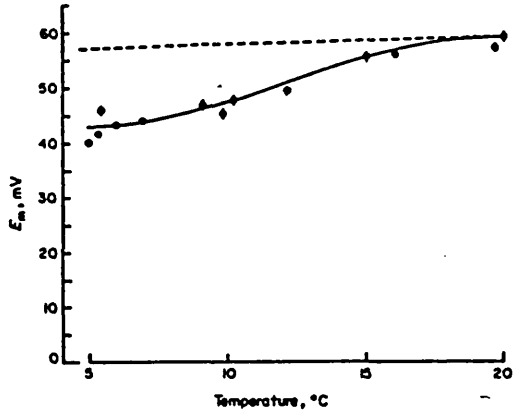


Fig. 22A The effect of temperature on the resting potential of cockroach coxal muscle. Muscles were equilibrated at each temperature for 2 hr. Standard errors are shown where these exceed the diameter of the points. Dashed line represents the expected fall in E_m when the temperature is decreased, as predicted by the Nernst equation. Solid line represents the observed response of E_m and is fitted by eye. (From Wareham *et al*, 1974)

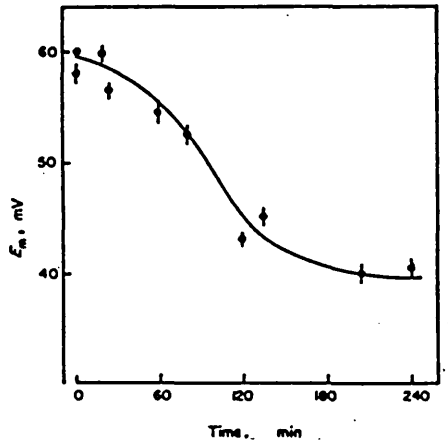


Fig. 22B Effect of 10^{-4} M dinitrophenol on E_m. The muscles were exposed to bicarbonate saline containing DNP (pH 7·1; room temperature). Standard errors are shown, and are calculated from at least thirty separate measurements. Abscissa: time (min) of exposure to saline containing DNP.
(From Wareham *et al*, 1974)

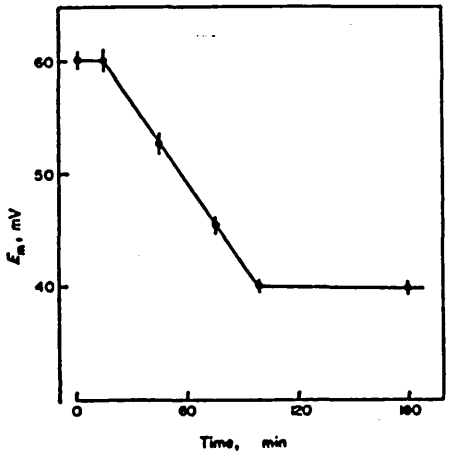


Fig. 22C Effect of 10^{-3} M NaCN on E_m (bicarbonate saline; pH 7·2; room temperature). Standard errors are shown and are calculated from at least thirty separate measurements. Abscissa: time (min) of exposure to saline containing 10^{-3} M NaCN. (From Wareham *et al*, 1974)

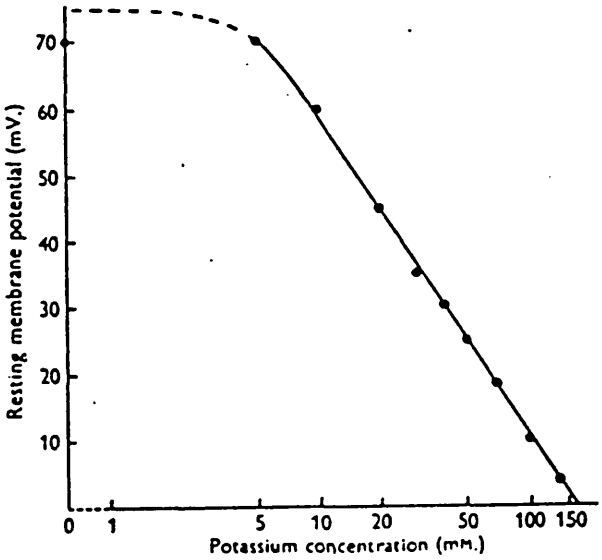


Fig. 23 The relationship between the membrane resting potential of fibres of the flexor tibialis muscle and external potassium concentration.

(From Hoyle, 1953).

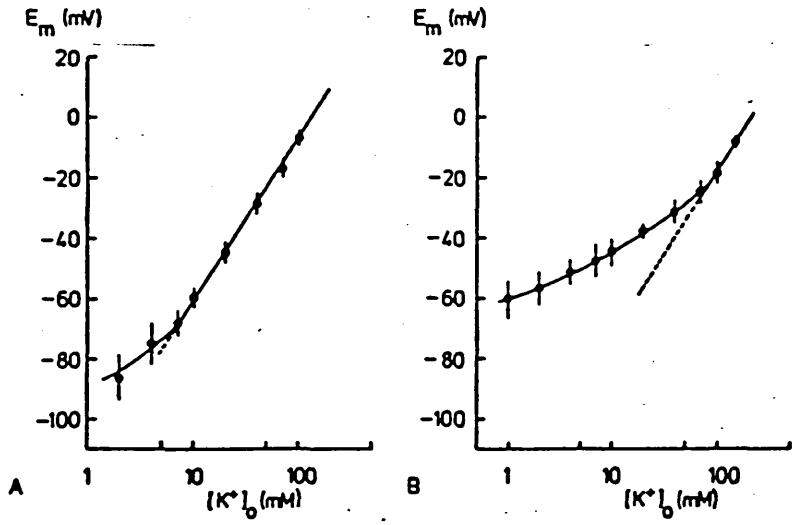


Fig. 24. Effect of external potassium concentration on the membrane potential of the retractor unguis muscle of *Schistocerca gregaria* at 20°C. The slope of the line is 54 mV for a tenfold change in $[K^+]_o$. The vertical bars represent the standard errors of the mean. B. Effect of $[K^+]_o$ on E_m at 5°C. The dotted line represents a slope of 54 mV per tenfold change in $[K^+]_o$. (C. A. Leech, unpublished observations) **(From Ashcroft, 1982)**

when the muscle was returned to low K^+ (10mM K^+) saline, however. (Usherwood, 1969) (fig. 25). This effect was attributed to anomalous rectification of the muscle fibre membrane.

Increasing extracellular Na^+ in this insect was found to cause a hyperpolarisation in E_m (Wood, 1963, table 6), but no conclusions were drawn from this observation.

Chloride was found to be passively distributed in this insect (Lea & Usherwood, 1973, fig. 26): a reduction in extracellular Cl^- (substituted by propionate) resulted in a transient depolarisation of E_m, an increase led to a transient hyperpolarisation.
In the stick insect, the recorded E_m's fit those calculated from the intra- and extra cellular K^+ concentrations for a K^+-selective membrane (Hoyle, 1955; Wood, 1957, 1963 (table 5)). Increasing extracellular Na^+ led to a small hyperpolarisation in E_m (fig. 27 A, table 6) and Ca^{2+} had a similar effect (fig. 27B). The membrane was found to be impermeable to Mg^{2+} (fig. 27 C).

Thus, in certain insect species, E_m appears to be determined by K^+ alone, whilst in others, a variety of additional ionic and metabolic mechanisms are involved in maintaining E_m.

I.5 Neuromuscular transmitters in insects

In the most extensively-studied insect neuromuscular preparation, the locust extensor tibiae, the muscle receives three neural inputs: 'fast' and 'slow' excitatory, and inhibitory. (Usherwood, 1967) (fig. 28).

L-glutamate is the putative transmitter at the excitatory synapse, and the presence of post-junctional receptors for this amino acid have been demonstrated in a variety of ways (Usherwood and Machili, 1966, 1968; Usherwood, 1967; Beranek and Miller, 1968). Application of glutamate to excitatory synapses on locust muscle activates glutamate-sensitive receptors on the post-synaptic membrane, causing an increase in membrane conductance. This increase results from the opening of cationic channels which are associated with, and whose function is 'gated' by the glutamate receptors. When in the open state, the channels increase membrane permeability to Na^+ and K^+, with Ca^{2+} making a minor contribution to the

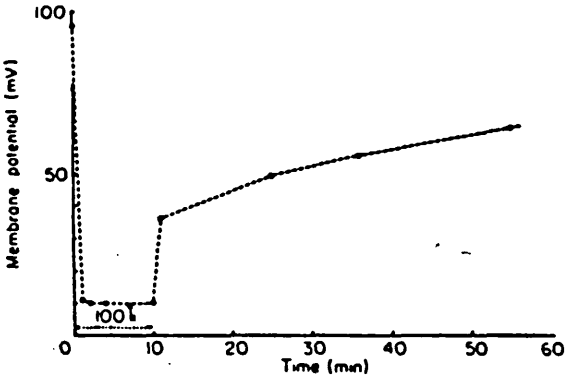


Fig. 25 Effect of changing the external potassium ion concentration, from 10 mmol l^{-1} to 100 mmol l^{-1}, and vice versa, at a constant chloride concentration (154 mmol l^{-1}), on the membrane potential of a *Romalea microptera* retractor unguis muscle fibre. The rate of depolarization is much greater than the rate of repolarization, the latter being characterized by an initial fast phase and a subsequent slow phase. (From Usherwood, 1969.)

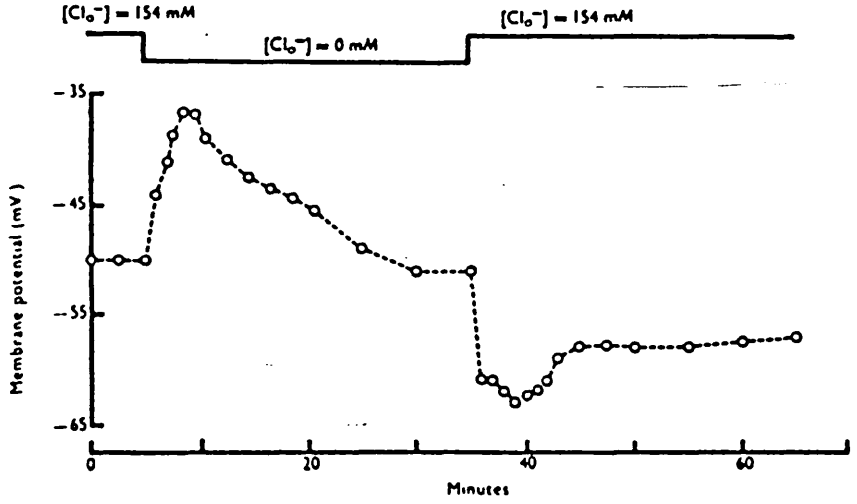


Fig. 26 Transient changes in membrane potential of a coxal adductor muscle fibre of *Schistocerca gregaria* caused by substituting of the chloride in the saline by sulphate. (From Lea and Usherwood, 1973 .)

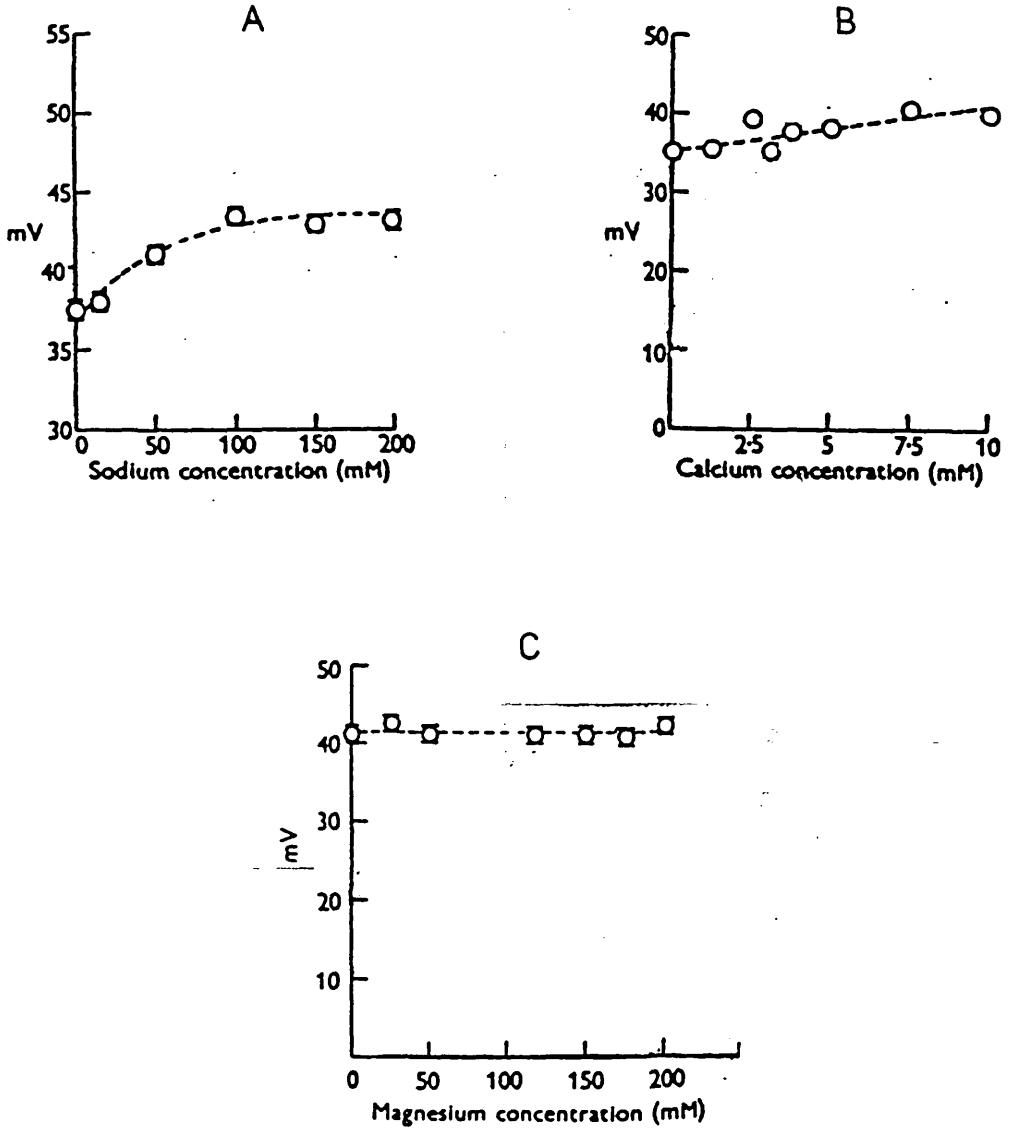


Fig. 27 Relation between the resting potential in *Carausius* and (A) external Na concentration, (B) external Ca concentration, (C) external Mg concentration. (From Wood, 1957)

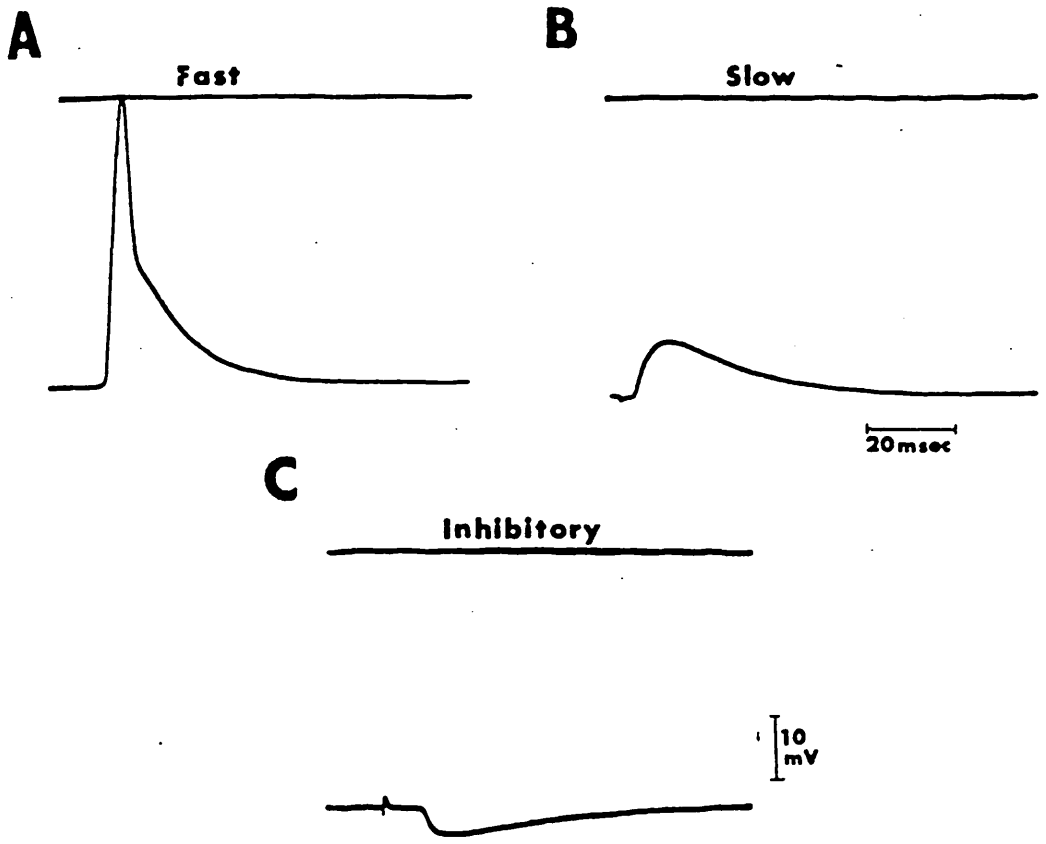


Fig. 28. Intracellular recordings from three different metathoracic extensor tibial muscle fibres of the locust to stimulation of (A) "Fast" excitatory axon; (B) "Slow" excitatory axon and (C) Inhibitory axon. Recordings made in 10 m eq/L potassium-saline. Time and voltage calibrations same for all three records. (From Usherwood, 1967).

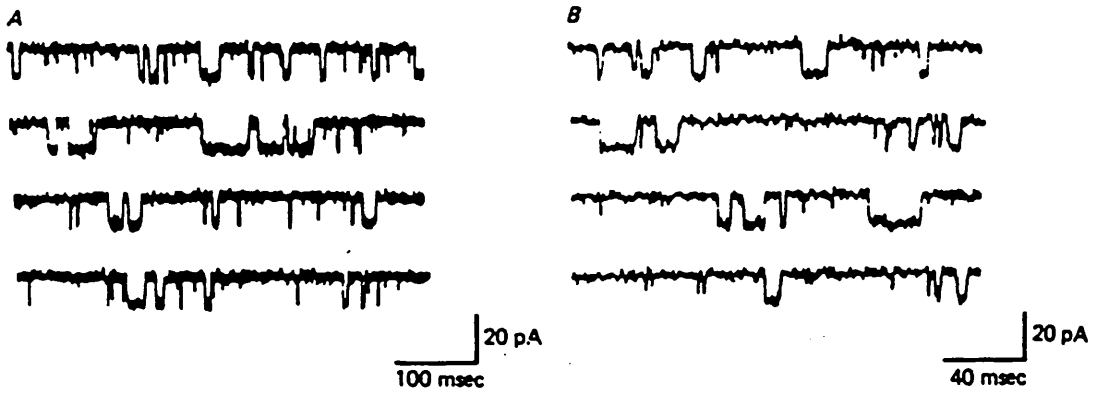


Fig. 29 A,B: Records of glutamate-induced single-channel activity from two con-A-treated muscle fibers; note the difference in sweep speeds. Chloride-free solution was used for the bathing medium and in the patch pipette; in both experiments, the pipette contained 100 μM glutamate. Fibers were voltage clamped to a potential of -110 mV with a conventional two-microelectrode clamp, and the patch pipette was placed between the recording and current-passing electrodes. Recording bandwidth was DC to 1 kHz. Inward current is shown as a downward deflection. $T = 22°C$; calibration, 100 or 40 msec and 20 pA. (From Cull-Candy *et al.*, 1981.)

current through the channel (Anwyl, 1977).

Glutamate receptors also occur on the extrajunctional membrane of locust muscle as two mixed, but pharmacologically distinct populations: one population gates an increase in Cl^- permeability (hyperpolarising or H-receptors); the second gates an increase in cation permeability (depolarising or D-receptors) (Lea & Usherwood, 1973; Cull-Candy & Usherwood, 1973).

Transmitter-receptor interaction is thought to cause the brief and transient opening of ionic channels. A number of techniques have been developed to obtain information about the operation of ionic channels associated with synaptic receptors. These include analysis of the membrane current noise that occurs in the prolonged presence of transmitter or agonist as a result of fluctuations in the number of open channels (Katz & Miledi, 1972; Anderson & Stevens, 1973). A second method is the patch clamp technique for measuring the currents passing through individual channels (Neher *et al*, 1978).

D-type receptors have proved to be particularly suitable for the application of patch-clamp analysis to individual receptor-chanel complexes for a number of reasons: 1. These receptors are present at low densities (Usherwood, 1981), so that recording from single receptor-channel complexes can routinely be obtained; 2. locust muscles are almost devoid of connective tissue, so that the muscles need not be pre-treated with enzymes (Patlak, *et al*, 1979); 3. the channels gated by D-receptors have large conductances (around 120pS) so that channel events with lifetimes as short as 100μ sec can be resolved with megohm seals (Patlak *et al*, 1979); 4. desensitisation of these receptors can be inhibited using the lectin, concanavalin A (Mathers & Usherwood, 1976, 1978 a); 5. the population density of the receptors can be modified through denervation (Usherwood, 1979; Mathers & Usherwood, 1978 b; Gration *et al*, 1979).

The values of channel conductance and mean lifetime obtained using patch-clamp (150pS and 2ms respectively, at 23°C) (Patlak *et al*, Cull-Candy *et al*, 1981) (fig. 29) were comparable to those obtained from the analysis of the membrane current noise (122 ± 0.4pS and 2.5 ± 0.13ms at 20°C; Anderson *et al*, 1978).

γ-aminobutyric acid (GABA) is the putative inhibitory transmitter at the locust neuromuscular junction. It activates locust, cockroach and grasshopper inhibitory nerve-muscle synapses and in most respects its mode of action at these sites is very similar to that of the natural transmitter, (Usherwood & Grundfest, 1965). GABA acts by increasing the permeability of the muscle fibre to Cl^-, leading to a hyperpolarisation of the muscle fibre membrane. GABA action on insect muscle fibres is reduced by picrotoxin at concentrations of 10^{-5}M (Usherwood & Grundfest, 1965) and by bicuculline at similar concentrations (Usherwood, unpublished, cited in Usherwood & Cull-Candy, 1975).

Current noise analysis gave a mean lifetime for junctional GABA-activated channels of around 4ms at 21°C, and a mean conductance of 22.6pS. Similar values of open time and conductance were obtained for extra junctional GABA-activated channels (Cull-Candy & Miledi, 1981).

In contrast to the situation in the locust, the ventrolateral body-wall muscles of cyclorrhaphan Diptera larvae have no inhibitory input, being innervated only by a single fast and a single slow excitatory axon (Hardie, 1976; Magazanik *et al*, 1979; Irving & Miller, 1980 a,b). The innervation of these muscles in *Calliphora erythrocephala* is shown in figure 30 a,b.

In *Musca domestica* larvae, L-glutamate was found to be a specific agonist at the fast transmitter receptor, and aspartate is a specific agonist at the slow transmitter receptor. (Irving & Miller, 1980 a). Fast and slow responses are believed to use different ionic channels, and it has been suggested that HCO_3^- affects the reversal potential of the slow excitatory post-synaptic potential (EPSP) by increasing the intracellular potassium concentration. The fast and slow EPSPs may therefore utilise channels whose conductances are differentially sensitive to intracellular K^+ concentration. (Irving & Miller,1980 b).

Other neurotransmitters

Acetylcholine (ACh) is a putative excitatory neurotransmitter at synapses in the insect central nervous system, but seems to play no part in neuromuscular transmission. The evidence for its transmitter action is summarised in several reviews (Pitman, 1971; Gerschenfeld, 1973; Callec,

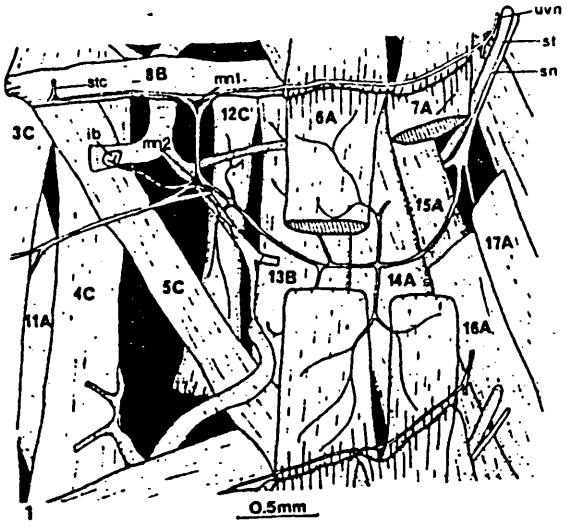


Fig. 30a The gross motor innervation of the longitudinal ventro-lateral muscles in an abdominal half segment. Muscle numbering according to CROSSLEY (1965). ib; imaginal bud, mn1; multipolar neurone 1, mn 2; multipolar neurone 2, sn; segmental nerve, st; segmental trachea, stc; strand of connective tissue, uvn; unpaired ventral nerve.

(From Hardie, 1976)

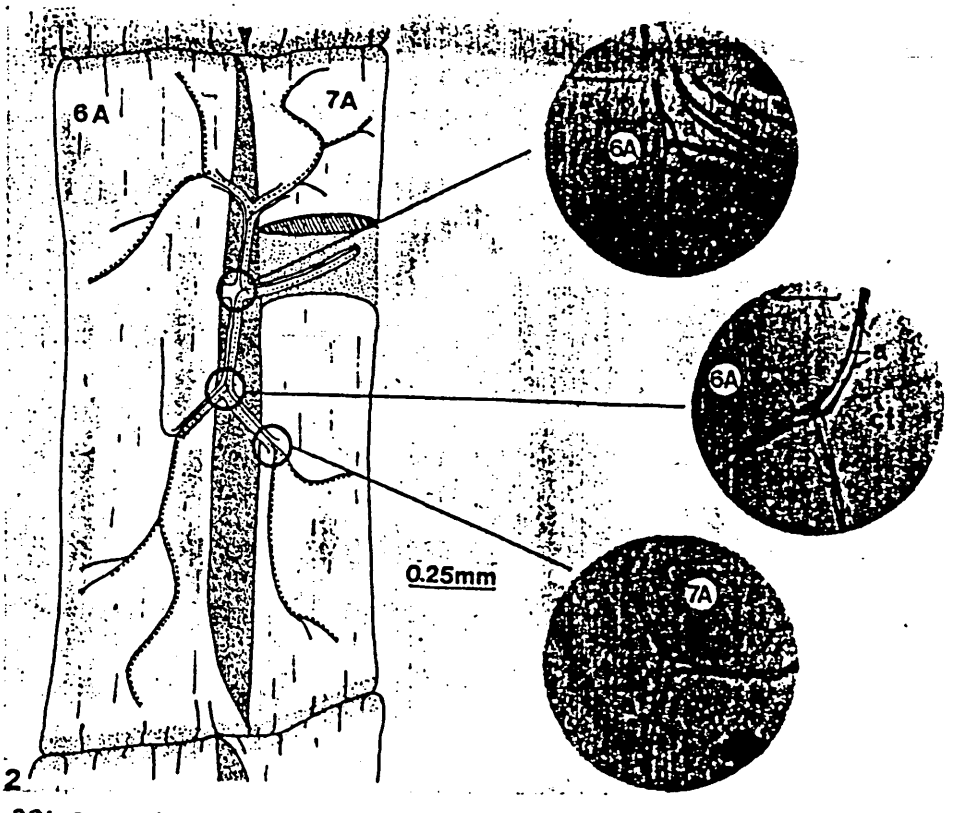


Fig. 30b Innervation of the longitudinal ventro-lateral muscles, 6A and 7A, at the axonal level. Diagramatic representation with photographic evidence from reduced silver stained preparations. Note the common branching of the axons. a, axon; ct, connective tissue; n, muscle nucleus. Scale = 20μm.

(From Hardie, 1976).

1974; Sattelle, 1977; Harrow *et al*, 1982). The CNS of several insect species have been shown to contain the essential components of a cholinergic system, including ACh, choline acetyltransferase (which catalyses the synthesis of ACh), and acetycholinesterase (which hydrolyses ACh and prevents further synaptic action). Insect nervous tissues have been shown to be capable of synthesizing ACh (Prescott *et al*, 1977) and certain insect central neurones are extremely sensitive to either locally- or bath-applied ACh when the endogenous acetycholin-esterase has been inhibited (Sattelle, 1980).

The evidence for a transmitter role for ACh is particularly strong in the antennal (olfactory) afferent input to the antennal lobes of the moth, *Manduca sexta* (Sanes & Hildebrand, 1976; Sanes *et al*, 1977), and in the cercal (mechanoreceptor) afferent input to the giant interganglionic interneurones of the abdominal ganglion of the cockroach, *Periplaneta americana* (Callec, 1974; Sattelle, 1980; Harrow & Sattelle, 1983).

The biogenic amine, octopamine, has been found to act as a neuromodulator in certain insects, modulating neuromuscular transmission and muscular contraction in skeletal muscle in insects. The most extensively studied preparation has been the large extensor tibae muscle of the hindleg of the locust, *Schistocerca americana gregaria* (Evans & O'Shea, 1977, 1978; O'Shea & Evans, 1979; Buchan & Evans, 1980; Evans & Siegler, 1982). This muscle is innervated by an octopamine-containing 'DUMETi' neurone (Hoyle, 1975; Hoyle & Barker, 1975; Evans & O'Shea, 1977, 1978) which inhibits a myogenic rhythm in the hindleg, modulates neuromuscular transmission and muscle contraction, and influences behaviour involving rapid movements eg. walking.

The pentapeptide proctolin is found in the central nervous system of a number of insect species (Starratt, 1979). In the cockroach, it is contained in bilaterally symmetrical neurones in all ganglia of the CNS (Bishop & O'Shea, 1982). Proctolin may behave as a neurotransmitter (Brown, 1975) and/or as a neuromodulator (Cook & Holman, 1979; O'Shea & Adams, 1981) to modulate muscle excitability. Both octopamine and proctolin have been found to mimic spontaneous membrane depolarisations in larvae of *Lucilia sericata* (Irving & Miller, 1980c.) This effect appears to be post-synaptic and mediated by receptors specific for each substance.

The Aims and Scope of the Present Study

This thesis reports an experimental investigation of the ionic bases of the resting membrane potentials of the body-wall muscle cells of larvae and prepupae of the blowfly *Calliphora erythrocephala* (Diptera) and larvae of *Chilo partellus* (Lepidoptera) the rice stem borer in a comparative approach. The aim of the present study has been to develop experimental methods in order to obtain direct, quantitative measurements of intracellular ionic activities from these muscle cells, and to monitor any changes in membrane potential and other properties corresponding to changes in the extracellular activities of the major inorganic ions. This was achieved in several stages:

1. The development of techniques for the manufacture of double-barrelled ion-sensitive microelectrodes for K^+, Na^+ and Cl^- which gave acceptable and reliable responses to the intracellular activity of the relevant ion.

2. The construction of a Faraday cage and assembly of a recording system suitable for intracellular recording from single muscle cells with both conventional microelectrodes and double-barrelled ion-sensitive microelectrodes. Refinement of the manufacturing technique for ISM's until they were capable of making reliable intracellular ionic activity measurements in practice.

3. Measurement of the intracellular activities of K^+, Na^+ and Cl^- in larval and prepupal body-wall muscle cells bathed in normal saline.

4. Performance of ionic substitution experiments to determine quantitatively the role of the major inorganic ions, particularly K^+, Na^+ and Cl^-, in resting membrane electrogenesis in *Calliphora* and *Chilo*.

CHAPTER II: MATERIALS AND METHODS

Apparatus was assembled to provide the following functions:-

1. A walk-in Faraday cage was erected around a heavy wooden bench to reduce to a minimum electrical noise and interference, and mechanical instability during experiments;
2. Manufacture of double-barrelled ion-sensitive microelectrodes (ISM's) with tip diameters 1.5 μm;
3. Calibration of ISM's for their response to ionic activity changes and general evaluation of their performance;
4. Intracellular recording with conventional microelectrodes (OM's) and ISM's from single body-wall muscle cells of insect larvae;
5. Amplification, visual display and recording on chart paper of the electrical signals produced by both ISM's and OM's;
6. Variation of the composition of the media bathing the muscle cells, allowing ionic activities to be changed and metabolic inhibitors to be applied;
7. Measurement of the membrane resistance of the impaled cells;
8. Localised application of brief pulses of a solution onto the surface of an impaled muscle cell from a broken micropipette by pressure.

II.1. Ion-sensitive microelectrodes

The manufacture of ion-sensitive microelectrodes (ISM's) involved the use of a number of procedures and devices which will be described in the following section.

1.i Method for production of double-barrelled glass micropipettes

Double barrelled ISM's were used to obtain simultaneous measurements of intracellular ionic activities and membrane potential from individual cells.

K^+-, Na^+- and a few Cl^--ISMs required electrolyte-filled reference barrels, whereas in the majority of Cl^--ISMs, the reference barrel needed to be filled with an organic reference liquid ion exchanger (RLIE, Thomas & Cohen, 1981). Use of RLIE overcame the problem of Cl^- leaking out of the reference barrel into a muscle cell and leading to artificially high values of intracellular Cl^- activity being recorded by the active barrel. It

was therefore necessary to employ two different methods for preparation of the double-barrelled micropipettes: One in which the reference barrel was not silanised, the other in which it was.

(a) Preparation of micropipettes with electrolyte-filled reference barrels

To make active barrels, borosilicate glass capillary tubes of 1.50mm O.D. (GC 150T-15 Clark Electromedical Instruments) were cut to give pieces 7.5cm in length. Twenty of these lengths were cleaned using a mixture of concentrated nitric acid (8 ml) and ethanol (2 ml), which reacted violently and thus removed any contaminants from the inner surfaces of the glass tubes. The tubes were washed ten times in distilled water and dried for one hour in an oven at 100°C.

After drying, these capillaries were paired with other capillaries which were to become the reference barrels. The latter were borosilicate glass capillary tubes with an internal filament to aid filling, an O.D. of 1.00mm and I.D. of 0.58mm (GC 100F-10, Clark Electromedical Instruments) which had been cut to produce 5 cm lengths. Active and reference barrels were glued together in parallel pairs using Araldite (CIBA-GEIGY) (fig. 31 A), and then baked at 100°C for 1 hour to polymerise the resin.

In order to ensure that when the capillaries were pulled into micropipettes, each would have a single 'combined' tip consisting of the two adjacent tips of the two barrels, each pair of tubes was twisted through 180° halfway along its length. In order to achieve this, the lower member of each pair was clamped at both ends in the chuck jaws of a vertical electrode puller (Narishige Scientific Instrument Lab. Type PE-2, Plate 1). The middle of the pair was positioned at the centre of a cylindrical heating coil with an I.D. of 6mm (fig. 31 B). The upper chuck of the puller was fixed by means of a clamping screw on the puller, and the lower chuck was held in place manually. After several seconds of heating, the glass softened and the lower chuck was rotated through 180° (fig. 31 C). The capillary pair was then stretched slightly in order to optimise the shape of the shank of the micropipettes when they were subsequently pulled (fig. 31 D). This was achieved by allowing the lower chuck to fall under gravity by around 2mm. The heat was then switched off and the capillary pair removed.

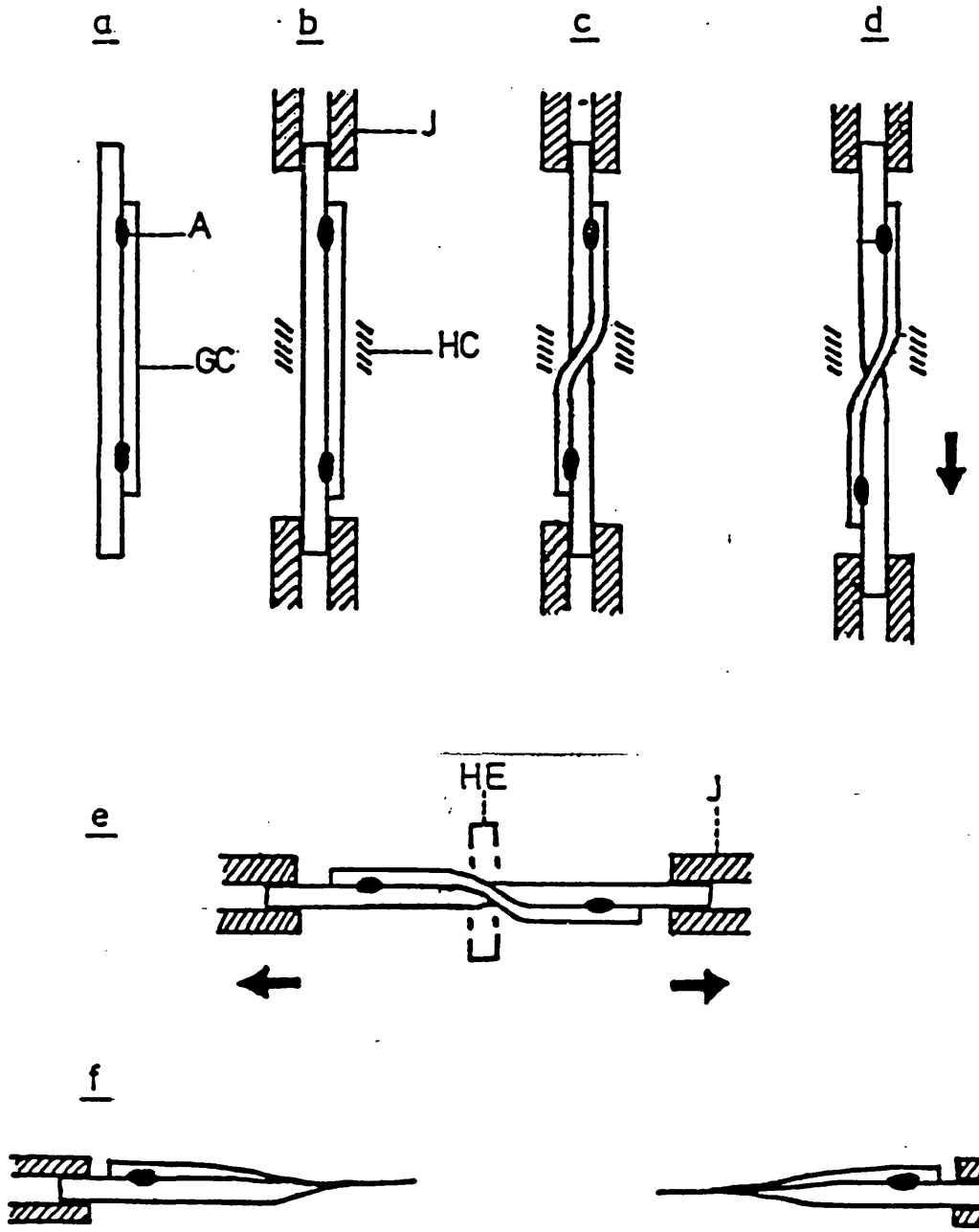


Fig. 31 a-f. Stages in the production of a double-barrelled micropipette from two separate glass capillary tubes. A - Araldite; GC - glass capillary; HC - heating coil; HE - heating element; J - chuck jaws of microelectrode puller. (From Laming, 1982)

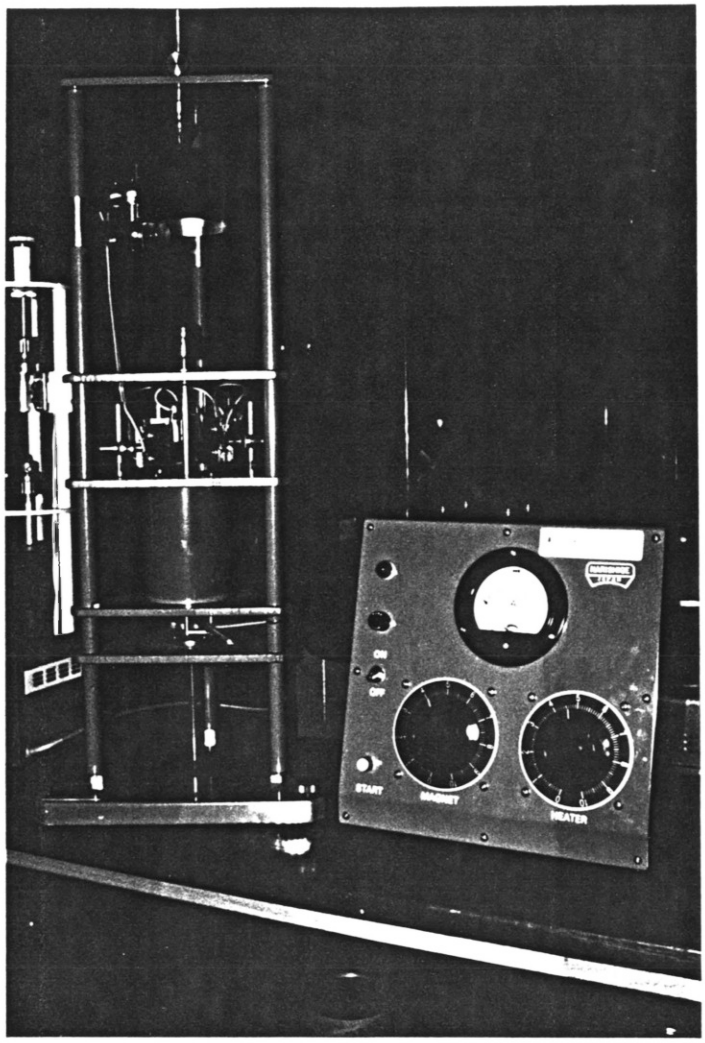


Plate 1. The Narishige vertical microelectrode puller.

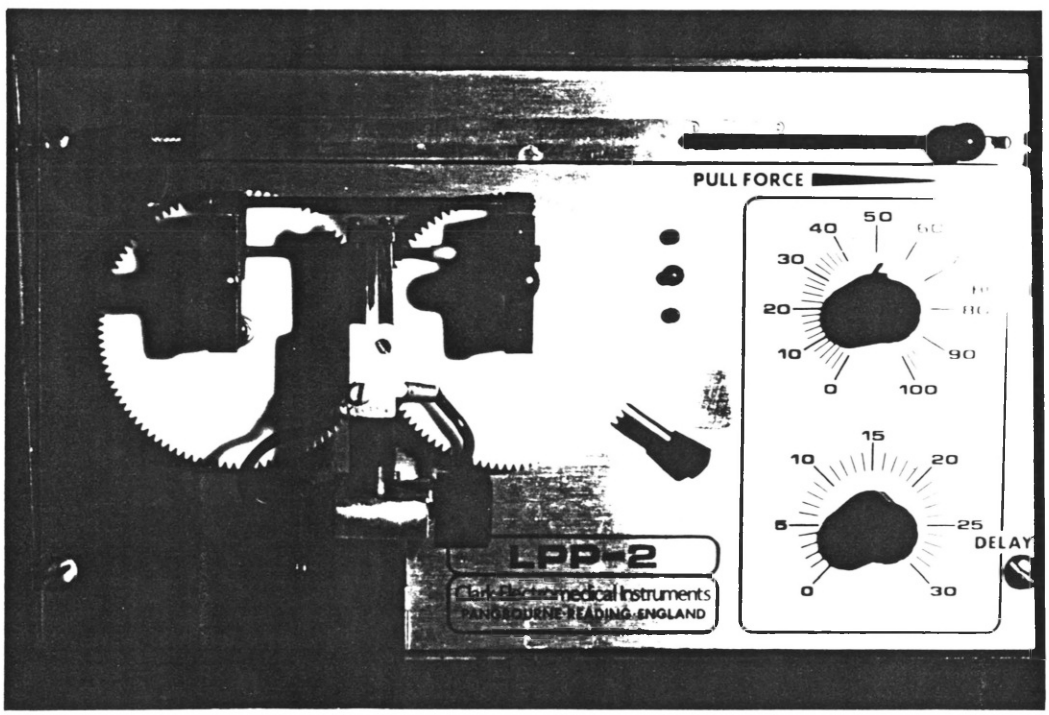


Plate 2. The Clark horizontal microelectrode puller.

The pulling of micropipettes from the capillary pair was performed by a Livingstone-type horizontal puller (Clark Electromedical Instruments, model LPP2, (Plate 2) which had controls for heating an element formed from a U-shaped strip of platinum, pulling force and time of delay before 'pull' was effected (after heating had started). This puller was used because it was found that the vertical puller could not produce double-barrelled micropipettes with sub-micron tips. To pull a pair of micropipettes from a twisted and stretched capillary pair, the latter was clamped at both ends in the jaws of the horizontal puller, so that the central twisted part of the double capillary was positioned centrally inside the heating element (fig. 31e). It was important that the glass was heated, as nearly as possible, symmetrically about the axis of the length of the capillaries so that when micropipettes were pulled they would have straight shanks terminating in fine tips (fig. 31f). Each micropipette was examined under a light microscope at x400 magnification to check that the shank was straight and tapered gently and that the tip was fine enough ($\leq$ 1·5μm in diameter). Several acceptable double-barrelled microelectrodes were also examined in the scanning electron microscope to confirm their shapes, dimensions etc. An example is shown in Plate 3. Microelectrodes with unacceptable features were discarded.

(b) Preparation of micropipettes for Cl^--ISM with RLIE-filled reference barrels

The method used was similar to that described in the preceeding section, except that the reference barrel was made from borosilicate glass capillary tubes with an O.D. of 1.50 mm and an I.D. of 1.05 mm (GC 150F, Clark Electromedical Instruments) which contained a glass fibre. Glass tubes for both active and reference barrels were cut into approximately 7.5 cm lengths and washed in the mixture of concentrated nitric acid and absolute ethanol described above. They were then dried and glued together in pairs. The twisting and pulling of these pairs of tubes was identical to that described above. When filling the two barrels, care was taken to ensure that solutions did not spill from the back of one barrel to the next and cause contamination.

II.1.ii. Silanisation of micropipettes

A clean glass surface is hydrophilic/organophobic, because it is covered

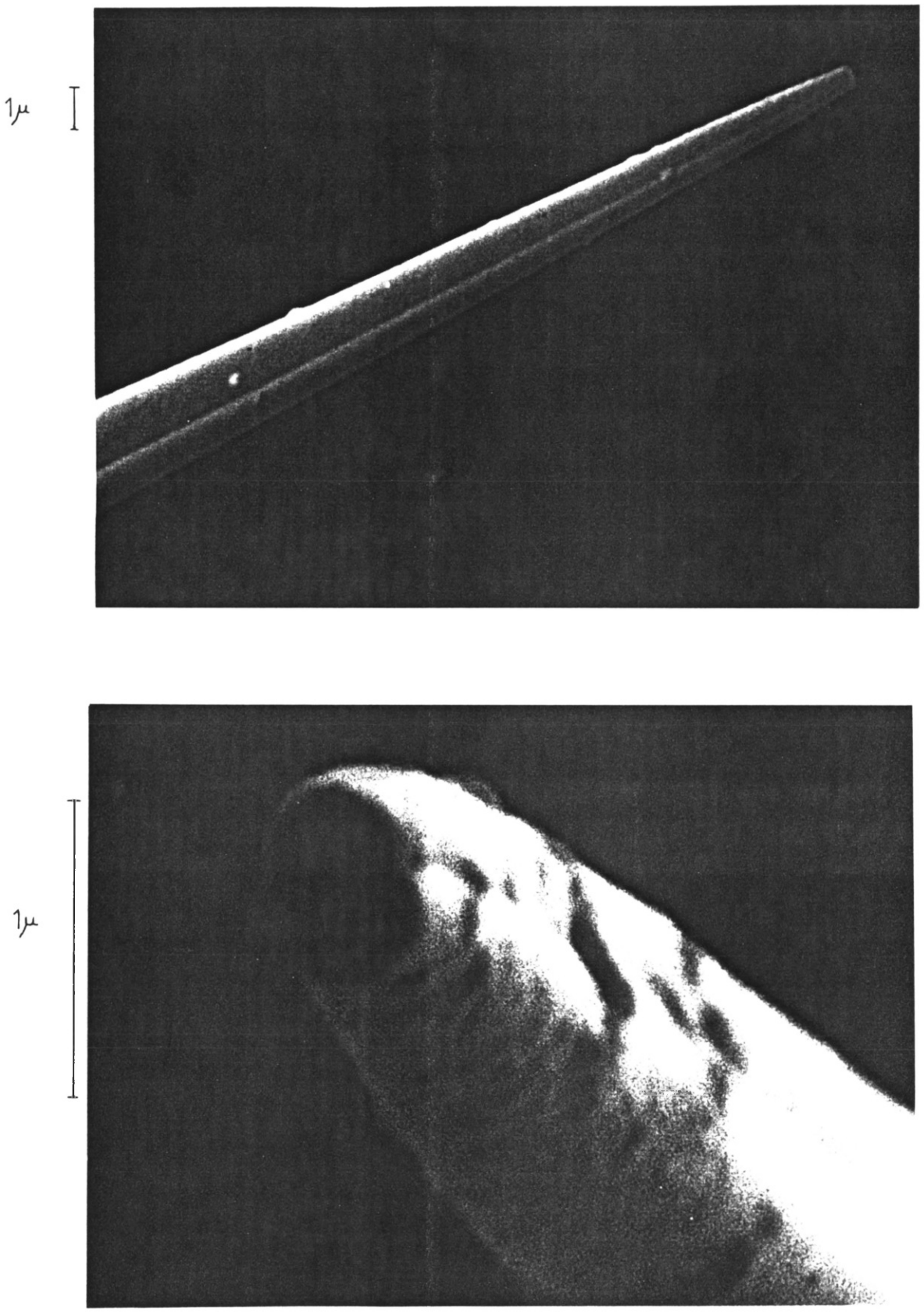


Plate 3. a, b. Scanning electron micrographs of the tip of a double-barrelled micropipette. Calibration bars show the size of the tip (<1μm diameter). (Dawson & Djamgoz, unpublished.)

with polar groups, primarily silanol (silicic acid) groups (Hair & Hertl, 1973). These groups must be masked by silanisation in order to render the surface hydrophobic/organophilic , and thus allow the formation of a stable organic liquid membrane. In addition, this treatment prevents the aqueous back-filling solution in the active barrel from creeping towards the tip of the ISM. If not masked, the silanol groups behave as cation exchangers, which under some conditions cause the micropipettes to behave as cation electrodes (Walker, 1971).

For ISMs requiring reference barrels filled with a salt solution (ie. K^+, Na^+ and some Cl^--ISMs), only the active barrel was silanised and precautions were taken to ensure that the reference barrels were not exposed to silane. For Cl^--ISMs in which the reference barrel was to be filled with organic RLIE, however, both barrels needed to be silanised.

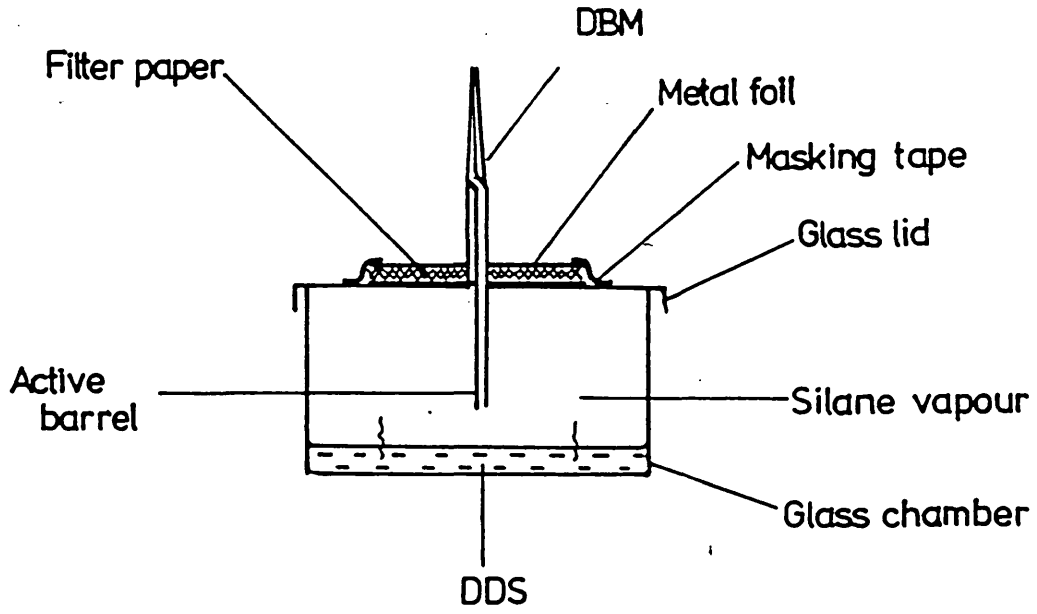
The procedure for silanisation was essentially similar for all types of micropipette, involving the exposure of inside surfaces to the vapour of an organic silicon compound.

Procedure used for silanisation of active barrels alone

Silane (dimethyldichlorosilane, DDS; Sigma) (2ml) was placed in a small glass jar in a fume cupboard. The jar was covered by a glass lid in the centre of which was a small hole with dimensions such that it accommodated the protruding back end of the active barrel of the double micropipette (fig. 32 A). Before silanisation of each batch of micropipettes, two small pieces of aluminium foil and two of filter paper were placed over the hole and secured using paper tape. A hole was then made through the foil and paper coincident with the hole in the lid, such that the protruding back end of a micropipette would fit tightly in the hole. This arrangement was designed to ensure that when the lid was placed onto the jar of silane and the shaft of a double micropipette introduced into the hole, the larger "active" barrel alone would be silanised by DDS vapour, whilst the smaller reference barrel was blocked and remained unsilanised.

The optimum silanisation times for K^+/Cl^-- and Na^+-ISMs were found to be 30 and 180 seconds respectively. ISMs silanised for shorter times than

a



b

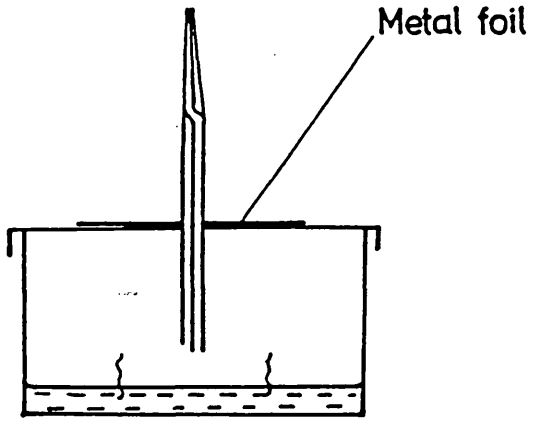


Fig. 32

a. Apparatus for silanising the active barrel of a double-barrelled micropipette (DBM) using dimethyldichlorosilane (DDS) vapour.
b. Apparatus for silanising both barrels of a double-barrelled micropipette using dimethyldichlorosilane vapour.

these had a tendency to show the symptoms of under-silanisation, ie. poor calibration curves with low slopes, and instability of behaviour; whilst those silanised for much longer tended to have blocked active and reference barrels (silane was thought to "spill" out of the tip of the active barrel and enter the tip of the reference barrel, thus preventing proper conduction).

Following silanisation, the batch of micropipettes, held vertically in a metal holder, was placed into an oven at 100°C for one hour. It was then stored in a desiccator until needed.

Procedure for silanisation of both active and reference barrels

The major difference between this and the procedure described above was that the hole in the lid of the silanisation chamber was made sufficiently large to accommodate both barrels of the double micropipette (figure 32 b). Thus, both active and reference barrels were silanised simultaneously using DDS. The optimum silanisation time was found to be around 30 seconds for Cl^-ISMs.

II.1.iii Filling the micropipettes

The filamented reference barrel was first filled with the appropriate compound to constitute the reference electrode. The compounds used are summarised in table 7, below.

Table 7. Compounds used to fill the reference barrels of ISMs.

Types of ISM	Reference barrel filling compound(s)
K^+	5M LiCl
Na^+	1M KCl
Cl^-	85% 0.6M K_2SO_4 +15% 1.5M KCl or RLIE

The reasons for filling the reference barrel before the active barrel are twofold. 1) In order to avoid filling the active barrel (a relatively complex process) only to discover that the reference barrel had not filled

properly and would therefore not conduct; 2) the presence of electrolyte in the reference barrel tip prevented the ion-sensor from the tip of the active barrel from crossing into the empty reference barrel tip and making the latter ion-sensitive when filled. The reference barrel was filled using a 30g syringe needle and a 1 ml syringe. The tubular fibre inside this barrel enabled it to fill with electrolyte up to the very tip so that it made a good conducting electrode.

In the case of Cl^--ISMs whose reference barrels were to be filled with the organic reference liquid ion exchanger (RLIE) a column only a few millimetres long was introduced into the reference barrel, and left for several hours or overnight to allow the barrel to fill. This was necessary because the RLIE is viscous in nature and hence takes longer to move to the tip than aqueous solutions.

In order to fill the active barrel, the double-barrelled micropipette (DBM) was clamped in a crocodile clip, the jaws of which had been shaped and filled with dental wax so as to optimally hold the DBM. This modified clip was in turn held on an arm on the right-hand side of a pair of Prior micromanipulators mounted on an optical bench (MM1, fig. 33a such that the shank and tip of the DBM could be viewed by a horizontal binocular microscope (fig. 33b Plate 4). The DBM tip was viewed using a x20 objective when its size was being checked immediately after the micropipette had been pulled. A x3, and sometimes a x10, objective was used to view the DBM shank when it was being filled.

The filling of the active barrel proceeded in a number of steps:

1. A 100mm long, 0.8mm OD micropipette with a broken tip was waxed onto a fine hypodermic needle, which was attached to the body of a 1 ml disposable syringe. This was in turn connected to a 50 ml syringe via a short length of plastic tubing. This whole assembly was held upright in one of the left-hand micromanipulators (MM2, fig. 33b) above the DBM held on the right-hand side. The tip of this broken micropipette was dipped into the pool of LIX in a small vial held by MM3 (fig. 33b) and a small quantity was sucked in. The 'electrode' was then lowered as far down as possible into the active barrel of the DBM under visual control, and a small drop of LIX was injected out by pressurising the syringe (fig. 33 a). The injection micropipette was then removed from the inside of the active barrel.

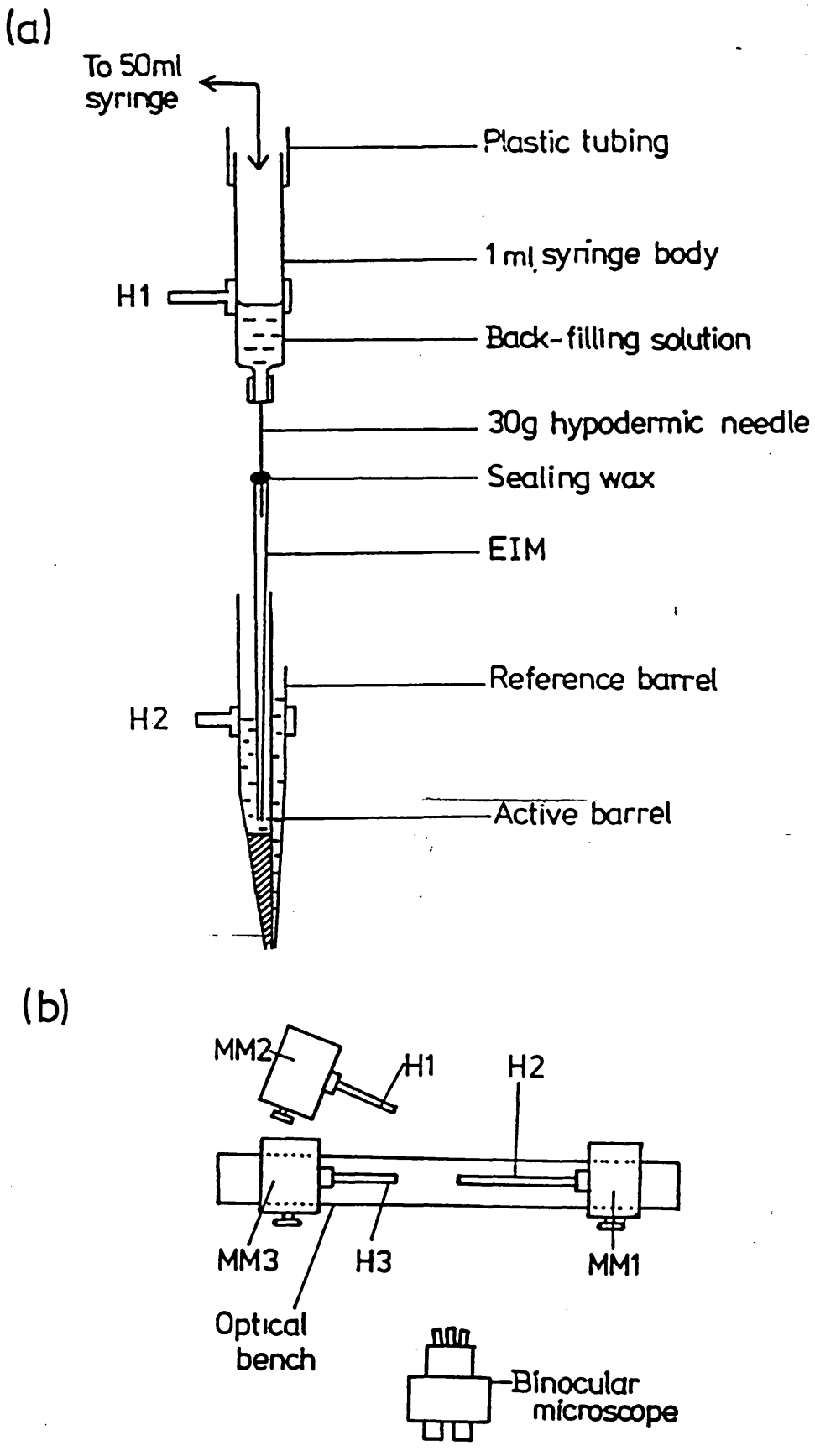


Fig. 33 Apparatus for filling the active barrel of an ISM.
a. Apparatus for back-filling the active barrel. H1 and H2 represent holders; EIM, the electrolyte-injection micropipette.
b. Plan view of apparatus used to fill the active barrel of an ISM; MM1, 2 and 3 represent micromanipulators; H1, 2 and 3 represent holders.

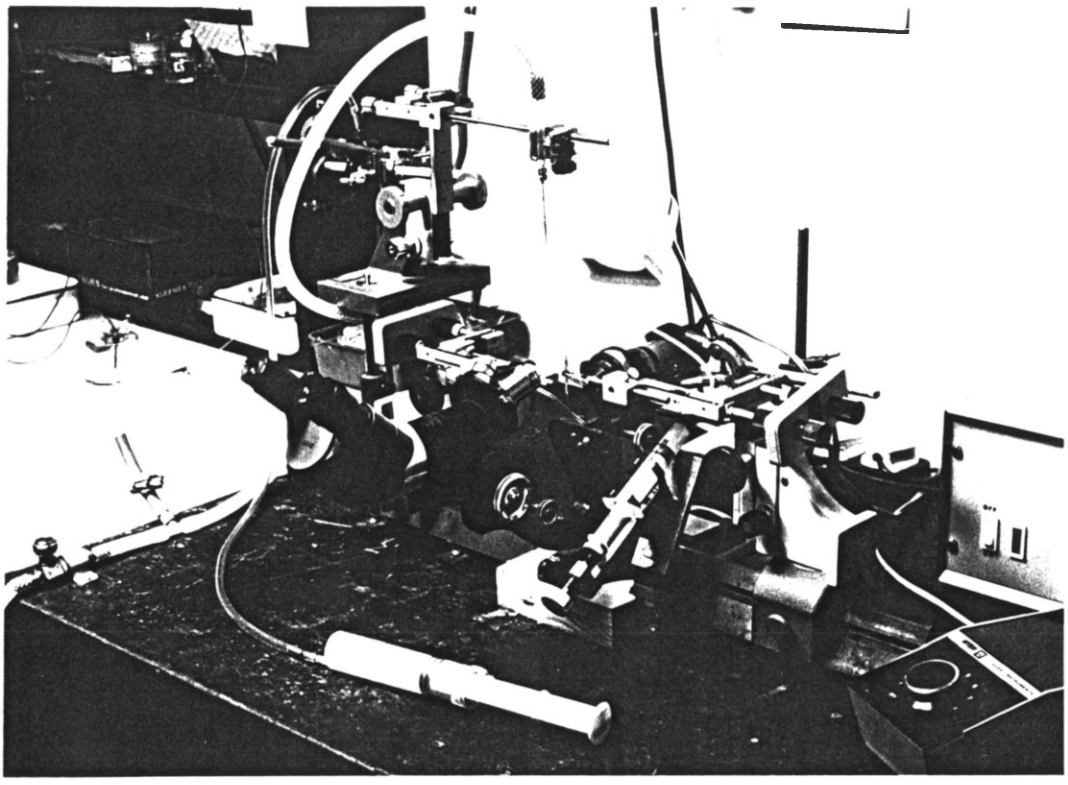


Plate 4. Apparatus for filling double-barrelled microelectrodes by injection of ion sensor and electrolyte. Compare with fig. 33 a, b to discern the various parts of this apparatus.

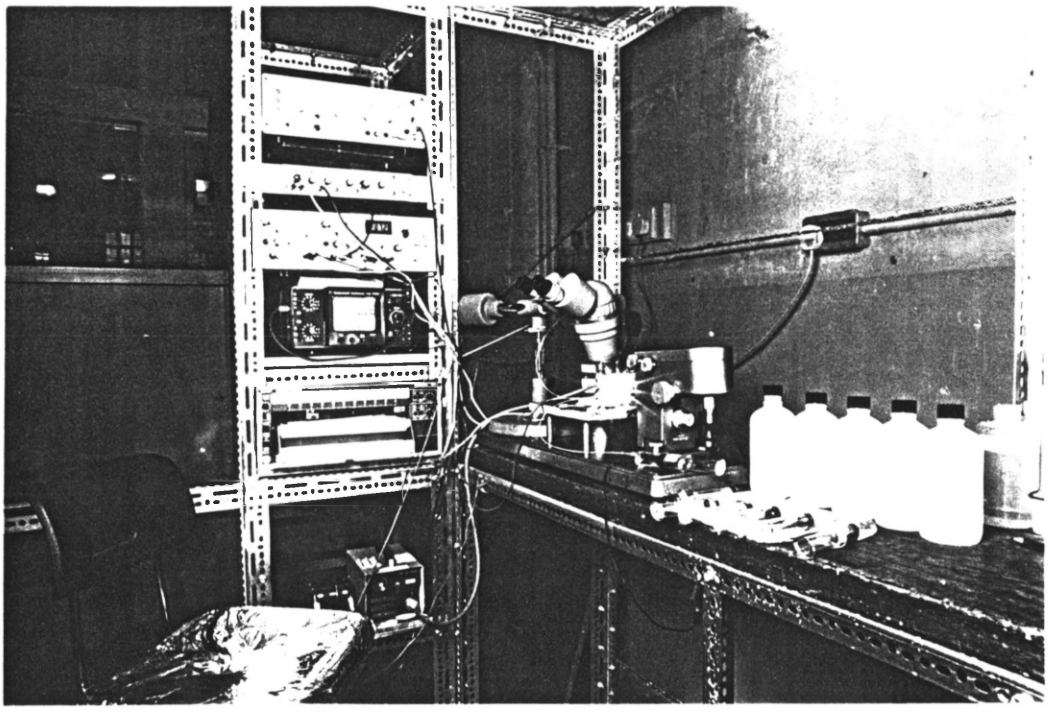


Plate 5. Position of equipment inside the Faraday cage (compare with fig. 44).

2. A tightly fitting plastic tube was attached to the back end of the active barrel, and pressure exerted from another 50 ml syringe to force the drop of LIX to the tip of the electrode. Sometimes such pressure was sufficient to move the LIX a short distance, after which it continued to move towards the tip by capillary action. By this means a few 100s μm - few mms of the tip of the active barrel was filled by a column of LIX.

3. Bevelling If the LIX did not move into the tip on its own or by pressure applied from the 50 ml syringe, the DBM was taken out of the apparatus and its tip bevelled slightly. For this a 'slurry beveller' of the type described by Lederer *et al*, (1979) was used. The bevelling medium consisted of about 10 ml of a mixture of (0.05μm diameter) Al_2O_3 powder (20% by volume) in distilled water. This was kept in a plastic petri dish of 10 cm diameter placed on a 5 mm thick circular perspex plate that was attached to the shaft of a mains-driven clock-motor. The slurry medium was thereby rotated at 10 RPM, and the microelectrode, held in a clip and holder, was lowered by a Prior micromanipulator, under visual control, until its tip just touched the thick sediment (fig. 34 a,b). The tip of the DBM was thus bevelled for a few seconds and then it was transferred to the microscope system to view its shank. Further application of back pressure usually moved the LIX to the tip; otherwise that DBM was discarded.

Back-filling the active barrel. The active barrel was back-filled with electrolyte from the upper meniscus of the ion sensor column to the top of the shaft using a second broken glass micropipette waxed to a hypodermic needle. The latter was attached to the 1 ml syringe body previously used for introduction of ion sensor (fig. 33a). The electrolyte was injected into the active barrel under pressure provided by the 50 ml syringe. The electrolytes used for back-filling are summarised in the following table:

Table 8. Compounds used to back-fill the active barrels of ISMs.

ISM type	Back-filling solution
K^+	0.5M KCl
Na^+	0.5M NaCl
Cl^-	0.5M NaCl

a

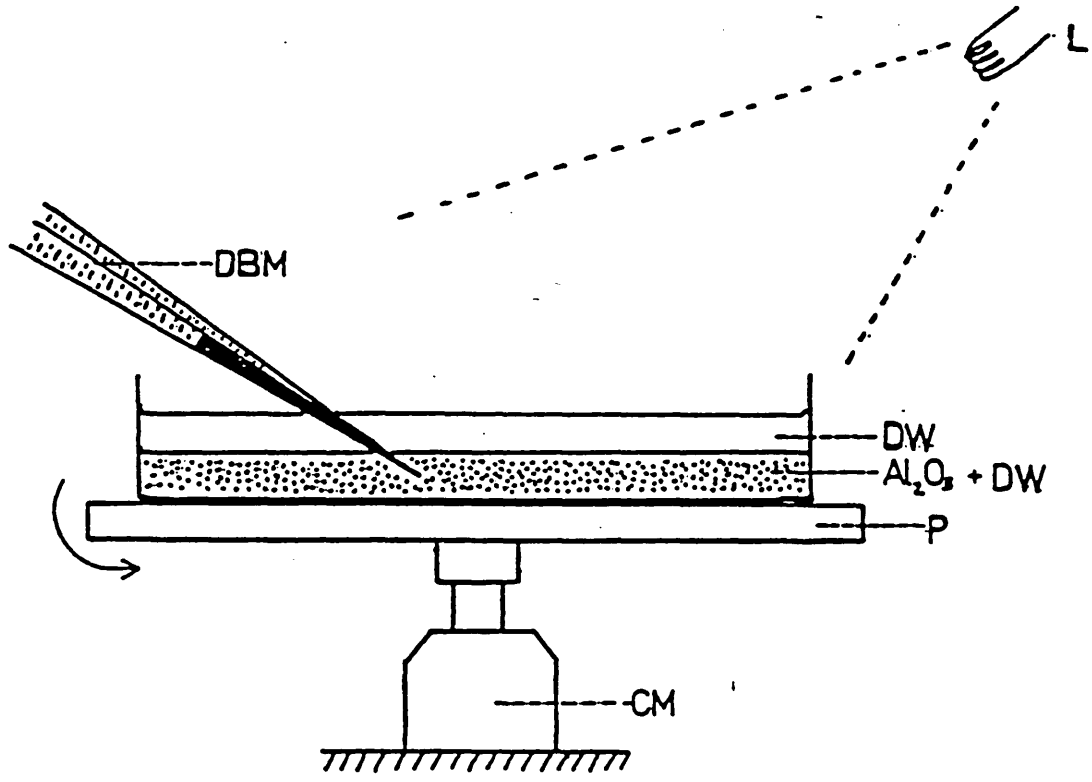
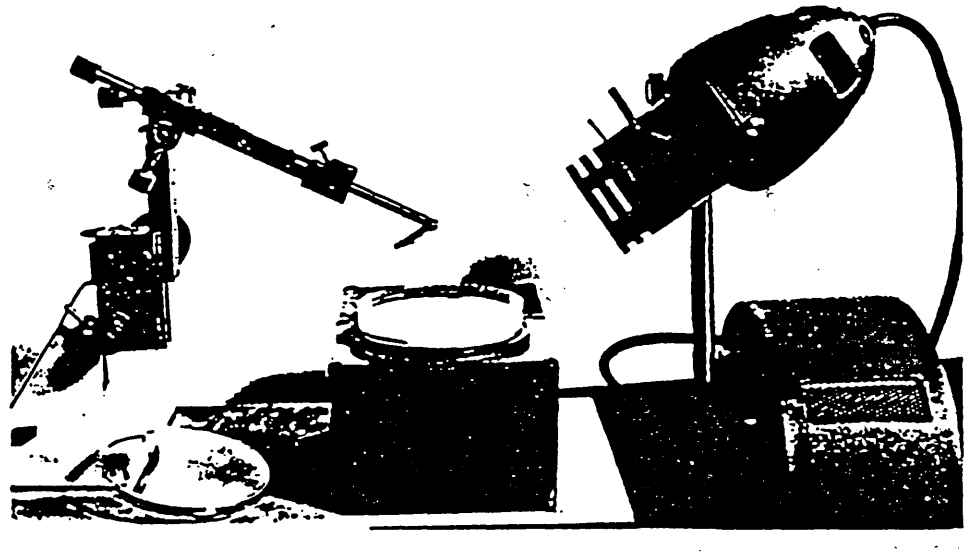


Fig. 34 a: diagram of; b: photograph of bevelling apparatus. DBM: double-barrelled micropipette; L: light; DW: distilled water; Al_2O_3: very fine particles of aluminium oxide; P: perspex plate; CM: clock motor.

(From Laming, 1982)

b



The electrolyte injection micropipette (EIM) was held in a micromanipulator (MM2, fig. 33b) and lowered into the active barrel until its tip was visible under the microscope inside the widest part of the shank. The micropipette was then slowly raised until the tip of the EIM was just above the upper meniscus of the ion sensor. Pressure was then applied using the 50 ml syringe, causing injection of the electrolyte and formation of a junction with the ion-sensor column. As the electrolyte filled the shank, the double-micropipette was lowered, keeping the EIM tip just below the upper meniscus of the electrolyte, thus preventing the formation of air bubbles. When the electrolyte column had passed the widest part of the shank, the EIM was withdrawn and the remainder of the shaft filled using an electrolyte-filled 1 ml syringe and 30 g needle. Thus, a continuous column of electrolyte was produced from the junction with the column of ion-sensor to the top of the shaft. Fig. 35 summarises the composition of each type of ISM used.

II.1.iv. Provision for Electrical Connection

Chlorided silver wires were used to make electrical contact with both active and reference barrels of the ISM. The reversible reaction between Cl^- ions in the electrolyte and in the solid AgCl coating on the silver wire reduces the junction potential between the wire and the solution to a negligible minimum and produces a stable potential. Some 2-3 cm each of a pair of 6 cm long silver wires were chlorided electrolytically in a 0.2M NaCl solution.

The silver wires constituted the anode and a carbon rod, the cathode, whilst a DC current was supplied by a stimulator (Model SD9, Grass Instruments). In order to provide a uniform coating of AgCl on the ends of the wires, a current of 2 mA was passed for 2 minutes. One wire was then introduced into the active, one into the reference barrel of the ISM, the AgCl coated ends making contact with the electrolyte solutions. Sealing wax was then applied to the end of each barrel, serving both to secure the wires and to prevent evaporation from the electrolyte solutions. The free ends of the wires were then soldered onto miniature metal pins which were connected to the electrometer probes.

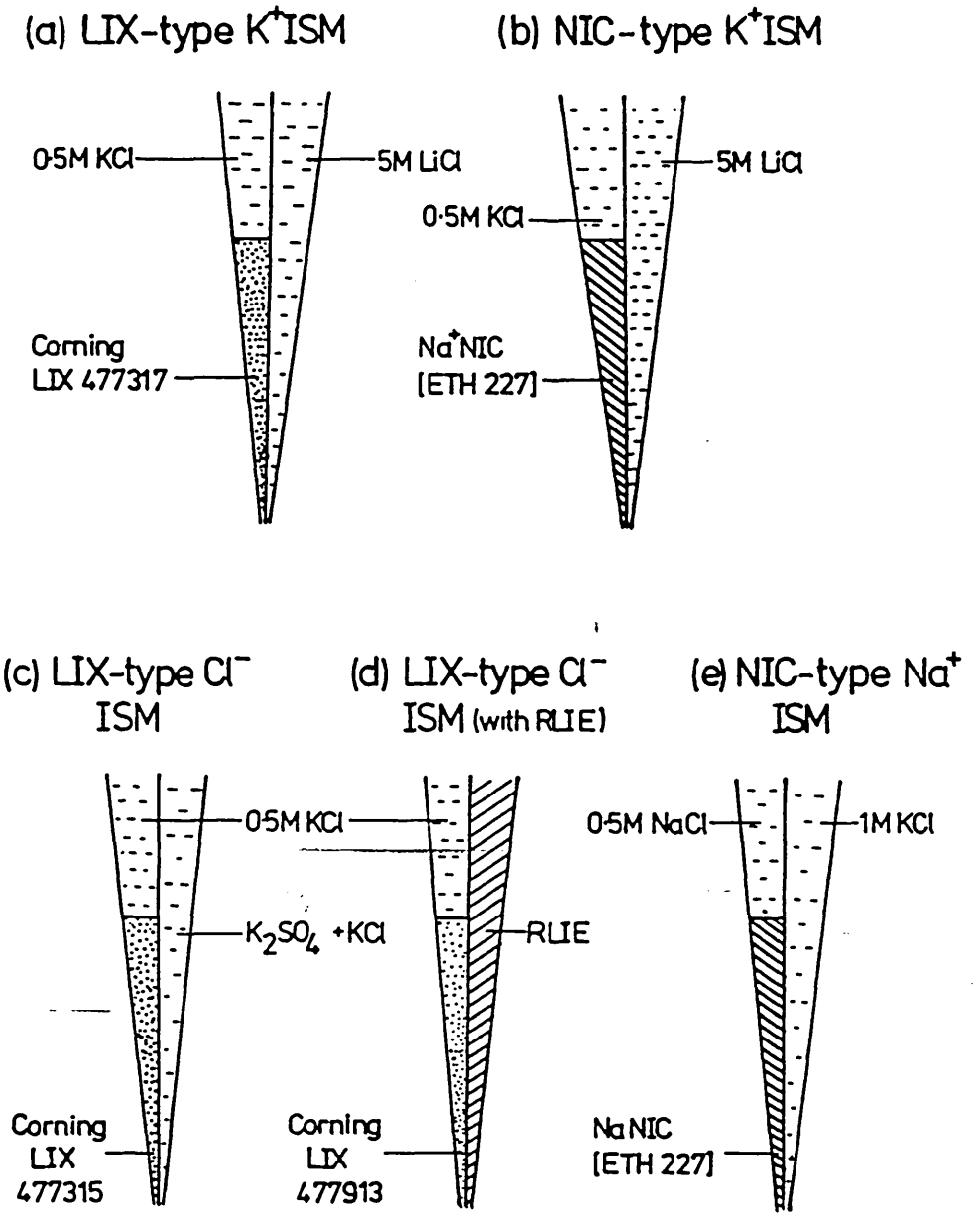


Fig. 35 Summary diagram of the composition of the types of ISM used in this study. LIX: liquid ion-exchanger; NIC: neutral ion carrier; RLIE: reference liquid ion-exchanger.

II.1.v. Recording circuitry

As previously stated, the electrical potential generated across the ion-sensitive membrane at the tip of the ISM comprises the sum of two parts:

$$V_{ISM} = V_{ION} + V_{REF}$$

where V_{ION} is a potential which depends on the activity of the ion to which the ISM is sensitive, and V_{REF} is a local potential that is recorded by the reference barrel.

The inclusion of a dual-differential electrometer in the recording circuit (fig. 36) permits the subtraction of V_{REF} from V_{ISM} to give V_{ION}. This is recorded by one channel of a chart recorder and is then referred to the calibration curve for the ISM to give the intracellular activity of the ion being monitored. V_{REF} is recorded by the second channel of the chart recorder, and monitors the membrane potentials of impaled cells.

The full electronic equipment (Plates 5, 6) consisted of:

1. A dual-differential electrometer (WPI Model FD 223) whose probes ('head amplifiers') were connected to the ISM via metal pin connectors. The active barrel of the ISM was connected to channel A and the reference barrel to channel B. Thus, the output of the B channel monitored the membrane potential of individual cells, whilst the differential output A-B represented the response of the ISM to ionic activity changes. The above circuit is given in fig. 9.
The manufacturers' specifications for the electrometer were as follows:
(i) Input impedance = $10^{15}\Omega$
(ii) Input capacitance = 1.0pF
(iii) Input leakage current = 10^{-14} A maximum
(iv) Response time = 0.5μ sec 10-90%.

2. A 2-channel chart recorder (W + W, model 314) for monitoring outputs A-B and B from the electrometer

3. A unity gain, high input impedance 'amplifier' (WPI, model M701).

4. A 2-beam oscilloscope (Telequipment, type D1010) connected to the

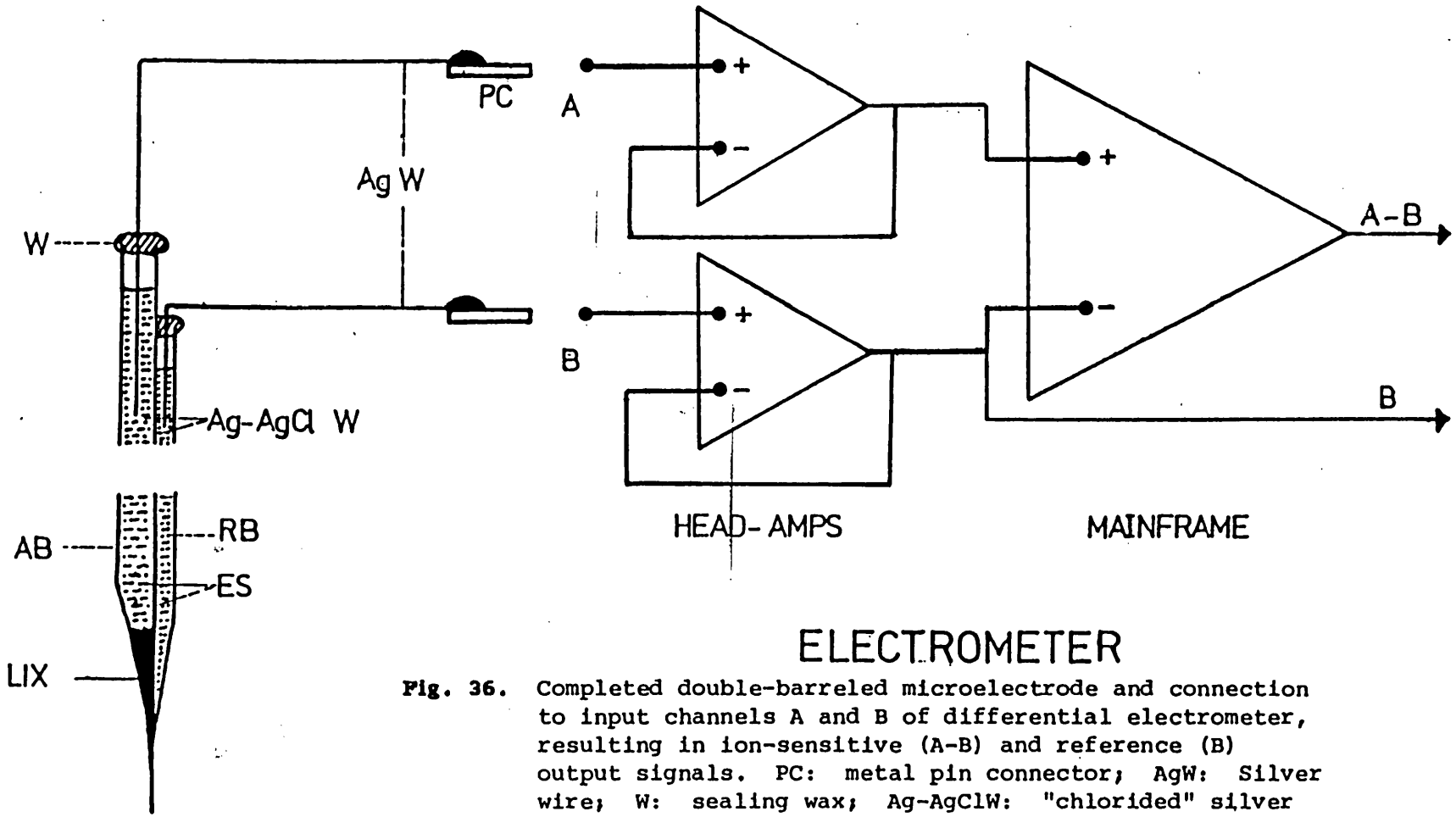


Fig. 36. Completed double-barreled microelectrode and connection to input channels A and B of differential electrometer, resulting in ion-sensitive (A-B) and reference (B) output signals. PC: metal pin connector; AgW: Silver wire; W: sealing wax; Ag-AgClW: "chlorided" silver wire; RB: reference barrel; AB: active barrel; ES: electrolyte solutions; LIX: liquid ion-exchanger.

(From Laming, 1982).

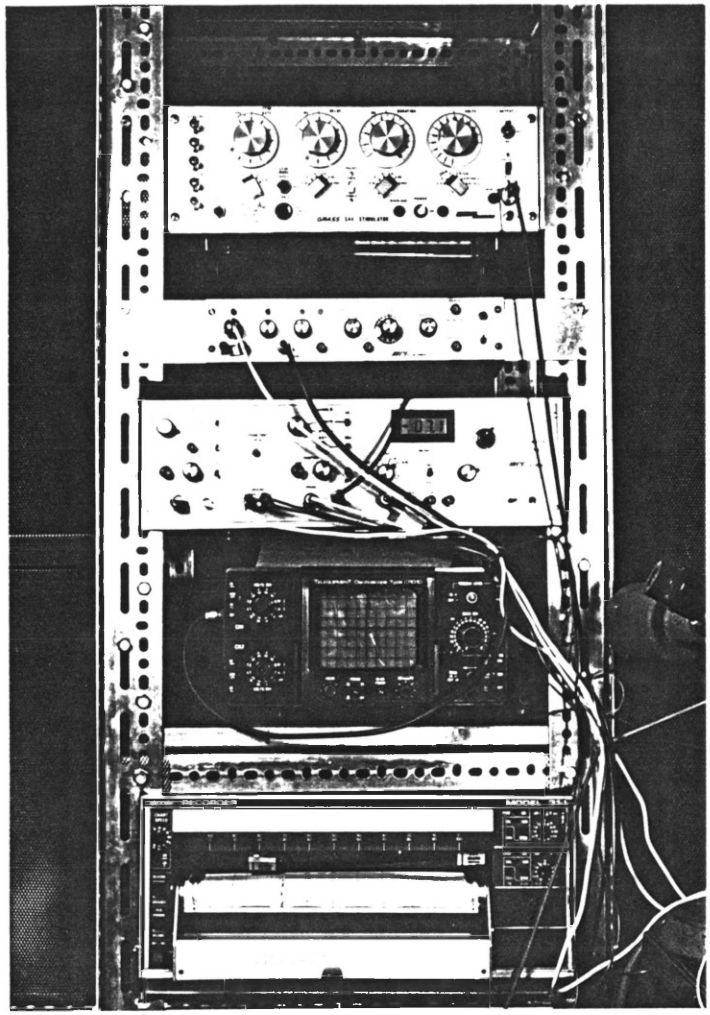


Plate 6. Photograph showing the electronic equipment: stimulator, amplifier, electrometer, oscilloscope and chart recorder (see text).

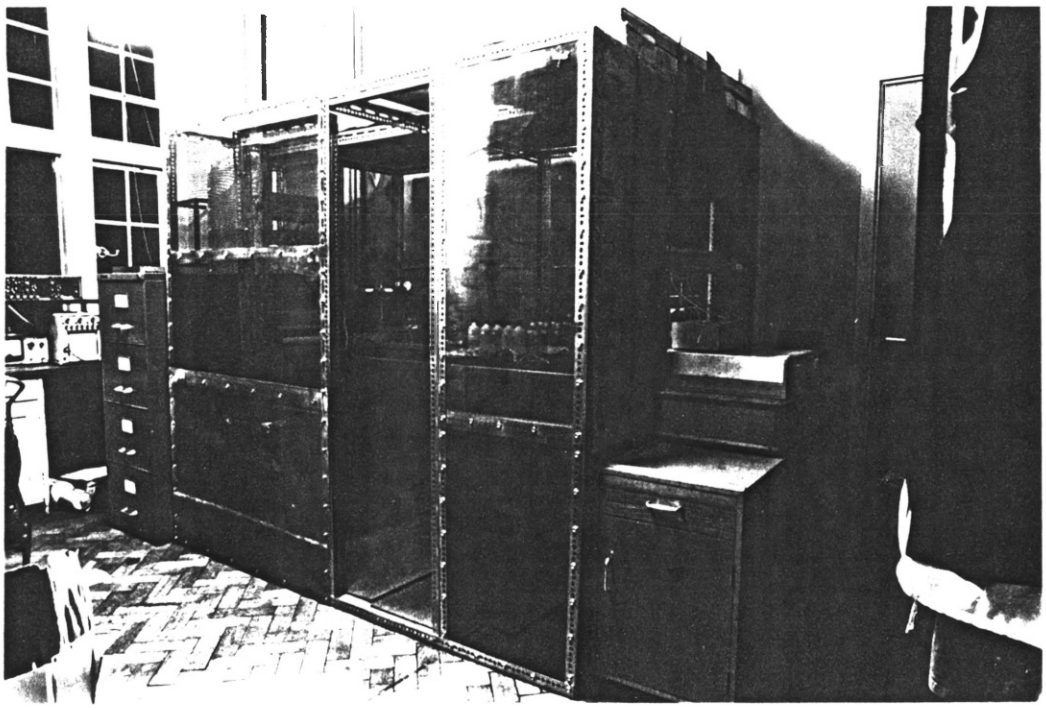


Plate 7. Photograph showing the Faraday cage, constructed from copper mesh and a Dexion framework for this study.

amplifier, used to measure reference barrel resistance.

5. A Grass (S44) stimulator.

The 'earth' connection in the mains plug of each instrument was disconnected, and each device was earthed on its panel by connecting its chassis to an aluminium common earthing bar at the back of the Faraday cage. This 'bus' bar was in turn connected to the mains earth via a plug, thereby ensuring that no earth loops were created.

II.1.vi. Calibration of ISMs

In order to calibrate ISMs, a calibrating chamber was constructed from perspex, into which solutions of varying ionic composition could be passed and quickly changed. The ISM tip was introduced into this chamber from above (fig. 37). The outlet of the chamber was connected to a vacuum pump via fine polythene tubing and a 0.5 l glass bottle which acted as a vacuum chamber to collect 'used' solution. Solutions whose compositions are given in appendices 3, 4 and 5 were passed into the chamber from a set of 20 ml syringes. The calibrating chamber was placed in the XY controls on the platform and the ISM held tightly in a modified crocodile clip on the end of a brass rod, clamped in the micromanipulator. Electrometer probes were mounted at the back of the platform. Before calibrating an ISM, the tip resistances of the two barrels were measured using the constant current supply ('electrode test') switches on the electrometer. Deflection of either of the two switches passed a constant 1 pA current across the corresponding electrode thereby causing a voltage deflection at the output of 1 mV per 1000 MΩ. If the resistance measurements showed that the ISM conducted well in both barrels with stable potential readings, then the ISM was calibrated. The ranges of resistances of the two barrels of each type of ISM used are given in table 9, below. The left-hand column gives the resistances of the active barrels (R_A) and the right-hand, the resistances of the reference barrels (R_R).

Table 9. Ranges of resistances of the active (R_A) and reference (R_R) barrels of the different types of ISM.(K=1000)

Type of ISM	R_A (MΩ)	R_R (MΩ)
K^+ LIX	8 - 94 K	50 - 150
K^+ NIC	26 - 160 K	75 - 200
Cl^- LIX (KCl/K_2SO_4)	21 - 88 K	75 - 150
Cl^- LIX (RLIE)	10 - 58 K	10 - 54 K
Na^+ NIC	62 - 154 K	100 - 200

The calibrating solutions for K^+ and Cl^- ISMs were based on Rice's and Weever's salines for *Calliphora* and *Chilo* respectively (Appendices 3 & 4). Those for K^+ ISMs used Na^+ to substitute for K^+, giving a range of K^+ activities for *Calliphora* experiments of between 0.97 and 97.2 mM, and for *Chilo* experiments of between 0.72 and 43.2 mM. Cl^--ISM calibrating solutions used gluconate to substitute for Cl^-, giving Cl^- activities between 18.2 and 137 mM for *Calliphora* experiments, and between 0.68 and 67.7 mM for *Chilo* ones. The use of gluconate necessitated the addition of extra Ca^{2+} to the calibrating solutions to compensate for sequestering of Ca^{2+} by gluconate (Kenyon & Gibbons, 1977; Vaughan-Jones 1979) . All K^+- and Cl^--ISM calibrating solutions were of constant ionic strength, with the result that the activity coefficient for the primary ion was constant throughout each series, at 0.72 (CRC Handbook of Chemistry & Physics, 52nd Edition).

Na^+ ISMs were found to calibrate very poorly in Ringer-based solutions, because the latter contained high Ca^{2+} concentrations which interfered significantly with the Na^+ neutral ion carrier (Steiner *et al*, 1979).

A series of solutions was therefore constructed in which sodium activity was varied against a constant ionic background which was based on the measured intracellular K^+ activity for each insect (115 mM for *Calliphora*, 60 mM for *Chilo*) in addition to a more realistic level of intracellular Ca^{2+} (0.01 mM), and a small amount of $MgCl_2$ (2.8 mM) and buffer (HEPES, 2.8 mM) (Bers & Ellis, 1981. see Appendix 5). Na^+ activities were thus varied between 1 and 99.3 mM for *Calliphora*, and between 1.1 and 101.5 for *Chilo* experiments. Na^+-ISMs were found to calibrate satisfactorily in these solutions. Unlike the calibrating solutions for K^+ and Cl^--ISMs, the above series of solutions was not of constant ionic strength. The activity coefficient for Na^+ was therefore not constant throughout the series, and variations in the value of

the activity coefficient are reflected in the calculated Na^+ activity in each solution (Appendix 5).

In order to calibrate the ISM, solutions were passed through the calibrating chamber, usually in order of decreasing activity of the primary ion. The solution in the calibrating chamber was 'earthed' by a glass capillary containing agar-Ringer (Appendix 1) and an Ag-AgCl contact connected to the chassis-earth of the electrometer (fig. 37). (This 'floating earth' system was devised so that the same 'earth' could be used both during the calibration of ISMs and to earth solutions in the recording chamber during experiments. Thus potential readings from an ISM during an experiment could be reliably referred to the ISM calibration recorded on the chart paper).

5 ml of each solution was passed through the chamber by injection from a 20 ml syringe, whilst the excess solution was removed in a controlled manner using the vacuum system (fig. 37). The last ~ 1 ml of each solution was left in the chamber and the ISM's response to that solution was recorded on chart paper. The responses of both barrels (channels A-B and B) were recorded simultaneously (fig. 36). This procedure was then repeated to ensure that the response of the ISM was stable and consistent before an experiment was carried out. After the experiment, the ISM was re-calibrated in order to check that no significant changes in the calibration had occurred during the course of the experiment (see Criteria for Selection of Results, section II.5).

The calibration traces on the chart recording were converted to calibration curves on log-linear graph paper. Activities were derived from concentrations of the primary ion in the solutions by means of standard activity coeficients, as previously described.

For the calibration curves of K^+- and Cl^--ISMs, the potential level given by the ISM when in Normal Ringer was defined as zero potential. For Na^+ ISMs, the potential level in the solution containing the highest concentration of Na^+ was defined as zero. Examples of the calibrations of ISMs showing the raw data from the chart recorder and the corresponding calibration curves are given in figure 38a, b for a LIX-type K^+ ISM, figure 39 a, b for a NIC-type ISM, figure 40 a,b, for a Cl^--ISM with the reference barrel filled with K_2SO_4 and KCl, figure 41 a,b, for a Cl^--ISM with the reference barrel

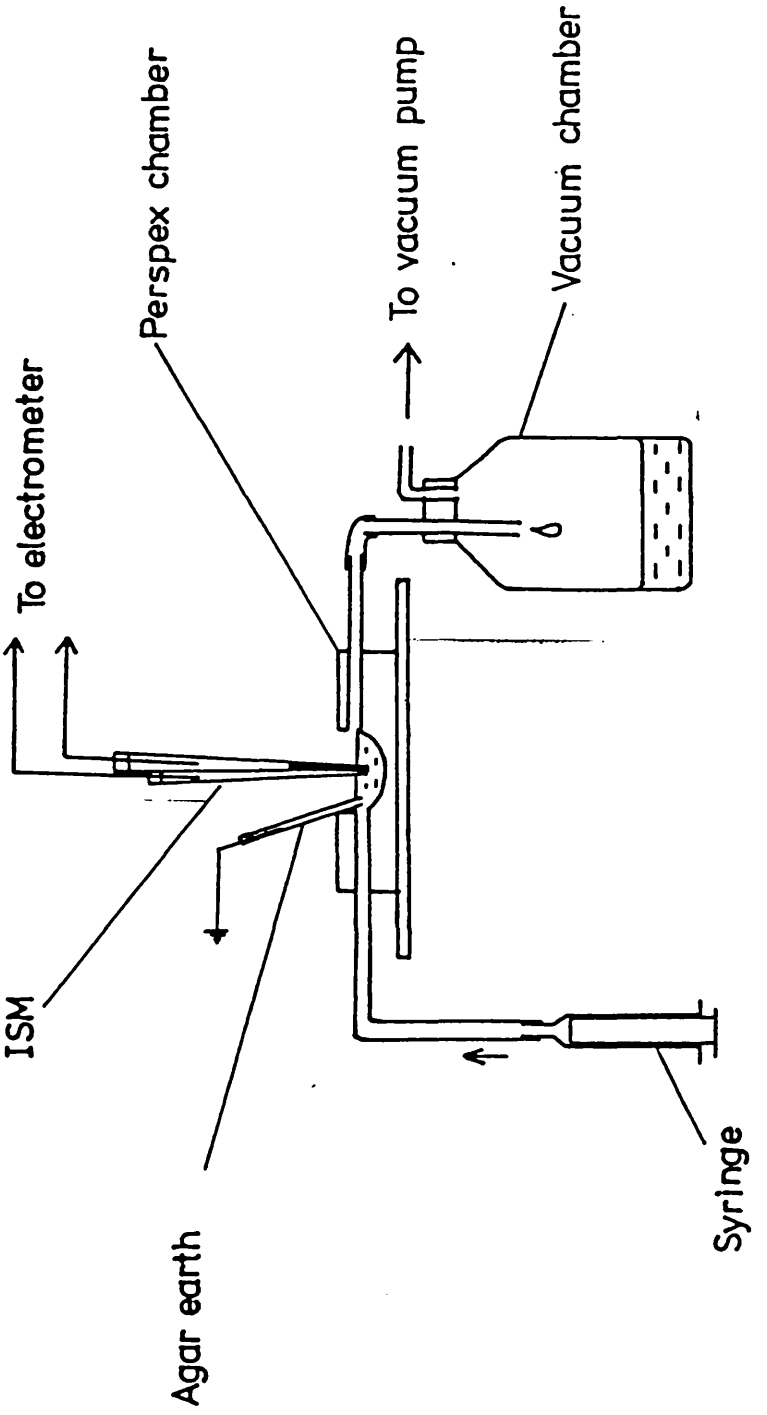


Fig. 37 Equipment for the calibration of ISM's. Solutions were introduced into the chamber via a syringe, and removed to a vacuum chamber.

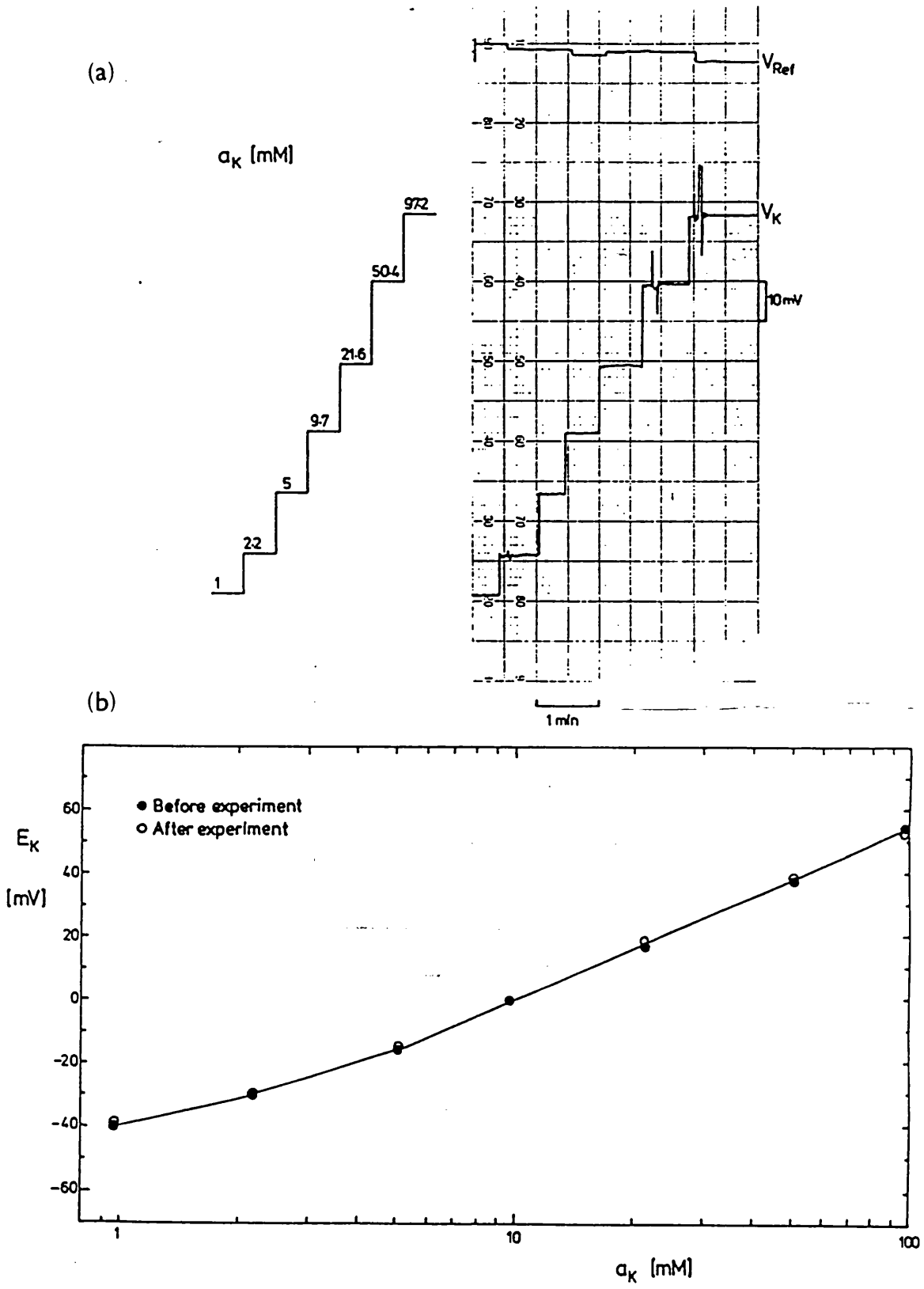


Fig. 38 a. Calibration of a LIX-type K^+ ISM and b. the resulting calibration curve. V_{Ref} is the potential seen by the reference barrel and V_K is the differential potential signal which is dependent on a_K.

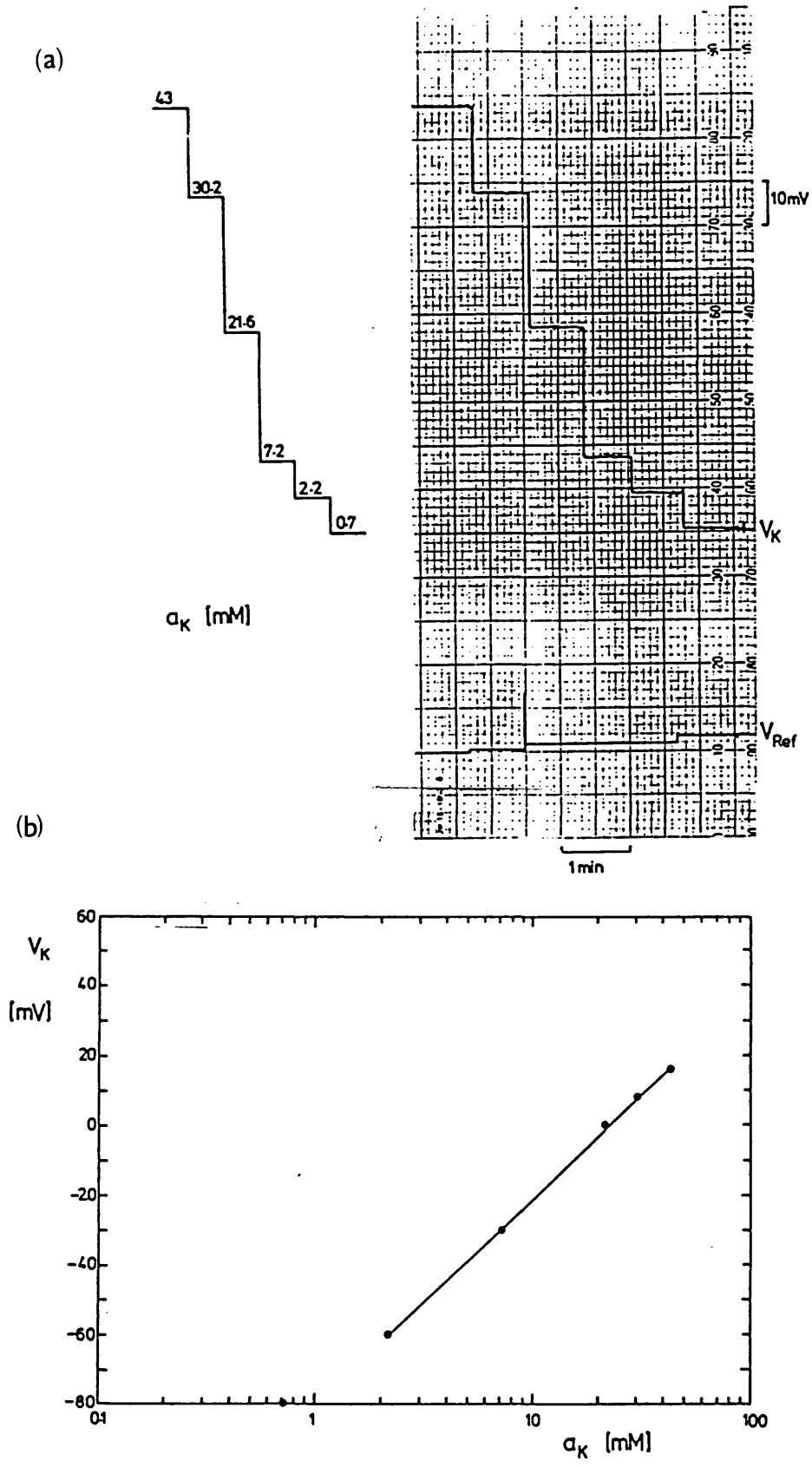


Fig. 39 a. Calibration of a NIC-type K^+ ISM and b. the resulting calibration curve. V_{Ref} is the potential seen by the reference barrel and V_K is the differential potential signal which is dependent on a_K.

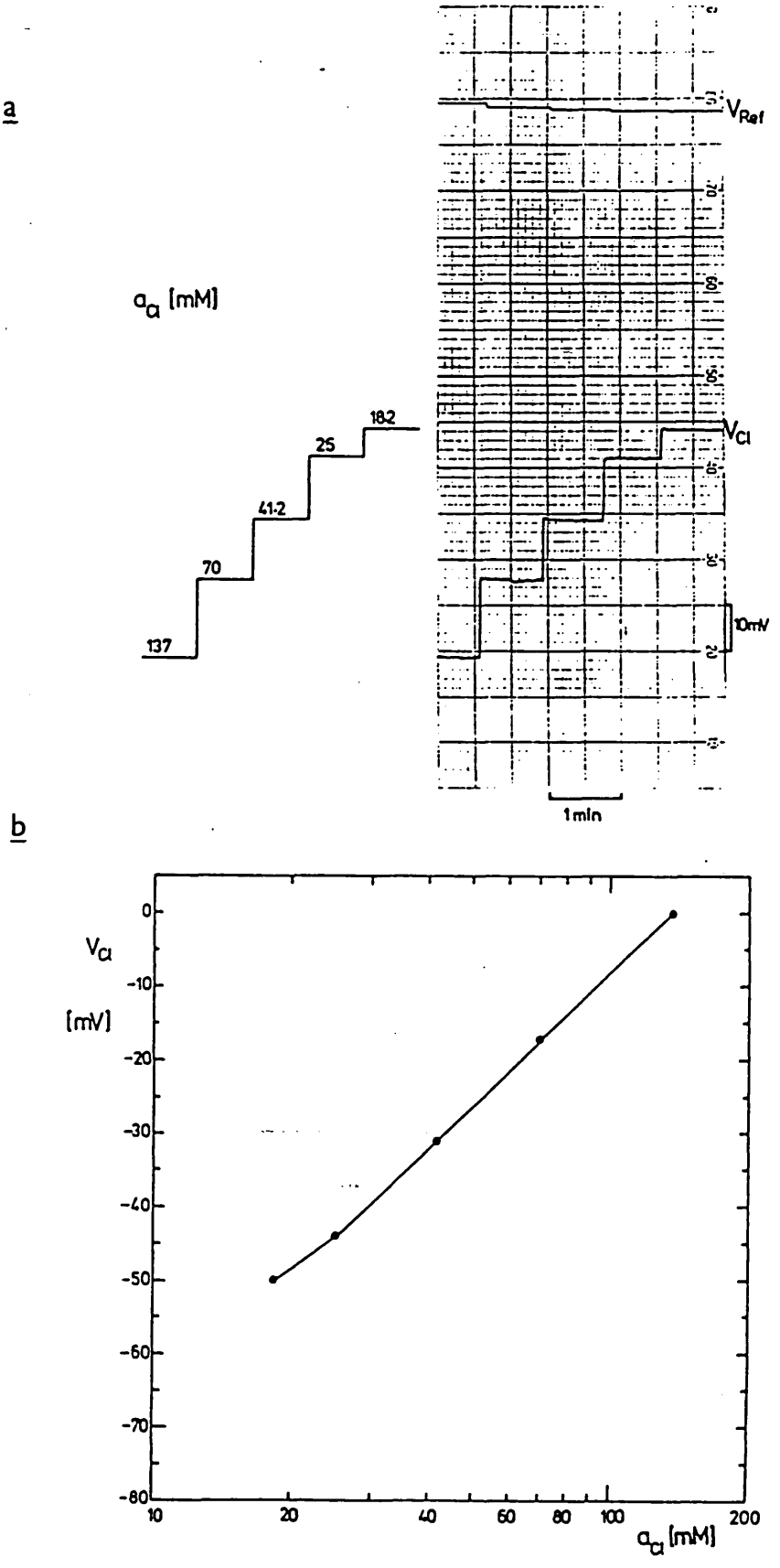


Fig. 40 a. Calibration of a Cl^- ISM with the reference barrel filled with KCl and K_2SO_4 and b. the resulting calibration curve. V_{Ref} is the potential seen by the reference barrel and V_{Cl} is the differential potential signal which is dependent on a_{Cl}.

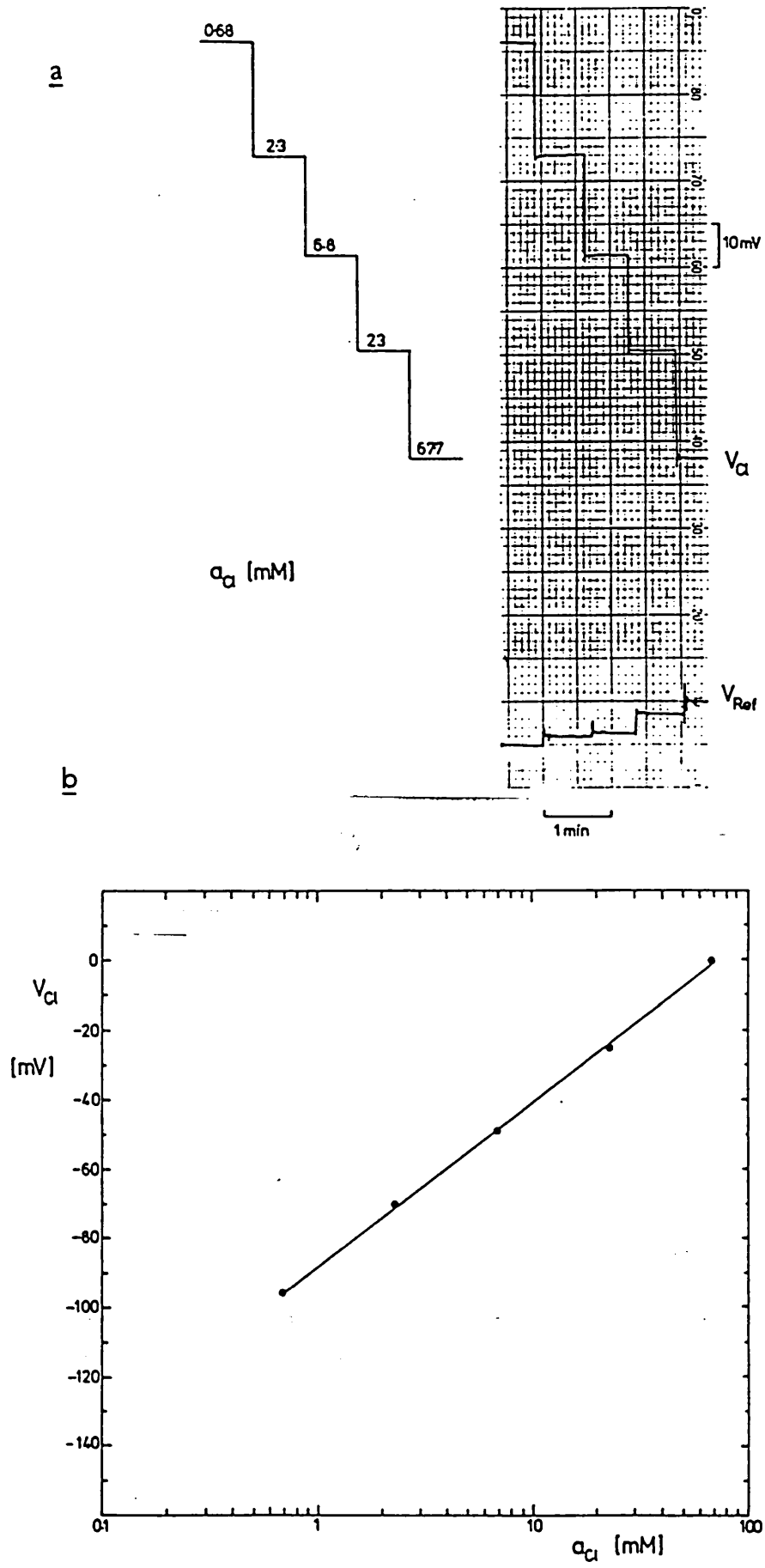


Fig. 41 a. Calibration of a Cl^- ISM with a RLIE-filled reference barrel and b. the resulting calibration curve. V_{Ref} is the potential seen by the reference barrel and V_{Cl} is the differential potential signal which is dependent upon a_{Cl}.

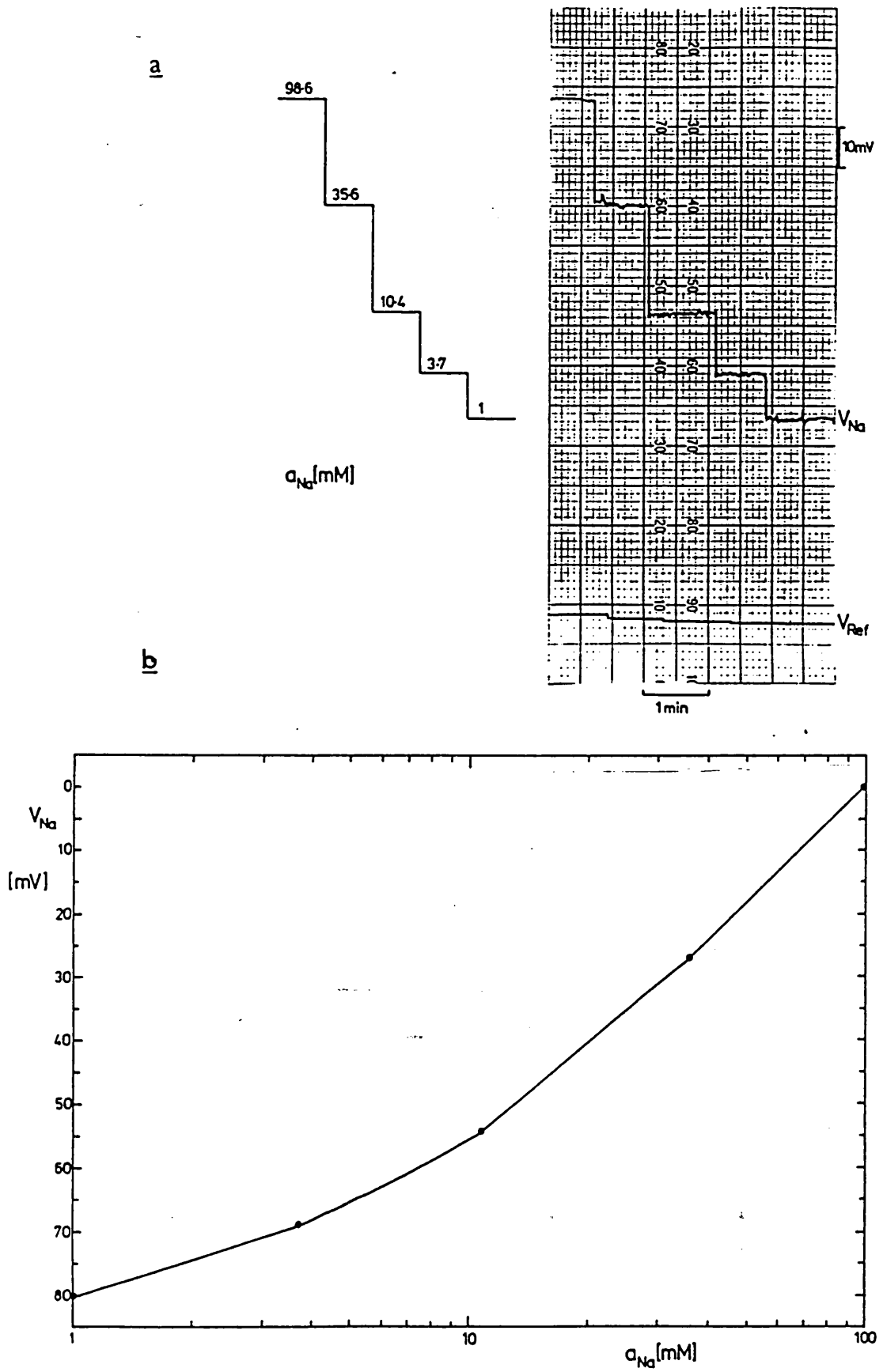


Fig. 42 a. Calibration of a Na^+ ISM and b. the resulting calibration curve. V_{Ref} is the potential seen by the reference barrel and V_{Na}, the differential potential signal which is dependent upon a_{Na}.

filled with reference liquid ion exchanger (RLIE), and figure 42 a,b for a Na^+ ISM. Figure 38 b shows the close correspondence typically found between the calibrations of an ISM before and after an experiment.

II.2. Ordinary microelectrodes

These were required for three types of experiment:

(i) To measure the E_m of muscle cells and to compare the mean and distribution of the population of values obtained with those measured using ISMs. A close correspondence between the values recorded using the two types of microelectrode in one preparation indicates that ISMs, despite their relatively coarse tips, do not cause significantly more damage to cells then OMs.

(ii) To perform ionic substitution experiments to quantify the contribution of particular ions to E_m.

(iii) To monitor membrane resistance during some ionic substitution experiments.

II.2.i. Manufacture of ordinary microelectrodes (OM's)

In all cases, OMs were made from borosilicate glass capillary tubes with an internal filament, an OD of 1.0 mm and an ID of 0.58 mm (GC 100 F-10, Clark Electromedical Instruments) and filled with 2.5 M KCl. Their resistances were then measured using the 'electrode test' facility on the WPI M701 amplifier. Two types of microelectrode puller were used, depending on the shape of electrode tip required. For OMs suitable for measuring E_m and performing ionic substituion experiments, a horizontal puller was used (Clark Electromedical Instruments, LPP-2). This gave fine electrodes, with long shanks and relatively high resistances (50-100 mΩ), which were generally found to give stable impalements. For monitoring membrane resistance, however, relatively low-resistance electrodes were required, to minimise the chance of the electrode resistance changing spontaneously during the experiment and causing recording errors. Such electrodes were made using a vertical micro-electrode puller (SRI), which gave short shanks and resistances between 10 and 40 MΩ.

II.2.ii Recording circuit

The microelectrode was connected via chlorided silver wire to a unity gain amplifier (WPI, model M 701) whose output was displayed on a chart recorder (W & W, model 314) and an oscilloscope (Telequipment, type D1010) (fig. 43).

II.3. Recording set-up

(i) Faraday cage

A Faraday cage was built from a Dexion framework covered by fine expanded copper mesh. The cage was large enough for the experimenter to work inside, thus reducing to a minimum electrical noise and interference from external sources. (Plate 7). The arrangement of the recording equipment within the Faraday cage is shown in fig. 44 and plates 5 to 8.

II.3.ii Recording Platform

A wooden bench was supported on strips of Dexion within the cage, and was found to provide a mechanically stable working platform for the testing of ion-sensitive microelectrodes and for electrophysiological intracellular recording experiments. A single precision micromanipulator (Zeiss) mounted on one side of heavy steel base-plate was placed on the bench (Plate 8), and a recording platform constructed in the centre of the base-plate. This platform consisted of a square 4" x 3" of 0.5 inch thick metal supported on metal legs, and was fitted with the XY controls of a microscope stage to allow movement of the recording chamber relative to the microelectrode. A binocular zoom stereomicroscope was positioned above the recording platform to permit visual examination of the preparation during experiments. Illumination was provided by a fibre optic light (Ealing).

The electronic equipment used was set in a recess inside a Faraday cage so that the cage interior was well-shielded from all a.c. mains inputs (plates 5 & 6).

II.3.iii Experimental recording chamber

A recording chamber was constructed from perspex as shown in figure 45 a,b

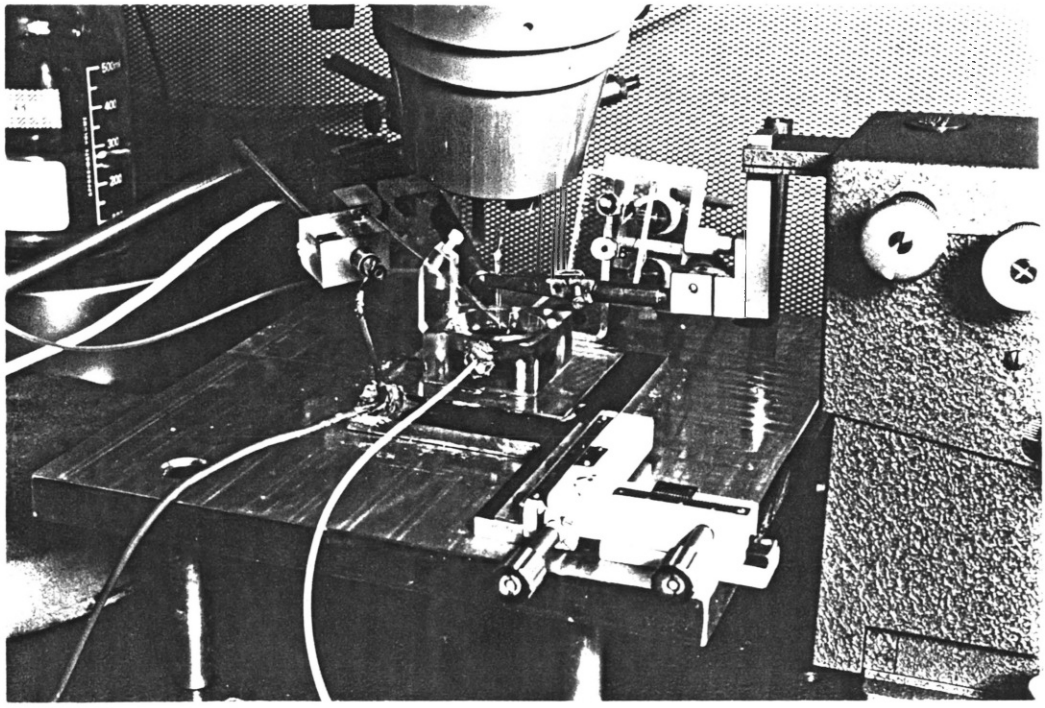


Plate 8. Photograph of recording platform and recording chamber, above which is seen a microelectrode held by a micromanipulator and the dissecting microscope.

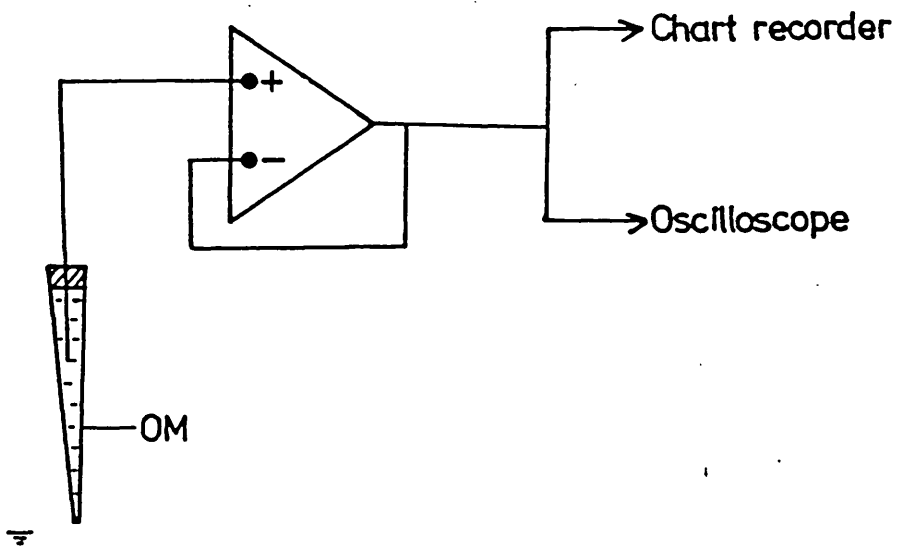


Fig. 43 Circuit diagram for the use of conventional microelectrodes (OM's). The OM was connected via an amplifier to a chart recorder and oscilloscope which displayed all electrical signals from the OM.

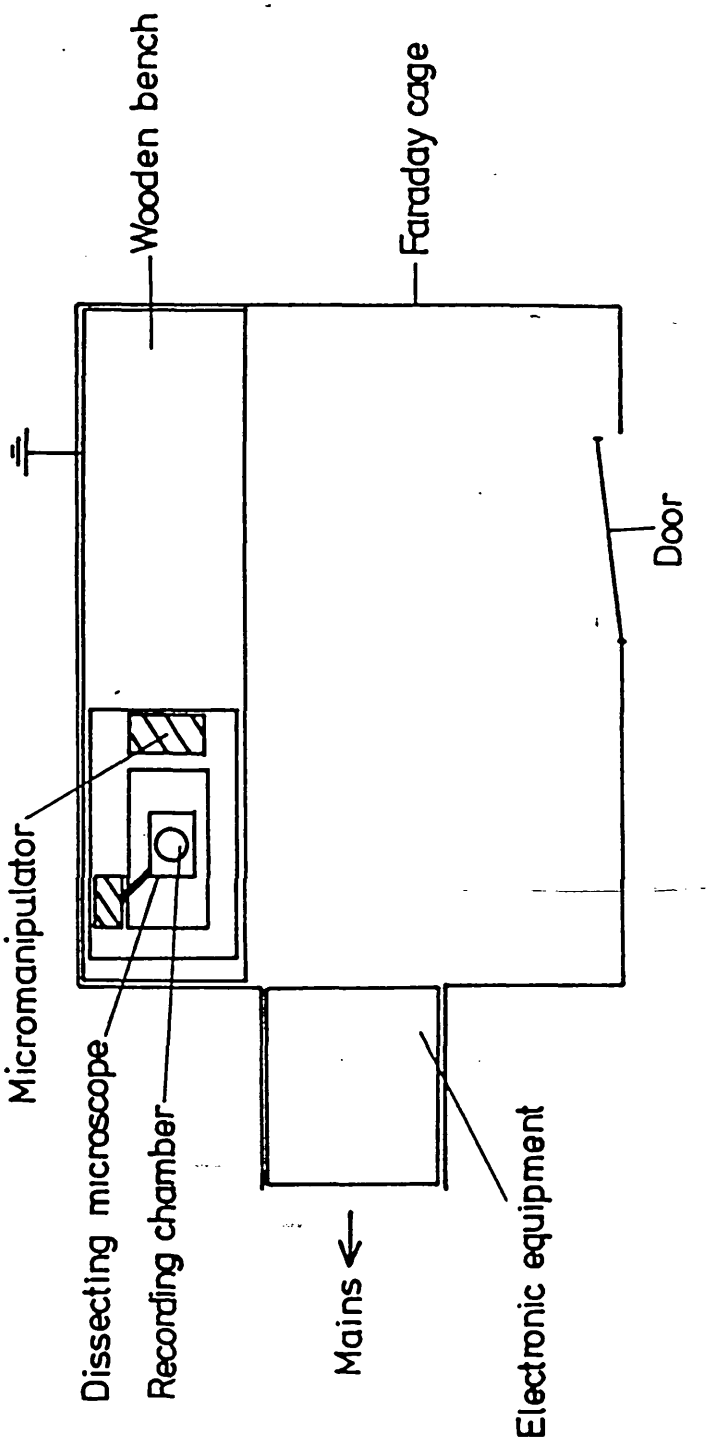


Fig 44. Schematic diagram of the Faraday cage and associated equipment from above.

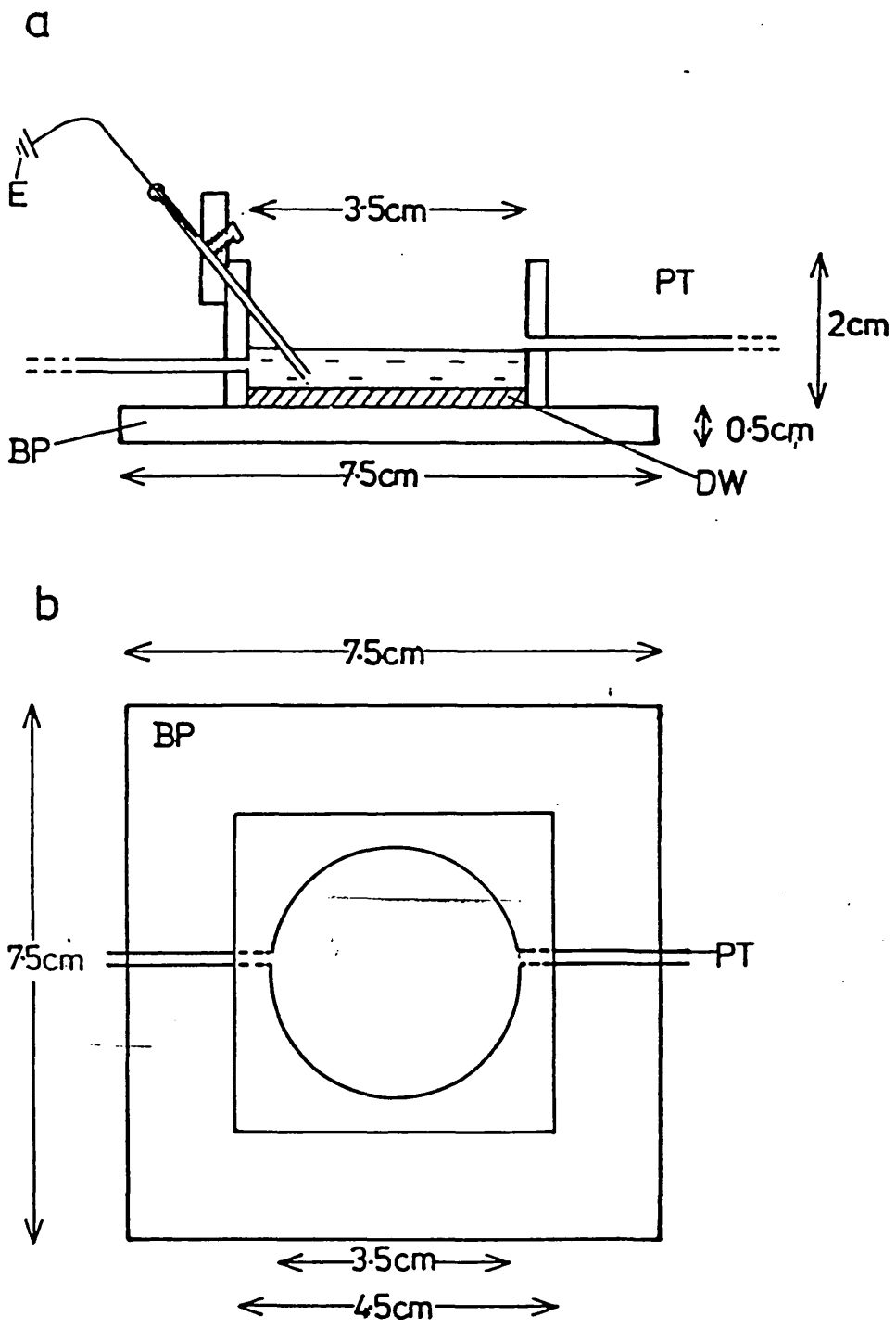


Fig. 45 The recording chamber. a. T.S of chamber. PT, polythene tubing; BP, baseplate; E, earth; and DW, dissecting wax. b. View of chamber from above.

and plate 8. It consisted of a square flat base which fitted into the microscope stage X-Y controls on the recording platform. Onto this was glued a perspex block into which a circular recess had been cut, to form the chamber. The chamber was designed so that it was large enough to accommodate both *Calliphora* and *Chilo* preparations, whilst holding a relatively small volume of fluid. The latter ensured that fast solution changes could be achieved during substitution experiments.

Solutions were introduced into the recording chamber via a length of polythene tubing (1.5 mm in diameter) which was inserted into a small hole in the side of the chamber. Waste solutions were removed from the chamber via a similar length of tubing, inserted slightly higher up the wall of the chamber, using the same vacuum system described under calibration of ISMs (Section II.1.vi, fig. 37). The position of the outlet hole relative to the inlet hole was such that the preparation remained covered with fluid at all times, whilst minimising the volume of fluid left in the chamber. The latter further facilitated fast solution changes.

The fluid in the recording chamber was earthed with the same 'floating earth' as that used duing ISM calibration (consisting of a glass capillary containing agar-Ringer and an Ag-AgCl contact connected to the chassis-earth of the electrometer).

II.4 Experimental procedures

II.4.i The Preparations

Two species of insect were used in this study: final instar larvae and prepupae of *Calliphora erythrocephala* Meig., the blowfly (Diptera) and final instar larvae of *Chilo partellus*, the rice stem borer (Lepidoptera). All preparations were dissected under saline in a similar manner. For *Calliphora*, Rice's saline was used (Finlayson & Osborne, 1970, Appendix 1) and for *Chilo*, Weevers' saline (Weevers, 1966; Appendix 2). Stainless steel entomological pins were used to impale the anterior and posterior ends of the larva or prepupa (dorsal surface upermost) and thus attach it to the wax in the base of the recording chamber. A lengthwise cut was made in the dorsal surface from posterior to anterior and the cut edges pinned to the wax. The gut and associated fat bodies and the major ganglia were than dissected out, exposing the body-wall muscles. Preparations were allowed to equilibrate for at least 30 minutes in

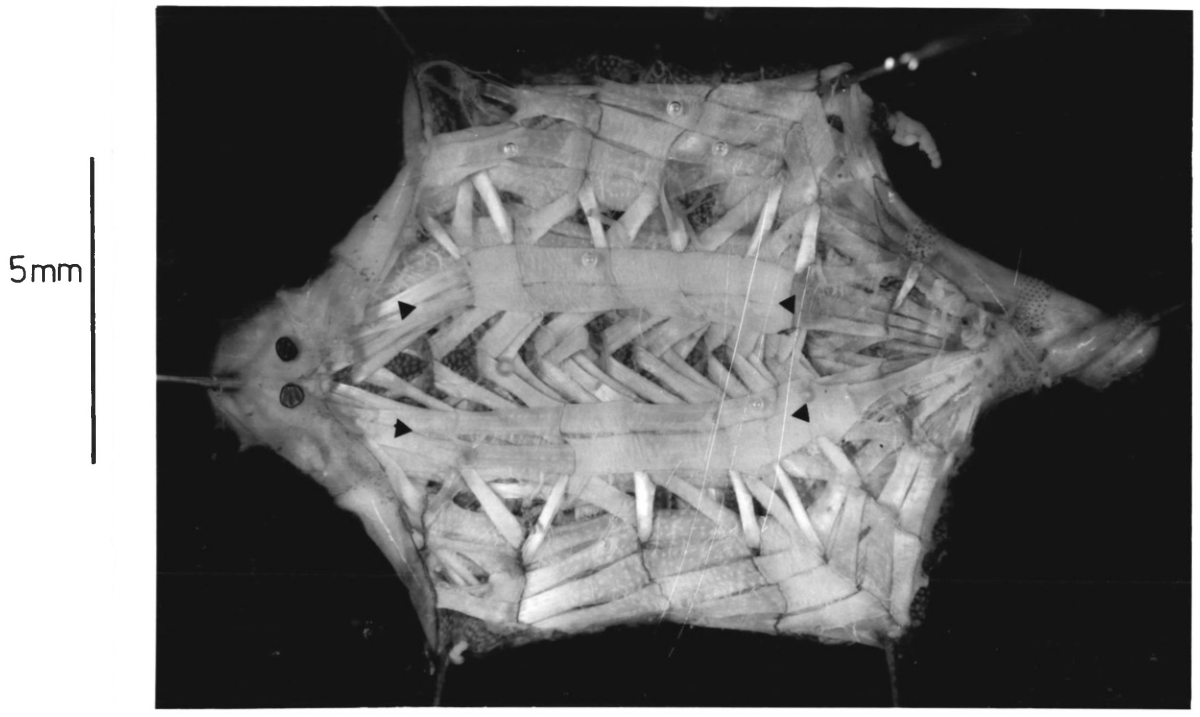


Plate 9. *Calliphora* larva preparation in Bouin's fixative: the insect was dissected from the dorsal surface and the gut and fat bodies removed. The cells studied were the ventral longitudinal muscle bands denoted by arrowheads at either end. Calibration bars show the size of the insect.

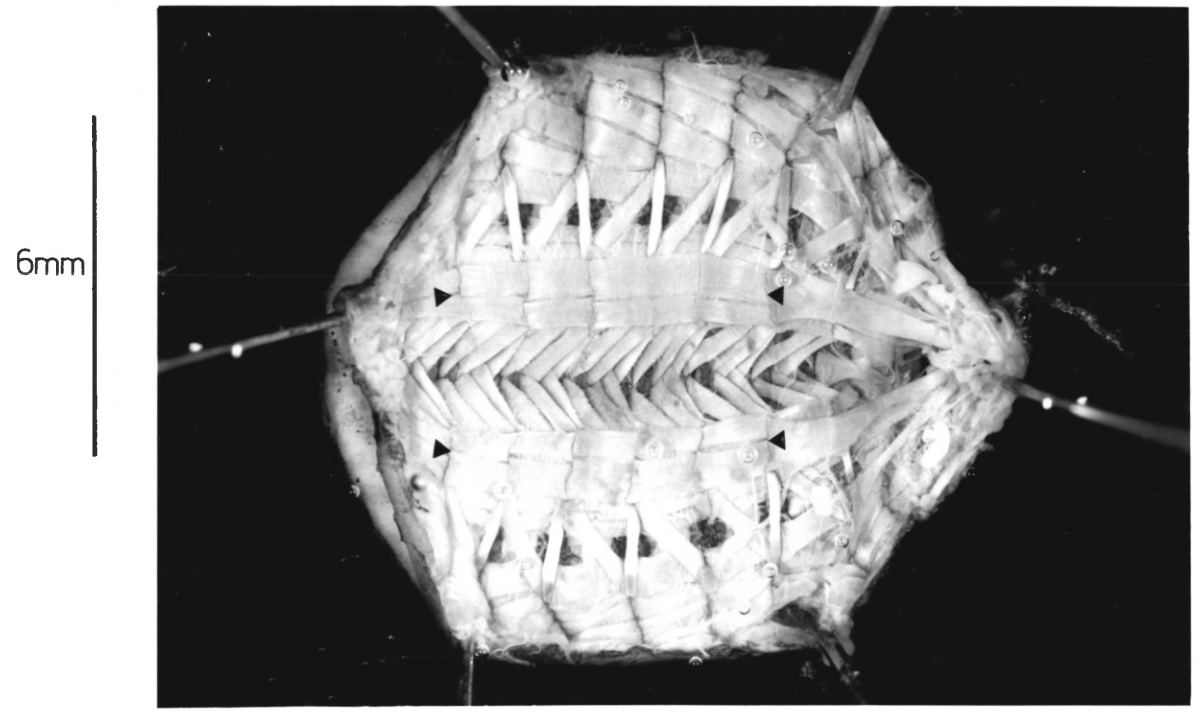


Plate 10. *Calliphora* prepupa preparation in Bouin's fixative, showing the ventral longitudinal muscles studied (denoted by arrowheads at either end).

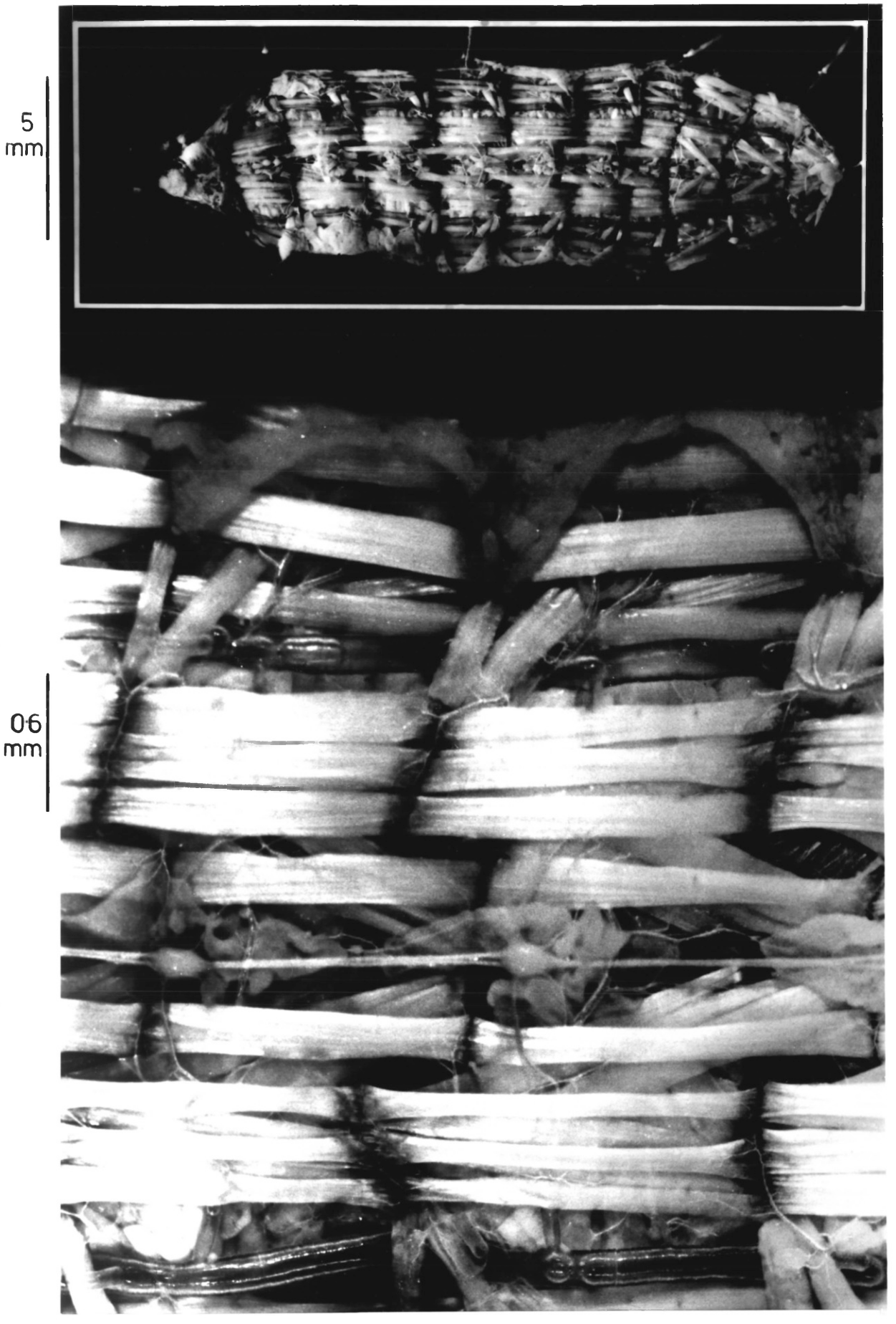


Plate 11. *Chilo* larva preparation in Bouin's fixative. The insect was dissected from the dorsal surface and the gut and fat bodies removed.

the saline. The preparations are illustrated in plate 9 (*Calliphora* larva) 10 (*Calliphora* prepupa) and 11 (*Chilo* larva).

II.4.ii Intracellular ionic activity measurements: Derivation of results from recorded traces

An ISM was manufactured, as described in section II.1.i and calibrated several times until two successive calibrations were exactly the same: this was taken to indicate that the ISM was stable.

The preparation was then earthed using the same Ag/AgCl - Agar earth electrode as that used for the calibration of the ISM, and the ISM was advanced from above into individual muscle cells under direct microscopical control (fig. 46).

The methods by which intracellular ionic activity measurements were derived from recorded traces were slightly different depending on whether K^+ and Cl^- ISMs or Na^+ ISMs were used. The derivation of intracellular K^+ and Cl^- data will therefore be considered separately from that of intracellular Na^+ data.

Intracellular K^+ and Cl^- activities

Since the method used to derive both K^+ and Cl^- activity data from chart recordings is the same, it will be described using K^+ as an example.

A typical chart recording from an experiment shows the calibration of an ISM followed by traces produced when the ISM touches the bathing medium in the chamber. It then records the extracellular activity of the primary ion (here K^+), a_K^o, by means of the a_K-dependent voltage, V_K (fig. 47a). In the presentation of the results of this study, the K^+-sensitive differential potential is denoted by V_K and the membrane potential (the electrical potential of the inside of the cell with respect to the outside) at any time is represented by V_m. The notation E_m exclusively represents the resting membrane potential. (Similarly, for the Na^+ and Cl^- data, the Na^+ and Cl^--sensitive potentials are denoted by V_{Na} and V_{Cl} respectively).

The ISM is then advanced into a muscle cell and a steady trace obtained. This gives a measure of the potential difference between the levels of V_K

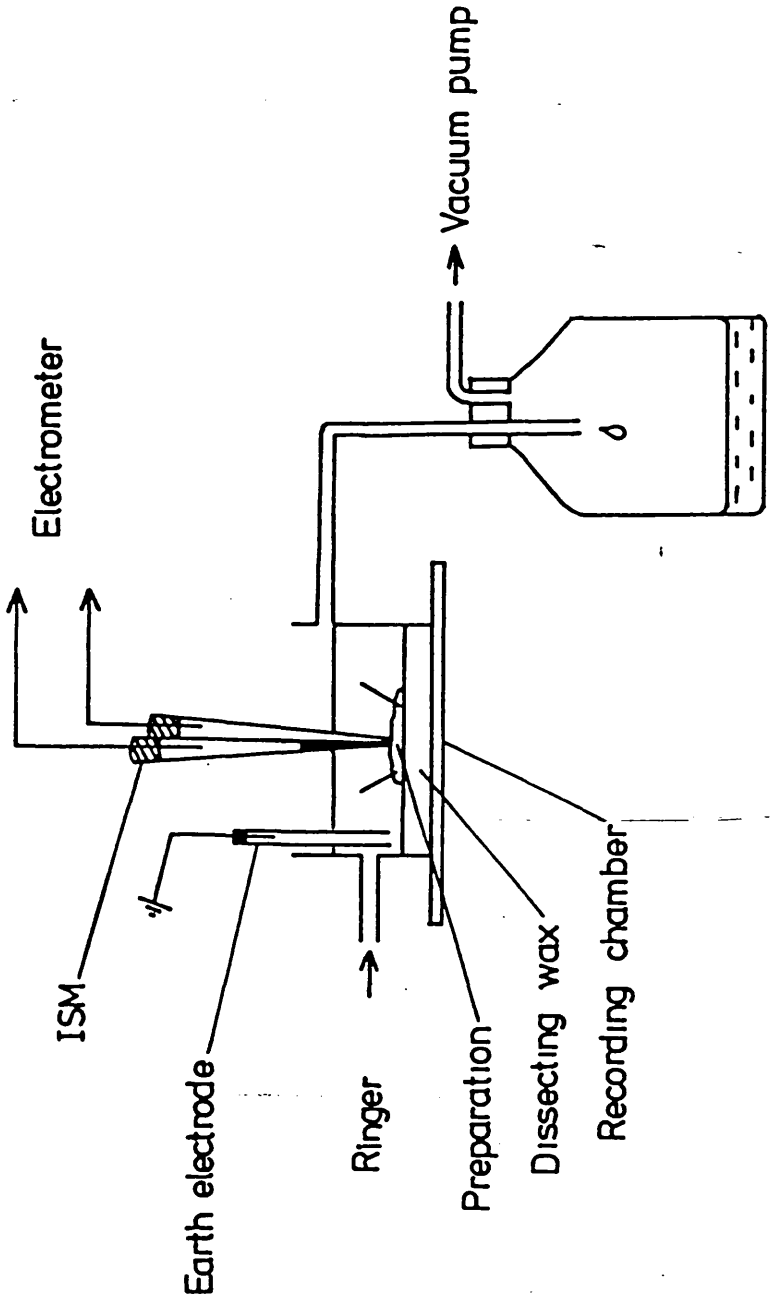


Fig. 46 The position of the preparation within the recording chamber. During substitution experiments, solutions were introduced into the chamber via polythene tubing and removed to the vacuum chamber by a vacuum pump.

inside and outside the cell, ΔV_K^i, and this voltage is referred to the ISM calibration curve to give the intracellular K^+ activity. (Fig. 47 a,b).

Intracellular Na^+ activities

As previously explained (section II.1.vi) the calibration solutions for Na^+ ISMs were not based on Ringer solutions, because the latter contain high levels of Ca^{2+} which interfere with the Na^+-NIC. Instead the calibration solutions were designed to include a constant background of interference mimicking the intracellular medium, which is assumed to contain very small amounts of Ca^{2+} (Campbell, 1982.). Since Normal Ringer was not included as one of the steps in the calibration of the ISM, the potential recorded from the Na^+ ISM when bathed in the extracellular fluid is meaningless. It was therefore necessary to take ΔV_{Na}^i as the difference between the level of V_{Na} (the Na^+-sensitive potential) and the zero potential on the ISM calibration trace (Fig. 48a) ΔV_{Na}^i was then referred directly to the calibration curve to give the intracellular Na^+ activity, a_{Na}^i (Fig. 48 b).

The equilibrium potential, E_X, for each ion, 'x', was calculated using the Nernst equation, as follows:

$$E_X = 58 \log_{10} \frac{a_X^o}{a_X^i} \quad (mV)$$

where a_X^i is the measured intracellular activity and a_X^o is the known extracellular activity of the ion, "x", present in the Ringer.

The value of E_m for each muscle cell was read directly from the hyperpolarising deflection of the reference barrel trace, V_m, upon impalement of the cell (figures 47a, 48a). The value of E_X was compared with that of E_m, in order to evaluate the possible role of each ion in the generation of the muscle cell membrane potential.

II.4.iii Membrane resistance measurements

These were carried out using a bridge circuit in order to monitor changes in muscle membrane resistance when the composition of the bathing medium was altered. The experimental procedure was as follows, and is illustrated in fig. 49. (i) Low-resistance (around 20 MΩ) OMs were manufactured. These

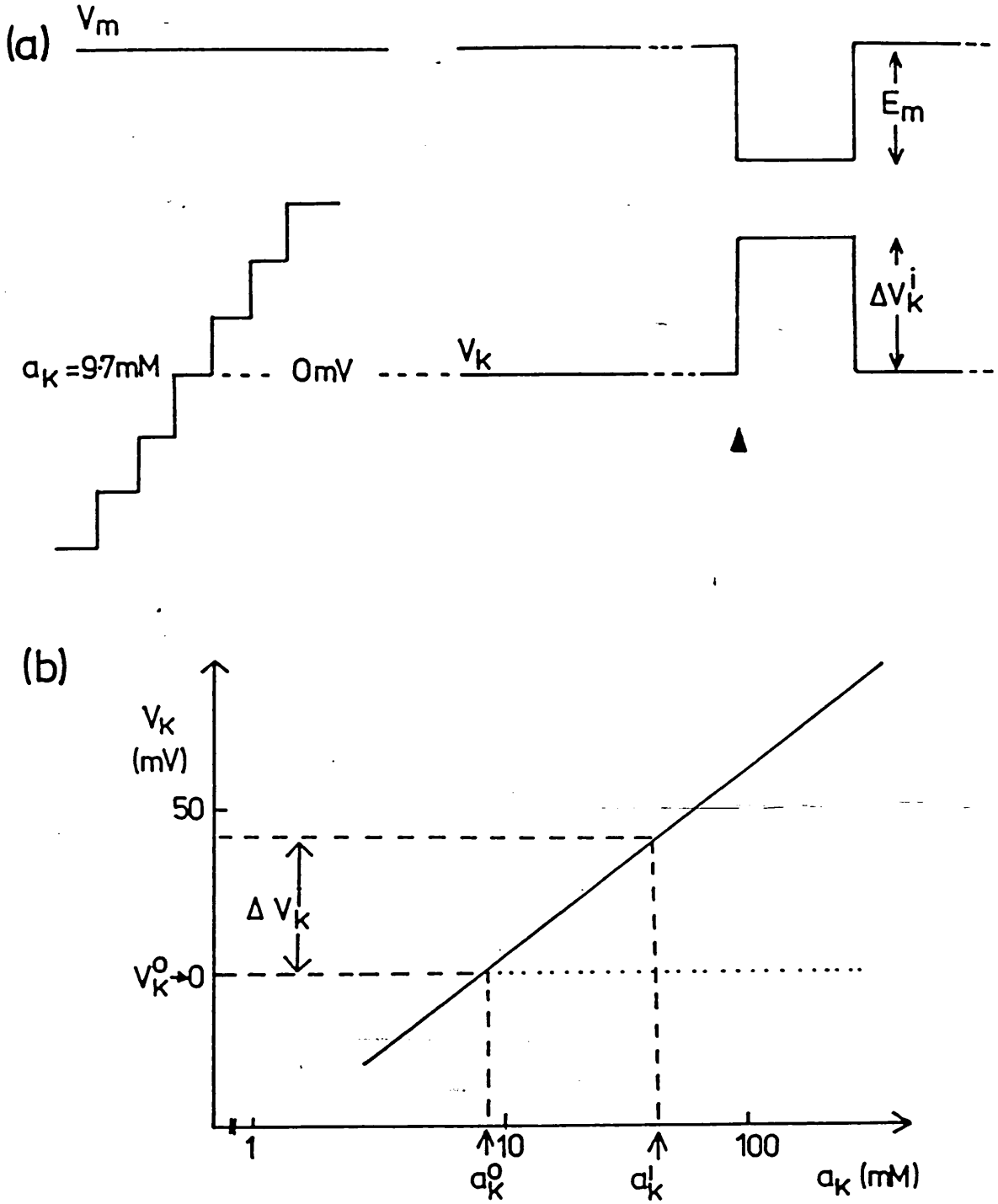


Fig. 47 a. Schematic diagram showing how V_K^i was determined from the ISM calibration trace and the recording of the extracellular potential and a cell penetration, starting at the arrowhead. V_m is the reference potential and V_K, the K^+-sensitive potential. b. Determination of the intracellular level of a_K from the ISM calibration curve (see text.)

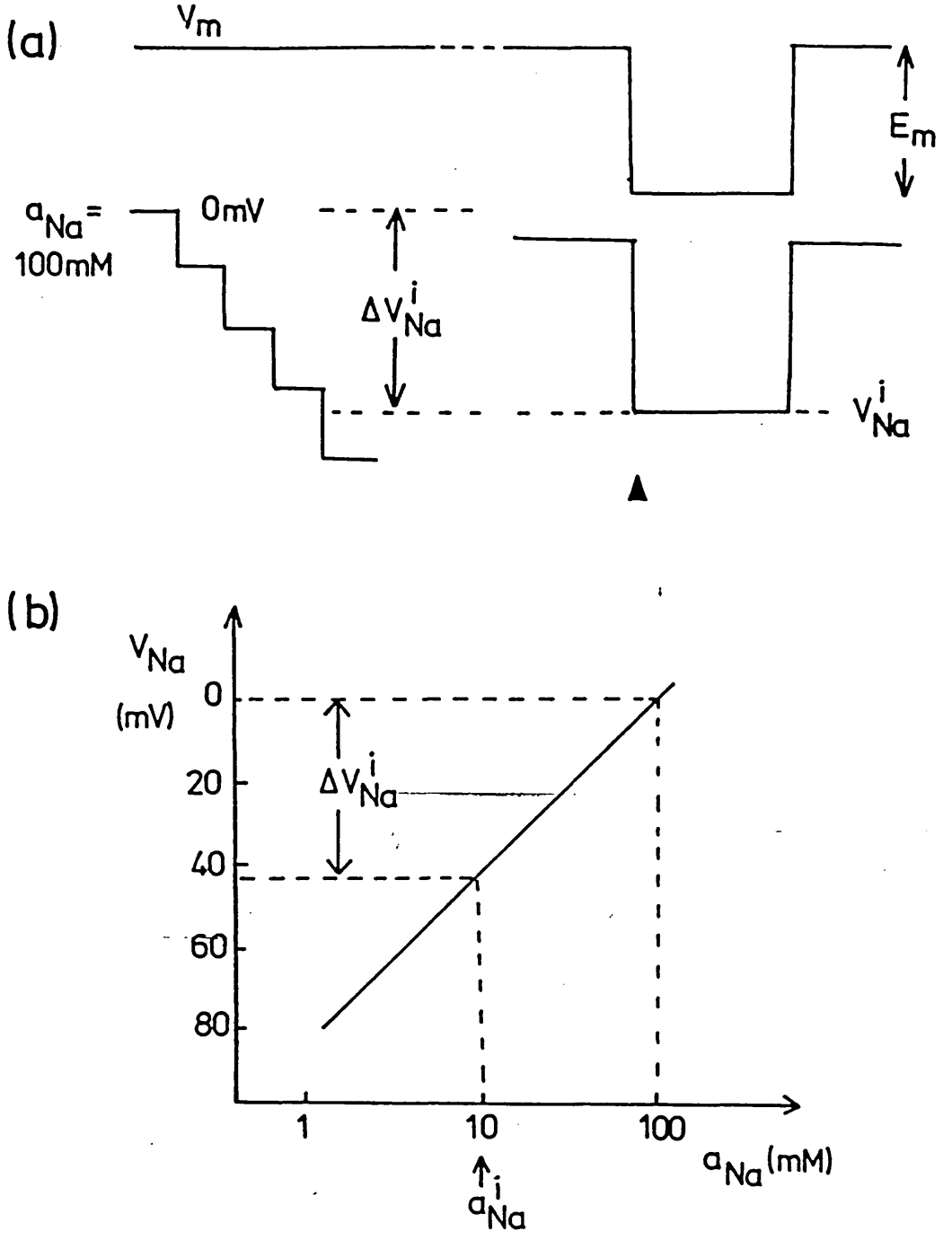


Fig. 48 a. Schematic diagram showing how V_{Na}^i was determined from the ISM calibration trace and the intracellular potential. V_m is the reference potential and V_{Na}, the Na^+-sensitive potential.
b. Determination of the intracellular level of a_{Na} from the ISM calibration curve.

were used in order to reduce the risk of tip blockage and possible resistance changes during the experiment. Such changes would lead to errors in membrane resistance measurements.

(ii) The OM was introduced into the recording chamber, and pulses of constant current (I_m) were applied (7.5×10^{-9} A) to the bridge circuit from a stimulator (Grass S44). (fig. 49 stage (i)). The corresponding voltage pulses across the electrode represented a measure of the electrode resistance and were balanced using the variable resistor on one side of the bridge circuit (Fig. 49, stage ii). The extent to which the variable resistance in the bridge circuit had to be adjusted provided a direct measure of the electrode resistance, which was always in good agreement with the value obtained using the "resistance test" facility on the amplifier.

(iii) A muscle cell was impaled, whereupon positive voltage pulses were recorded, (V_m) representing the resting membrane resistance, (Fig. 49, stage iii) which was calculated from Ohm's law:

$$R_m = \frac{V_m}{I_m}$$

After obtaining a steady V_m reading, the bridge circuit was rebalanced, and the solution bathing the preparation changed, (Fig 49, stage v).

(iv) Any subsequent changes in membrane resistance were monitored, and the cell was finally returned to normal Ringer to check the reversibility of any effects observed (Fig. 49, stage vi).

(v) The electrode was withdrawn from the cell, providing a check that the E_m and microelectrode resistance had the same value as before the experiment ie. $|V_m| = |-V_m|$ which indicated that the cell had not been damaged and the OM resistance had not changed, (Fig. 49, stage vii).

II.4.iv. Ionic substitution experiments

The aim of these experiments was to provide a quantitative assessment of the contribution of an ion 'x' to E_m. The experimental procedure involved impaling a muscle cell in Normal Ringer with an ordinary microelectrode and obtaining a steady value of E_m for several minutes. Ringer solutions

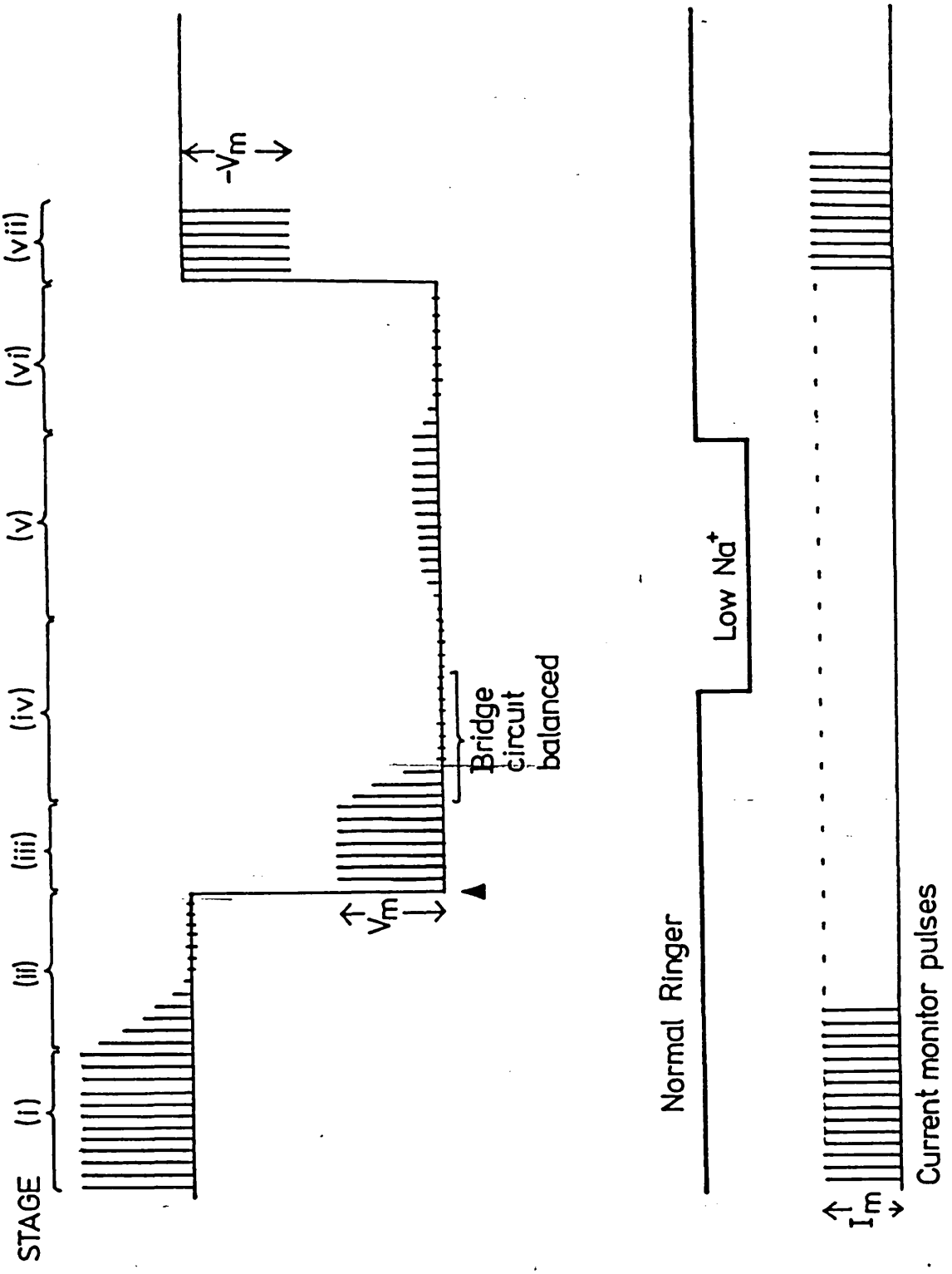


Fig. 49 Membrane resistance measurements during a substitution experiment. Stages (i) to (vii) are explained in the text. V_m represents the membrane resistance and I_m, the applied current pulses.

containing a range of a_x's were then substituted into the recording chamber and a steady value of E_m obtained in each. In each case, the reversibility of the effect(s) was checked.

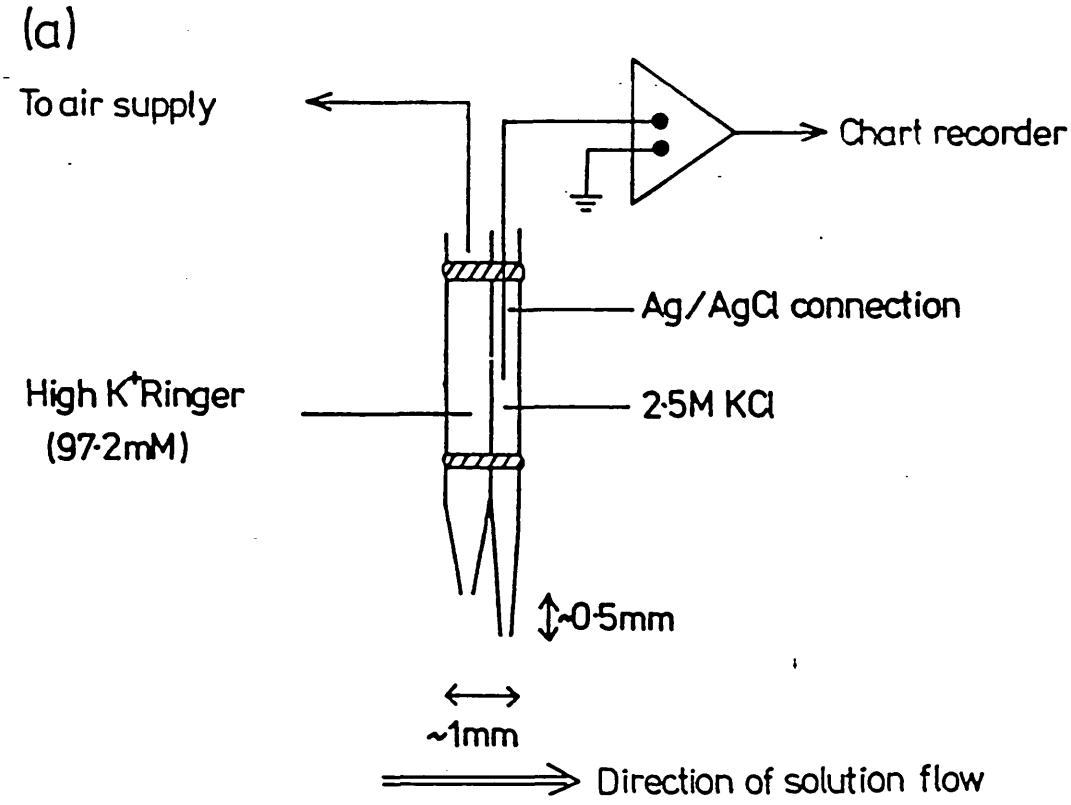
K^+, Na^+ and Cl^- substitution experiments were performed on the two insects. The composition of Ringer solutions used are given in Appendices 3, 4, 6 and 7. All solutions were based on the Normal Ringer for the insect concerned, and were of constant ionic strength. In the K^+ substitution solutions, Na^+ was used as a substitute for K^+. In the *Calliphora* Na^+ substitution solutions a variety of substitutes were used: choline chloride, glucose, tetramethylammonium chloride, n-methyl D-glucamine and magnesium chloride. In *Chilo*, only $MgCl_2$ was used. Gluconate salts were used to substitute for Cl^- in the Cl^- substitution solutions, and extra Ca^{2+} was added to these solutions to compensate for sequestering of Ca^{2+} by gluconate (Vaughan-Jones, 1979; Kenyon & Gibbons, 1977).

II.4.v. K^+ pulsation experiments

The purpose of these experiments was to determine whether the permeability of the muscle cell membrane of *Calliphora* to K^+ changes when the cell is exposed to low Na^+ Ringer. The experiments involved impaling a cell bathed in Normal Ringer, and monitoring its membrane response to a series of pulses of high K^+ Ringer of constant size, applied from a broken microelectrode. Low-Na^+ Ringer was then introduced into the recording chamber, whilst high-K^+ pulses continued to be applied. Any change in the size of the membrane response to high K^+ following the introduction of low-Na^+ Ringer would indicate a change in the K^+ permeability of the membrane.

Fig. 50 (a) shows the arrangement by which a broken micropipette pulled from 1.5 mm OD glass (GC 250T, Clark Electromdical Instruments) and filled with high-K^+ Ringer (97.2 mM K^+; solution no. 7, Appendix 3) was attached to a conventional 2.5 M KCl-filled microelectrode, pulled from 1mm OD glass (GC 100P Clark Electromedical Instruments). The two microelectrodes were arranged with their tips positioned as shown in figure 50a to allow the formation of high-K^+ droplets as close as possible to the tip of the recording microelectrode without the broken microelectrode touching the muscle cell itself.

Figure 50 b shows a schematic layout of the apparatus used to apply air pulses to the back of the broken micropipette and hence produce



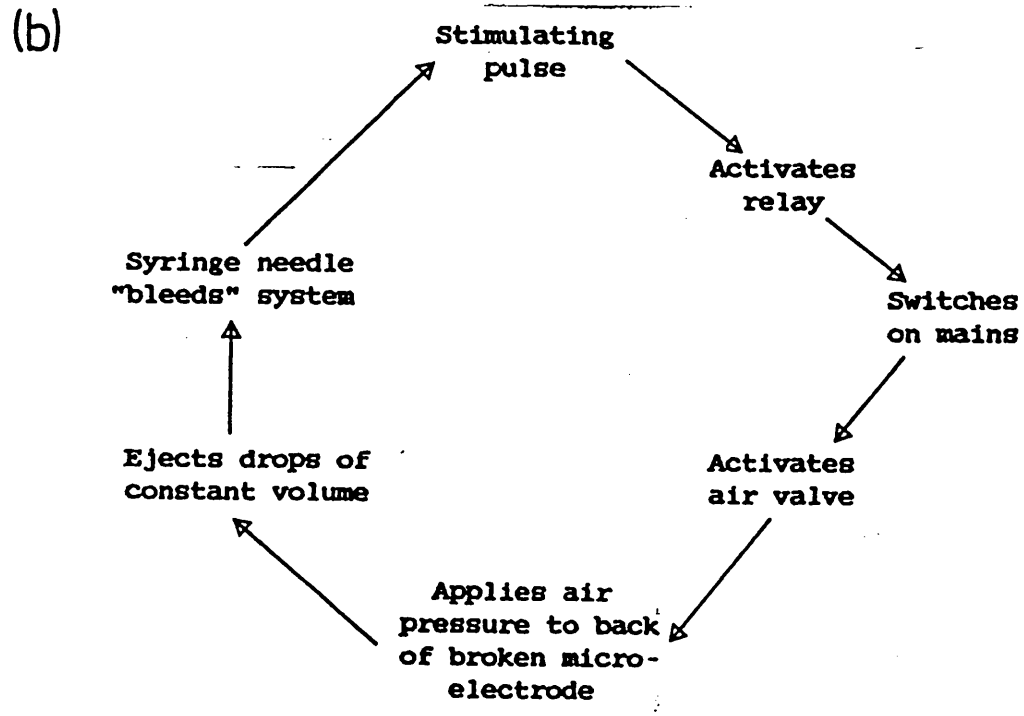


Fig. 50 a. Schematic diagram illustrating the arrangement of the two microelectrodes used to apply droplets of high-K^+ Ringer to a cell, whilst simultaneously recording its membrane potential.
b. 'Flow' diagram illustrating the system devised to apply pulses of high-K^+ Ringer to the outside of a cell.

constant-sized (approx 4 µl) droplets of high K^+ Ringer. A stimulator generating pulses of around 1 second duration (Grass S44) was used to control a relay (RS Type 22) which in turn regulated the opening of an air valve (Dewroswitch Model 8263/B206) via mains. Thus, a pulse from the stimulator led to the opening of the valve and hence to the application of pressure (1 - 5lb.square inch) to the back of the broken micropipette. This system ensured that constant-sized droplets of high-K^+ Ringer were ejected from the micropipette at regular intervals, controlled by the stimulator.

A vital feature of this layout was the piercing of the polythene tubing between the air supply and the broken micropipette with a hypodermic syringe needle. The latter remained in place during the experiment and allowed air to escape from the system between pulses, thus preventing the build-up of pressure.

The positioning of the double-microelectrode within the recording chamber is shown in fig. 50 a. Its orientation with respect to the direction of flow of the Ringer is particularly important: the broken micropipette must be "upstream" of the recording microelectrode to ensure that the high K^+ Ringer pulses are washed towards the impaled cell and not away from it.

II.4.vi. Cooling experiments

These were carried out in order to determine the effect of reduced temperature on muscle cell membrane potentials in *Chilo* larvae. Experiments involved impaling a cell with a conventional microelectrode at room temperature, RT (around 20°C) and recording a steady E_m level. The bath temperature was then reduced to a constant 8°C by continuous perfusion with cooled Ringer (kept on ice). Temperature was monitored using a Conmark 3002 digital thermometer with micro-probes which were placed very close to the muscle cell concerned. When a steady E_m had been recorded for several minutes, Ringer at RT was substituted back into the chamber, and the preparation left to equilibrate for several minutes before withdrawing the microelectrode from the cell.

II.5. Criteria for the selection of results

A. Ion-sensitive microelectrode measurements

In order to select the most reliable data from the recordings available, the

following criteria were used. These eliminated, as far as possible, the sources of error to which ISMs are prone.

1. Ionic activity measurements were accepted only if the calibrations of the ISM before and after the experiment were within 5 mV of each other at all points.

2. Prior to the impalement of a cell, the level of potential and ionic activity in the recording chamber must be steady to within 1 mV for at least 2 minutes to ensure that the calibration of the ISM remained unchanged.

3. The change in reference potential when an ISM penetrates a muscle cell should be abrupt, indicating that minimal damage has been caused to the cell membrane by the ISM during the impalement.

4. The recorded potential should be constant for longer than two minutes, and equal to the potential achieved immediately after the cell was impaled, for intracellular K^+ and Cl^- data. This ensures that the intracellular ionic activities are not affected by leakage from the reference barrel. Steady impalements were obtained for up to several hours which showed no significant changes in potential from the initial readings. In the case of intracellular Na^+ data, Na^+ ISMs respond more slowly than K^+ or Cl^--ISMs, and more time must therefore be allowed for the recorded potential to reach a new steady equilibrium level following the impalement of a cell. Recordings were therefore accepted from Na^+ ISMs only when a steady impalement had been held for three or more minutes. 5. Cells with membrane potentials of less than -30 mV were discarded, because a low E_m indicates either that the cell is unhealthy or that it was damaged during impalement.

6. The same agar earth was used both for the ISM calibration and for the experimental recordings.

7. The distribution of membrane potentials obtained from a given preparation should be similar when measured using either a conventional or an ion-sensitive microelectrode.

B. Conventional microelectrode measurements.

Ionic substitution experiments. (section II.4.iv).

Following all ionic substitution experiments, the cell was returned to Normal Ringer and a steady or E_m value obtained. Data was accepted only from those cells in which the E_m before and after the experiment differed by no more than 1 mV, indicating that the cell had not been damaged or become less healthy during the experiment.

Membrane resistance measurements. (section II.4.iii)

In experiments in which membrane resistance was monitored, data was accepted only from those experiments in which (i) the electrode resistance read from the balanced bridge circuit following the impalement of a cell was the same as the value obtained prior to the impalement using the 'constant current' switch facility on the amplifier. (ii) the voltage pulses recorded following withdrawal of the OM from the cell were identical to those which corresponded to membrane resistance immediately after the initial impalement of the cell. These ensured that there had been no change in the resistance of either the OM or the cell membrane during the course of the experiment.

K^+ pulsation experiments (section II.4.v)

In K^+ pulsation experiments data was accepted only from those cells in which the responsiveness of the membrane to high K^+ recovered following removal of low Na^+. This ensures that there has been no irreversible change in the properties of the cell membrane or movement of the OM within the cell during the experiment.

Cooling experiments (section II.4.vi)

In cooling experiments on *Chilo*, only those experiments in which E_m returned to its original level following exposure to cold Ringer were considered acceptable. This ensured that the OM had not damaged the cell or slipped out of the cell to some extent.

CHAPTER III. INTRACELLULAR IONIC ACTIVITY MEASUREMENTS IN *CALLIPHORA*

III.1. Conventional microelectrode measurements of membrane potentials

In order to establish the 'normal' resting potential, (E_m) values of the cells, ordinary ultrafine microelectrodes (OM's) filled with 2.5 M KCl were used (tip resistances in the range 60 to 80 MΩ). In addition, it was then possible to check that ISMs did not cause significantly more damage to the cells being studied than OMs, by comparing the mean and distribution of membrane potentials measured using the two types of microelectrode. Membrane damage would be expected to result in depolarisation of E_m, and if the relatively coarse tips of ISMs ($\leq$ 1.5μm c.f. $\leq$ 1μm for OMs) were causing damage, the population of E_m values recorded using ISMs would be expected to have a lower mean and a more asymmetrical distribution than those recorded with OMs. Thus, data were obtained from a minimum of 167 cells from 9 preparations, and the frequency histograms for the E_m's measured in larvae and prepupae are shown in figure 51 a,b, respectively.

Membrane potentials recorded in larvae ranged between -33 and -63 mV, with a mean value of -48 ± 0.4 mV; those recorded in prepupae ranged from -35 to -62 mV, with a mean of -47 ± 0.5 mV. In both preparations, the E_m values were distributed normally, with the mean value falling in the modal class. The mean E_m values recorded from larvae and prepupae (-48 and -47 mV respectively) are not significantly different. (t-test, $p > 0.1$)

The means and distributions of E_m values subsequently measured using the reference barrels of ion-sensitive microelectrodes (ISMs) were compared with the total population of E_m values measured using conventional microelectrodes (figure 51 a,b). Data was accepted from ISMs only when measured values of E_m fell in the range recorded by conventional microelectrodes.

III.2. Intracellular ionic activity measurements in larvae and prepupae of *Calliphora*

K^+-, Na^+- and Cl^--sensitive microelectrodes were manufactured and calibrated by the methods described in section II. Each ISM was advanced into a preparation under direct microscopical control, and used to impale individual muscle cells bathed in Rice's saline (for composition, see appendix 1). Results were selected on the basis of the criteria listed in section

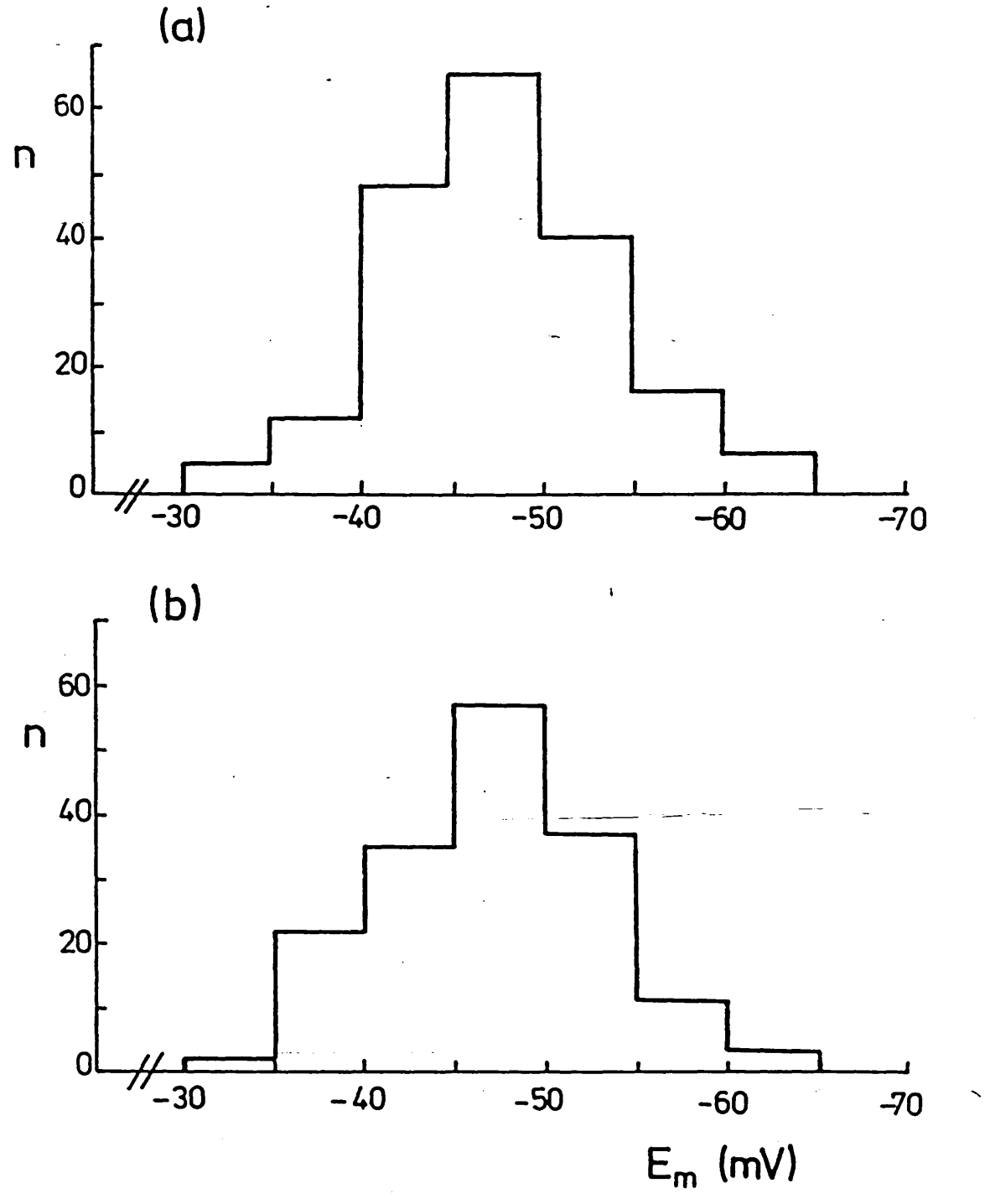


Fig. 51 Frequency histograms showing the distribution of E_m values measured using OM's a. in *Calliphora* larvae b. in prepupae.

II.5, and derived from the raw data recorded on chart paper as described in section II.4.ii. Full lists of data from individual cells are given in appendices 8, 9 and 10. Data from different preparations are separated by short spaces. The first column lists the membrane potentials of the cells (E_m), the second, the voltage response of the ISM to the ion 'x' (either K^+, Na^+ or Cl^-), V_x. The third column shows the intracellular activities of 'x' corresponding to the column 2 values, a_x^i, and the fourth, the corresponding equilibrium potential, E_x. The fifth column indicates the difference between E_x and E_m for each cell.

III.2. Intracellular K^+ activities

Intracellular K^+ activities, a_K^i's were measured in larval and prepupal preparations using K^+-sensitive microelectrodes based on each of two types of K^+-sensor: a liquid ion-exchanger, LIX (Corning code 477317), and a valinomycin-based neutral ion carrier, NIC (Oehme & Simon, 1976).

The reason for using the two types of K^+-sensor was that the Corning LIX was known to be more prone to interference (see section I.3.i) and it therefore seemed crucial to double-check measurements made using the LIX.

III.2.i. Larvae

Typical K^+-ISM recordings obtained from *Calliphora* larvae are shown in figures 52 (LIX-) and 53 (NIC-type ISMs). In each, the upper trace shows the reference potential and the lower, the K^+-sensitive potential. Cells were impaled at the point marked by the arrowhead, where rapid deflections are seen in each trace, giving new values for each parameter which remained steady for many minutes.

The LIX-type ISM gave a membrane potential, E_m, of -52 mV and an intracellular K^+ activity, a_K^i, of 109 mM for the cell shown in figure 52. This a_K^i value corresponds to a potassium equilibrium potential, E_k, of -61 mV, which is 9 mV more negative than the E_m. The NIC-type ISM gave an E_m of -44 mV, an a_K^i of 100 mM and an E_K of -59 mV for the cell in figure 53. This E_K is also more negative than E_m, by 15 mV. Similar data was obtained from 80 cells (10 preparations) using LIX-type ISMs and from 115 cells (11 preparations) using NIC-type ISMs. The average values for a_K^i, E_K and E_m obtained are given in table 10 below.

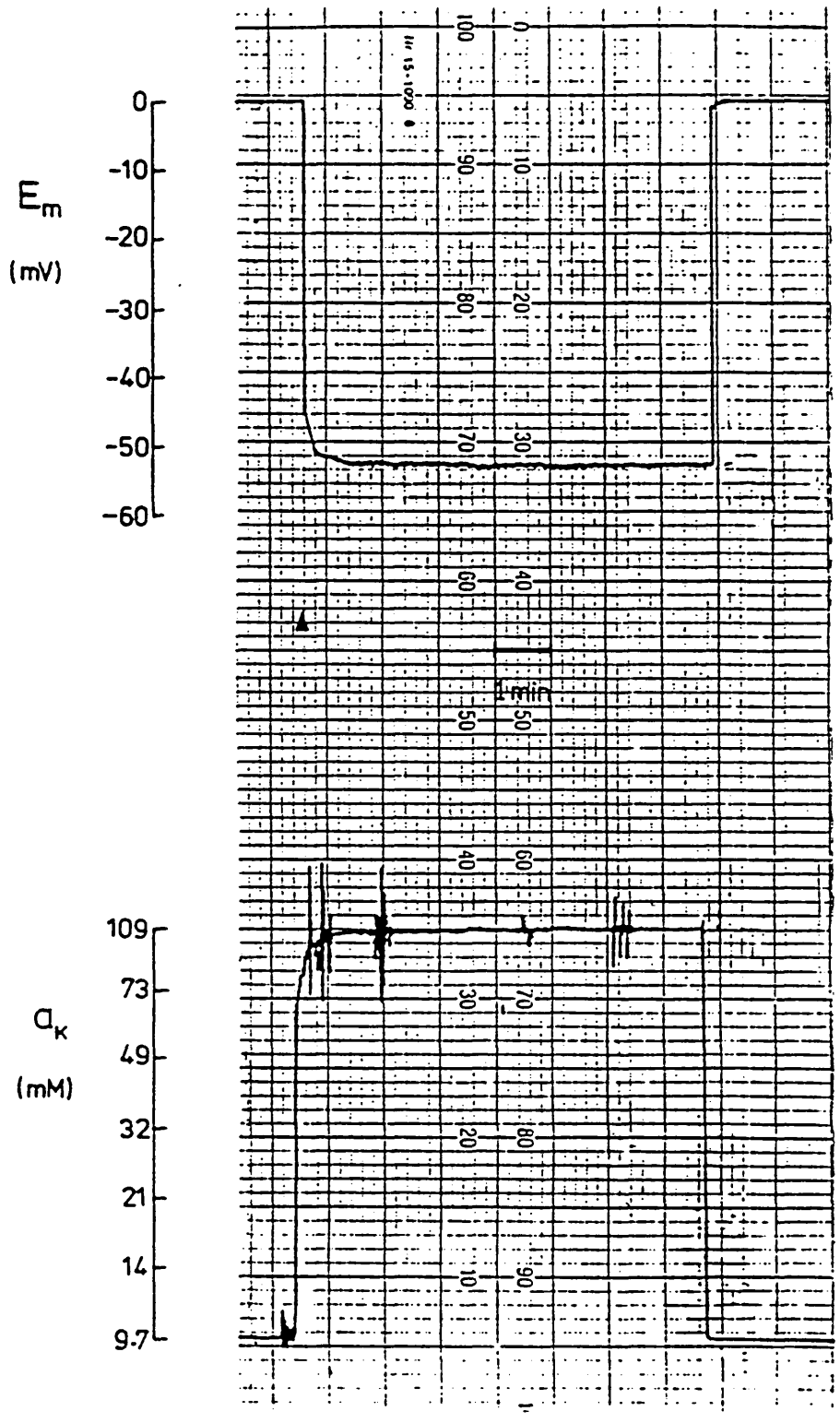


Fig. 52 Chart recording showing a typical impalement of a *Calliphora* larval muscle cell with a LIX-type K^+ ISM. E_m denotes the potential recorded by the reference barrel, and a_K, the potassium activity. The cell was impaled at the point indicated by an arrowhead.

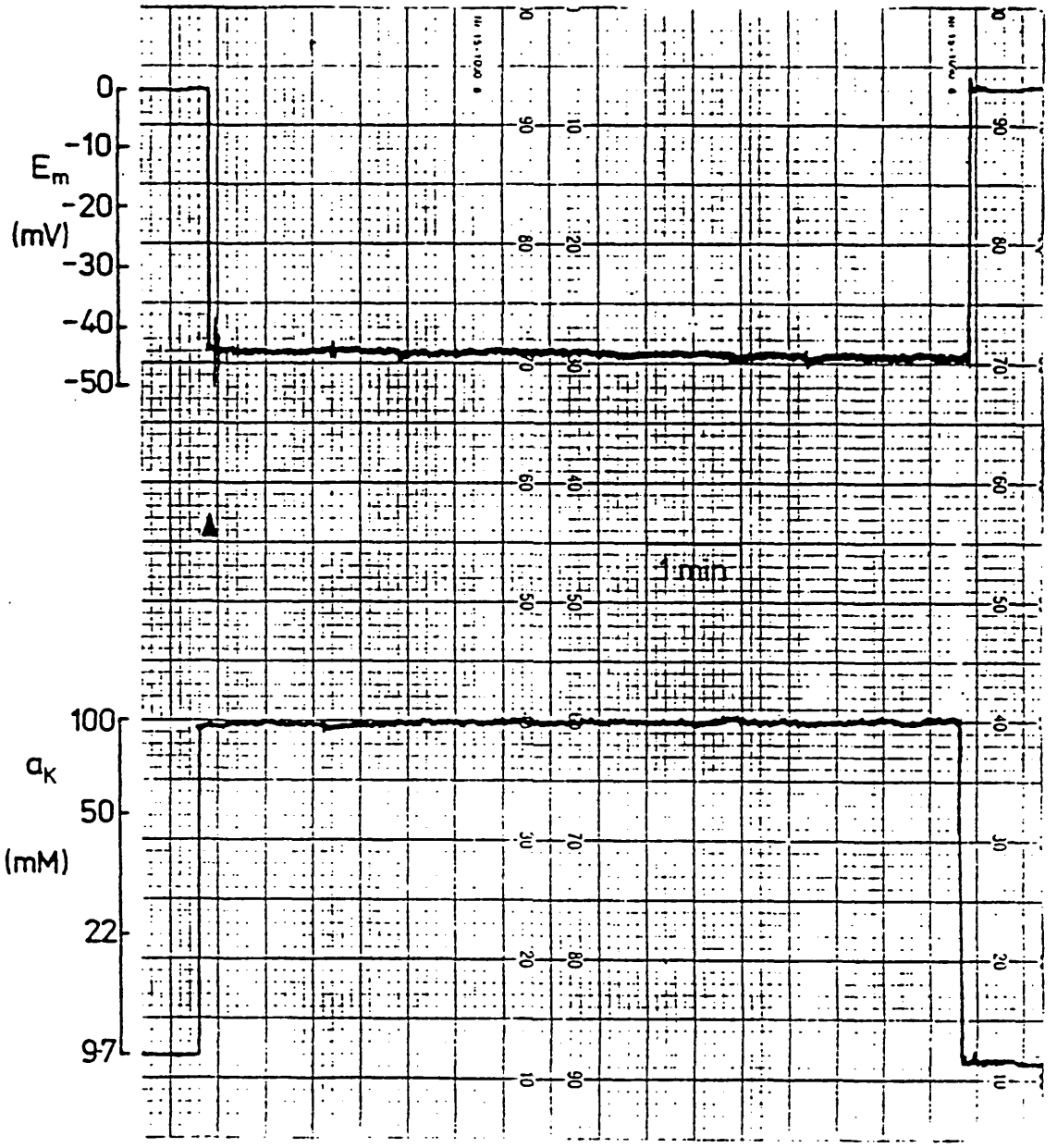


Fig. 53 Chart recording from a *Calliphora* larval muscle cell with a NIC-type K^+ ISM, showing changes in potential and a_K during an impalement.

Table 10 Intracellular K^+ activity data from *Calliphora* larvae (Data from 80 cells, 8 preparations for LIX-type ISMs; from 115 cells, 8 preparations for NIC-type ISMs. Data given as mean ± S.E.)

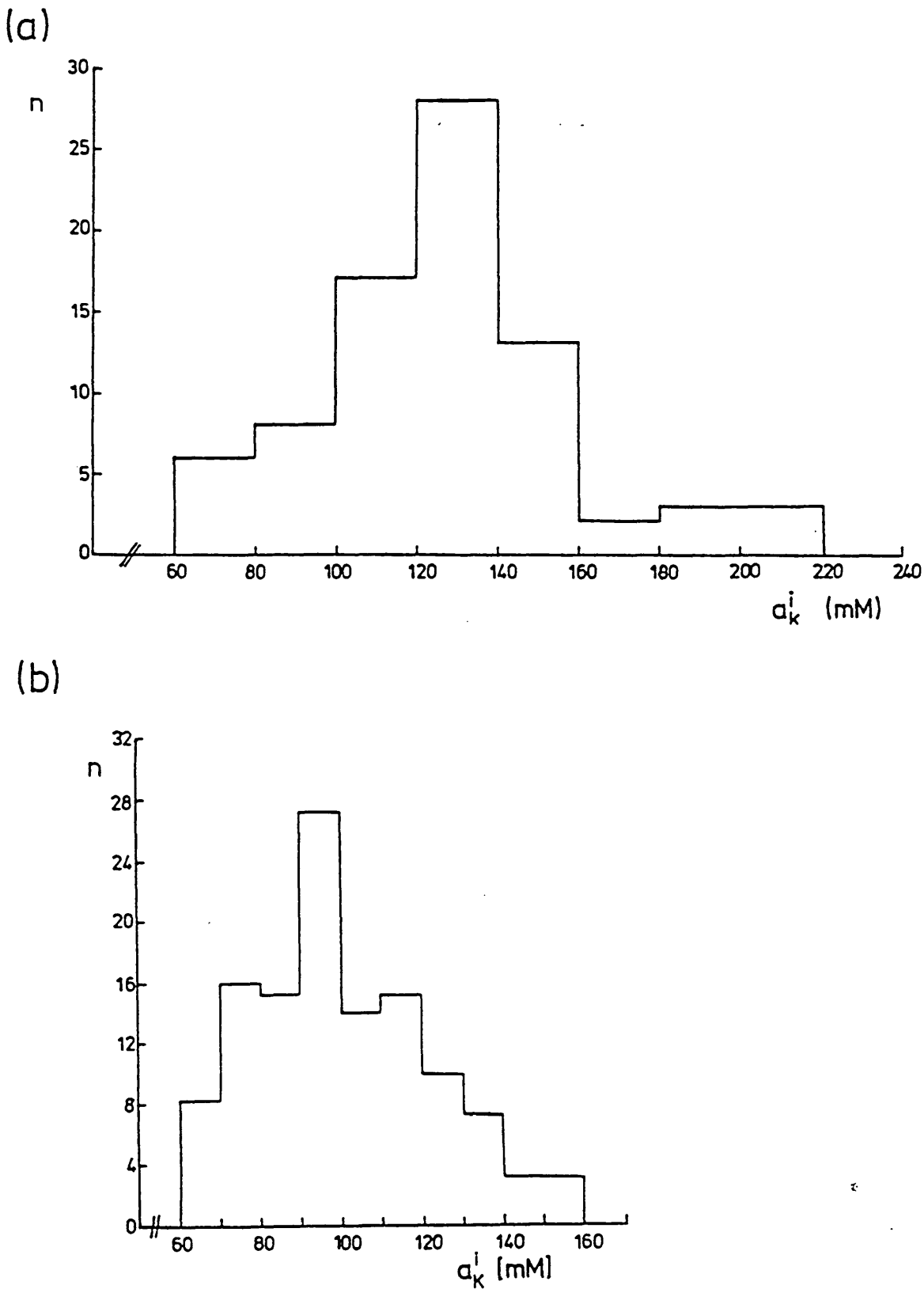
	LIX	NIC
a_K^i(mM)	129 ± 4	102 ± 2
E_K (mV)	-64 ± 1	-59 ± 1
E_m (mV)	-46 ± 1	-47 ± 1
E_K-E_m (mV)	-18 ± 1	-11 ± 1

Thus, the average a_K^i recorded using LIX-type ISMs is significantly higher than that recorded using NIC-type ISMs ($p < 0.001$, t-test). This is likely to be due to the presence of an interferent to which the LIX responds, giving atifically high values for apparent a_K^i.

The frequency histogram for intracellular K^+ activities, a_K^i, measured in larval muscle cells using LIX- and NIC-type K^+ ISMs is shown in figure 54 a,b. (In this and all subsequent histograms, the abscissa is divided into suitable intervals, with results being grouped into classes accordingly. A given class contains values greater than its lower limit, up to and including the upper limit. The ordinate represents the frequency (number of cells) with which values fall into each class).

The values of a_K^i recorded using the two types of ISM followed approximately normal distributions. Those obtained using LIX-type ISMs ranged from 61 to 215 mM, and the mean (129 mM) falls in the modal class, 120 to 140 mM. This range is considerably wider than that of values recorded using NIC-type ISMs (62 to 165 mM), with a mean of 102 mM, which falls close to the modal class.

The populations of values obtained for potassium equilibrium potentials, E_K's, and the corresponding membrane potentials, E_m's measured using the two types of ISM are compared in the form of frequency histograms in figures 55 and 56. Data from LIX-type ISMs is illustrated in figure 55, which shows that both E_m and E_K are normally distributed, with mean values (-64 mV forE_K, -46 mV for E_m) close to the peaks of the histograms. The ranges of the two parameters are comparable in width: E_K ranged from -46 to -77 mV, E_m, from -34 to -63 mV. E_K was more negative than E_m by an average of 18



Pig. 54 Frequency histogram showing the distribution of a_K^i values measured in *Calliphora* larval muscle cells, a. using LIX-type K^+ ISM's and b. using NIC-type K^+ ISM's.

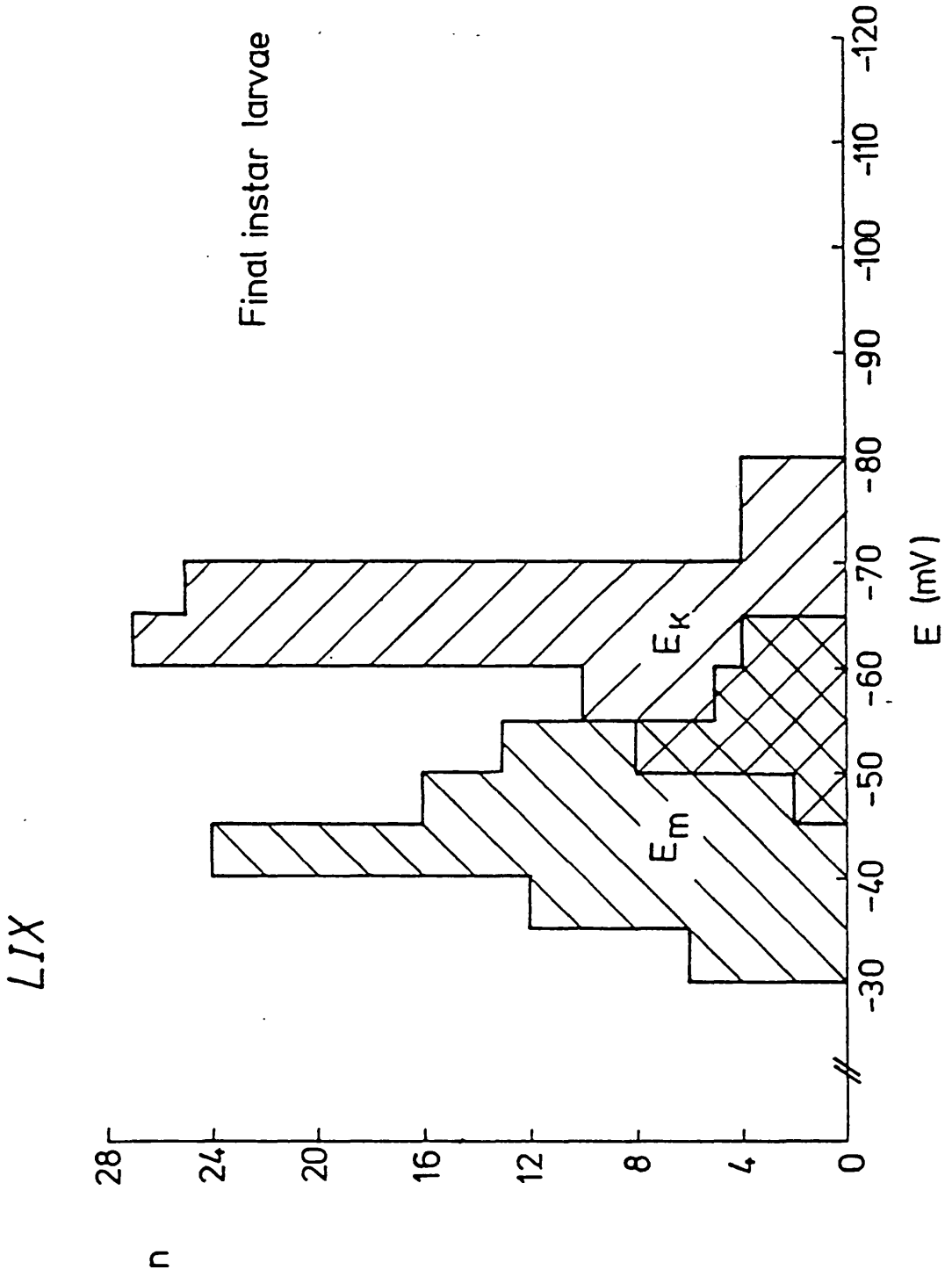


Fig. 55 Frequency histograms illustrating the distributions of membrane potentials (E_m) and potassium equilibrium potentials (E_K) as measured in *Calliphora* larvae using LIX-type K^+ ISMs, on the same abscissa for comparison.

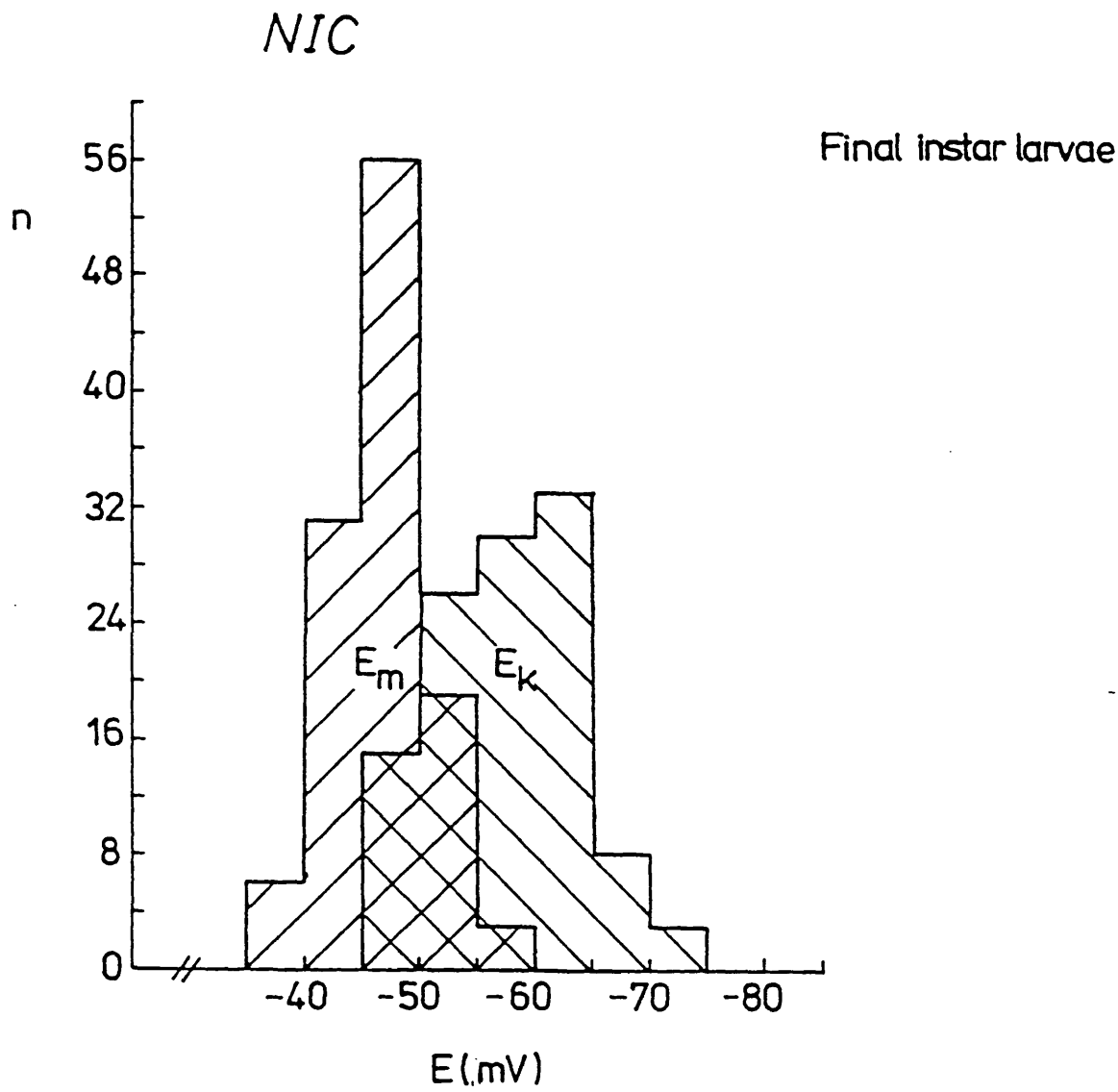


Fig. 56 Frequency histograms illustrating the distributions of membrane potentials (E_m) and potassium equilibrium potentials (E_K) as measured in *Calliphora* larvae using NIC-type K^+ ISMs, on the same abscissa for comparison.

mV, which is reflected to some extent by the separation of the peaks of the E_K and E_m histograms.

Data from NIC-type ISMs is shown in figure 56. The form of the histograms is very similar to that of the LIX-type ISM data (cf. figure 55). Both E_m and E_K values are normally distributed, with the mean values (-47 mV for E_m, -59 mV for E_K) falling close to the modal class in each case. E_K values were between -48 and -69 mV, E_m's between -38 and -58 mV: thus, the widths of the distributions of the two parameters were comparable. As for the LIX-type ISM data, E_K was consistently more negative than E_m in all cells impaled, by an average of 11 mV (cf 18 mV in the case of LIX-type ISM data).

A comparison between the mean and distribution of E_m values recorded in larvae using LIX- and NIC-type K^+-ISMs (figures 55 and 56, respectively) with those recorded using conventional microelectrodes (OM's) (figure 51a) confirmed that ISMs did not cause significant damage to the muscle cell membranes during the impalement of cells. The E_m values recorded using LIX-type ISMs ranged between -34 and -63 mV, with a mean of -46 mV; those recorded using NIC-type ISMs between -38 and -58 mV with a mean of -47 mV. These correspond closely to E_m values obtained using OMs, which were between -33 and -64 with a mean of -48 mV. (The latter does not differ significantly from-46 mV or -47 mV (t-test, $p < 0.05$).

Thus the potassium equilibrium potential, E_K, as calculated from a_K^i values measured using both LIX- and NIC-type K^+ ISMs, was consistently more negative than the membrane potential. This indicates that K^+ is not the only ion involved in generating E_m in *Calliphora* larvae: if E_m were generated solely by K^+, E_K would be close to E_m in value.

III.2.ii. Prepupae

Figures 57 and 58 show typical recordings obtained from prepupal muscle cells using LIX- and NIC-type K^+ ISMs, respectively. The upper trace shows the reference potential, and the lower, the potential corresponding to K^+ activity. The cell was impaled at the point marked by the arrowhead. The LIX-type ISM gave a membrane potential, E_m, of -60 mV, and intracellular K^+ activity, a_K^i of 355 mM for the cell shown in figure 57. This a_K^i value corresponds to a potassium equilibrium potential, E_K, of -91 mV,

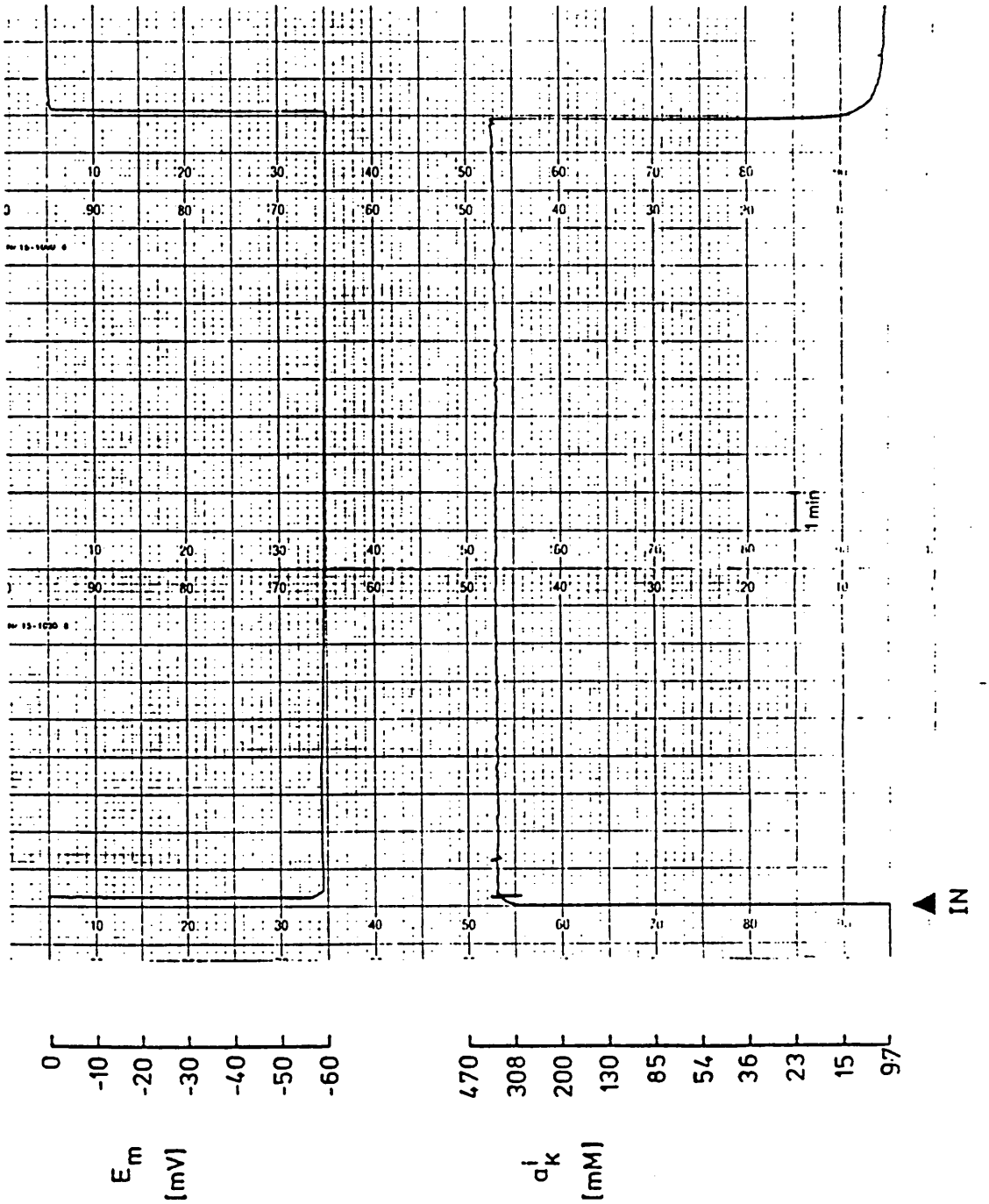
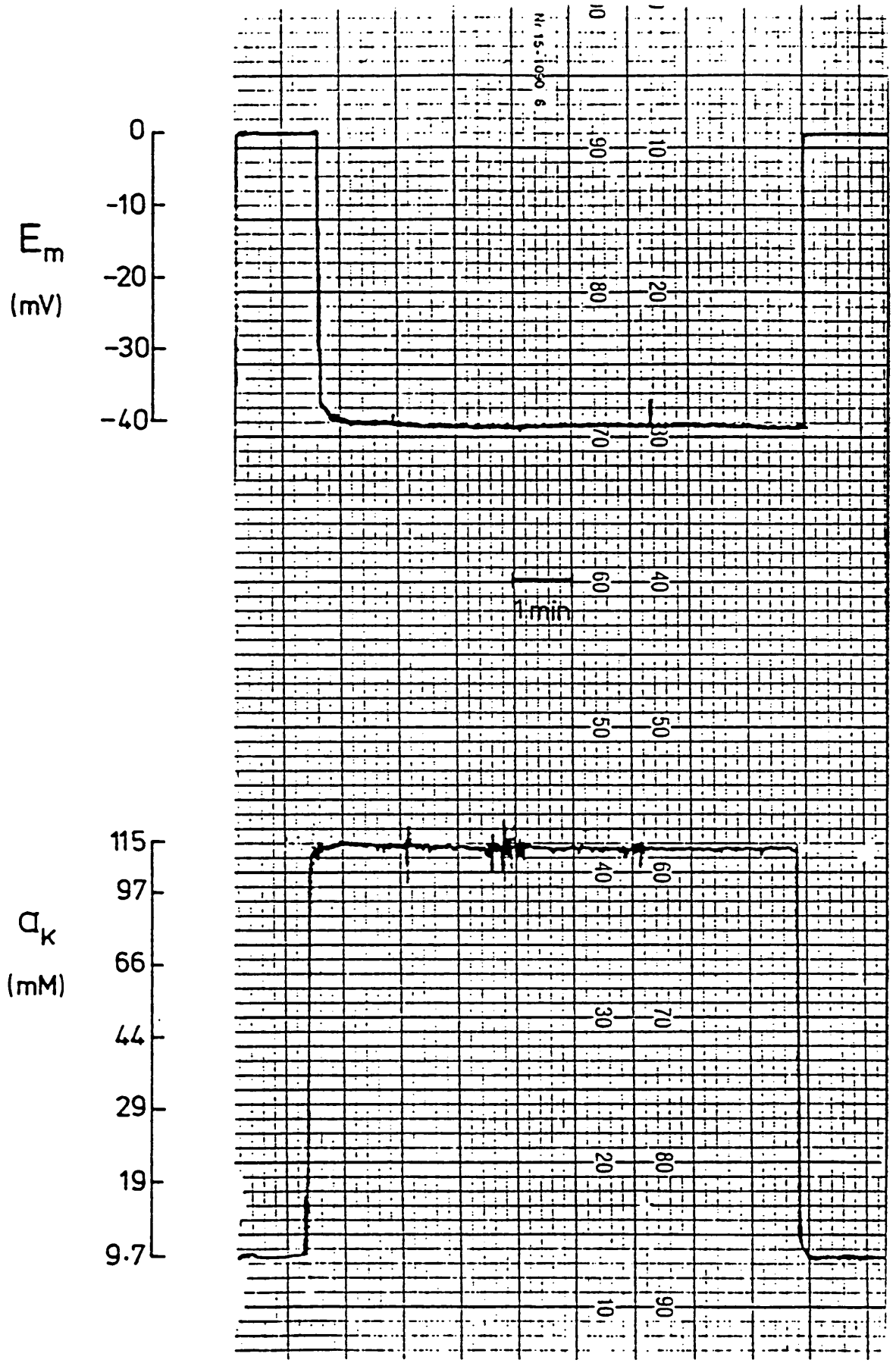


Fig. 57 Chart recording of the impalement of a *Calliphora* prepupal muscle cell using a LIX-type K^+ ISM.



Pig. 58 Chart recording of the impalement of a *Calliphora* prepupal muscle cell using a NIC-type K^+ ISM.

which is 31 mV more negative than E_m. The NIC-type ISM recorded an E_m of -40 mV and an a_K^i of 115 mM corresponding to an E_K of -62 mV for the cell shown in figure 58. This E_K is 22 mV more negative than E_m. Similar data was obtained from 96 cells (7 preparations) using LIX-type ISMs and from 85 cells (10 preparations) using NIC-type ISMs. The average values recorded for a_K^i, E_K and E_m are given in table 11 below.

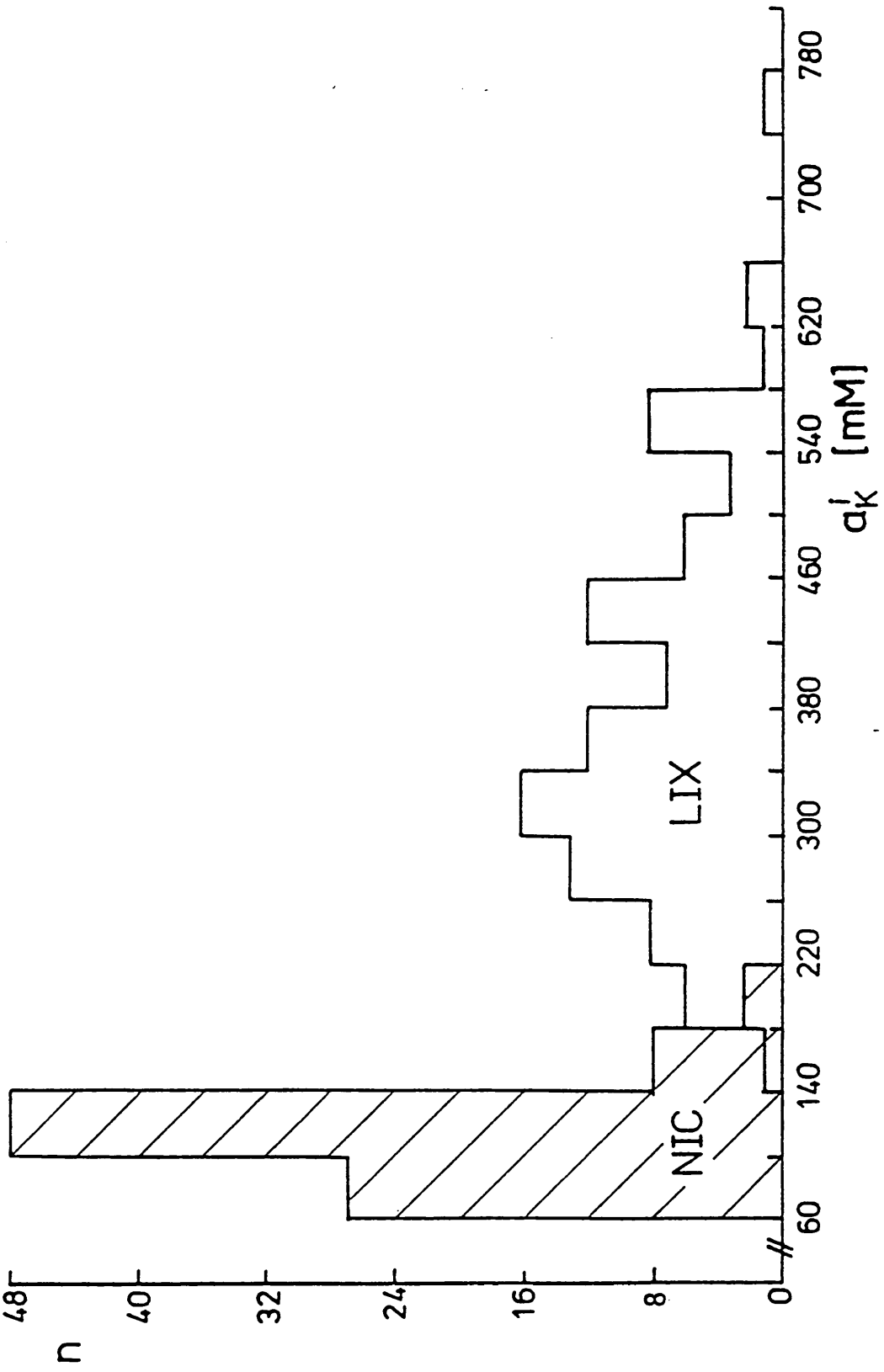
Table 11 Intracellular K^+ activity data from *Calliphora* prepupae

Data is given as mean ± SE for 96 cells, 7 preparations (LIX-type ISMs); 85 cells, 10 preparations (NIC-type ISMs)

	LIX	NIC
a_K^i (mM)	382 ± 12	115 ± 3
E_K (mV)	-91 ± 1	-62 ± 1
E_m (mV)	-50 ± 1	-47 ± 1
E_K-E_m (mV)	-41 ± 1	-15 ± 1

Thus, the average a_K^i value recorded using LIX-type ISMs (382 mM) was more than three times larger than that recorded using NIC-type ISMs (115 mM). This may be attributed to the presence of an interferent in prepupal muscle cells to which the K^+ LIX responds, giving very high values for apparent a_K^i. The frequency histograms for the above a_K^i data are shown in figure 59. Both LIX- and NIC-type ISM data are approximately normally distributed with the mean values falling in or close to the modal class. The range of a_K^i values recorded using LIX-type ISMs was far wider than that recorded using NIC-type ISMs (150 to 760 mM cf a total range of 68 to 210 mM using NIC-type ISMs, with 98% of values falling between 68 and 170 mM).

The populations of E_K and E_m values obtained using the two types of ISM are compared in figures 60 and 61. The E_K values recorded using LIX-type ISMs ranged between -69 and -114 mV and E_m varied from -34 and -68 mV (figure 60). Both parameters were normally distributed, with the mean value close to the modal class. Values of E_K were consistently more negative than E_m values in all cells studied, by an average of 41 mV. This fact is illustrated by the clear separation between the two populations of values. The E_K values recorded using NIC-type ISMs fell in the range -49 to -77 mV, with E_m varying between -34 and -63 mV (figure 61). In both histograms, the mean falls in the modal class. Thus, as described for



Pig. 59 Frequency histograms illustrating the distributions of a_K^i values measured in *Calliphora* prepupae using LIX- and NIC-type K^+-ISMs, on the same abscissa for comparison.

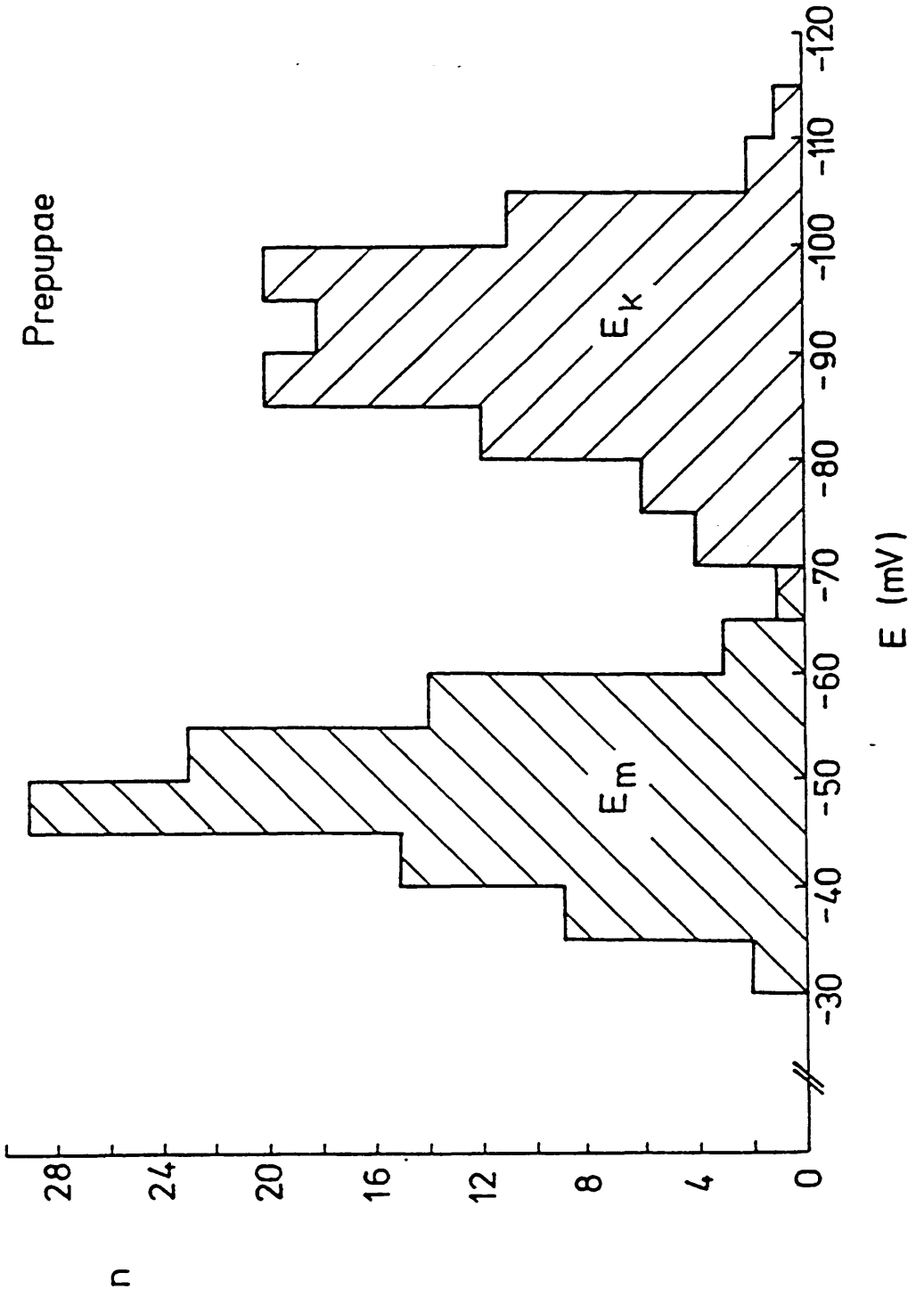


Fig. 60 Frequency histograms illustrating the distributions of membrane potentials (E_m) and potassium equilibrium potentials (E_K) measured in *Calliphora* prepupae using LIX-type K^+-ISMs, on the same abscissa for comparison.

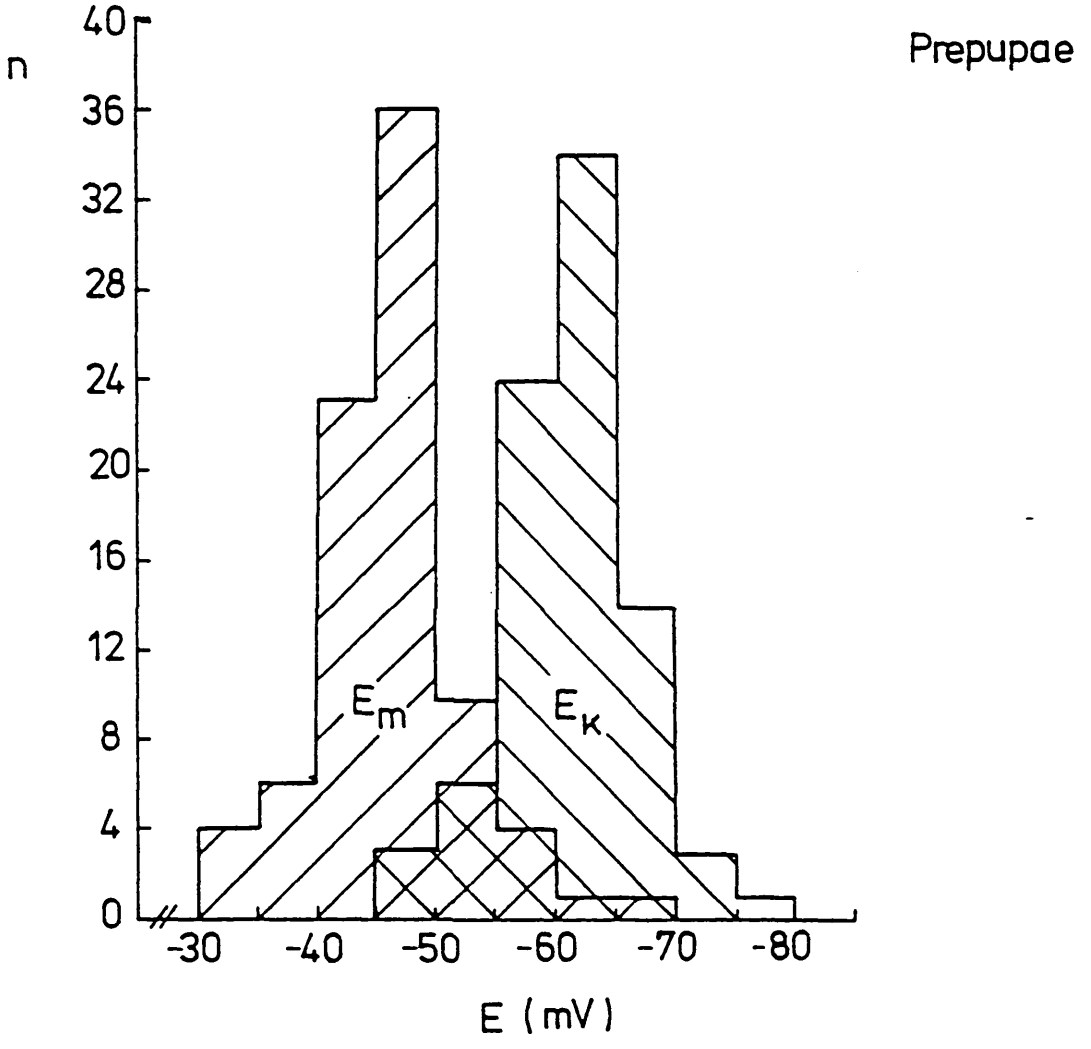


Fig. 61 Frequency histograms illustrating the distributions of E_m and E_K values measured in *Calliphora* prepupae using NIC-type K^+-ISMs, on the same abscissa for comparison.

LIX-type ISM data, E_K was consistently more negative than E_m, by an average of 15 mV (cf. 41 mV for LIX-type ISM data). This again indicates that K^+ is not the only ion involved in generating E_m.

The mean and distributions of E_m values recorded from prepupae using LIX- and NIC-type ISMs were compared with those obtained using conventional microelectrodes (figure 51 b), confirming that ISMs did not cause significantly more damage to the cell membranes than conventional microelectrodes. The E_m values recorded using LIX-type ISMs ranged between -34 and -68 mV (mean -50 mV), and those recorded with NIC-type ISMs were between -34 and -63 mV (mean -47 mV). Both the ranges and means of these populations of E_m values are similar to those recorded in prepupae using conventional microelectrodes: -35 to -62 mV with a mean of -47 mV (figure 51 b). This confirms that ISMs record the 'real' situation in cells.

II.2.iii Comparisons of larval and prepupal K^+ data, obtained using LIX- and NIC-type K^+-ISMs

The data obtained for larvae and prepupae using liquid ion exchanger (LIX) and neutral ion carrier (NIC)-type K^+-sensitive microelectrodes is summarised in table 12 below.

Table 12. Intracellular K^+ activity data from *Calliphora* larvae and prepupae obtained using LIX- and NIC-type K^+ ISMs. (Data is given as mean ± S.E)

	LARVAE		PREPUPAE	
	LIX	NIC	LIX	NIC
a_K^i (mM)	129 ± 4	102 ± 2	382 ± 12	115 ± 3
E_K (mV)	-64 ± 1	-59 ± 1	-91 ± 1	-62 ± 1
E_m (mV)	-46 ± 1	-47 ± 1	-50 ± 1	-47 ± 1
E_K-E_m (mV)	-18 ± 1	-12 ± 1	-41 ± 1	-15 ± 1
	n = 80 cells	115 cells	96 cells	85 cells

Thus, the Corning LIX, 477317, is clearly prone to interference by one or more compounds which are present in both larval, and, to a greater extent, prepupal, muscle cells. There is, however, a significant difference between the average a_K^i values in larvae and prepupae as measured using NIC-type

ISMs (102 and 115 mM, respectively) ($P < 0.001$, t-test), and a corresponding difference between the calculated values of E_K in the two preparations (-59 and -62 mV, respectively). This indicates that there is a real increase of around 10% in intracellular K^+ activity during the 'development' from larva to prepupa. This may reflect the maturation of a K^+ pumping mechanism.

A frequency histogram comparing the populations of a_K^i values in prepupal cells, measured using the two types of ISM (fig. 59) shows that the range of the distribution is widest and the mean highest for the data obtained using LIX-type ISMs. The latter results from the presence of interfering ions in the prepupal muscle cells. The discrepancy between the a_K^i values measured by the two methods is reflected in the size of the difference between E_m and E_K in each case (figures 60, 61; table 12). The mean difference given by LIX-type ISMs is 41 mV; that given by NIC-type ISMs, 15 mV. The range of a_K^i and hence E_K values is also much larger for LIX than NIC data (figures 59, 60 and 61).

The fact that the potassium equilibrium potential is more negative than the E_m in both preparations, irrespective of the type of K^+ ISM used, indicates that K^+ is not the only ion involved in resting membrane electrogenesis. A second ion 'x', with its equilibrium potential, E_x, more positive than E_m, might also be expected to play a part. The most likely candidate for this ion is Na^+. The following sections describe measurements of intracellular Na^+ and Cl^- activities, designed to obtain information about the values of the sodium and chloride equilibrium potentials, E_{Na}, and E_{Cl}, respectively, relative to the membrane potential.

III.3. Intracellular Na^+ activities

Intracellular Na^+ activity measurements were made in larval and prepupal preparations using ISMs based on a neutral ion carrier, ETH 227 (Steiner *et al*, 1979). The properties of the latter are discussed in sections I.3.iii and II.1.vi.

III.3.i. Larvae

A typical impalement of a larval muscle cell with a Na^+-sensitive microelectrode is shown in figure 62. The upper trace shows the potential

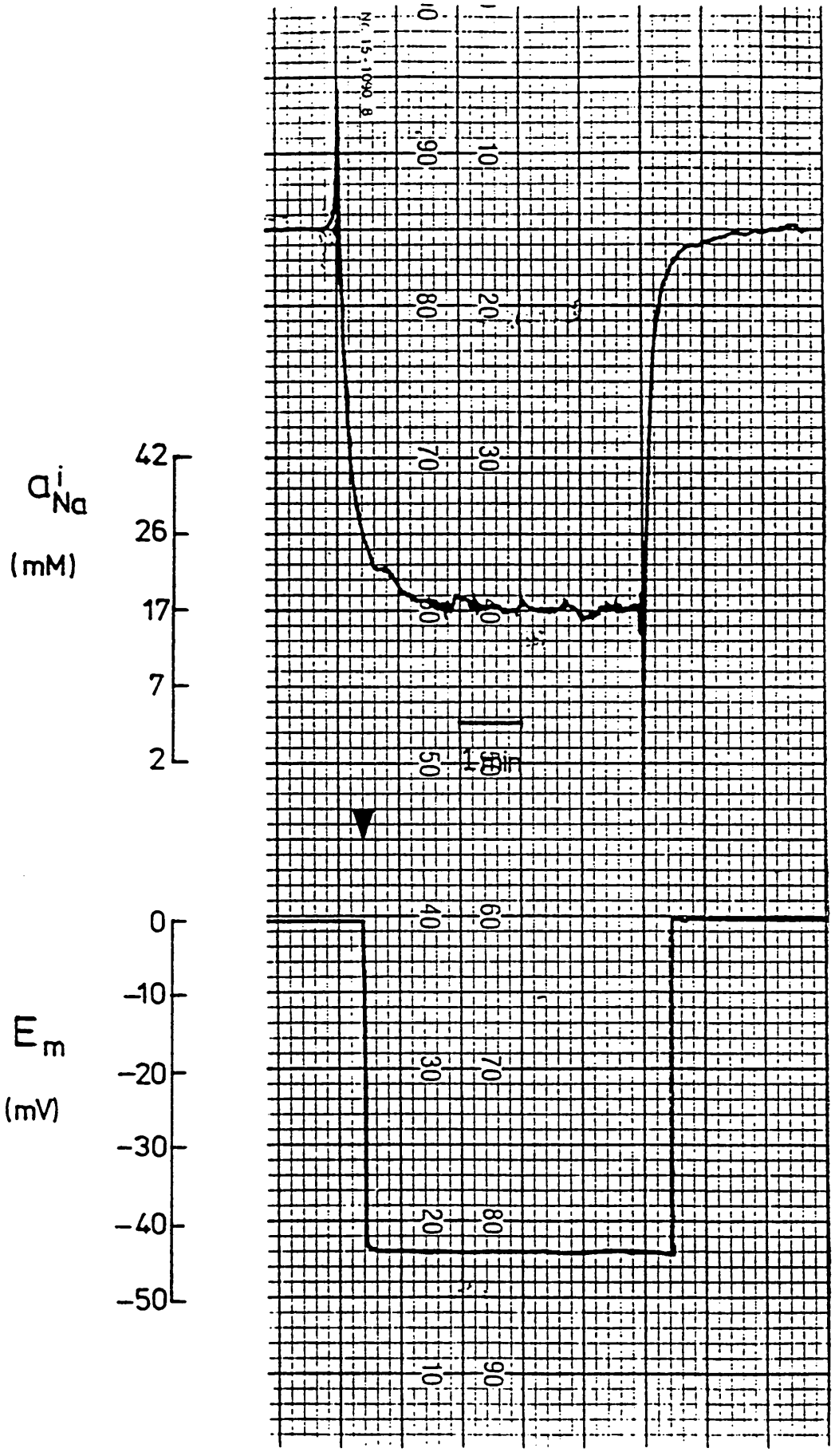


Fig. 62 Chart recording of the impalement of a *Calliphora* larval muscle cell with a Na^+ ISM. a^i_{Na} represents the level of intracellular Na^+, E_m, the reference potential.

which corresponds to the sodium activity, V_{Na}, and the lower one, the reference potential. The ISM peneterates the cell at the point marked by an arrowhead, and an immediate sharp deflection is seen in both traces. A new steady level is almost instantaneously reached by the reference potential. Due to the rather slow response time of the Na^+- NIC, however, the Na^+-sensitive potential takes up to 3 minutes to reach a new steady state after impaling a cell. Since Na^+ ISMs were calibrated in solutions which resembled the intracellular medium (section II.1.vi), the intracellular value of V_{Na} was referred directly to the calibration curve of the ISM. For the same reason, the a_{Na}^i scale has been drawn adjacent only to the intracellular level of potential. Recordings were accepted only from cells where the impalement had been maintained for 4 minutes or longer, as described under 'criteria for selection of results', section II.5. For this reason, data satisfying these criteria were difficult to obtain, and smaller numbers of reliable impalements were made using Na^+-sensitive microelectrodes, than using K^+ or Cl^- sensitive ones.

The trace shown in figure 62 is a recording made with a double-barrelled Na^+ sensitive microelectrode from a cell with an intracellular Na^+ activity, a_{Na}^i, of 17 mM (upper trace) and an E_m of -44 mV. This a_{Na}^i value corresponded to a sodium equilibrium potential, E_{Na}, of 50 mV. Similar recordings were made from 30 cells in 5 preparations, giving the average data shown in table 13 below.

Table 13 Intracellular Na^+ activity data from *Calliphora* larvae.
(Data is given as mean ± SE from 30 cells, 5 preparations).

a_{Na}^i :	11 ± 1 mM
E_{Na} :	65 ± 2 mV
E_m :	-48 ± 1 mV
E_{Na}-E_m:	113 ± 2 mV

Frequency histograms illustrate the distributions of these parameters (figures 63a, 64a, 65a). The a_{Na}^i histogram (figure 63a) has a normal distribution with a range of 4.5 to 24 mM and the mean (11 mM) falls in the modal class.

The sodium equilibrium potential values, E_{Na}, calculated from these a_{Na}^i values were consistently positive, with a range of 41.5 to 83.6 mV and a

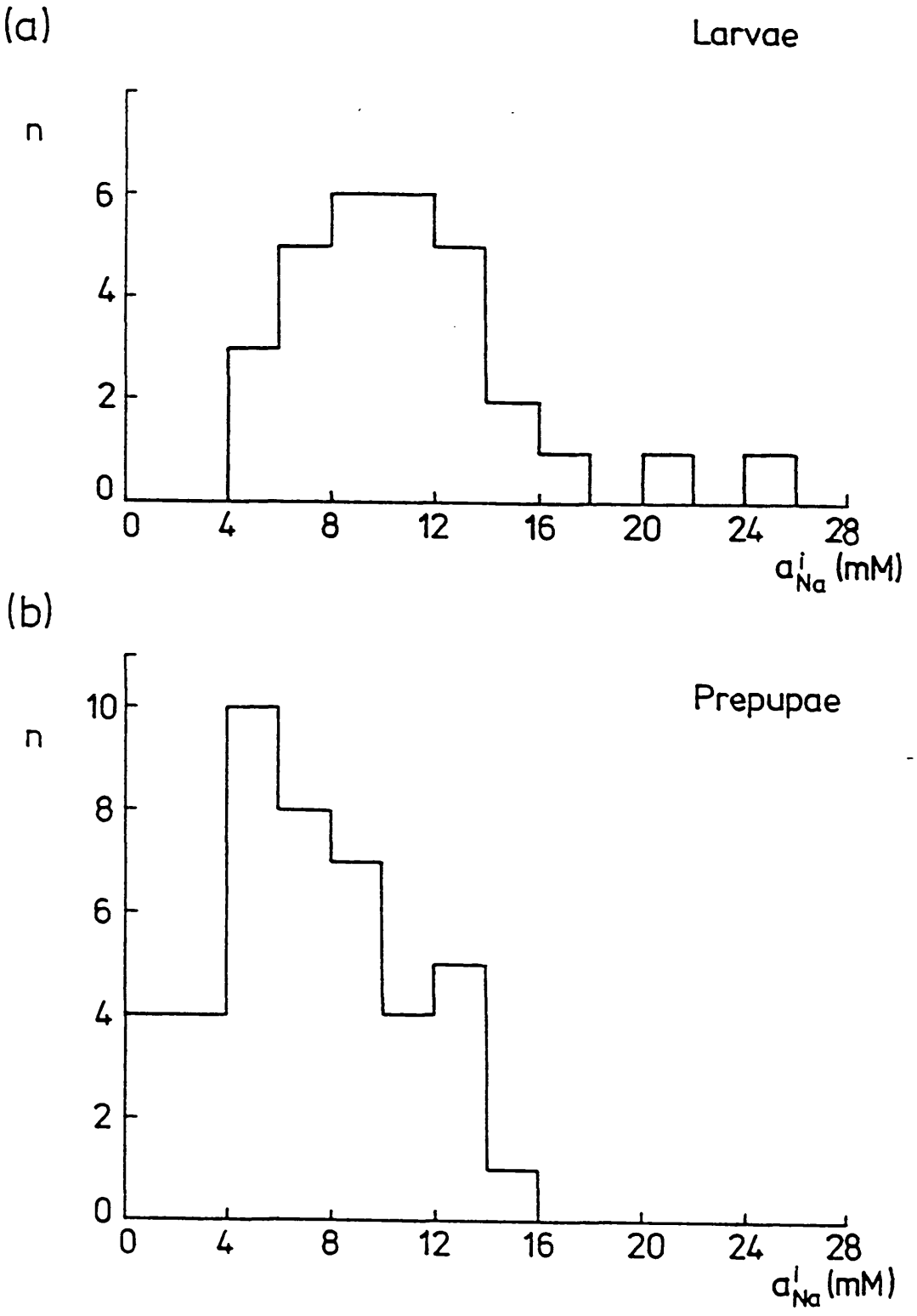
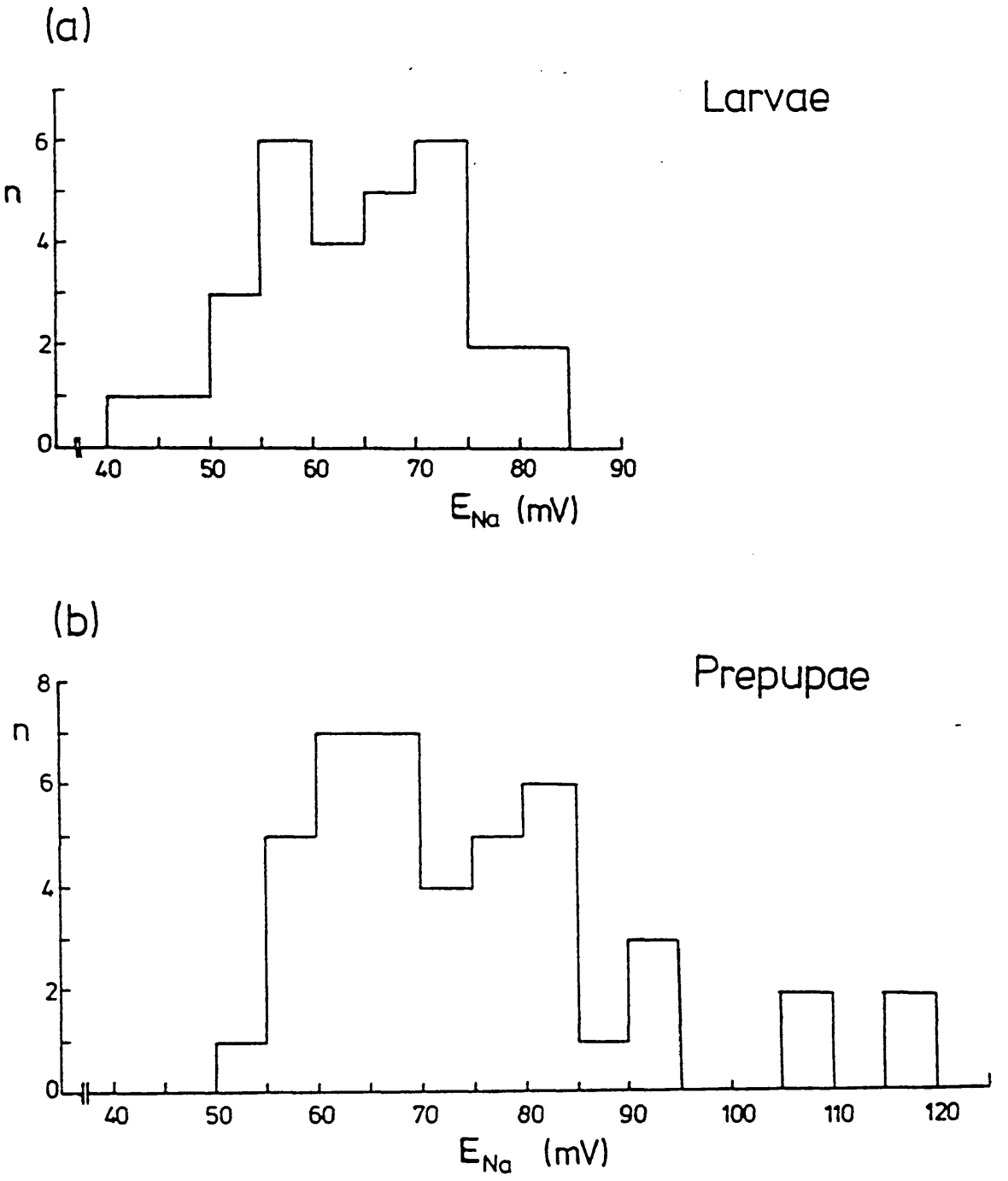


Fig. 63 Frequency histograms illustrating the distributions of a_{Na}^i values measured, a. in *Calliphora* larvae and b. in prepupae.



Pig. 64 Frequency histograms illustrating the distributions of sodium equilibrium potential values E_{Na}, a. in *Calliphora* larvae and b. in prepupae.

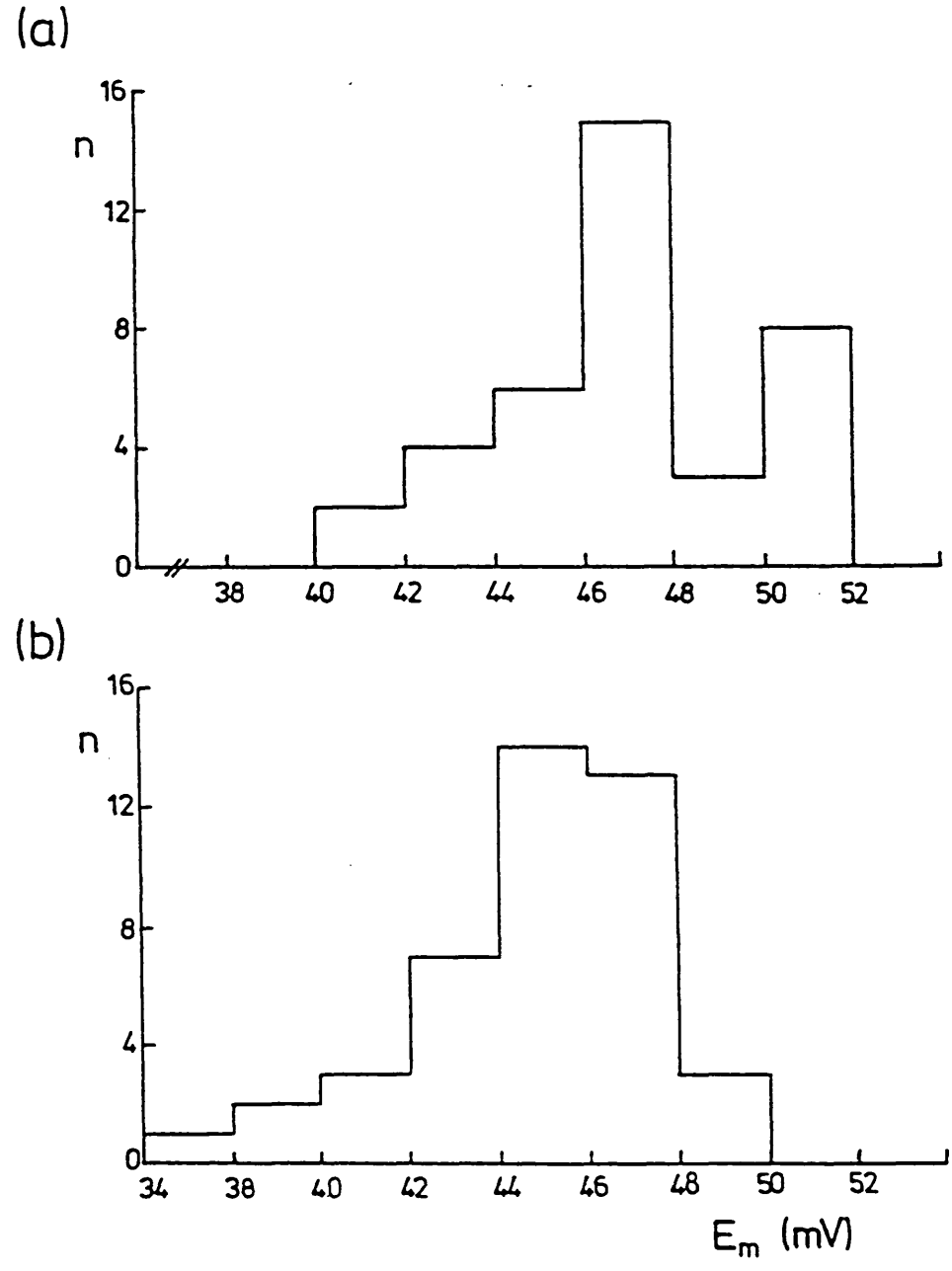


Fig. 65 Frequency histograms illustrating the distributions of E_m values recorded, a. in *Calliphora* larvae and b. in prepupae using Na^+-ISMs.

somewhat irregular distribution. This, together with the asymmetry of the distribution of E_m values recorded using Na^+-ISMs (figure 64a) is likely to be due to the small number of cells impaled. A comparison between the distributions of E_m values measured using conventional and Na^+-sensitive microelectrodes (figures 51, 65a) shows that, although a narrower range of values was recorded with Na^+-ISMs (-41 to -52 mV, cf. -33 to -64 mV recorded using OMs) the peaks of the two histograms fell in the same class. This indicates that Na^+ ISMs were not causing significant damage to the cells' membranes during impalements.

III.3.ii. Prepupae

A typical recording obtained from prepupal muscle cells is illustrated in figure 66. As in figure 62, the upper trace corresponds to Na^+ activity, and the lower one is the reference potential. The intracellular Na^+ activity, a_{Na}^i, of the cell was 9 mM (which remained steady for around 4 minutes), its sodium equilibrium potential, E_{Na}, 66.2 mV, and its membrane potential, E_m, -46 mV. Average data for these parameters from 43 cells, 6 preparations, are shown in table 14, below.

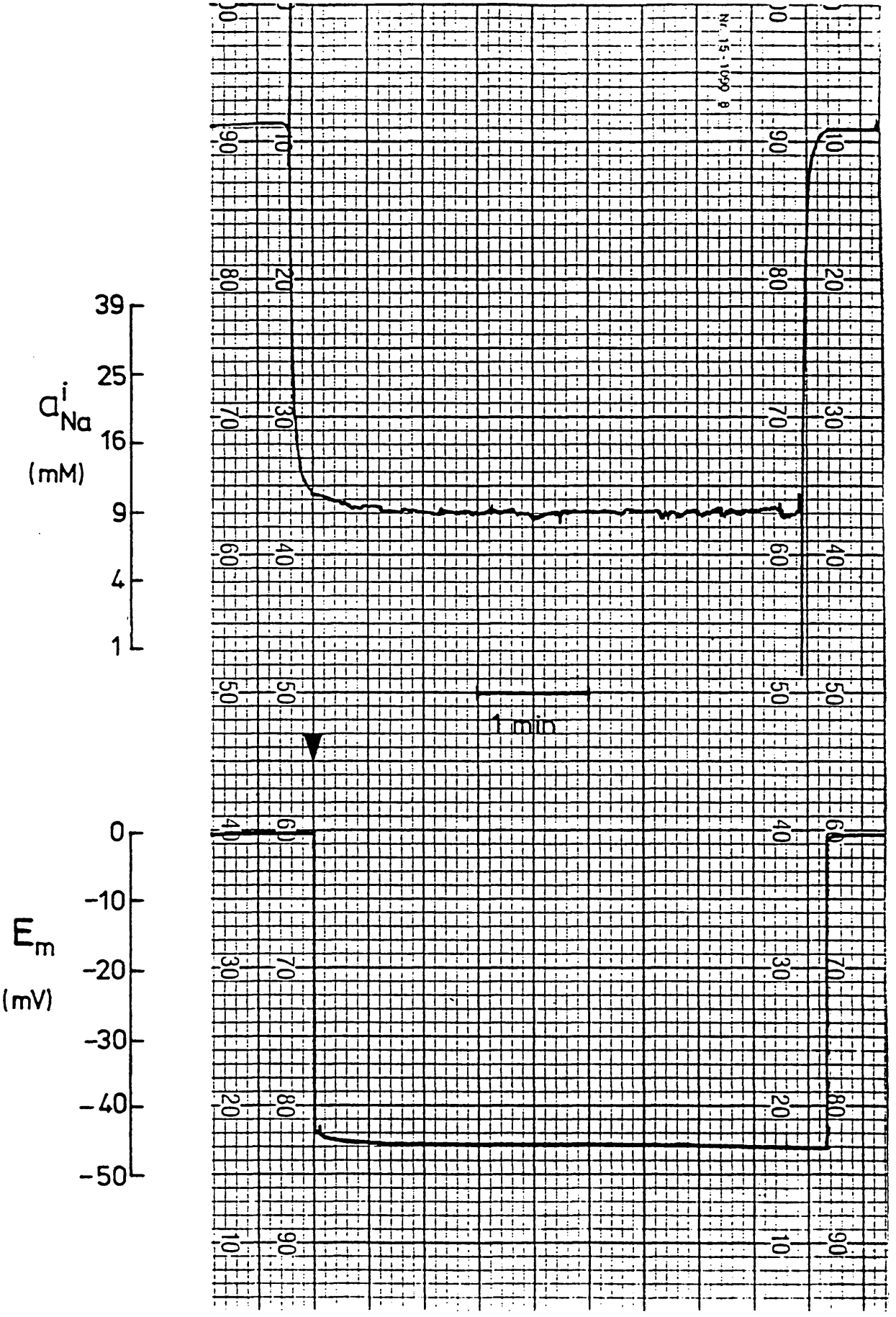
Table 14 Intracellular Na^+ activity data from *Calliphora* prepupae. Data from 43 cells, 6 preparations, given as mean ± SE)

a_{Na}^i :	7 ± 1 mM
E_{Na} :	76 ± 2 mV
E_m :	-46 ± 1 mV
E_{Na}-E_m:	122 ± 3 mV

The distributions of the population of values for each parameter are illustrated in frequency histograms (figures 63b, 64b, 65b). The histogram showing a_{Na}^i data (figure 63b) has a somewhat irregular distribution. This is likely to be due to chance alone since data from only a relatively small number of cells were accepted. The calculated E_{Na} values were consistently positive, covering a wide range (56.5 to 116.9 mV) (figure 64b) with an approximately normal distribution.

The values of E_m recorded in prepupae using Na^+ ISMs ranged between -38 and -49 mV, and the mean (-46 mV) falls in the modal class of the frequency histogram (fig. 65b).

Fig. 66 Chart recording of the impalement of a *Calliphora* prepupal muscle cell using a Na^+-ISM.



III.3.iii Comparison between larval and prepupal Na^+ data

The intracellular Na^+ data obtained in *Calliphora* larvae and prepupae using NIC-based ISMs is summarised in table 15 below.

Table 15. Intracellular Na^+ activity data from *Calliphora* larvae and prepupae (Data from 30 cells, 5 preparations for larvae, 43 cells 6 preparations for prepupae, listed as mean ± SE.)

	LARVAE	PREPUPAE
a_{Na}^i (mM)	11 ± 1	7 ± 1
E_{Na} (mV)	65 ± 2	76 ± 2
E_m (mV)	-48 ± 1	-46 ± 1
E_{Na}-E_m (mV)	113 ± 2	122 ± 3

The average intracellular Na^+ activity is thus significantly greater in larvae than in prepupae ($p < 0.01$, t-test), (figure 63). This result is consistent with the earlier suggestion (section 3.I.iii) that there may be a maturation of a pumping mechanism during development, tending to pump more K^+ into the cell. Such a pump would also tend to remove Na^+ from the cell, hence the relative lack of Na^+ in prepupal muscle cells, which contain 36% less Na^+ than larval cells.

In all cells studied in both larvae and prepupae, E_{Na} had a positive value. This suggests that Na^+ may be the ion 'x' referred to at the end of section III.2.iii, with its equilibrium potential more positive than E_m, which, in addition to K^+, contributes to resting membrane electrogenesis. The average E_{Na} in prepupae was higher than in larvae (76 mV cf. 65 mV in larve) (figure 64) which reflects the fact that a_{Na}^i tends to be smaller in prepupae than in larvae. The average membrane potentials in the two preparations were similar (-48 mV in larvae, -46 mV in prepupae (figure 65)).

III.4. Intracellular Cl^- activities

III.4.i. Preliminary measurements

Preliminary measurements of intracellular Cl^- activities, a_{Cl}^i's, were made in larvae using ISMs based on the Corning Cl^- exchanger (code 477315) with

the reference barrel filled with a mixture of potassium chloride and potassium sulphate (section II.1.iii, table 7). A typical impalement of a muscle cell is illustrated in figure 67. The upper trace shows the membrane potential of the cell (-53 mV), the lower trace, the chloride-sensitive potential, V_{Cl}. The latter corresponded to an a_{Cl}^{i} of 59 mM, and a chloride equilibrium potential, E_{Cl} of 21 mV. This E_{Cl} value was more positive than E_m by 32 mV. It was, however, noted that the intracellular Cl^- activity of the cell appeared to increase with time following the impalement of the cell (see lower trace, figure 67) and that it did not seem to reach a completely steady level.

Data was obtained using this type of ISM from a total of 48 cells from 4 preparations, giving the average values of a_{Cl}^{i}, E_{Cl} and E_m shown in table 16 below.

Table 16 Intracellular Cl^- activity data for *Calliphora* larvae, measured using ISMs with K_{Cl}/K_2SO_4-filled reference barrels. (Data from 48 cells, 4 preparations, given as mean ± SE).

a_{Cl}^{i}	28 ± 1 mM
E_{Cl}	41 ± 1 mV
E_m	48 ± 1 mV
$E_{Cl}-E_m$	7 ± 1 mV

Figure 68a shows a frequency histogram for the distribution of intracellular Cl^- activity values measured. The latter were all in the range 15 to 50 mM, and were distributed asymmetrically. The distribution of chloride equilibrium potential values calculated from the above a_{Cl}^{i} data is shown in figure 68c and had a range of -25.4 to -54.1 mV.

A comparison between the distributions of E_{Cl} and E_m (fig 68 b,c) showed that in the vast majority (81%) of cells, E_{Cl} was apparently more positive than E_m. In the remainder, E_{Cl} was close to E_m. This unexpected result suggests that Cl^- may not be passively distributed in this insect. A number of other factors could also account for this result, however. Firstly, the Corning Cl^- LIX 477315 is known to be rather unselective (Baumgarten, 1981), responding to a range of anions in addition to Cl^-, eg. HCO_3^-. The presence of such anions in the cell could thus have led to the active barrel

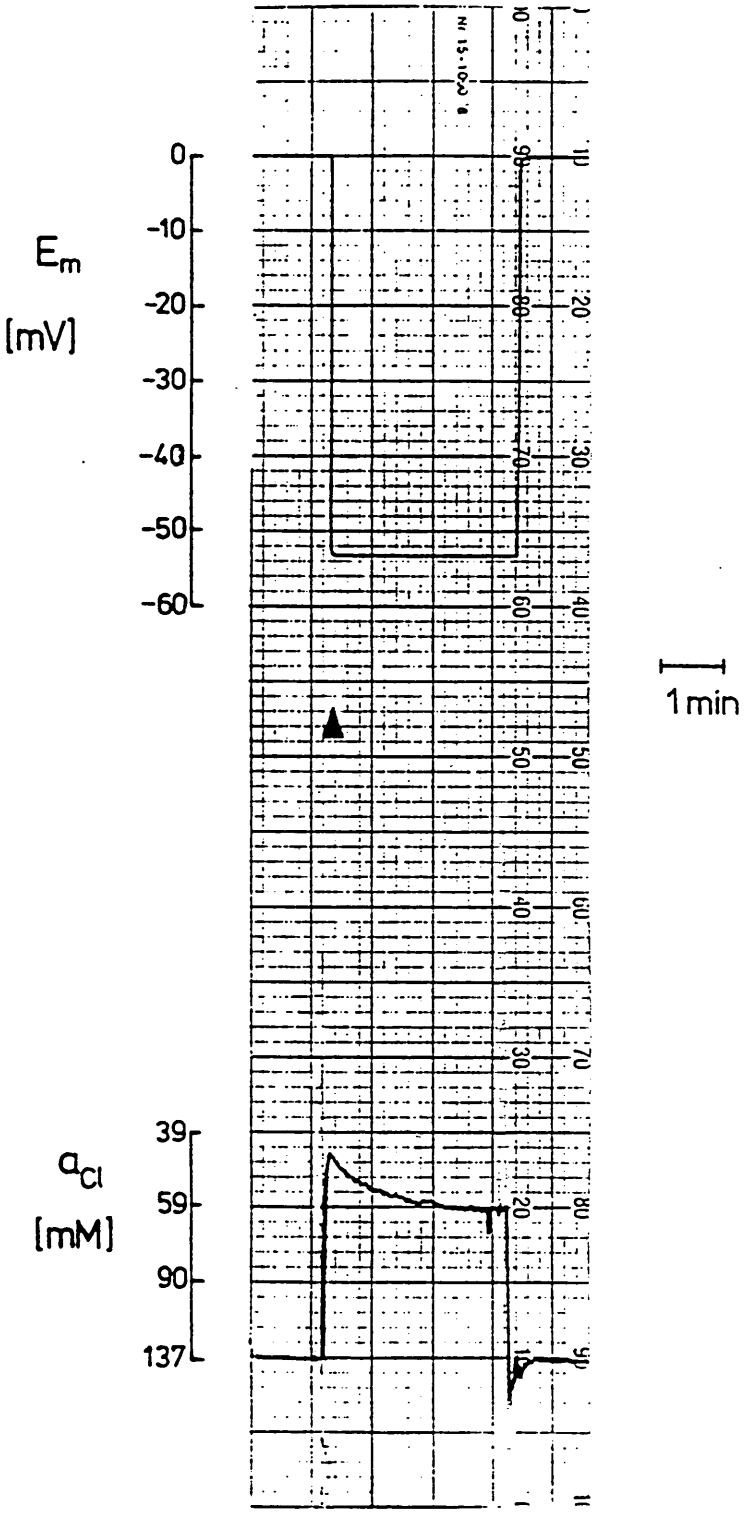


Fig. 67. Chart recording of the impalement of a *Calliphora* larval muscle cell using a Cl^- ISM with the reference barrel filled with KCl/K_2SO_4.

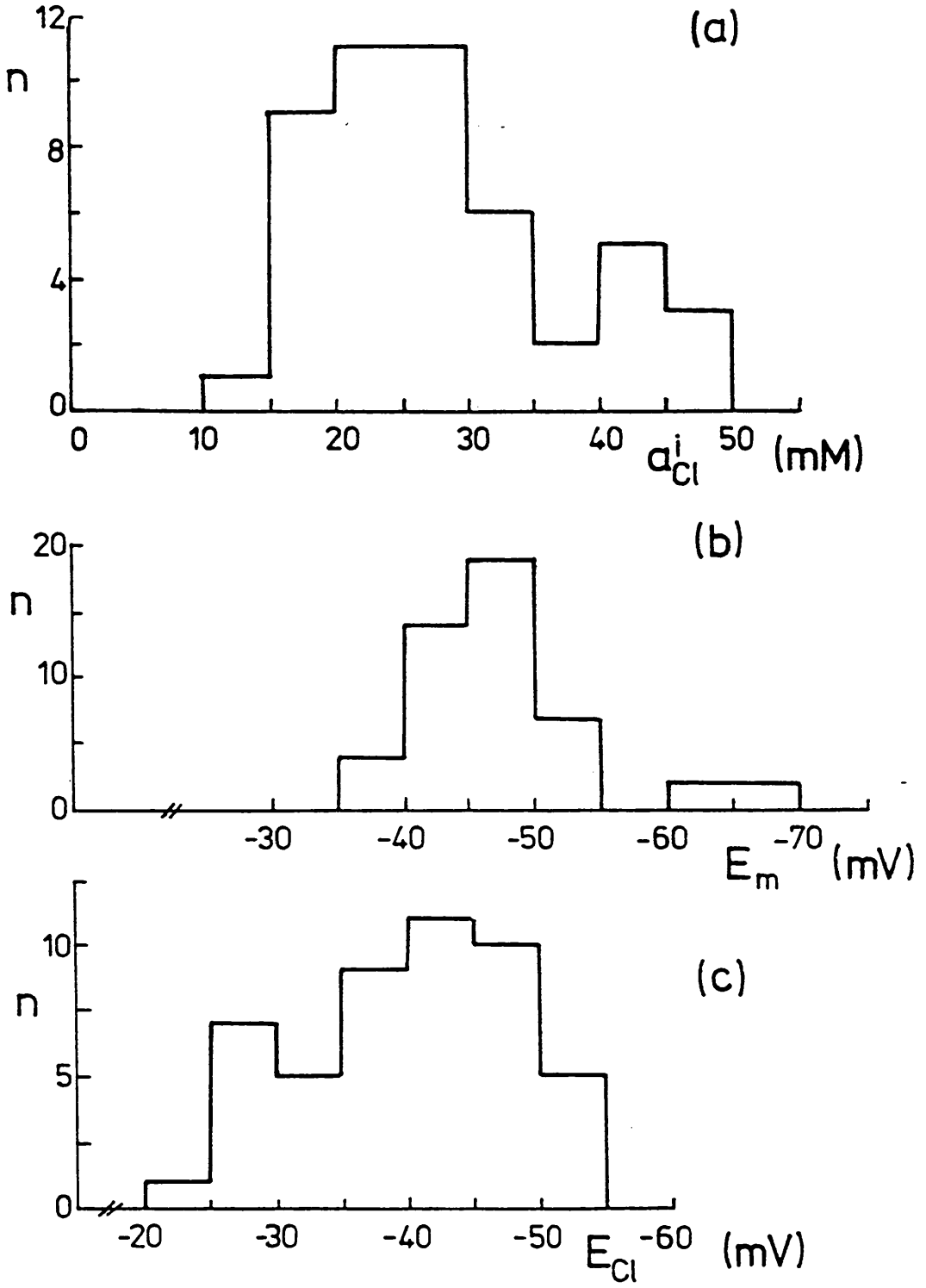


Fig. 68 Frequency histograms illustrating the distributions of, a. a^i_{Cl} values; b. E_m values and c. E_{Cl} values measured in *Calliphora* larvae using Cl^- ISMs with K_{Cl}/K_2SO_4-filled reference barrels.

recording a high value for the apparent intracellular Cl^- activity. Secondly, the reference barrels of this type of ISM contained K_{Cl} and K_2SO_4. Leakage of these anions from the reference barrel into the muscle cell following impalement could therefore account for the high values of apparent a_{Cl}^i recorded. Evidence for the latter suggestions was derived from the form of the chart recordings of impalements of cells (see figure 67) which clearly indicate that a_{Cl}^i increased with time following the introduction of the ISM into the cell. The a_{Cl}^i level did not appear to reach a steady value, but continued to rise indefinitely.

In order to test the hypothesis that the high a_{Cl}^i values recorded using ISMs with KCl/K_2SO_4-filled reference barrels were due to leakage of anions from the reference barrels into the muscle cells. These intracellular Cl^- activity measurements were repeated, using ISMs whose reference barrels were filled with an organic reference liquid ion-exchanger, RLIE. This latter eliminated the possibility that leakage from the reference barrel could influence the a_{Cl}^i levels recorded by the active barrel. In addition, a newly-available improved version of the Corning Cl^- exchanger (Corning 477913; Baumgarten, 1981) was used in the active barrel of the ISM. The latter helped to reduce the effect of intracellular anions other than Cl^- on the recorded value of a_{Cl}^i. The results obtained using this type of ISM are described in the next section.

III.4.ii. Intracellular Cl^- activities: Larvae

A typical impalement of a larval muscle cell is given in figure 69. The upper trace shows the reference potential, corresponding to a membrane potential of -52 mV, the lower, the Cl^--sensitive potential, V_{Cl}, corresponding to an intracellular Cl^- activity, a_{Cl}^i, of 19 mM and a chloride equilibrium potential, E_{Cl} of -50 mV. It should be noted that this recording and others made using the same type of ISM showed no tendency for a_{Cl}^i to increase from the value recorded immediately following the impalement of the cell.

Similar recordings were obtained from a total of 50 cells from 7 preparations, giving the average values for a_{Cl}^i, E_{Cl} and E_m shown in table 17 below.

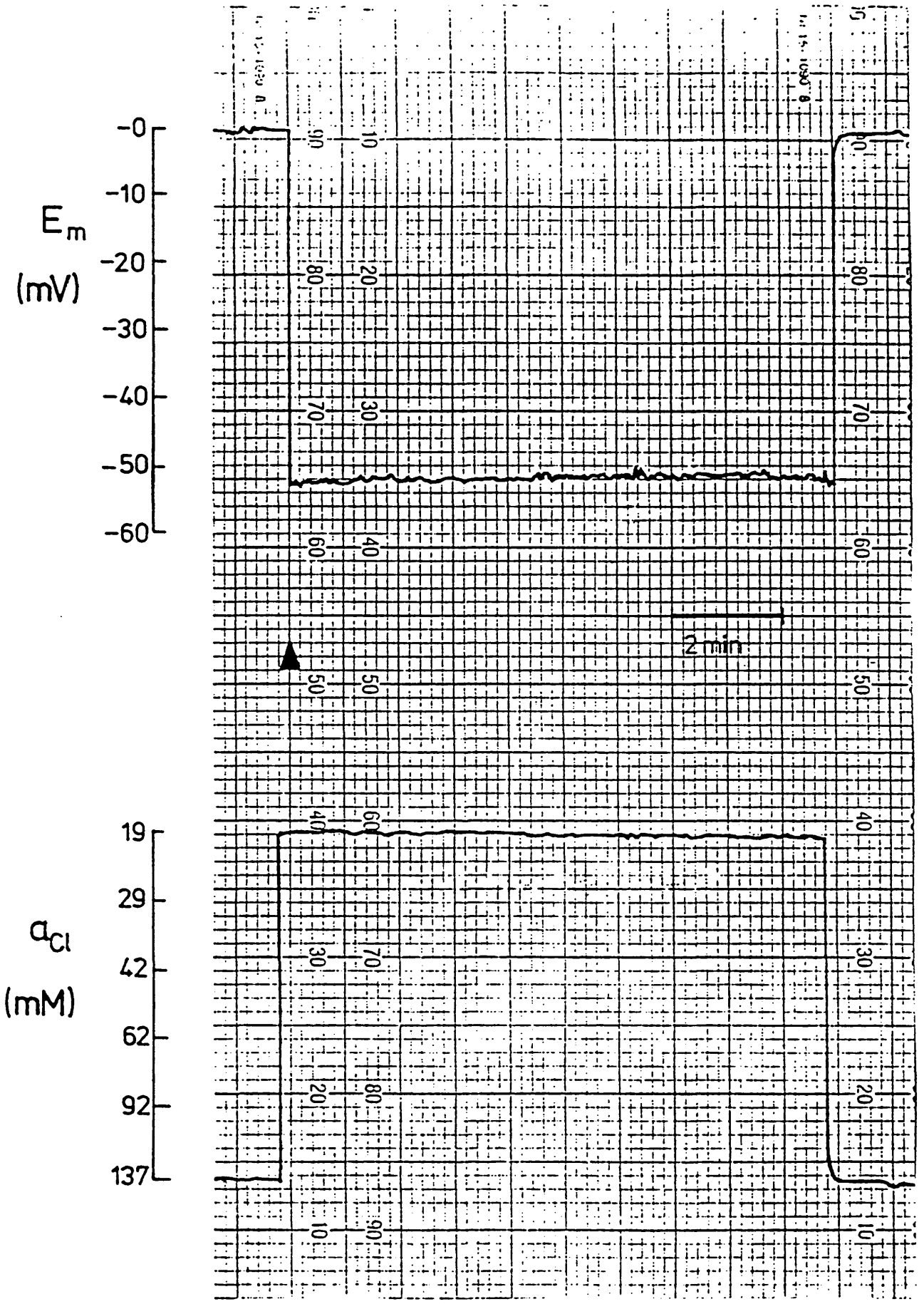


Fig. 69 Chart recording of the impalement of a *Calliphora* larval muscle cell with a Cl^-ISM with a RLIE-filled reference barrel.

Table 17 Intracellular Cl^- activity data for *Calliphora* larvae, measured using ISMs with RLIE-filled reference barrels. (Data from 50 cells, 7 preparations, given as mean ± SE).

a_{Cl}^i	17 ± 1 mM
E_{Cl}	-53 ± 1 mV
E_m	-53 ± 1 mV
$E_{Cl}-E_m$	0.1 ± 0.3 MV

The distributions of the values for each parameter are illustrated as frequency histograms in figures 70 and 71. a_{Cl}^i values have a somewhat asymmetrical distribution (figure 70) ranging between 12.7 and 28 mM (mean 17 mM) but with the vast majority (88%) of values falling between 12.7 and 22 mM. The mean of those a_{Cl}^i values which are between 12.7 and 22 mM is 16.3 ± 0.5, which falls in the modal class of the frequency histogram.

Frequency histograms comparing the distributions of membrane potential and chloride equilibrium potential values are shown in figure 71. The two parameters have comparable distributions, both with ranges of -40 to -60 mV, and identical means (-53 mV). In all cases, the value of E_{Cl} calculated for a cell is very close to the measured E_m, indicating that Cl^- is passively distributed in *Calliphora* larvae. This result is also illustrated by plotting individual E_{Cl} values against the E_m value for the same cell (fig. 72). All points fall very close to the line $E_{Cl} = E_m$ (the actual slope of the line along which the points fall is 0.98), which is extremely close to the slope of 1 for the line along which $E_{Cl} = E_m$. The correlation coefficient for this data is 0.94 (principle of least squares)

The possibility that Cl^- ISMs damage cell membranes more than conventional microelectrodes was effectively eliminated by comparing the total population of E_m values recorded using these Cl^- ISMs (-40 to -60 mV, with a mean of -53 mV fig. 71 b) with the total population recorded using conventional microelectrodes, OM's (-33 to -64 mV, with a mean of -48 mV, figure 51 a). Both populations are similar in means and distributions, indicating that Cl^-ISMs do not cause significantly more damage to the cell membrane than conventional microelectrodes, despite their slightly larger tip sizes. In fact, the average E_m recorded using the Cl^- ISMs is significantly higher than that obtained using OMs (-53 mV cf. -48 recorded using OMs) (t-test, $p < 0.01$). In order to establish that this difference was due to chance alone and did not reflect erroneous measurements by the RLIE-filled reference barrels, values of E_m

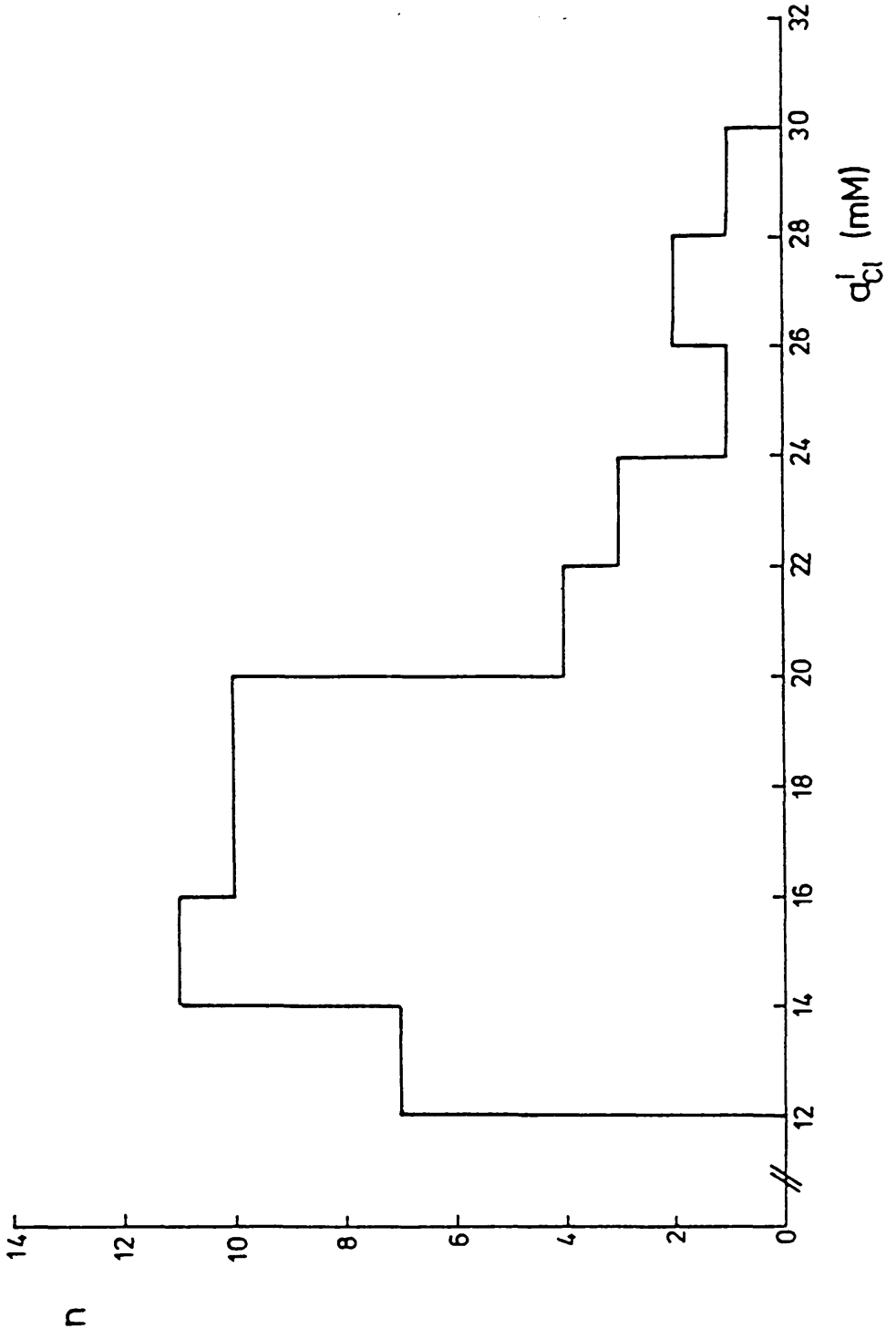


Fig. 70. Frequency histogram showing the distribution of a^i_{Cl} values recorded in *Calliphora* larvae using Cl^- ISMs with RLIE-filled reference barrels.

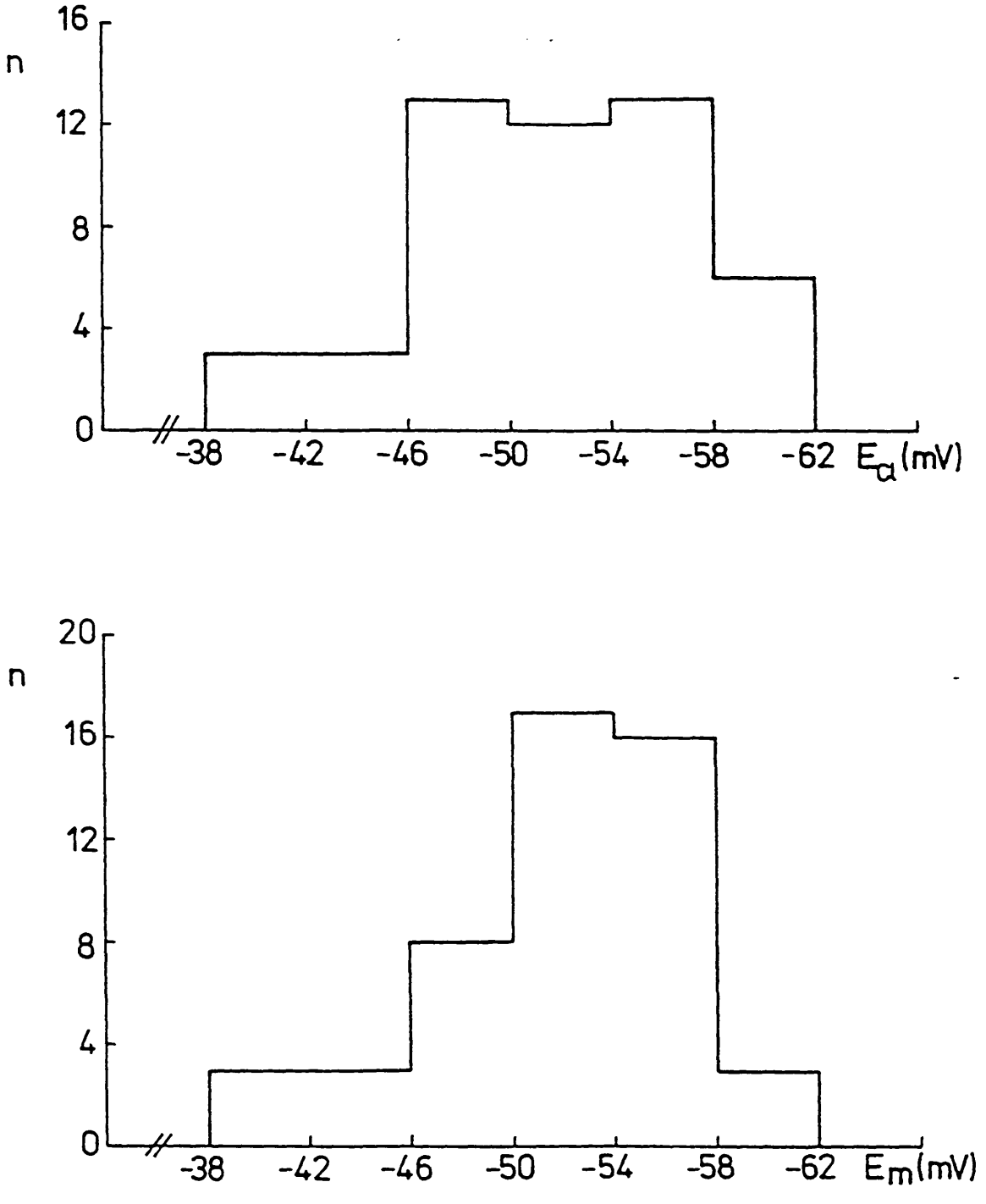


Fig. 71. Frequency histogram showing the distribution of a. E_{Cl} and b. E_m values obtained in *Calliphora* larvae using Cl^- ISMs with RLIE-filled reference barrels.

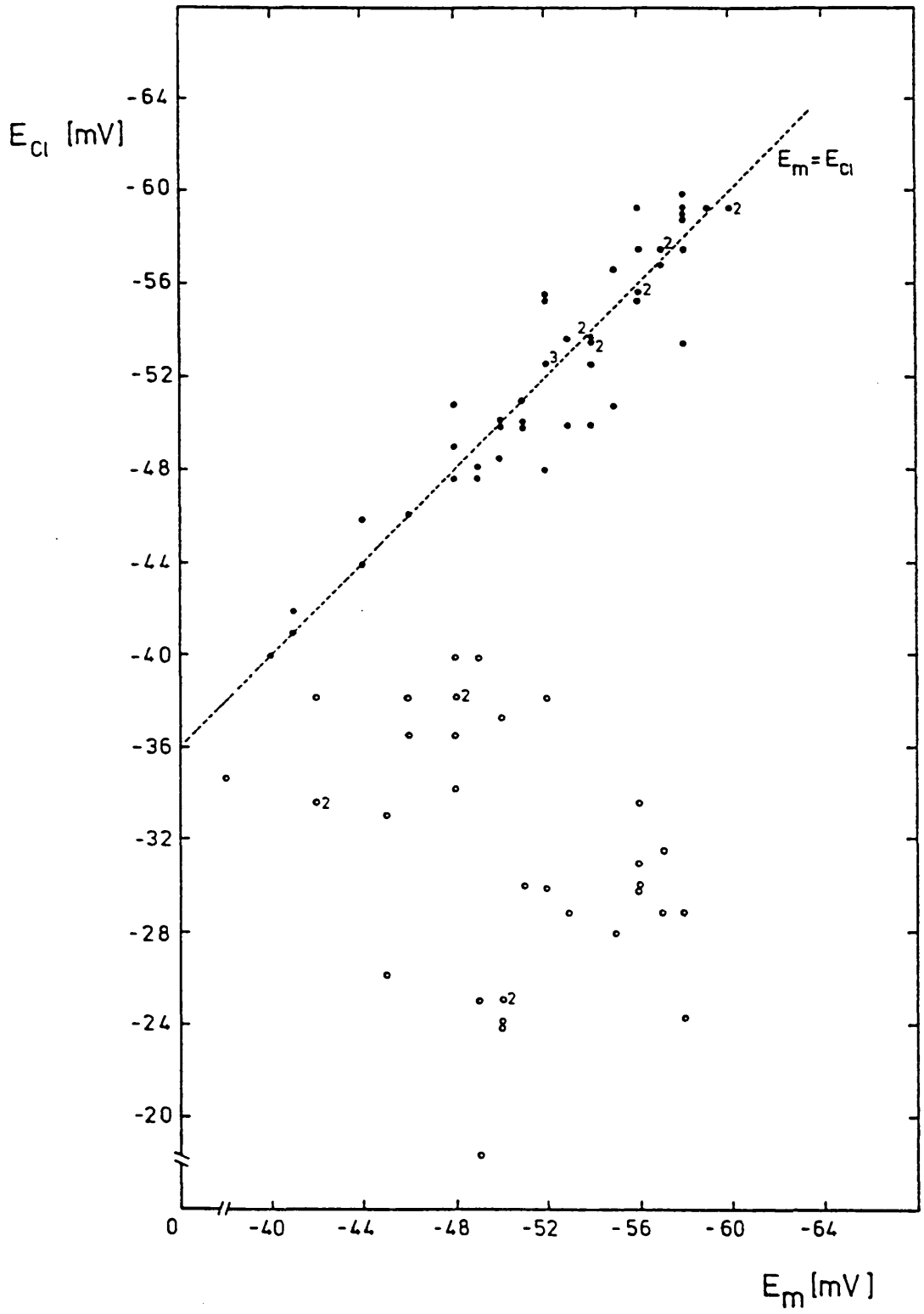


Fig. 72 Graph to illustrate the relationship between E_{Cl} and E_m in larvae (filled circles) and prepupae (hollow circles). The dashed line denotes the equality $E_{Cl} = E_m$, showing that for all larval cells, E_{Cl} is close to E_m, whilst in prepupae, E_{Cl} is consistently more positive than E_m. (The coincidence of two or more data points is indicated by a small number adjacent to that point.)

were measured in one preparation in which relatively high E_m values had been encountered using both an ISM and an OM. The results obtained are illustrated in figure 73, which shows that, whilst a wider range of E_m values was measured using the OM (-46 to-60 mV as opposed to -50 to -58 mV using the ISM), the mean E_m recorded (-53 mV) was identical using the two types of microelectrode. It was therefore concluded that RLIE-filled reference barrels reflect the 'true' situation in muscle cells.

Thus, the above data confirms that Cl^- is apparently passively distributed in *Calliphora* larvae, and that the unexpectedly high values of intracellular Cl^- activity recorded in preliminary studies using ISMs with KCl/K_2SO_4-filled reference barrels were artefactual, probably resulting from leakage of Cl^- and SO_4^{2-} from the reference barrel into the cell. All subsequent measurements of intracellular Cl^- data were therefore made using ISMs based on the Corning Cl^- exchanger 477913, with RLIE-filled reference barrels.

III.4.iii. Prepupae

The type of recording obtained when a prepupal muscle cell was impaled using a Cl^- sensitive microelectrode is illustrated by figure 74. The upper trace is the reference potential and the lower one, the potential corresponding to Cl^- activity. Both remained completely steady for ten minutes. For this cell, E_m was -48 mV, a_{Cl}^i, 30 mM and E_{Cl} -38.3 mV. Similar recordings made from a total of 35 cells (6 preparations) gave the average values of a_{Cl}^i, E_{Cl} and E_m shown in table 18 below.

Table 18 Intracellular Cl^- activity data for *Calliphora* prepupae. (Data from 35 cells, 6 preparations, given as mean ± SE).

a_{Cl}^i	40 ± 2 mM
E_{Cl}	-31 ± 1 mV
E_m	-50 ± 1 mV
$E_{Cl}-E_m$	19 ± 1 MV

Frequency histograms illustrating the distributions of the values of these three parameters are given in figures 75 and 76. The histogram for a_{Cl}^i values (fig. 75) has a total range of 28.6 to 66 mM, with all values but one falling between 28.6 and 53 mM. The distribution is rather flattened in shape, with

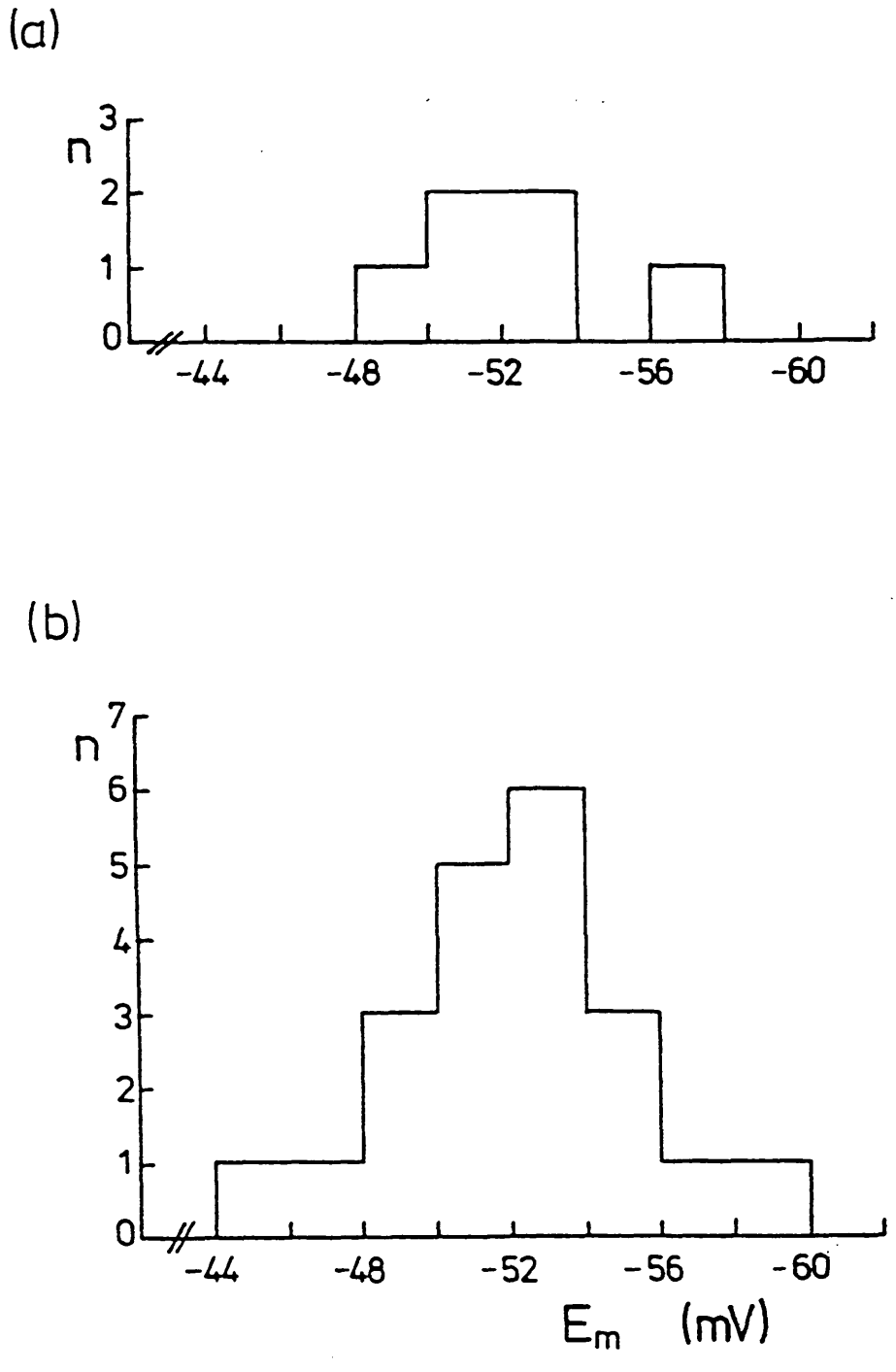


Fig. 73 Frequency histograms to compare the distributions of E_m values in a *Calliphora* larva recorded using, a. a Cl^- ISM and b. a conventional electrode.

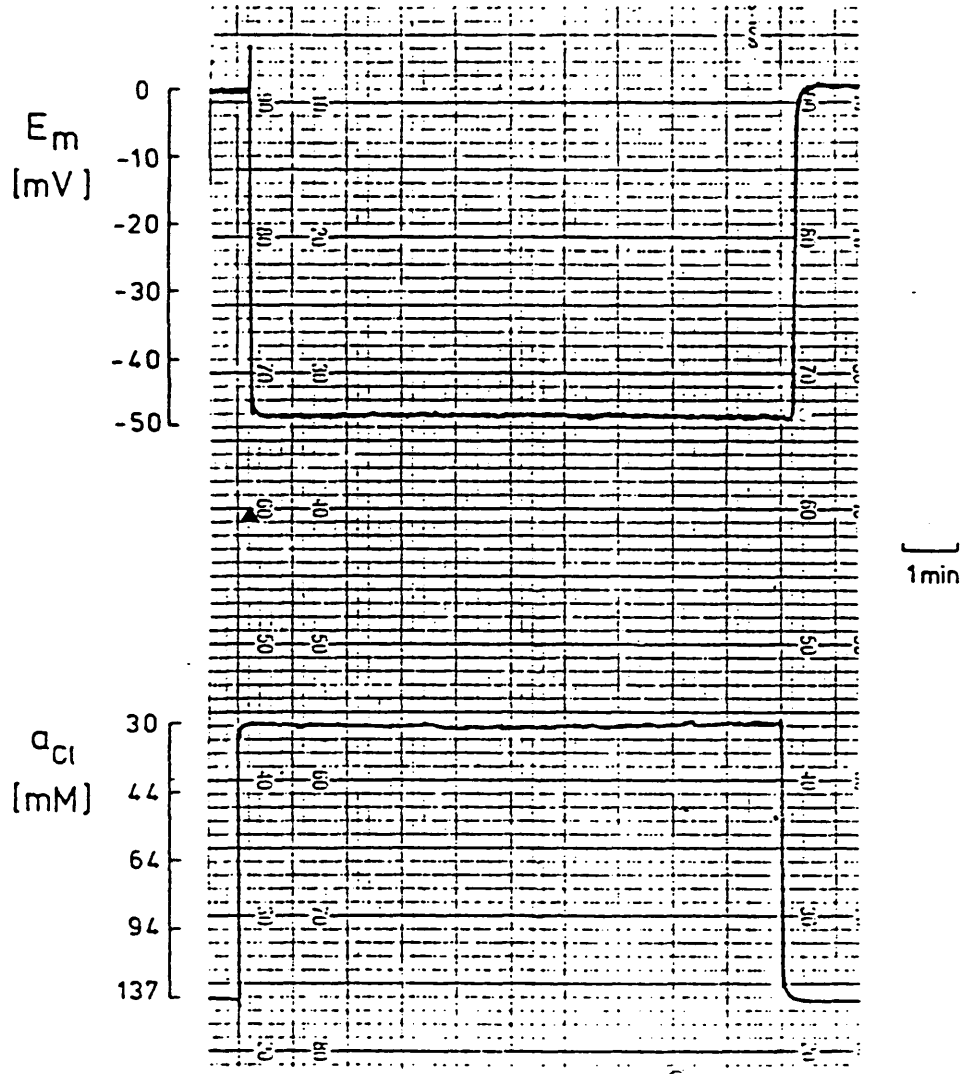


Fig. 74 Chart recording of the impalement of a *Calliphora* prepupal muscle cell using a Cl^-ISM with a RLIE-filled reference barrel.

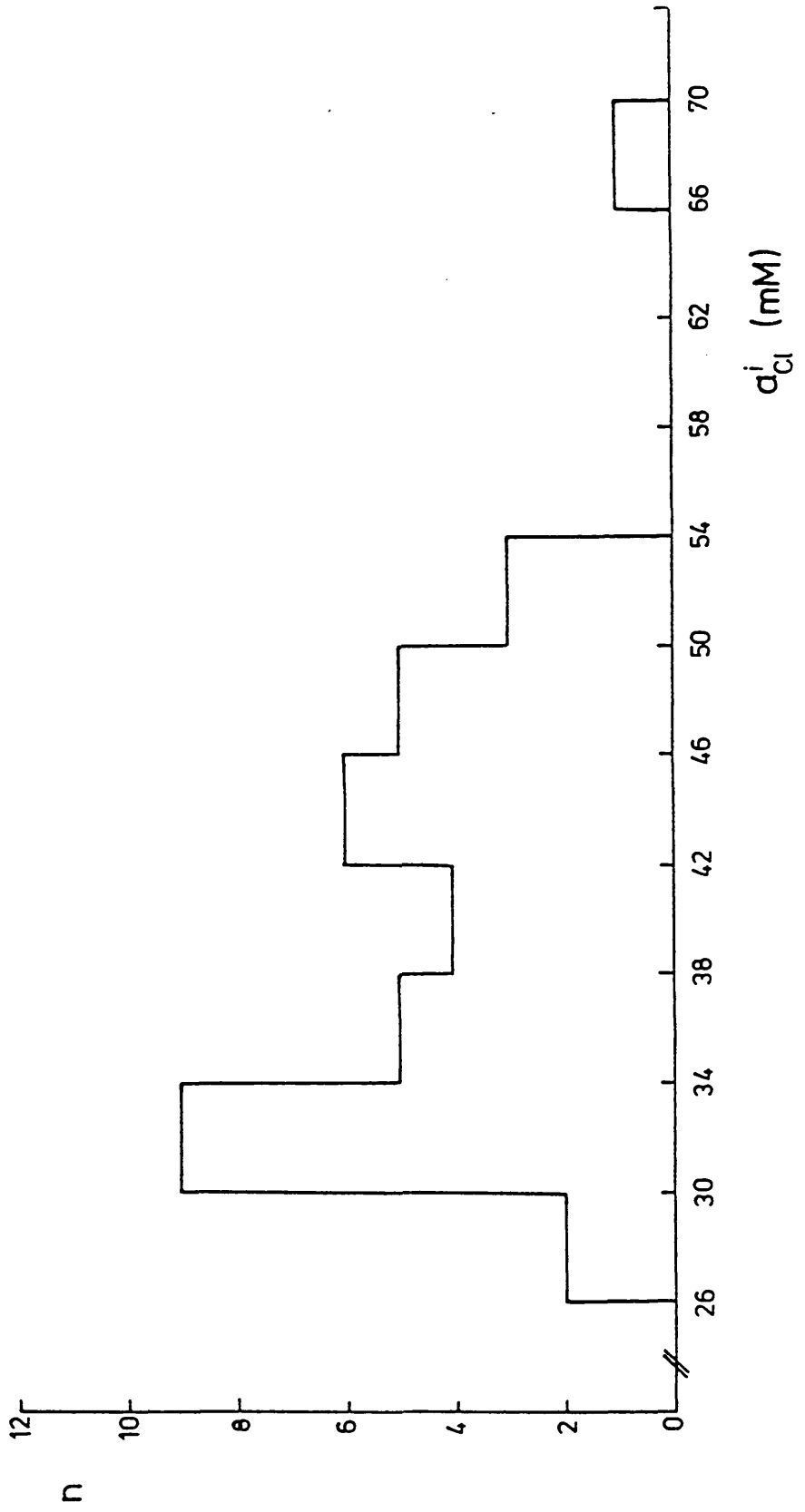


Fig. 75 Frequency histogram illustrating the distribution of a_{Cl}^{i} values in *Calliphora* prepupae.

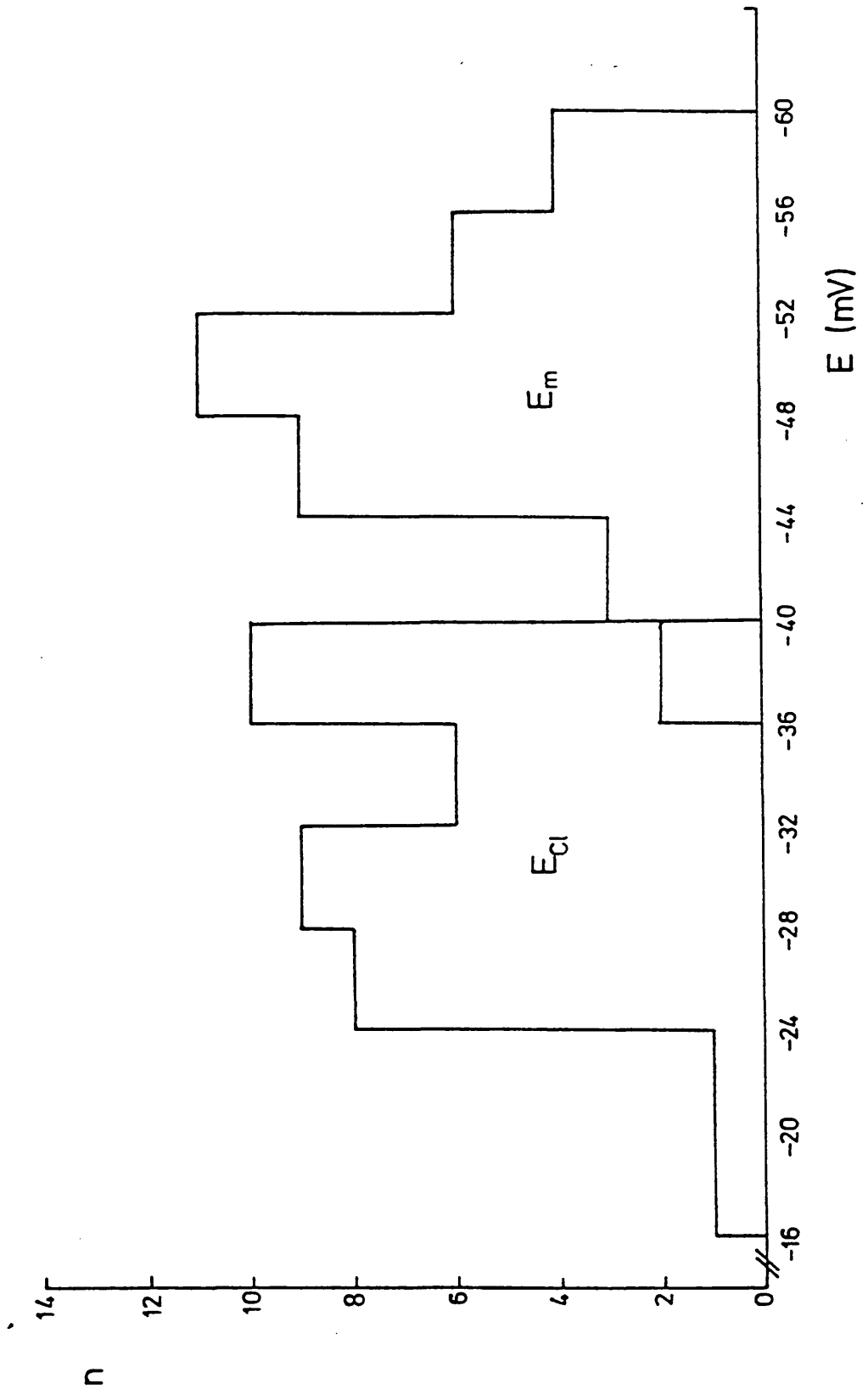


Fig. 76 Frequency histogram illustrating the distribution of E_{Cl} and E_m values in *Calliphora* prepupae on the same abscissa for comparison.

the mean (40 mM) falling close to the midpoint of the distribution.

The distribution of chloride equilibrium potentials, E_{Cl}, calculated from the above data is rather irregular, with a range of 18.4 to 39.5 mV (figure 76a) E_{Cl} was found to be consistently more positive than E_m in all cells studied (E_m ranged from -38 to -58 mV, with a mean of -50 mV and an approximately normal distribution, figure 76 b). This suggests that Cl^- may not be distributed passively in this preparation. There are three possible explanations for this. Firstly, Cl^- may be involved in generating E_m. However, Cl^- substitution experiments on prepupae (section IV.1) showed conclusively that changes in extracellular Cl^- activity led to only transient alterations in E_m, ie. that Cl^- was indeed passively distributed. Secondly, the high values of intracellular Cl^- activity recorded may have resulted from damage to the muscle cell membrane during its impalement. This possibility was eliminated by comparing the mean and distribution of E_m values recorded in a single preparation, using both conventional microelectrodes (OM's) and Cl^--sensitive microelectrodes (fig. 77). Both the mean and range of the two populations of values were similar: OMs recorded a mean E_m of -46 mV and a range of -40 to -52 mV; ISMs recorded a mean of -47 mV and a range of -38 to -52 mV, (fig. 73). Further, the E_m values recorded from all 6 prepupal preparations using Cl^--ISMs were compared with the total population of values recorded in prepupae using OMs (figs. 76 b and 51 b, rspectively). Cl^- ISMs gave a range of -38 to -58 mV, with a mean E_m of -50 mV; OMS gave a range of -35 to -62, with a mean of -47 mV. The two distributions were thus very similar, with the mean E_m recorded using Cl^--ISMs being slightly higher than that obtained using OMs, confirming the earlier conclusions that Cl^--ISMs did not cause more membrane damage than OMs.

Thirdly, the presence of an interferent in prepupal muscle cells to which the Corning Cl^- exchanger responded would explain the high values of apparent a_{Cl}^i recorded in this insect. This seems the most likely explanation for E_{Cl} being apparently more positive than E_m, and is considered further in section IV.1.

The graph of the E_{Cl} value for each cell against the recorded E_m for that cell (fig. 72) shows that there is no clear relationship between these two parameters in prepupae (the points follow a line with slope -0.26 and correlation coefficient -0.24). This may reflect the presence of varying

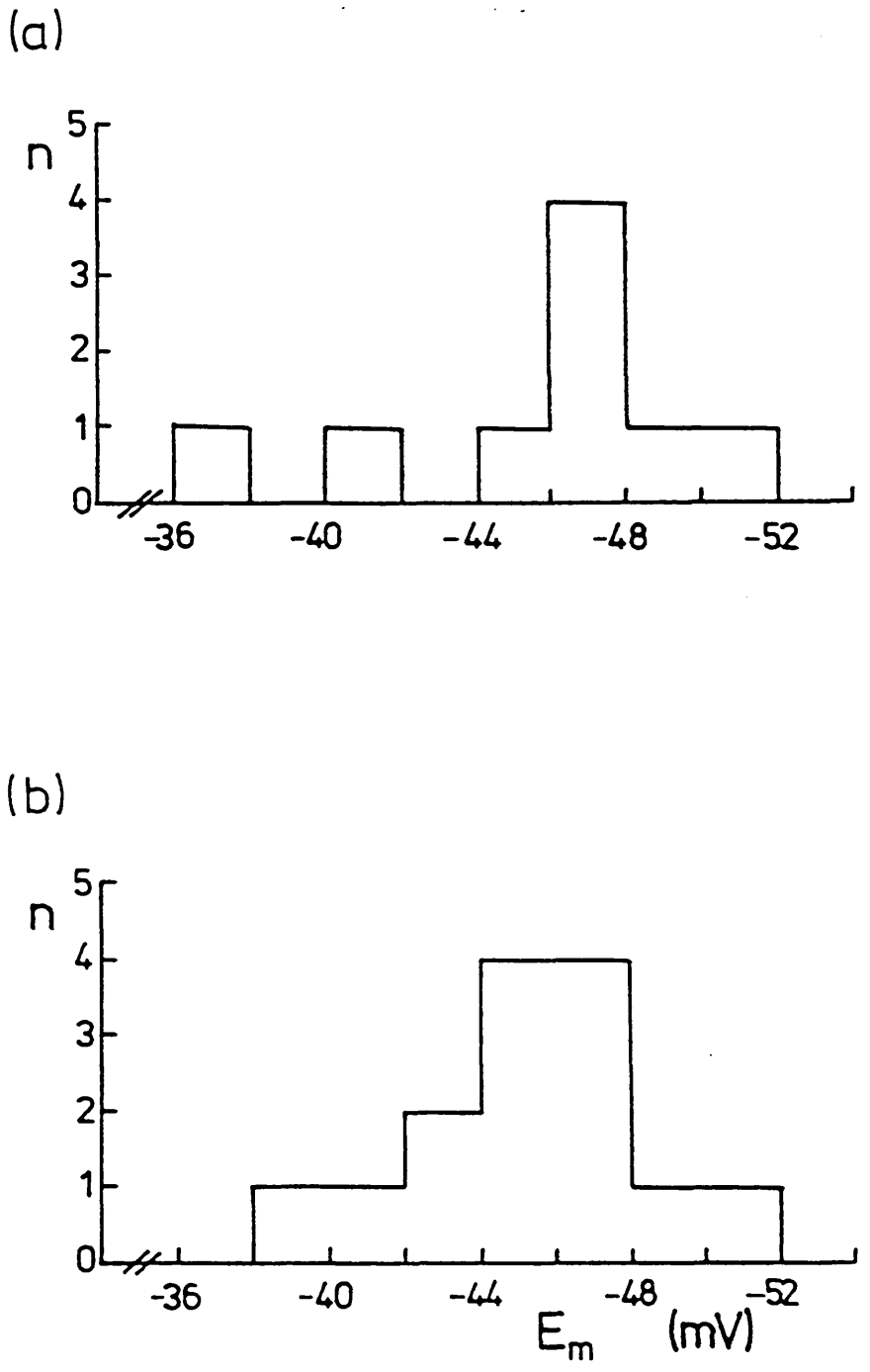


Fig. 77 Frequency histograms comparing the distributions of E_m values in a *Calliphora* prepupa recorded using, a. a Cl^-ISM and b. a conventional microelectrode.

amounts of interferent in the population of cells, which would mask any relationship that might exist.

In conclusion, in larvae, E_{Cl} was very close to the measured E_m in all cells impaled, and a graph of E_{Cl} against E_m showed that all points fall near the line along which $E_{Cl} = E_m$ (fig. 72). In contrast, in prepupae E_{Cl} was consistently more positive than E_m. This was tentatively attributed to the presence of an interferent.

III.4.iv. Comparison between larval and prepupal intracellular Cl^- activity data

The intracellular Cl^- activity data obtained from larvae and prepupae is summarised in table 19 below:

Table 19 Intracellular Cl^- activity data for *Calliphora* larvae and prepupae. (Data from 43 cells, 7 preparations for larvae; 35 cells, 6 preparations for prepupae, given as mean ± SE).

	LARVAE	PREPUPAE
a_{Cl}^i (mM)	17 ± 1	40 ± 2
E_{Cl} (mV)	-53 ± 1	-31 ± 1
E_m (mV)	-53 ± 1	-50 ± 1
$E_{Na}-E_m$ (mV)	0.1 ± 3	19 ± 1

The intracellular Cl^- activity, a_{Cl}^i, values measured for larvae and prepupae are thus very different. There is a large separation between the means of the two populations (23 mM on average) and the distribution of prepupal a_{Cl}^i values is considerably wider than that of larval a_{Cl}^i values (fig. 78). There is very little overlap between the two populations. These observations may be attributable to the presence of an interferent in prepupal muscle cells, and this will be considered further in chapters IV and VII.

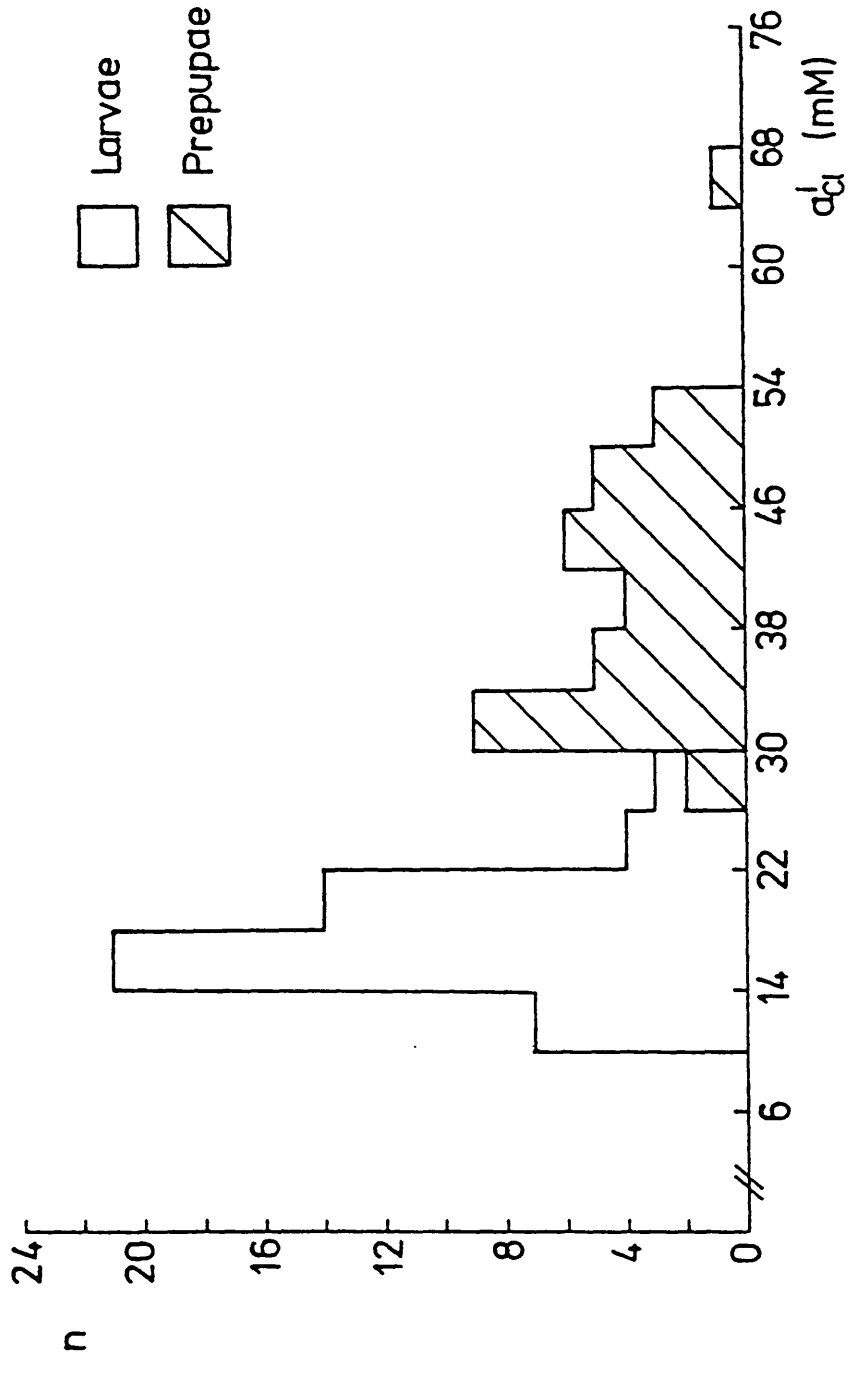


Fig. 78 Frequency histograms comparing the distribution of a_{Cl}^{i} values in larvae and prepupae on the same abscissa.

IV. IONIC SUBSTITUTION EXPERIMENTS ON *CALLIPHORA*: A MODEL OF RESTING MEMBRANE ELECTROGENESIS

The aim of these ionic substitution experiments was to obtain a quantitative assessment of the contribution of K^+, Na^+ and Cl^- to the membrane potential, E_m, of *Calliphora* muscle cells, and to construct a quantitative model of resting membrane electrogenesis in this insect.

All experiments were carried out on prepupal preparations. In prepupae, the muscle cells do not contract, whilst appearing to retain their electrochemical responsiveness (Jan & Jan, 1976; Irving & Miller, 1981). The problem of cells contracting in high-K^+ solutions and expelling the microelectrode was thus eliminated. Experiments were performed only on cells which, when impaled, gave steady recordings of E_m. Cells were then allowed to equilibrate in each of a series of Ringer-based solutions until a new, steady value of E_m was recorded in each.

IV.1. Chloride substitution experiments

Previous measurements of intracellular chloride activities in larval and prepupal muscle cells (section III.4) suggested that Cl^- is passively distributed in larvae (the Cl^- equilibrium potential, E_{Cl} was close to E_m in all cells, both having a mean value of -53 mV). In prepupae, however, E_{Cl} was more positive than E_m by an average of some 18 mV. This discrepancy reflected either that Cl^- was involved in generating E_m, or that an interferent was present in the cells to which the ISM responded, giving artificially high apparent intracellular Cl^- levels.

The aim of Cl^- substitution experiments was to determine whether Cl^- is involved in generating the membrane potential in this insect, or whether it is distributed passively across the cell membrane. The substitution experiments were carried out on both larvae and prepupae using the solutions listed in appendix 4, in which gluconate was substituted for Cl^-. (Extra Ca^{2+} was added to these solutions to compensate for the known Ca^{2+}-sequestering properties of gluconate (Kenyon & Gibbons, 1977; Vaughan-Jones, 1979)).

V.1.i. Larvae

A typical recording obtained when low-Cl^- (1.4 mM) Ringer (Appendix 6) was

substituted for Normal (137 mM Cl^-) Ringer is shown in figure 79. The trace shows a transient hyperpolarisation of 5 mV in E_m when the extracellular chloride activity, a_{Cl}^o, was reduced. The membrane then gradually depolarised, returning to the original, pre-treatment, E_m within 1 to 3 minutes. When Normal Ringer was re-introduced into the recording chamber, a second transient hyperpolarisation of 4 mV occurred. The E_m subsequently depolarised to its initial level within 1 to 3 minutes. Similar data was obtained from 6 cells (6 preparations) giving transient hyperpolarisations of 5-10 mV when a_{Cl}^o was reduced, and of 4-9 mV when Normal Ringer was reintroduced.

Thus, these experiments confirmed the suggestion from the intracellular chloride activity data for larvae, that Cl^- is passively distributed in this preparation, since changes in a_{Cl}^o produced no sustained alterations in E_m.

IV.1.ii. Prepupae

In contrast to the situation in larvae, where E_{Cl} was approximately equal to E_m, intracellular Cl^- activity measurements in prepupae showed that E_{Cl} was apparently more positive than E_m. This implied either that Cl^- was not passively distributed, and was involved in the generation of E_m, or that an interferent was present in prepupal muscle cells, to which the Cl^--exchanger responded, giving elevated values of apparent a_{Cl}^i. In order to investigate these two possibilities, Cl^--substitution experiments were performed using Cl^--free Ringer whilst monitoring a_{Cl}^i and E_m using a Cl^- ISM. The new steady a_{Cl}^i level recorded after the cell had been soaked in Cl^--free Ringer to deplete the cell of Cl^- provided a measure of any interferent present in the cell. Such an experiment is illustrated in figure 80. The upper trace shows the apparent a_{Cl}^i and the lower one, the membrane potential. The cell was initially bathed in Normal Ringer (137 mM Cl^-), and was impaled with a chloride-sensitive microelectrode. Steady readings of intracellular Cl^- activity (58 mM) and membrane potential (-44 mV) were obtained, and chloride-free Ringer substituted in for Normal Rice's saline (shown as a solid bar beneath the E_m trace). A transient hyperpolarisation of 10 mV was seen in E_m, followed by a depolarisation to the pre-treatment level within 1 minute. The cell was bathed in Cl^--free Ringer until a new steady value of apparent a_{Cl}^i was reached (in this case, around 13 mM) which represented the ISMs response to the interferent. To test that the removal of Cl^- from the cell was reversible, Normal Rice's saline was re-introduced into the

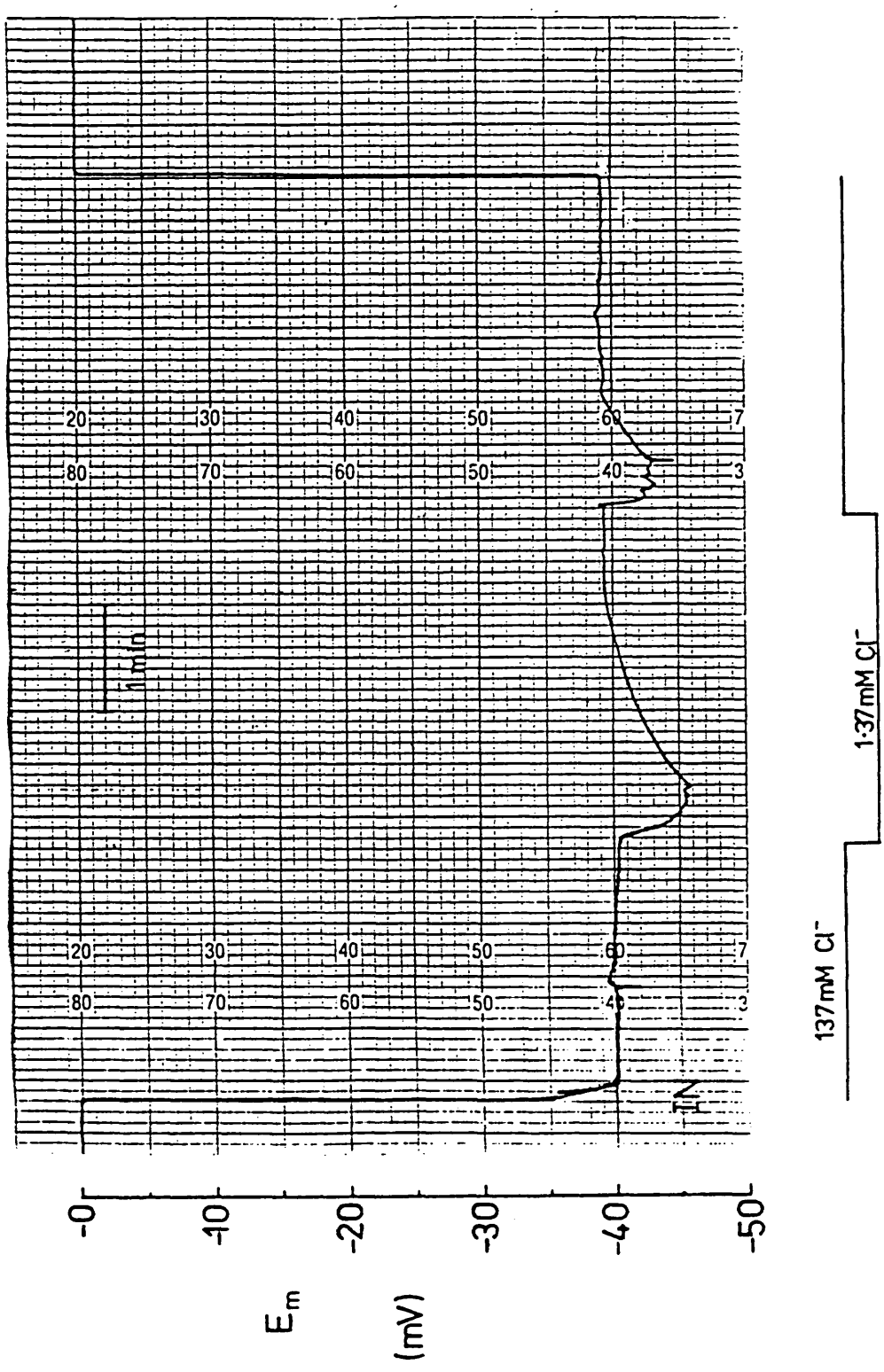


Fig 79. Chart recording of a Cl^- substitution experiment on a *Calliphora* larva, showing the transient responses of E_m to changes in a_{Cl}.

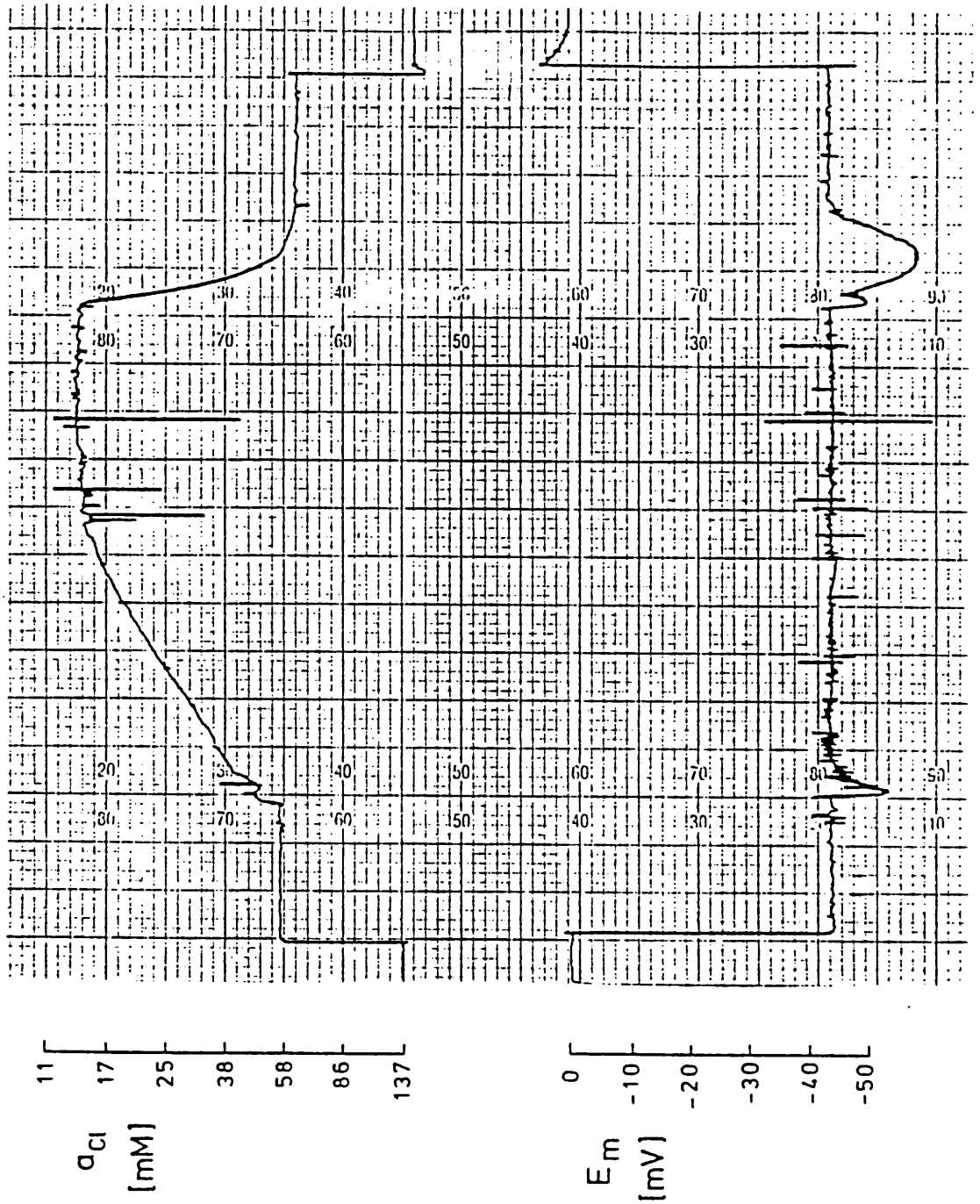


Fig 80. Chart recording of a Cl^- depletion experiment on a *Calliphora* prepupa, showing the transient responses of E_m to changes in a_{Cl}^o, together with the loss of Cl^- from the cell when a_{Cl}^o was reduced.

recording chamber. Chloride quickly entered the cell, the a_{Cl}^{i} returning to its original value within 2 minutes. A simultaneous hyperpolarisation of E_m of some 14 mV was observed, which recovered to its original, pre-treatment level within 2 minutes this recovery was rather slower than that recorded when the cell was first exposed to Cl^--free Ringer (1 minute). Similar results were obtained from a total of 7 cells from 7 preparations, giving transient hyperpolarisations of 9 to 14 mV when a_{Cl}^{o} was reduced and of 12 to 16 mV when Normal Ringer was re-introduced. The intracellular Cl^- data is summarised in table 20, below. A full list of results is given in appendix II.

Table 20. Data from Cl^--depletion experiments on *Calliphora* prepupae. (Data from 7 cells (7 preparations) is given as mean ± SE).

E_m (mV)	-50 ± 3
a_{Cl}^{i}, when cells were bathed in Normal Ringer (mM)	43 ± 5
a_{Cl}^{i}, when cells were bathed in zero Cl^- Ringer (mM)	10 ± 1

Thus, changes in extracellular Cl^- activity produced no sustained alteration in E_m, indicating that Cl^- is passively distributed in this preparation. The intracellular Cl^- activity, a_{Cl}^{i}, is markedly lower in cells bathed in zero Cl^- Ringer than in those bathed in Normal Ringer, which is also consistent with Cl^- being passively distributed and moving down its concentration gradient out of the cell. The earlier suggestion that the apparent difference between E_m and E_{Cl} in prepupae was due to interference was confirmed by the fact that the Cl^- ISMs recorded an average apparent a_{Cl}^{i} of 10 mM after the cell had been depleted of Cl^-. This value provides a measure of the quantity of interferent present in these cells.

Chloride substitution experiments on both larvae and prepupae have thus shown conclusively that Cl^- is passively distributed in the two preparations, playing no part in resting membrane electrogenesis. An interferent occurs in prepupal cells, however, accounting for some 10 mM of the total apparent intracellular Cl^- activity recorded by the ISM.

IV.2. Potassium substitution experiments

Measurements of intracellular K^+ activities in *Calliphora* prepupae (section 3.I) showed that the potassium equilibrium potential, E_K, is consistently more negative than the membrane potential in this preparation. This implies that K^+ is not the only ion involved in generating E_m. In order to determine the extent of the contribution of K^+, K^+ substitution experiments were carried out using Ringer-based solutions containing K^+ activities, a_K^+'s, between 0.97 and 97.2 mM, using Na^+ as the substitute (Appendix 3). The level of E_m measured in each solution was taken to be steady when it remained constant to within ± 1 mV over a 15 minute period.

A typical recording of the changes in E_m obtained during this type of experiment is shown in figure 81. The cell was impaled at the point marked by an arrowhead and a steady E_m of -40 mV recorded. Solutions containing a range of K^+ activities were then substituted in as indicated above the E_m trace, and a steady E_m obtained in each following equilibrium periods of at least 30 minutes. The cell was twice returned to Normal Rice's saline to ensure that the E_m changes were reversible, and that the cell remained generally healthy throughout the experiment. Changes in E_m following alterations in a_K^+ were found to be fastest when a_K^+ was reduced (see figure 81) eg. when a_K^+ was reduced from 9.7 to 3.6 mM, the E_m reached a new, steady level within around 15 minutes; when a_K^+ was increased from 36 to 97.2, the E_m did not reach a steady value for more than 30 minutes. (It should be noted that this result was not simply due to cells becoming less responsive towards the end of a long experiment, because the same slow responses to high K^+ Ringer were observed when the latter were applied at the start of the experiment).

A summary of the results obtained from 11 cells (each from a different preparation) is given in table 21. Thus, changes in a_K^+ result in sustained alterations in E_m, confirming that K^+ is involved in generating E_m. The relationship between E_m and the logarithm of a_K^+ (fig. 82) has a maximum slope of only 31 mV per tenfold change in a_K^+, however, which is considerably less than the 58 mV per tenfold change in a_K^+ predicted by the Nernst equation for a membrane that is permeable only to K^+.

These experiments were, however, rather lengthy, lasting for up to four hours, and, although each cell was repeatedly returned to Normal Ringer to

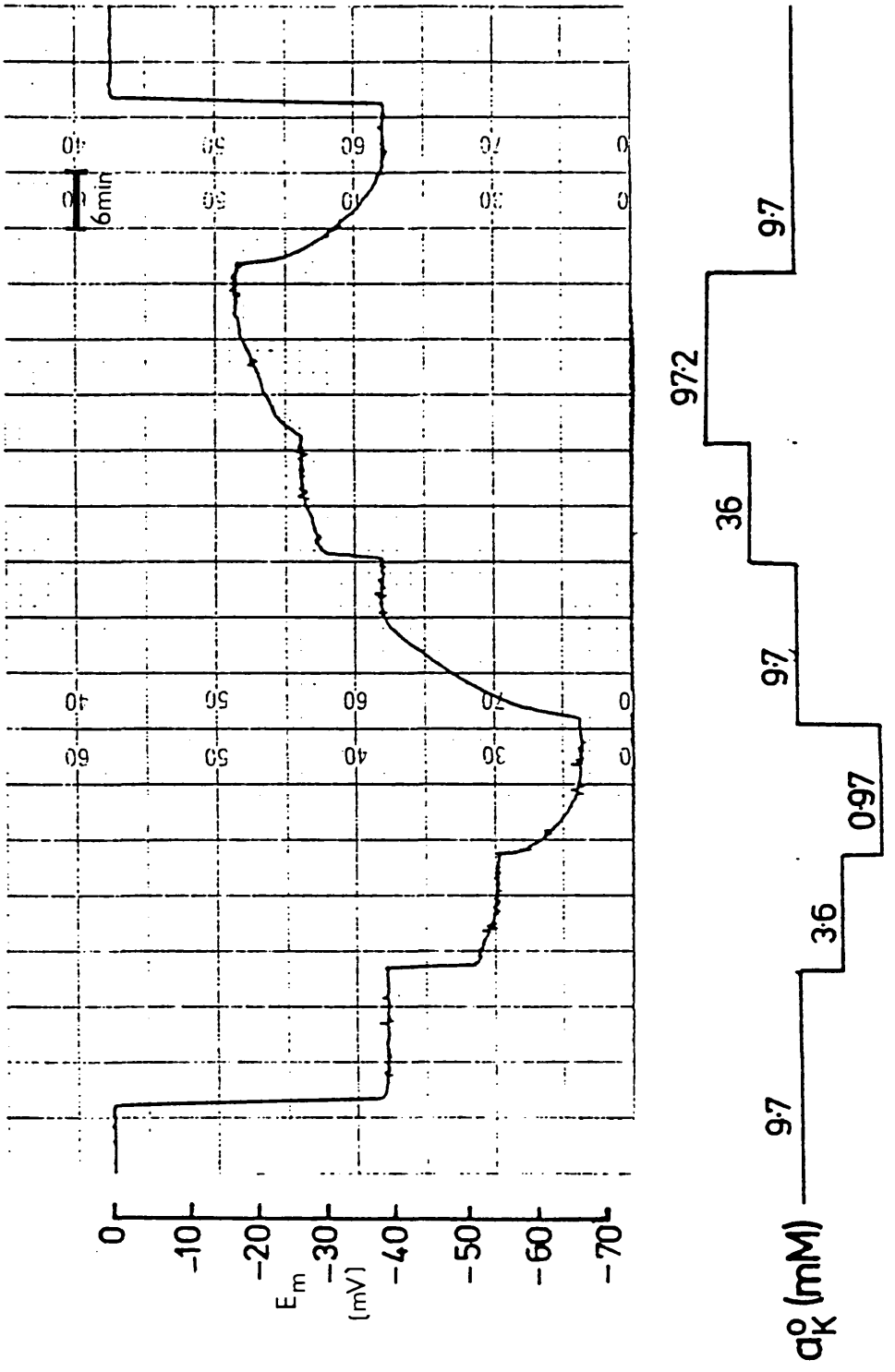


Fig 81. Chart recording of a K^+ substitution experiment on a *Calliphora* prepupa, showing the sustained changes in E_m which resulted when a^o_K was varied.

Table 21. Results from K^+ substitution experiments on *Calliphora* prepupae. (Data from 11 cells, 11 preparations)

Cell no.	Extracellular K^+ activity, a_K^o (mM)				
	0.97	3.6	9.7	36	97.2
	Membrane potentials, E_m (-mV)				
1	65	52	43	24	12
2	74	60	49	23	13
3	64	56	44	26	14
4	74	60	48	31	17
5	68	60	50	28	16
6	81	66	54	34	18
7	64	58	48	21	11
8	68	61	47	28	16
9	68	56	39	27	18
10	66	53	36	26	14
11	68	57	48	23	10
$\bar{x}$	69.1	58.1	46	26.5	14.5
SE	1.6	1.2	1.5	1.1	0.8

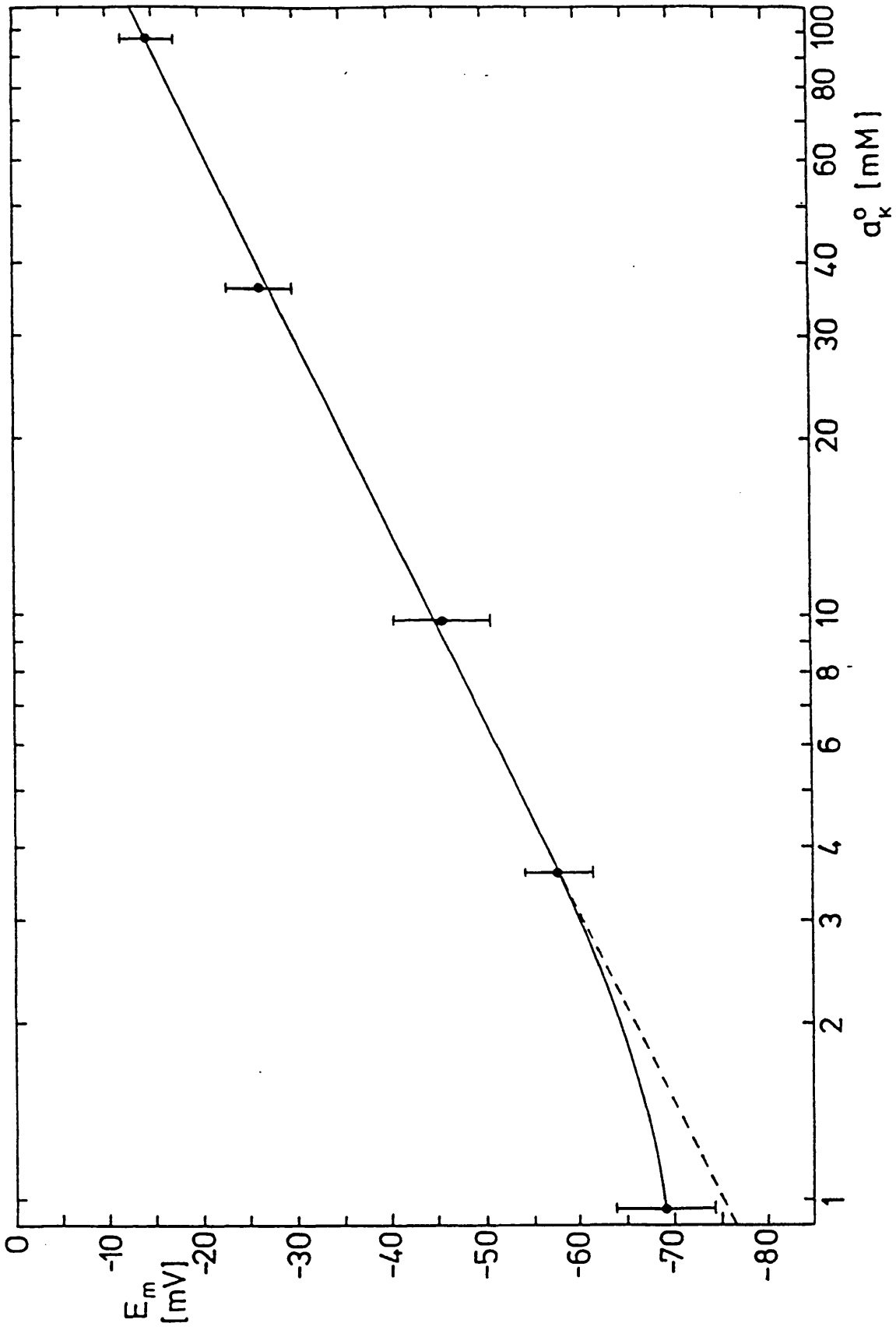


Fig. 82 Graph showing the relationship between E_m and the logarithm of a_K^o. (Bars represent S.D's)

ensure that it was in a healthy state throughout the experiment, it was conceivable that cells were becoming less responsive to changes in extracellular ionic activities with time. If this were the case, it might account, at least in part, for the discrepancy between the observed slope of the E_m against the logarithm of extracellular K^+ activity, a_K^o, graph (a maximum of 31 mV) and the 58 mV slope predicted by the Nernst equation, if the membrane were permeable only to K^+. In order to test this possibility, a number of shorter substitution experiments were performed which involved a maximum of three solution changes. A cell was impaled in Normal Ringer (9.7 mM K^+) and a steady E_m recorded. Low-K^+ Ringer (0.97 mM K^+) was then substituted in and the cell allowed to equilibrate. This was followed by high-K^+ Ringer (97.2 mM K^+), and finally the cell was returned to Normal Ringer. Using this protocol, a maximum slope of 30 mV was recorded for a_K^o's between 9.7 and 97 mM (cf. 31 mV for this range of a_K^o values obtained in full substitution experiments) and a maximum slope of 24 mV was recorded for a_K^o values between 0.97 and 9.7 mM (cf. 23 mV from the full substitution experiments). The slopes obtained for given a_K^o ranges using the two types of protocol are thus not significantly different. It was therefore concluded from these experiments that the shallow slope of the E_m against the logarithm of a_K^o graph obtained from the full K^+ substitution experiments provided a true reflection of the physiology of the cell, rather than resulting from deterioration of the health of the cell during the course of the experiment. The deviation from the 58 mV slope expected for a pure K^+ electrode is consistent with the fact that the potassium equilibrium potential was not equal to the membrane potential, but was consistently more negative than E_m. This confirms that at least one ion in addition to K^+ must contribute to E_m. A candidate for this ion is Na^+.

IV.3. Construction of a model for resting membrane electrogenesis in *Calliphora* prepupae

Evidence from intracellular K^+ activity measurements (section III.2) and K^+ substitution experiments (section IV.1) on *Calliphora* suggested that K^+ was not the only ion involved in generating the membrane potential, E_m. This was implied firstly by the fact that the potassium equilibrium potential, E_K, calculated for each cell from its intracellular K^+ activity, was consistently more negative than the E_m of the cell; and secondly by the observation that the slope of the graph of E_m against the logarithm of the extracellular K^+ activity, a_K^o, was significantly shallower than the 58 mV per tenfold change in

a_K^o predicted by the Nernst equation for a membrane permeable only to K^+. The additional ionic mechanism which would be expected to contribute to E_m would have an equilibrium potential more positive than E_m. Cl^- was known from the substitution experiments described in section IV.1 not to be involved in resting membrane electrogenesis. Thus, the most likely candidate for this ionic mechanism was Na^+. Further, since Na^+ was used as the substitute for K^+ in the K^+ substitution experiments, then if Na^+ was involved in generating E_m, varying the extracellular Na^+ activity would be expected to affect E_m. The changes in E_m observed during the substitution experiments were therefore considered in relation to the changes in both extracellular K^+ and Na^+. Assuming that the cell membrane was permeable only to K^+ and Na^+, with Cl^- being passively distributed, resting membrane electrogenesis should behave according to the simplified Goldman-Hodgkin-Katz equation:

$$E_m = \frac{RT}{F} \ln \left[\frac{a_K^o + \alpha\, a_{Na}^o}{a_K^i + \alpha\, a_{Na}^i} \right] \text{ (mV)} \qquad (1)$$

(where $\alpha = p_{Na}/p_K$ and all other terms are defined in section I.1).

If the cell membrane obeyed the above equation, a tenfold change in $(a_K^o + \alpha\, a_{Na}^o)$ would give rise to a 58 mV change in E_m. Thus, a value of α (the ratio of the partial permeability of the cell membrane for Na^+ to that for K^+ ie. p_{Na}/p_K) was calculated by numerical substitution from the K^+ substitution data described in the previous section (section IV.2, table 21) such that the above condition was met: its value was 0.086. This value was then substituted into equation (1), together with the values of a_K^o and a_{Na}^o, known from the composition of Normal Ringer (appendix 1) as follows:

$$E_m = 58 \log \left[\frac{9.7 + (0.086 \times 124.6)}{a_K^i + 0.086\, a_{Na}^i} \right] \text{ (mV)}$$

$$= 76 - 58 \log \left[a_K^i + 0.086\, a_{Na}^i \right] \text{ (mV)} \qquad (2)$$

Equation (2) provided a hypothesis to explain resting membrane electrogenesis in *Calliphora* prepupae. It suggests that the major ion involved in generating E_m is K^+, with Na^+ making a small contribution. According to this hypothesis, the ratio of the partial permeability of the cell membrane for Na^+ to that for K^+, α, has a value 0.086.

The graph of E_m against the logarithm of $(a_K^o + 0.086\, a_{Na}^o)$ (fig. 83) shows that all points fall close to a line with a slope of 58 mV per tenfold change in $(a_K^o + 0.086\, a_{Na}^o)$, and have a high correlation coefficient (0.94). It

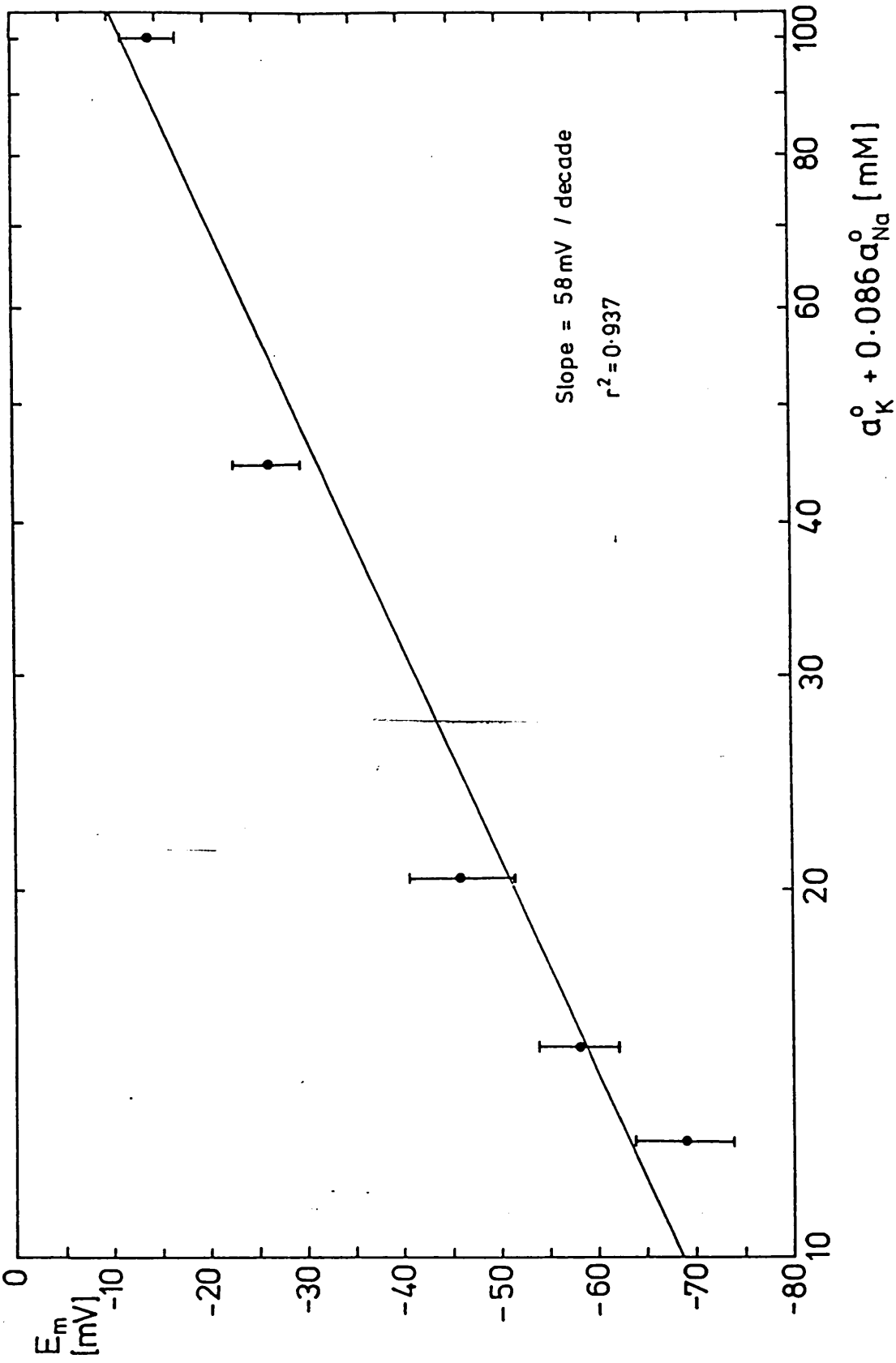


Fig. 83 Graph showing the relationship between E_m and the logarithm of $(a^o_K + 0.086\ a^o_{Na})$. (Bars represent S.D.'s).

was noted, however, that the points clearly followed a smooth curve rather than a true straight line. The greatest deviation from the straight line occured at high values of $(a_K^o + 0.086\ a_{Na}^o)$. In view of the fact that the properties of the muscle cell membrane had been found to change markedly when bathed in low-Na^+ Ringer (showing an increase in resistance and a reduction in permeability to K^+, see sections IV.4.ii and IV.4.iii), E_m data obtained in high K^+ Ringers (where a_{Na}^o was lower than, or equal to, that in Normal Ringer) and in low K^+ Ringers (where a_{Na}^o was higher than, or equal to, Normal) were considered separately. An α value of 0.169 was thus calculated from E_m data obtained in Ringers with a_K^o levels between 9.7 and 97 mM, and corresponding a_{Na}^o levels of 124.6 to 37.1 mM; and one of 0.036 was calculated from E_m data measured in Ringer solutions with a_K^o levels between 0.97 and 9.7 mM, and corresponding a_{Na}^o levels of 133.3 to 124.6 mM. These values are summarised in table 22 below.

Table 22. α values for *Calliphora* prepupae, calculated from E_m data obtained in Ringer solutions of various compositions (see table 21)

Ringer compositions	α
All a_K^o & a_{Na}^o values	0.086
High a_K^o / low a_{Na}^o	0.169
Low a_K^o / high a_{Na}^o	0.036

Figures 84 and 85 illustrate the straight line relationships between E_m and the logarithm of $(a_K^o + \alpha a_{Na}^o)$ for the two additional values of α. Both sets of data have very high correlation coefficients: 0.92 for the high K^+/low Na^+ data where $\alpha = 0.169$ (fig. 84); 0.99 for the low K^+/high Na^+ data where $\alpha = 0.036$ (fig. 85). (Principle of least squares.) Thus, considering separately data from high K^+/low Na^+ and low K^+/high Na^+ Ringers appear to provide a more accurate description of the behaviour of the cell membrane than considering all the data together.

IV.4. Tests of the model of resting membrane electrogenesis

IV.4.i. Sodium substitution experiments

These were carried out in order to test directly whether Na^+ had an effect on E_m, and, if so, whether the effect was of the right order of magnitude to

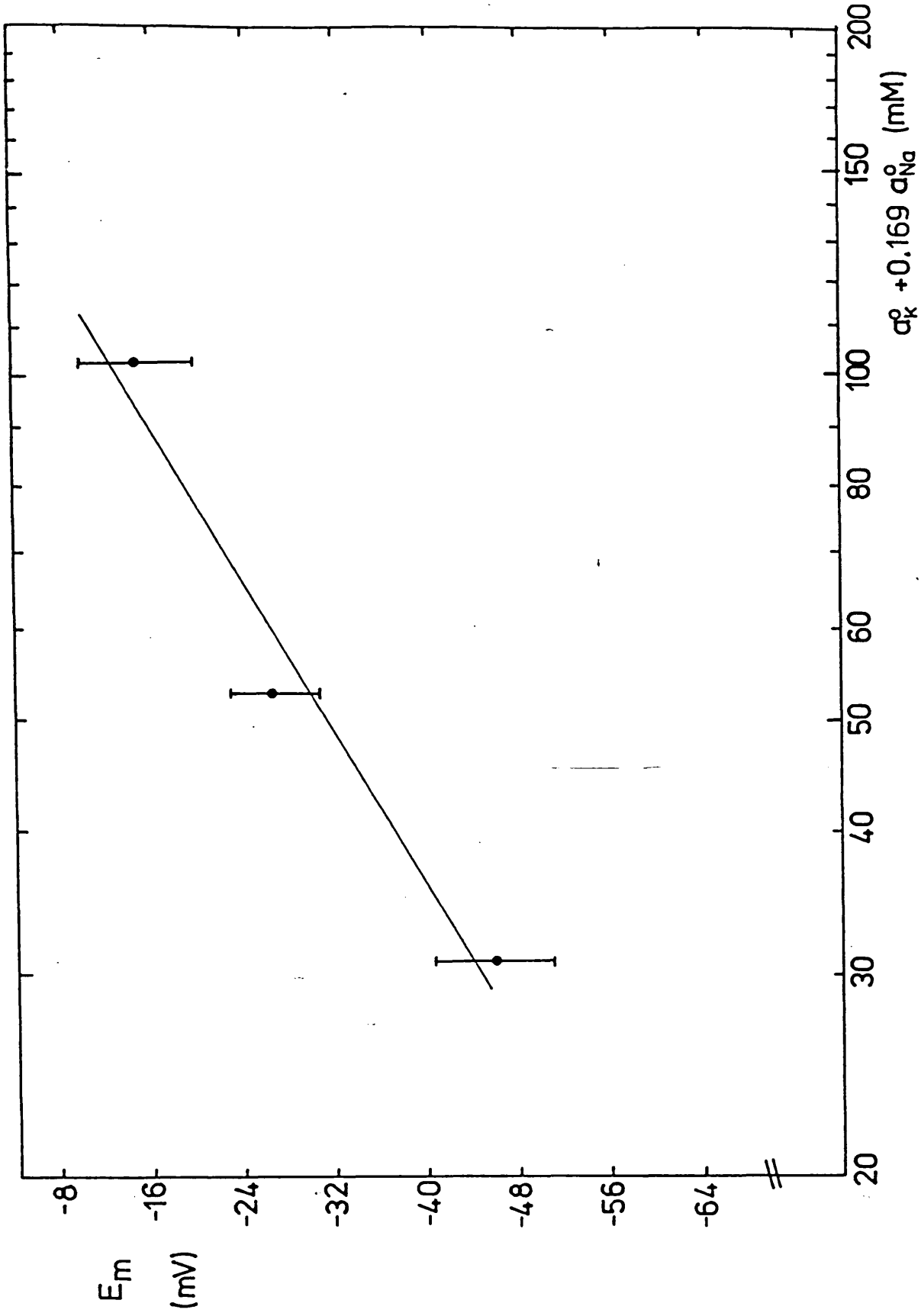


Fig. 84 Graph illustrating the relationship between E_m and the logarithm of $(a_K^o + 0.169\ a_{Na}^o)$. (Bars represent S.D:s). Straight line fitted by eye.

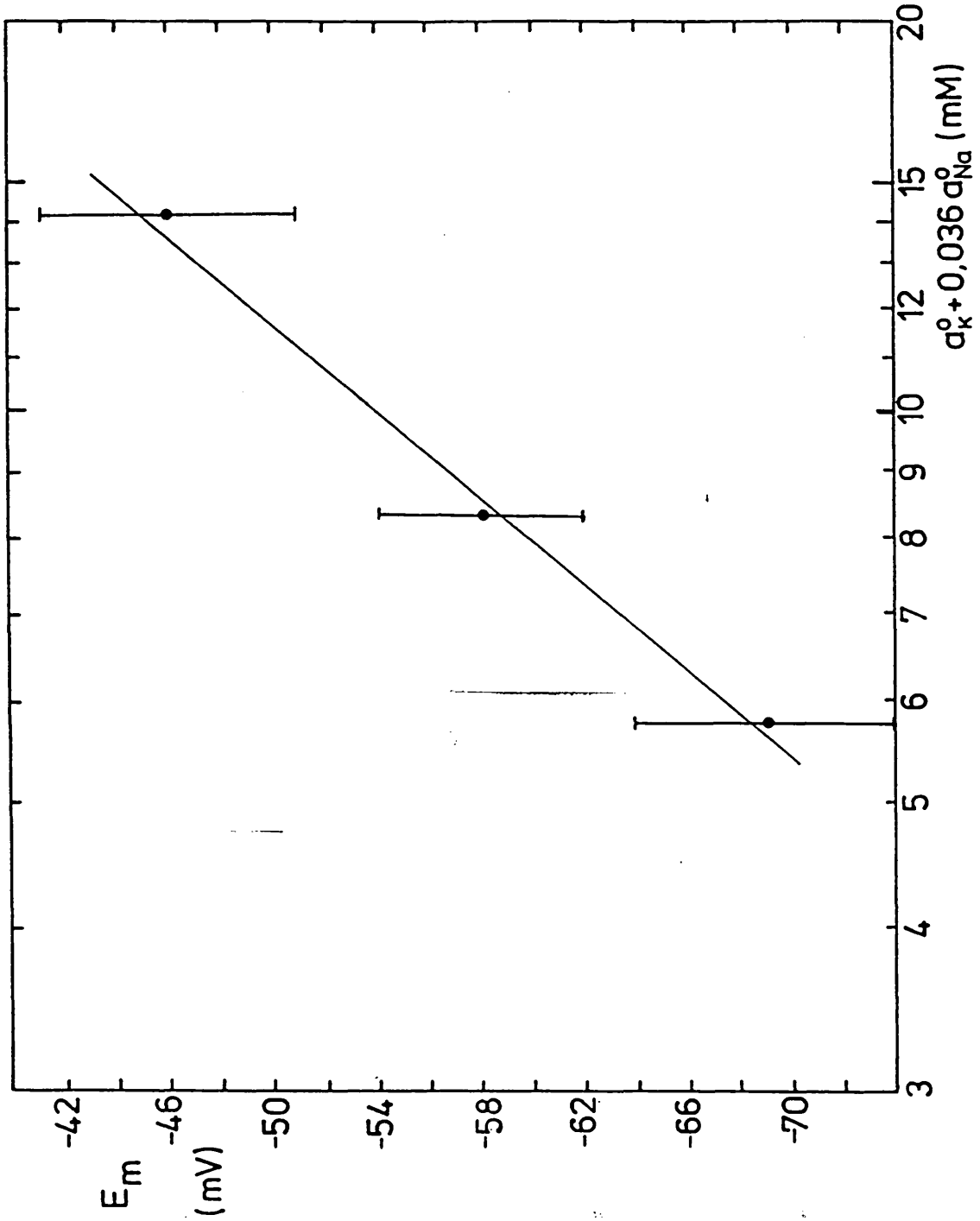


Fig. 85 Graph illustrating the relationship between E_m and the logarithm of (a_K^o + 0.036 a_{Na}^o). (Bars represent S.E's). Straight line fitted by eye.

account for the difference between the expected 58 mV per decade slope of the graph of E_m against the logarithm of the extracellular K^+ activity, and the observed slope of no more than 31 mV per decade.

Figure 86 shows a typical recording of the effect on E_m of reducing extracellular Na^+ activity from 124.6 mM to 1.25 mM, using $MgCl_2$ as a substitute (the cell membrane was apparently not permeable to the latter: a tenfold change in a_{Mg}^{o}, using glucose as a substitute caused no more than 1 mV change in E_m). Immediately after the introduction of low-Na^+ Ringer into the recording chamber, the E_m showed an initial hyperpolarisation of some 8 mV from its resting level of -50 mV. This was followed after less than 1 minute by a sustained depolarisation of some 18 mV to a steady E_m level of -40 mV which was reached 10 minutes after the introduction of the low-Na^+ Ringer. This effect reversed completely within 5 minutes of the return of Normal Ringer to the recording chamber.

In order to test that this unexpected result was not due to the unsuitability of $MgCl_2$ as a Na^+ substitute, this type of experiment was repeated using a variety of substitutes: choline chloride, n-methyl D-glucamine (nMDG), tetramethylammonium chloride (TMA chloride), glucose and, for comparison, magnesium chloride ($MgCl_2$). In all cases, similar results were obtained (fig. 87). When Low-Na^+ Ringer was substituted in for Normal saline, an initial hyperpolarisation of 2 to 7 mV was seen. This is the type of result expected if Na^+ were involved in generating E_m. This initial hyperpolarisation was, in all cases, followed by an unexpected, sustained depolarising phase, which began within one minute of the application of low-Na^+ Ringer. This phase depolarised E_m to levels 2 to 8 mV more positive than their original resting values within the duration of the experiment.

Thus, instead of the sustained hyperpolarisation in E_m expected if the permeability of the cell membrane to Na^+ were to account for the difference between the expected 58 mV per decade slope of the graph of E_m against the logarithm of a_K^o and the observed 31 mV slope, only a transient hyperpolarisation occurred. This was followed by an unexpected sustained depolarisation in E_m. Two possible explanations for this depolarising phase would be (a) an increase in a_K^i and a corresponding depolarisation in E_K when the cell was bathed in low-Na^+ Ringer, which would account for the depolarisation in E_m, or (b) a change in the relative permeability of the

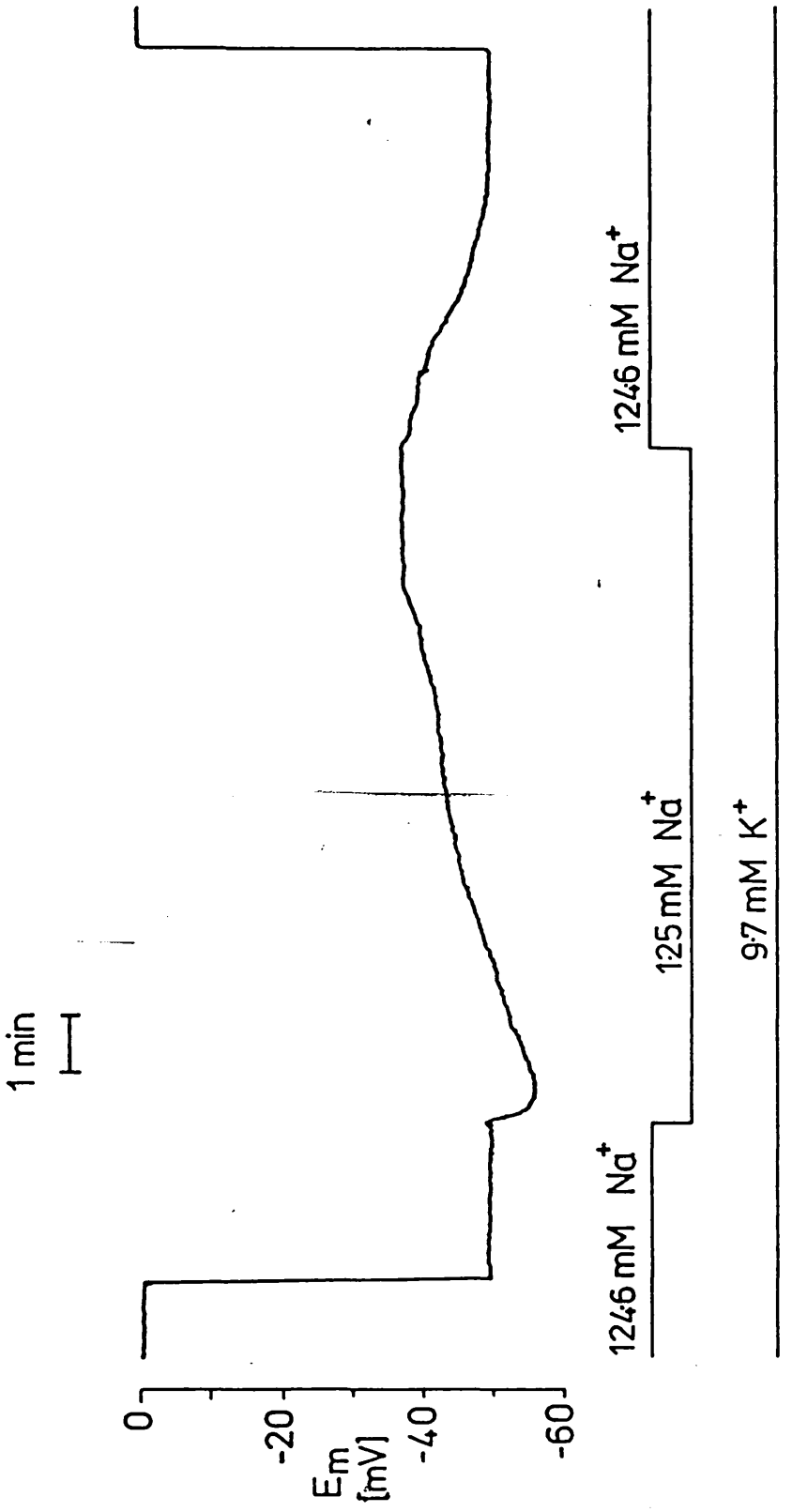


Fig. 86 Chart recording of a Na^+ substitution experiment on a *Calliphora* prepupa, illustrating the effect on E_m of reducing the extracellular Na^+ activity, a_{Na}^o.

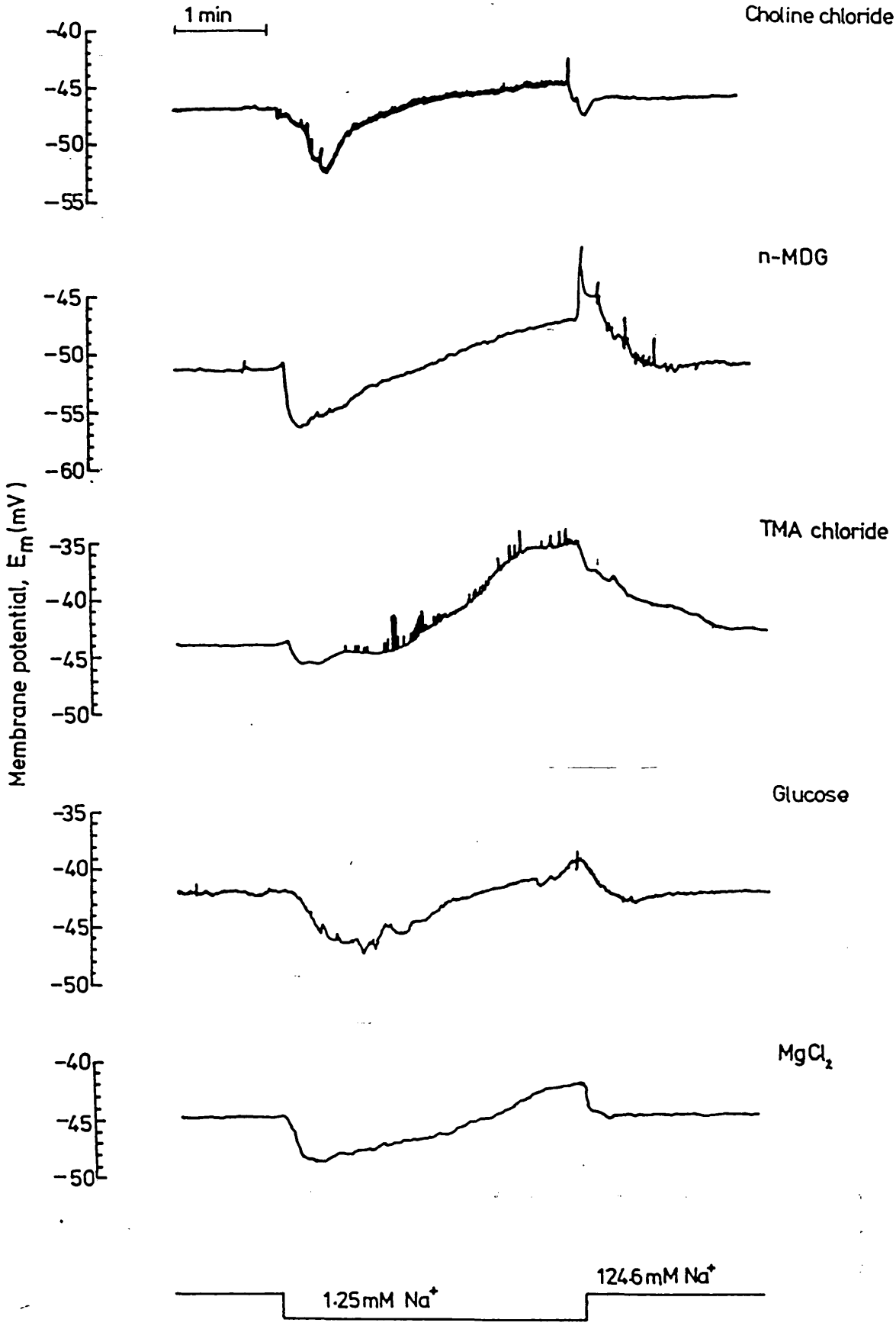


Fig. 87 Tracings of chart recordings of Na^+ substitution experiments on *Calliphora* prepupae using a variety of Na^+ substitutes (listed to the right of each trace). This illustrates the consistency of the response of E_m to reduced a_{Na}^{o}, regardless of the substitute used.

muscle cell membrane to Na^+ and K^+ in the presence of low extracellular Na^+. For example, a reduction in the permeability of the cell membrane to K^+ would result in the level of E_m moving away from that of E_K and hence E_m would depolarise.

IV.4.ii. The effect of low-Na^+ Ringer on E_K

The depolarising phase of the response of E_m to low-Na^+ Ringer could be explained if the intracellular K^+ activity, a_K^i, increased when the cell was exposed to low a_{Na}^o's. If this were the case, E_K, and hence E_m, would depolarise as a_K^i rose. In order to test this possibility experiments were designed in which a_K^i was monitored whilst a_{Na}^o was reduced.

A typical chart recording obtained from such an experiment is shown in figure 88. The upper trace shows the membrane potential of the cell (initially 38 mV), and the lower, the potassium-sensitive potential, which corresponded to an a_K^i of 80 mM. When low-Na^+ Ringer (1.25 mM Na^+) was applied to the cell as indicated beneath the trace, E_m initially hyperpolarised by some 4 mV and then depolarised to a level 9 mV more positive than its original resting value. (This type of result was consistent with data from earlier Na^+ substitution experiments). Similar data were obtained from a total of 3 cells. The a_K^i of the cells, however, remained unchanged.

Thus, the fact that E_m gave a sustained depolarisation in response to low levels of a_{Na}^o could not be explained in terms of a change in the E_K of the cell, since low-Na^+ Ringer had no effect on a_K^i.

IV.4.iii. The effect of low-Na^+ Ringer on membrane resistance.

Any change in the relative permeability of the cell membrane to Na^+ and K^+ might be reflected as a net change in the resistance of the membrane. In order to test the possibility that such a permeability change was occurring in low-Na^+ Ringer, the membrane resistances of cells were monitored during low-Na^+ substitution experiments (with Mg^{2+} as the substitute).

A typical recording from one such experiment is given in figure 89. The lower trace is the current monitor, each constant current pulse being denoted by an upward deflection of the trace. Current pulses of 7.5×10^{-9}A were applied to the muscle cell. The upper trace shows the membrane potential of

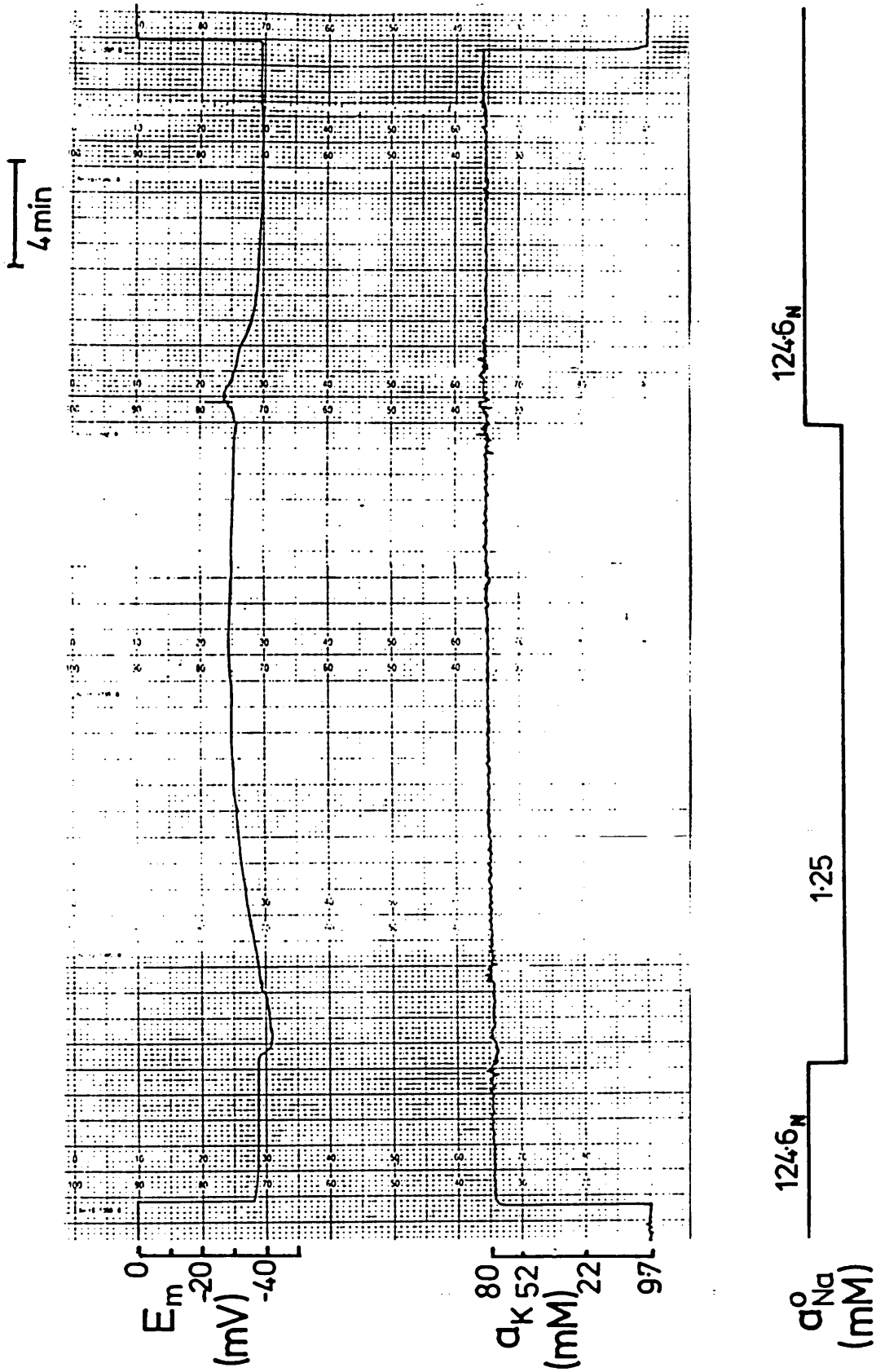


Fig. 88 Chart recording from an experiment in which a_K^i was monitored whilst a_{Na}^o was reduced. This shows that a_K^i remains unchanged in low-Na^+ Ringer.

the cell (initially -42 mV) and its responses to the application of the current pulses. These responses provide a measure of the membrane resistance. The derivation of results from the chart paper in this type of experiment is outlined in section II.4.iii. Data were obtained from 7 cells, each from a different preparation, and are summarised in table 23. The large pulses observed immediately following the impalement of the cell (fig. 89) represent the membrane resistance (column 1, table 23). These pulses were then balanced using the bridge circuit in order to make any subsequent small changes in membrane resistance easier to record on chart paper. Following the introduction of low-Na^+ (1.25 mM) Ringer (Mg^{2+} as substitute) into the recording chamber, an increase in membrane resistance was observed (columns 2 to 4, table 23). The mean value of the membrane resistance, R_m, in Normal Ringer was 96 ± 9 kΩ, and this increased by an average of 26% in low-Na^+ Ringer to give a mean of 121 ± 10 kΩ.

Thus, the observation that the membrane resistance increased when the cell was exposed to low-Na^+ Ringer is consistent with the earlier suggestion that the relative permeability of the cell membrane to K^+ and/or Na^+ appears to change in the presence of low extracellular Na^+. It is not possible, however, to deduce from these experiments whether the permeability of the cell membrane was changing specifically to K^+ or Na^+.

IV.4.iv The effect of low-Na^+ Ringer on the 'K^+ permeability' of the cell membrane

In order to determine whether the membrane resistance increases observed when a cell is exposed to low Na^+ Ringer were due to a reduction in the permeability of the cell membrane to K^+, potassium pulsation experiments were carried out. These involved the application of constant-sized pulses of high (97.2 mM) K^+ Ringer to a muscle cell bathed in Normal Ringer and obtaining membrane responses to these pulses. Low-Na^+ (1.25 mM) Ringer was then substituted in for the Normal Ringer, and any change in the membrane response to the high K^+ pulses noted. This type of experiment is illustrated in figure 90, which shows the depolarising responses of the membrane potential to high-K^+ pulses, the application of which are denoted by short bars beneath the E_m trace), and low-Na^+ Ringer (1.25 mM Na^+). In Normal Ringer (125 mM Na^+) the pulses depolarised the E_m by some 15 mV. In low-Na^+ Ringer, however, the membrane responses were reduced to around 3 mV. Shortly after the re-introduction of Normal Ringer into the

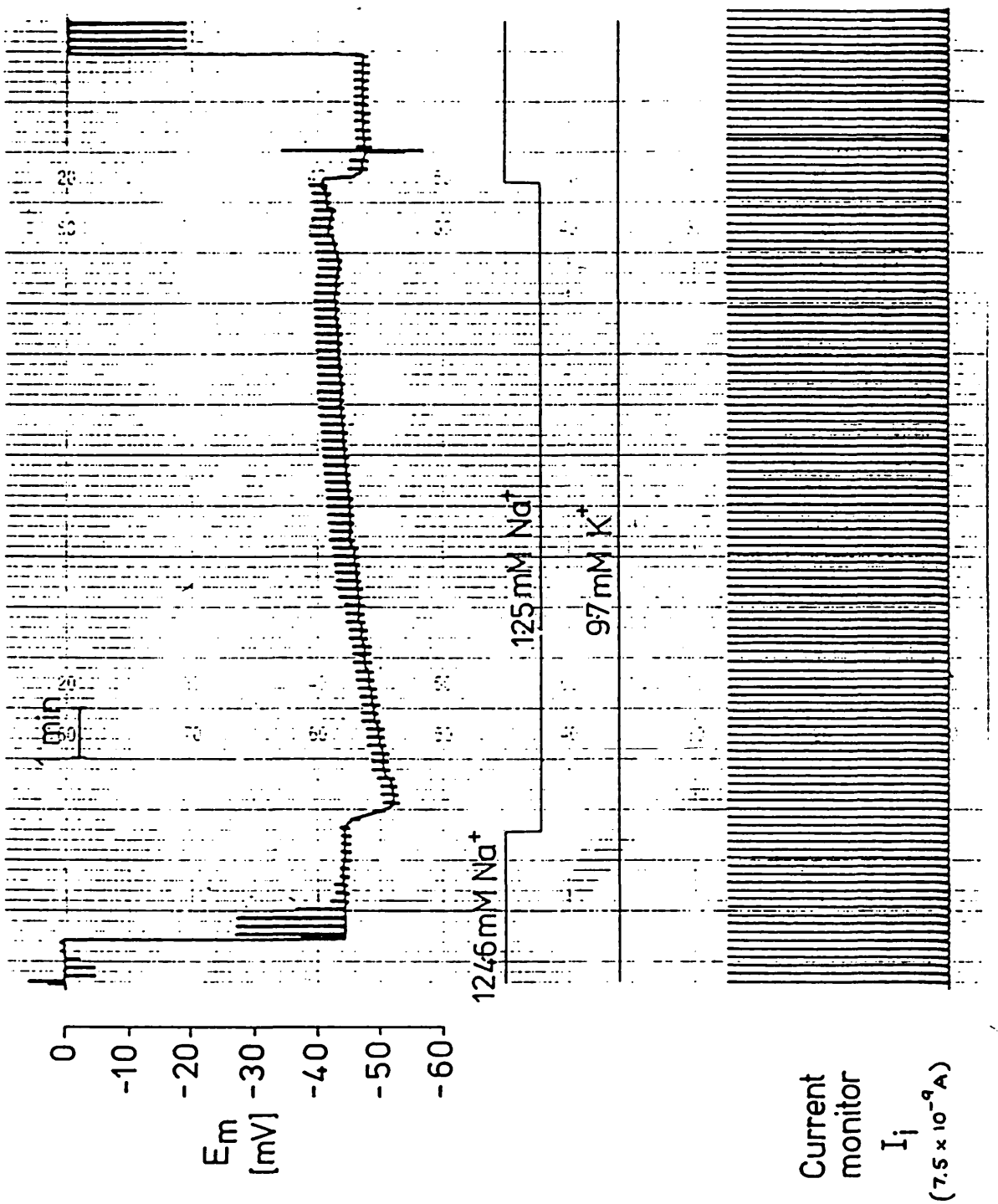


Fig. 89 Chart recording of a Na^+ substitution experiment on a *Calliphora* prepupa during which membrane resistance was monitored by the repeated application of constant-sized current pulses. It shows that membrane resistance increased when a_{Na}^{o} was reduced.

Table 23 Changes in membrane resistance recorded during low-Na^+ substitution experiments on *Calliphora* prepupae (Data from 7 cells)

Cell no.	Normal R_m (membrane resistance) kΩ	Low Na^+ (membrane resistance) kΩ	Δ R_m in low Na^+ kΩ	% Δ R_m in low Na^+
1	100	150	50	50
2	85	115	30	35.3
3	70	85	15	21.4
4	140	160	20	14.3
5	80	95	15	18.8
6	100	120	20	20
7	97	120	23	23.5
$\bar{x}$	96	120.7	25	26.2
SE	8.5	10.2	4.6	4.7

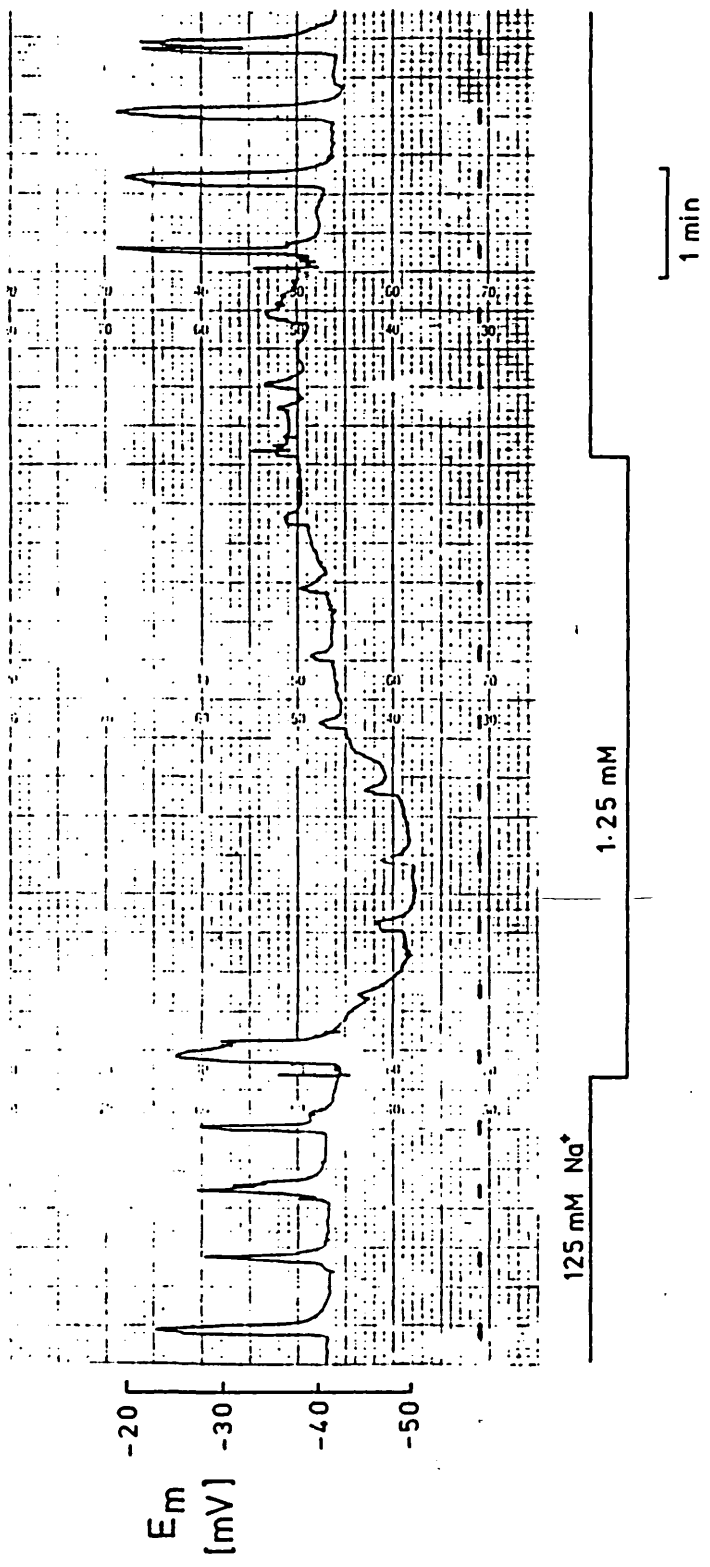


Fig. 90 Chart recording of a K^+ pulsation experiment on a *Calliphora* prepupa. This shows that the response of the cell membrane to constant-sized pulses of high K^+ Ringer was markedly reduced when the cell was exposed to low-Na^+ Ringer.

Table 24. *Calliphora* muscle cell membrane responses to constant-sized pulses of high K^+ (97.2 mM) Ringer when bathed in Normal Rice's saline (124.6 mM Na^+) and low-Na^+ (1.25 mM) Ringer.

	Membrane response as % of initial response								
t (x 100s)	Cell 1	Cell 2	Cell 3	Cell 4	Cell 5	Cell 6	Cell 7	$\bar{x}$	SE
0	96	100	64	117	117	113	91	99.7	7.1
1	93	100	109	100	89	100	86	96.7	3.0
2	100	100	91	100	100	120	109	102.9	3.5
3	100	100	100	100	89	77	114	97.1	4.3
4	100	131	27	150	--	77	111	99.3	17.7
5	3.6	7.7	18	--	11	77	0	19.6	11.8
6	0	19	9	17	0	13	0	8.3	3.2
7	5.4	23	18	0	0	13	0	8.5	3.6
8	1.8	23	9	0	0	10	0	6.3	3.2
9	0	19	0	0	0	10	0	4.1	2.8
10	0	19	0	0	0	7	0	3.7	2.7
11	0	23	9	0	0	7	0	5.6	3.2
12	0	15.4	9	0	0	7	14	6.5	2.5
13	1.8	23	9	0	0	7	14	7.8	3.2
14	0	31	18	0	22	10	36	17.2	5.5
15	1.8	154	73	0	0	7	9	34.9	22.1
16	1.8	169	91	33	0	7	0	43.1	24.4
17	0	177	82	33	11	10	9	46.0	24.2
18	3.6	154	73	33	11	10	100	54.9	21.4
19	93	154	91	66	11	10	105	75.7	19.5
20	93	162	64	66	11	10	109	73.6	20.4
21	86	154	73	167	156	87	109	118.9	14.8
22	89	154	73	100	122	80	109	103.9	10.5
23	79	154	91	167	156	73	82	114.5	15.9
24	86	154	64	100	144	73	118	105.6	13.1
25	89	150	64	66	156	73	109	101.0	14.6
26	--	--	91	100	144	95	100	106.0	9.6

Low Na^+

recording chamber, the response of the membrane recovered completely. Similar results were obtained from a total of 7 cells (table 24).

The effect of low extracellular Na^+ on the permeability of the cell membrane to K^+ is illustrated by figure 91, a graph showing the variation in the membrane response to constant-sized pulses of high K^+ Ringer throughout the experiment. (The membrane response is expressed as a percentage of the initial pretreatment response to the pulse of K^+). This shows clearly the reduction in the responsiveness, ie. permeability of the cell membrane to K^+ which results when the cell is exposed to low extracellular Na^+. A hundredfold reduction in extracellular Na^+ leads to an average reduction in membrane response to 4% of its original value.

The above attempt to test the hypothetical model of resting membrane electrogenesis in *Calliphora* prepupae (equation 2), by performing Na^+ substitution experiments was thus only partially successful. A reduction in the extracellular Na^+ activity of a cell gave an initial hyperpolarisation in E_m, confirming that Na^+ was involved in generating E_m. This hyperpolarisation was, however, followed by an unexpected depolarisation in E_m, which occurred simultaneously with a marked reduction in the permeability of the cell membrane to K^+.

Thus, Na^+ appears to influence E_m. However, in low-Na^+ solutions the partial permeability of the cell to K^+ (and possibly other ions) changes, thereby altering the value of α and invalidating the model being tested.

IV.4.v. Measurement of both intracellular K^+ and Na^+ activities in the same population of cells

According to the model for resting membrane electrogenesis based on the simplified version of the Goldman-Hodgkin-Katz equation, which taken into account only the transmembrane gradients of K^+ and Na^+ (equations 1 and 2, section IV.3) it should be possible to predict the E_m of a cell from a knowledge of the intra- and extra-cellular activities of K^+ and Na^+, together with the value of α (p_{Na}/p_K):

$$E_m = 58 \log \left[\frac{9.7 + \alpha.124.6}{a_K^i + \alpha\, a_{Na}^i} \right] \quad (mV)$$

Thus, a series of experiments was undertaken, involving the use of NIC-type

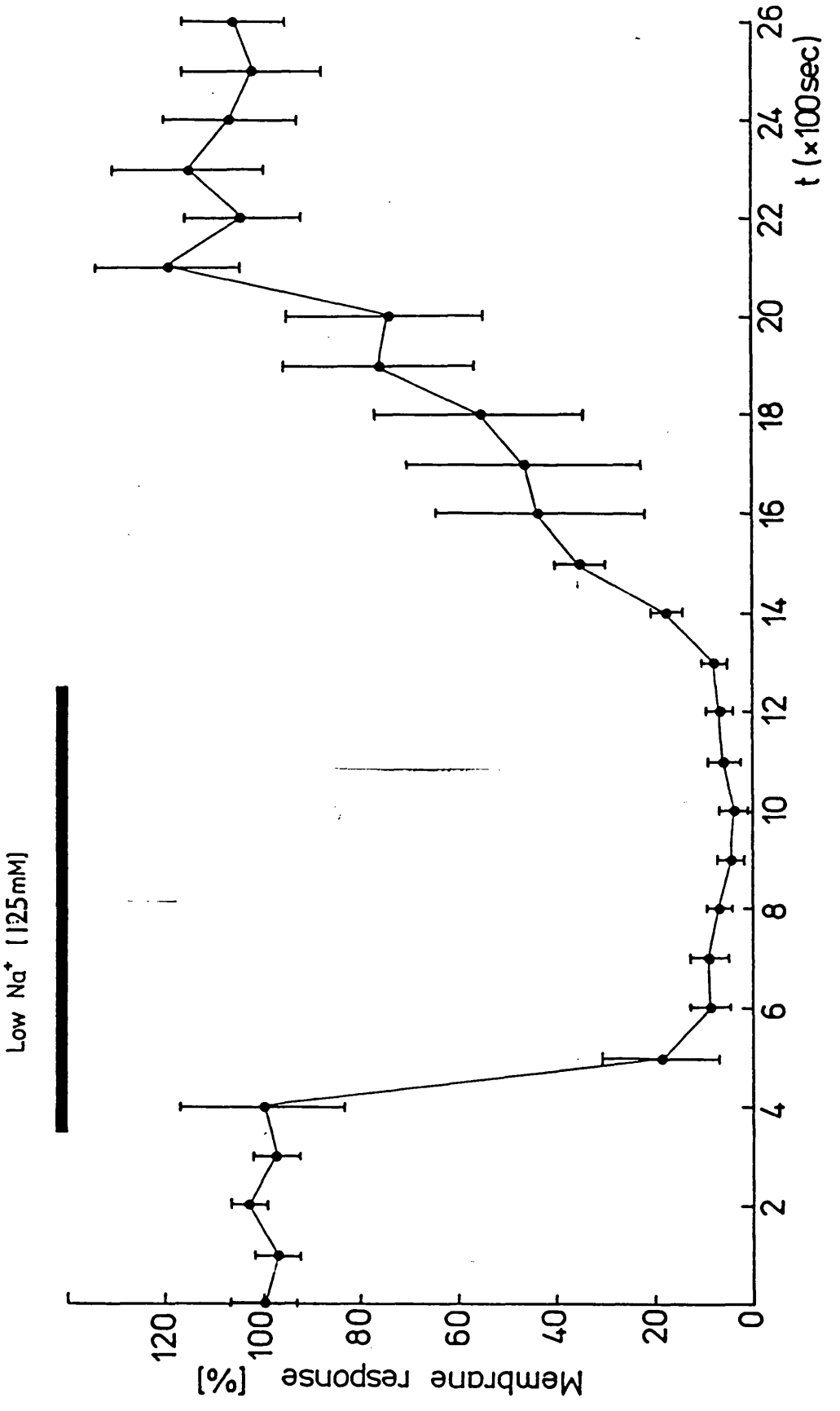


Fig. 91 Graph illustrating the change in the magnitude of the membrane response to constant-sized pulses of high K^+ Ringer when the cells were exposed to low Na^+ Ringer. This shows the marked reduction in P_K which occurred in the presence of low levels of extracellular Na^+. (Bars represent standard errors, n = 7.)

K^+- and Na^+-ISMs to measure intracellular K^+ and Na^+ activities (a_K^i and a_{Na}^i, respectively) together with the membrane potentials in a population of cells. The aim of these experiments was to substitute measured values of a_K^i and a_{Na}^i from single cells into the modified Goldman-Hodgkin-Katz equation given above, and to determine which of the three values of α calculated (0.086, 0.169 or 0.036, see section IV.3, table 22) gave the most accurate prediction of the E_m of the cell. Values of a_K^i, a_{Na}^i and E_m were therefore measured in a total of 18 cells from 3 preparations, and are listed in appendix 12 (columns 1, 2 and 3 respectively).

The values of E_m predicted for each cell using the α values 0.086, 0.169 and 0.036 are listed in appendix 12 (columns 4, 5 and 6) and table 25 where they are compared with the average measured value of E_m.

Table 25 Comparison between E_m values predicted using α values of 0.086, 0.169 and 0.036 and measured E_m values (Data is given as mean ± SE).

	α		
	0.086	0.169	0.036
E_m (predicted) (mV):	-39 ± 1	-27 ± 1	-48 ± 1
E_m (measured) (mV) :	-48 ± 1	-48 ± 1	-48 ± 1
E_m (predicted) - E_m (measured):	9 ± 1	21	0

The membrane potential predicted using an α value of 0.086 was thus more positive than the measured membrane potential in all cells, by an average of 9 mV, which is highly significant ($p < 0.001$, t-test). This is illustrated by figure 92, a graph of predicted E_m against measured E_m. These points give a correlation coefficient of 0.61 and a slope of 1.3, and have a rather wide scatter. It was therefore clear that the above value of α did not provide an accurate prediction of the E_m of a cell, implying that it did not truly reflect the membrane properties.

The α value calculated from the high K^+/low Na^+ data (0.169) gave predicted E_m values on average 21 mV more positive than the measured E_m values, reflecting perhaps the "abnormal" behaviour of the cell membrane in the presence of low extracellular Na^+ levels. The α value calculated from the low K^+/high Na^+ data (0.036), however, provided, on average, a very accurate prediction of E_m (the mean predicted E_m was equal to the mean measured E_m). Figure 93 shows the relationship between E_m (predicted) and

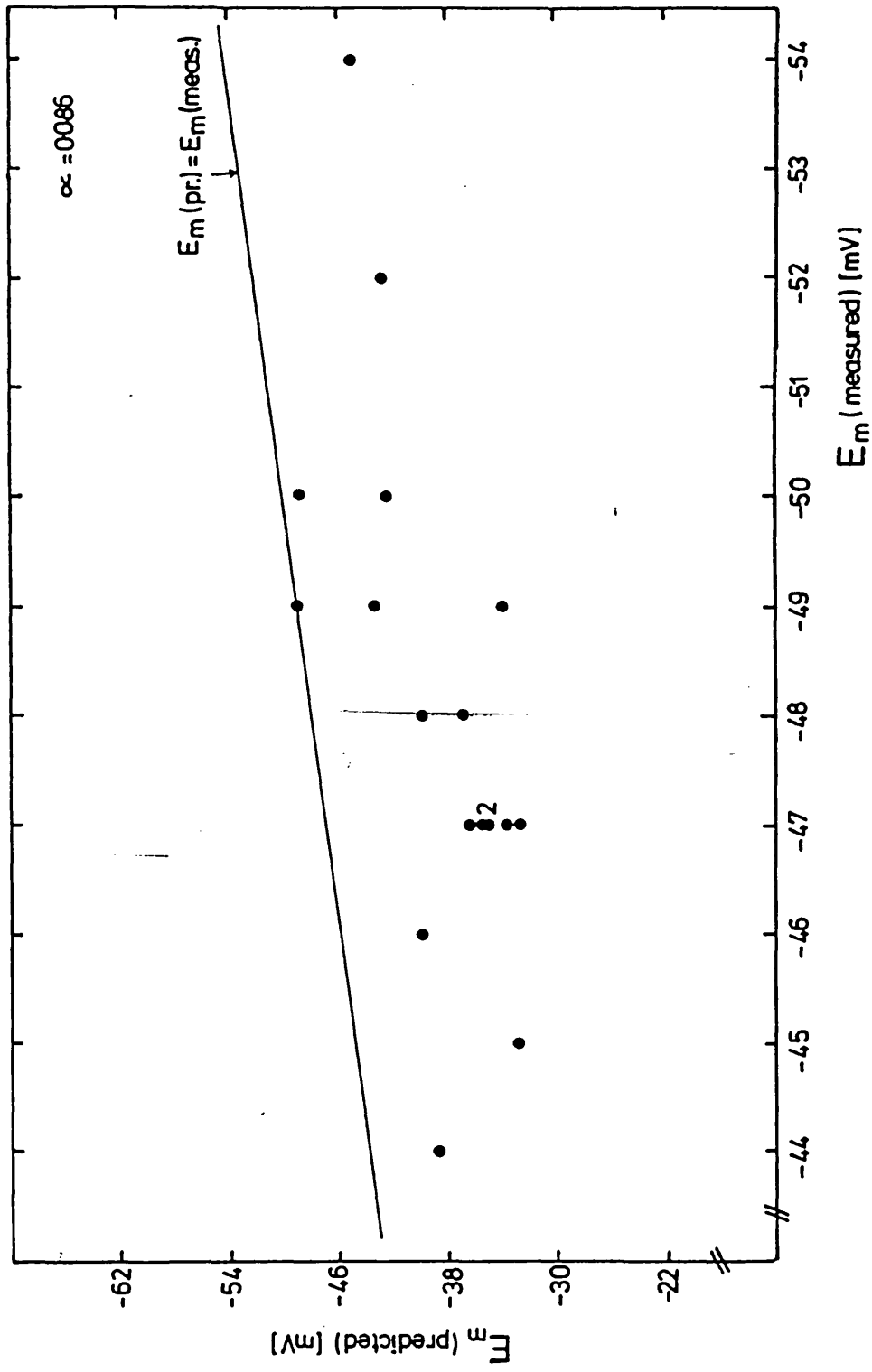


Fig. 92 Graph showing the relationship between the E_m values predicted for a population of cells from the Goldman-Hodgkin-Katz equation using an α value of 0.086, and the values measured in the same cells. It illustrates the fact that the majority of the predicted values were more positive than the measured E_m's.

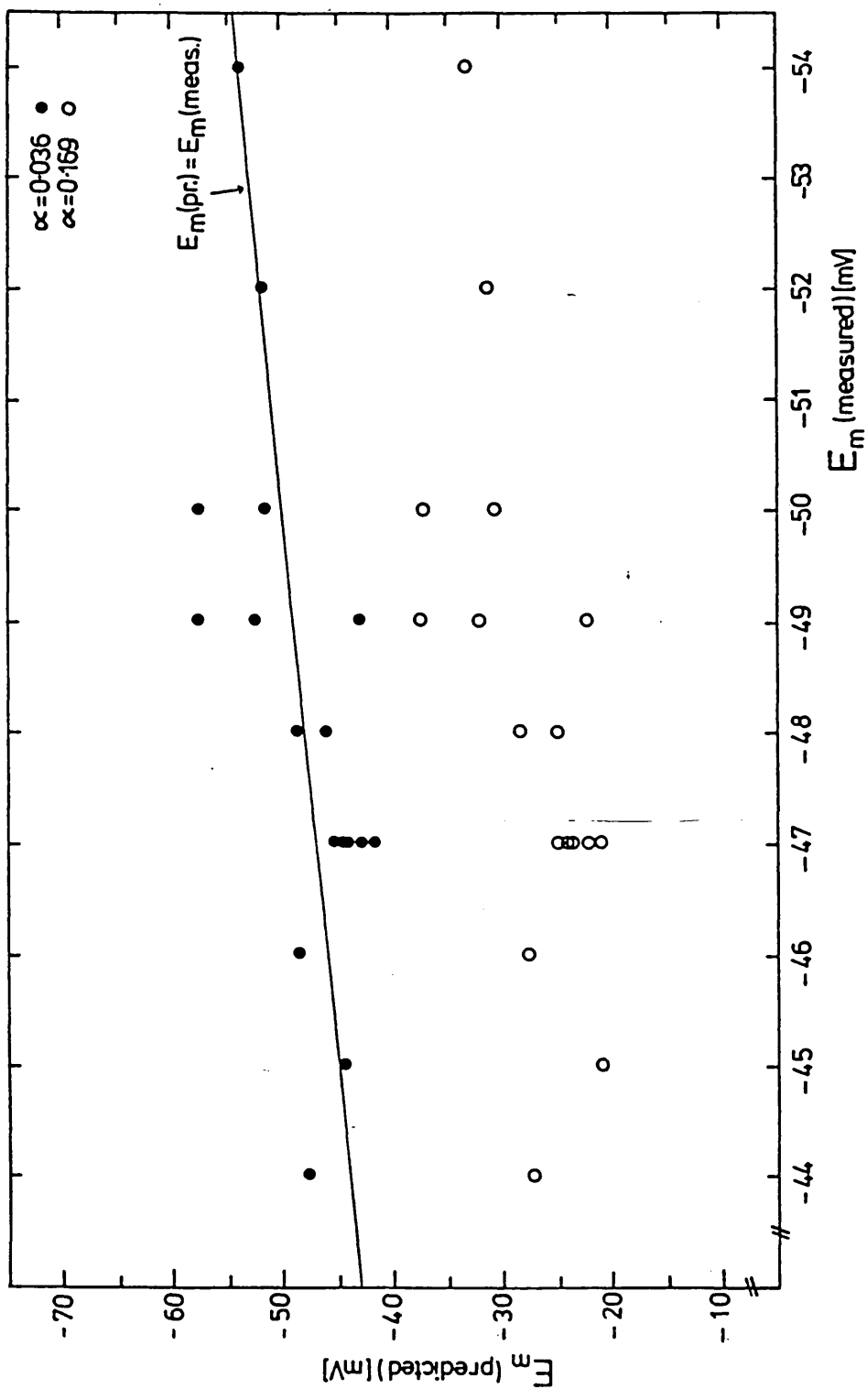


Fig. 93 Graph showing the relationship between the E_m values predicted for a population of cells from the Goldman-Hodgkin-Katz equation using α values of 0.036, (filled circles) and 0.169 (hollow circles), and the measured E_m values in the same cells. It illustrates that the α value at 0.036 provides the most accurate prediction of E_m.

E_m (measured) using the two additional values of α. This illustrates the greater accuracy of the α value of 0.036 in predicting E_m. The correlation coefficients for the points are, however, low for both values of α (0.59 for α = 0.036, 0.61 for α = 0.169), reflecting the high degree of scatter of the points, relative to the range of E_m values involved.

Thus the value of α (0.036) calculated using data points from substitution experiments in which the extracellular Na^+ levels were equal to or greater than that in Normal Ringer (ie. where extracellular K^+ varied betwen 0.97 and 9.7 mM) provided the best predictions of E_m. The final model for resting membrane electrogenesis was therefore modified from that proposed initially (equation (2)), to include the α value of 0.036. The latter was substituted into the simplified Goldman-Hodgkin-Katz equation together with the known values of a_K^o (9.7 mM) and a_{Na}^o (124.6 mM) to give the following:

$$E_m = 58 \log \left[\frac{9.7 + (0.036 \times 124.6)}{a_K^i + 0.036 \times a_{Na}^i} \right]$$

$$\boxed{E_m = 66.8 - 58 \log (a_K^i + 0.036\, a_{Na}^i)} \qquad (3)$$

The above model remained to be tested by a further series of substitution experiments which will be discussed in the next section.

IV.4.vi <u>The effect of varying (a_K^o + 0.036 a_{Na}^o) on E_m, whilst keeping (a_K^o + 0.036 a_{Na}^o) x a_{Cl}^o constant</u>

According to the model for resting membrane electrogenesis proposed in the preceding section (equation (3)), the E_m of a muscle cell is explicable in terms of the transmembrane gradients of K^+ and Na^+, with the contribution of Na^+ being weighted by a factor, α (p_{Na}/p_K) with a value of 0.036. If this were correct, a tenfold change in (a_K^o + 0.036 a_{Na}^o) would be expected to lead to a 58 mV change in E_m. Since Cl^- was known to be passively distributed in this preparation (sections III.4, IV.1.ii) substitution solutions were constructed such that (a_K^o + 0.036 a_{Na}^o) x a_{Cl}^o were kept constant (Appendix 6). The latter ensured that Cl^- and water did not move across the cell membrane, in accordance with the Donnan equilibrium, when a_K^o and a_{Na}^o were altered. Thus, changes in a_K^o and a_{Na}^o would be expected to produce rapid changes in E_m.

As expected, all E_m changes were quick and reversible, occurring within less than a minute of the completion of the solution change (fig. 94). This confirmed the conclusions from intracellular Cl^- activity measurements and Cl^- substitution experiments that Cl^- is passively distributed in this insect.

The results obtained from 7 cells (7 preparations) when (a^o_K + 0.036 a^o_{Na}) was varied between 12.9 and 18.3 mM are listed in appendix 13, and the mean E_m changes are shown in table 26, below.

Table 26. Summary of the results obtained from substitution experiments on *Calliphora* in which (a^o_K + 0.036 a^o_{Na}) was varied whilst keeping (a^o_K + 0.036 a^o_{Na}) x a^o_{Cl} constant

(a^o_K + 0.036 a^o_{Na}) (mM)	E_m (mM)	± SE
12.9	-56	2
14.2_N	-54	2
15.5	-51	2
17.2	-49	2
18.3	-47	2

The changes in E_m with changes in (a^o_K + 0.036 a^o_{Na}) are represented graphically in figure 95. The latter illustrates the linear relationship between E_m and the logarithm of (a^o_K + 0.036 a^o_{Na}). The slope of the line is 59 mV per tenfold change in (a^o_K + 0.036 a^o_{Na}) with a correlation coefficient of 0.996. This slope is extremely close to 58 mV, providing conclusive evidence that the model for resting membrane electrogenesis proposed (equation (3)) accounts fully for the ionic bases of the resting membrane potential.

In conclusion, in *Calliphora* prepupae, both the K^+ and Na^+ gradients are involved in generating the resting membrane potential of the body-wall muscle cells. The membrane potential can best be explained by assuming that the ratio of the Na^+ : K^+ permeabilities of the membrane, $\alpha = p_{Na}/p_K$, has a value of 0.036.

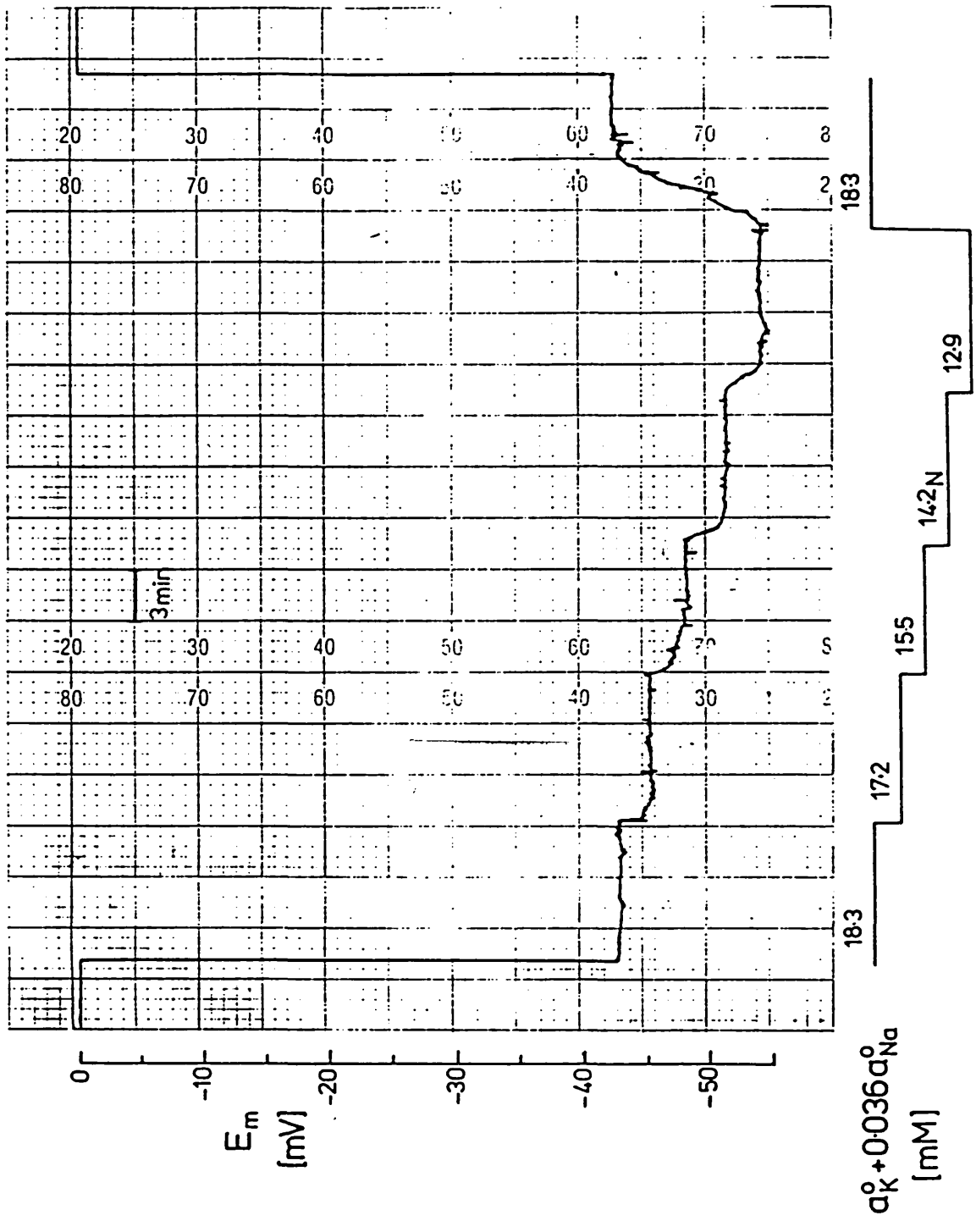


Fig. 94 Chart recording showing a substitution experiment on a *Calliphora* prepupa in which (a^o_K + 0.036 a^o_{Na}) was varied whilst (a^o_K + 0.036 a^o_{Na}) x a^o_{Cl} was kept constant. It illustrates the rapid and sustained nature of the changes in E_m in response to changes in (a^o_K + 0.036 a^o_{Na}).

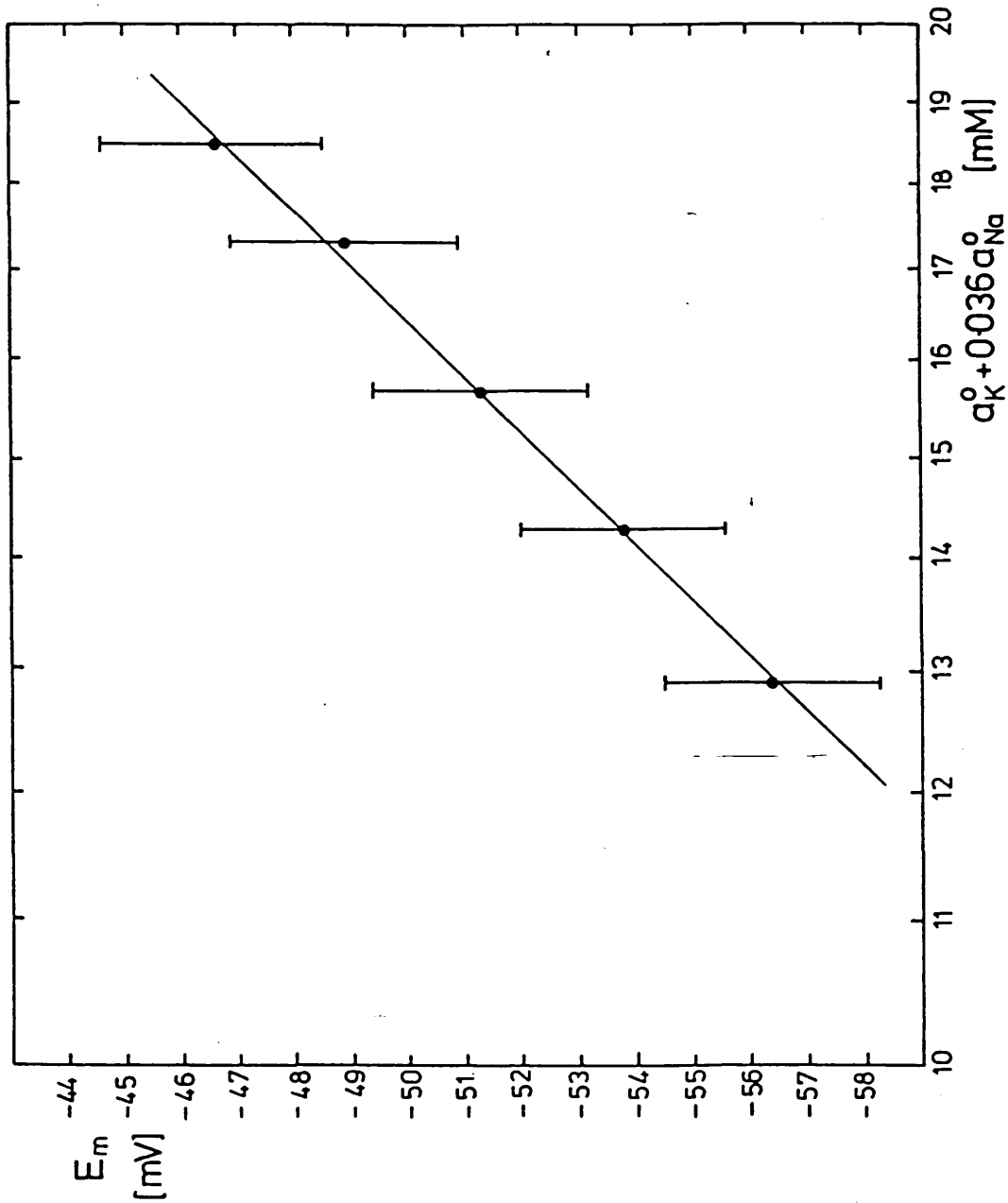


Fig. 95 Graph illustrating the relationship between E_m and the logarithm of $(a^o_K + 0.036\ a^o_{Na})$. It shows that all points fall extremely close to a line with a slope of 59 mV per tenfold change in $(a^o_K + 0.036\ a^o_{Na})$. (Bars indicate S.E.'s)

V. INTRACELLULAR IONIC ACTIVITY MEASUREMENTS IN *CHILO* LARVAE

V.1. Conventional microelectrode measurements of membrane potentials

Conventional 2.5 M KCl-filled microelectrodes (OM's) were used to establish the 'normal' levels of resting potentials, E_m, in *Chilo* preparations, as described in section III.1 for *Calliphora*. Using this information, it was possible to test that ISMs did not inflict significant damage on *Chilo* muscle cell membranes during the impalement of the cells, by comparing the mean and distribution of membrane potential values measured using the two types of microelectrode. If damage were occurring, depolarised levels of resting potential would be recorded. Thus, if the relatively coarse tips of ISMs ($\leq$ 1.5μm cf $\leq$ 1μm for OMs) were leading to poor impalements being obtained, the E_m values recorded using this technique would be expected to have a lower mean and a more asymmetrical distribution than the values recorded using OMs. Control data was obtained from a total of 99 cells from 13 preparations using OMs (with tip resistances between 60 and 80 MΩ) and a frequency histogram illustrating the distribution of the values measured is shown in figure 96. E_m's of between -35 and -59 mV were recorded, giving a mean of -45 mV. The distribution of these values was normal, with the mean falling very close to the modal class.

The means and distributions of E_m values subsequently measured using the reference barrels of ion-sensitive microelectrodes (ISMs) were compared with the above population of values recorded using OMs (fig. 96). Data from ISMs was accepted only if the E_m values measured in a given preparation were comparable in both mean and distribution to those measured with OMs.

Intracellular ionic activity measurements in *Chilo* larvae

K^+, Na^+- and Cl^--sensitive microelectrodes were made and calibrated as decribed in section II.1. Single cells in preparations bathed in Weevers' saline (Appendix 2) were impaled with ISMs under microscopical control. The results described below were derived from chart recordings by direct measurement (for membrane potentials) and by referring the recorded potential from the active barrel to the calibration curve for the ISM (ionic activity measurements) (section II.4.ii). Full lists of data from individual cells are given in appendices 8 (K^+ data), 9 (Na^+ data) and 10 (Cl^- data). In each list, the data from different preparations is separated by a space.

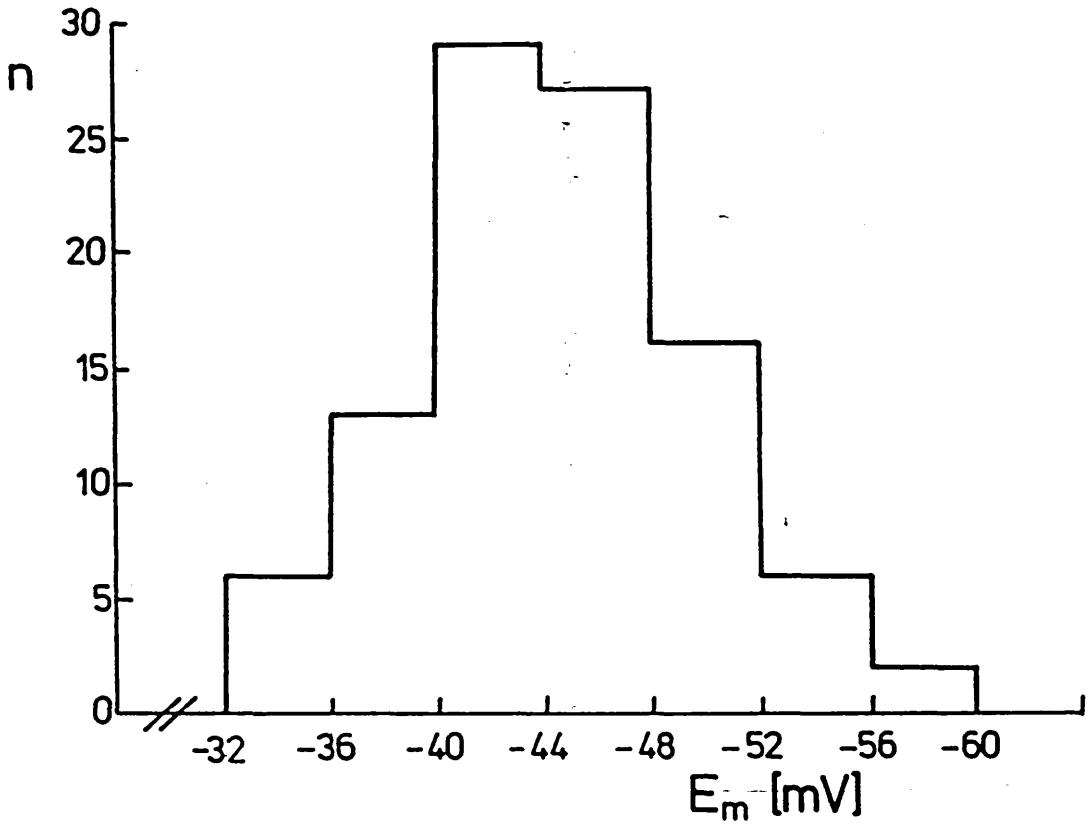


Fig. 96 Frequency histogram illustrating the distribution of E_m values measured in *Chilo* larvae with conventional microeletrodes.

The first column gives the membrane potential of each cell, E_m; the second, the potential response to the primary ion (K^+, Na^+ or Cl^-), V_X; the third, the intracellular activity of the primary ion, a_X^i; the fourth, the corresponding equilibrium potential, E_X, and the fifth, the difference between the equilibrium potential for the primary ion and the membrane potential for each cell, $E_X - E_m$.

It should be noted, however, that the muscle cells of *Chilo* larvae are markedly smaller than those of *Calliphora* larvae or prepupae (~ 0.2 x 1.5 mm cf. 0.5 x 2 mm in *Calliphora*) with the result that *Chilo* cells were more difficult to impale without inflicting damage on the cell membrane. This resulted in more variability in the data recorded and necessitated the discarding of a large amount of data which was not in accordance with the criteria set down for the selection of results (section II.5) for example, a total of 63 cells from 10 preparations were impaled using Na^+ ISMS, but only 13 cells (21% of the total Na^+ data) were accepted.

V.2. Intracellular K^+ activities

Measurements of intracellular K^+ activities, a_K^i's, were made using two types of K^+ ISM: one based on the Corning potassium exchanger (code 477317), LIX, and the second on the valinomycin-based neutral ion carrier, NIC (Oehme & Simon, 1976). A typical impalement using each type of K^+ ISM is shown in figures 97 and 98. In each, the upper trace corresponds to the membrane potential, E_m, and the lower the potassium-sensitive potential, V_K, which was referred to the calibration curve of the ISM to give the intracellular K^+ activity, a_K^i. Figure 97 shows the impalement of a cell with a LIX-type K^+ ISM giving an E_m of -44 mV and an a_K^i of 90 mM which corresponded to a potassium equilibrium potential, E_K, of -36 mV. The latter was more positive than E_m by 8 mV. Figure 98 shows an impalement made using a NIC-type K^+ ISM, giving an E_m of -40 mV, an a_K^i of 69 mM and a corresponding E_K of -29 mV. As noted for the LIX-type ISM data, E_K was more positive than E_m, here by 11 mV. Data were obtained from a total of 78 cells from 7 preparations using LIX-type ISMs, and from 77 cells, 8 preparations using NIC-type ISMs. The averaged data is summarised in table 27, below.

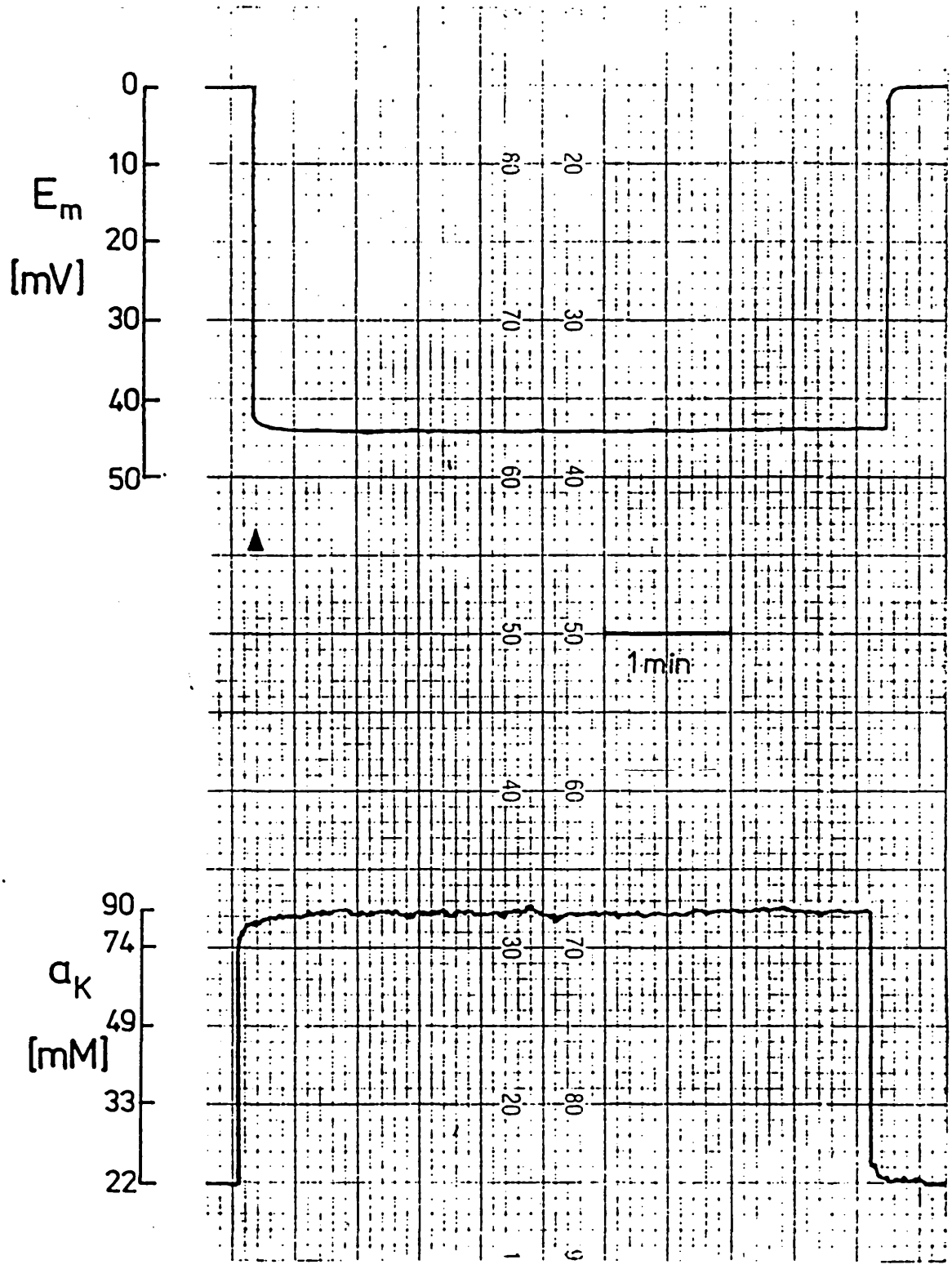


Fig. 97 Chart recording showing a typical impalement of a *Chilo* larval muscle cell with a LIX-type K^+ ISM.

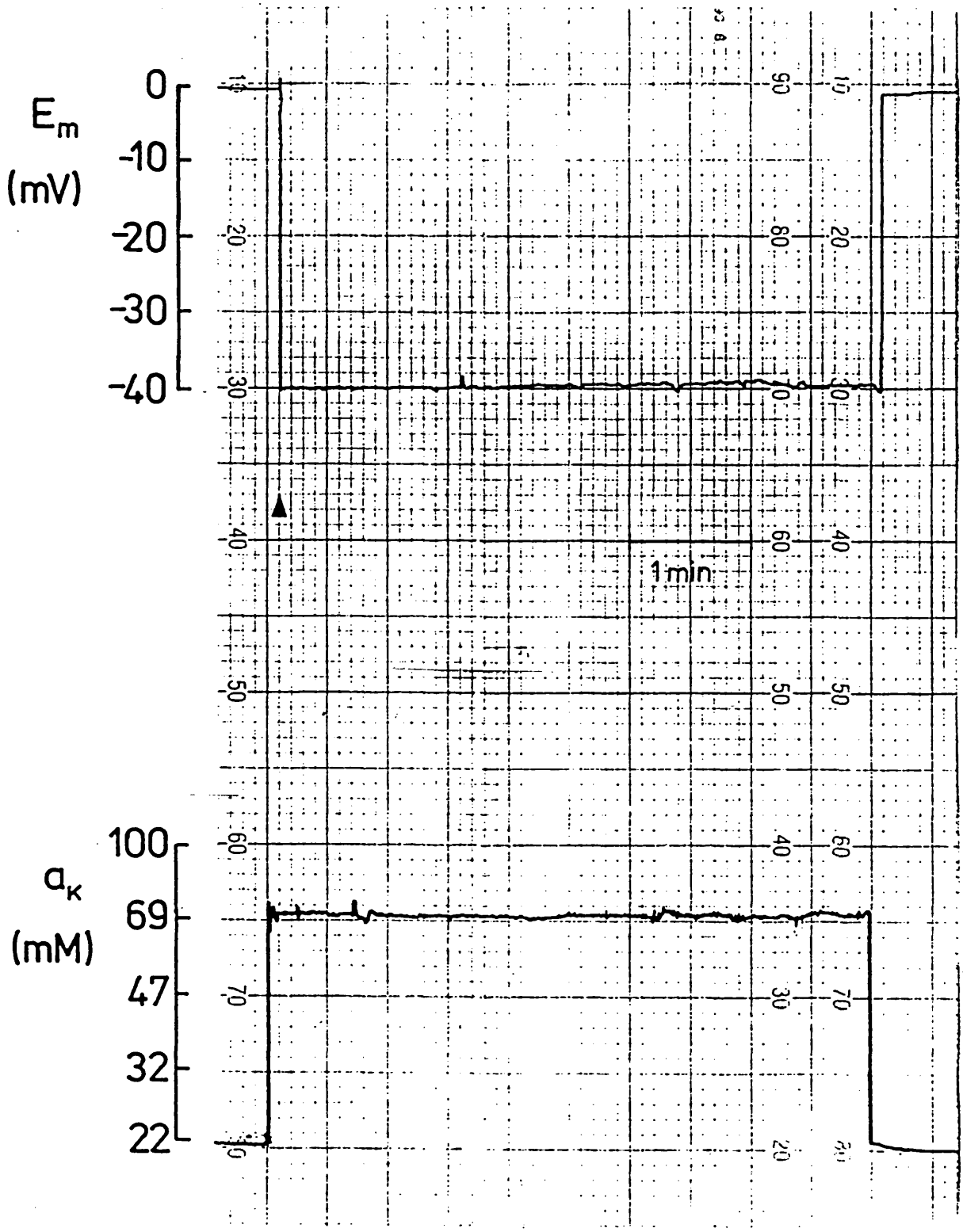


Fig. 98 Chart recording showing a typical impalement of a *Chilo* larval muscle cell with a NIC-type K^+ ISM.

Table 27 Intracellular K^+ data from *Chilo* larvae (Data from LIX-type (78 cells, 7 preparations) and NIC-type (77 cells, 8 preparations) ISMs are given as mean ± SE)

	LIX	NIC
a_K^i (mM) :	65 ± 1	62 ± 1
E_K (mV) :	-27 ± 1	-26 ± 1
E_m (mV) :	-46 ± 1	-45 ± 1
E_K-E_m (mV):	19 ± 1	19 ± 1

The intracellular K^+ activity, a_K^i, values recorded using LIX-type ISMs ranged from 43 to 96 mM with a mean of 65 mM. The distribution of these values, illustrated in the form of a frequency histogram in figure 99a, is somewhat skewed but approximately normal, with the mean (65 mM) falling in the class adjacent to the modal class. Similar trends were observed in the data recorded using NIC-type ISMs (fig. 99b). Values were in the range 44 to 82 mM, with a mean of 62 mM.

The corresponding potassium equilibrium values, E_K, for LIX-type ISM data were between -20 and -38 mV (mean -27 mV) and followed an approximately normal distribution (fig. 100) E_K was consistently more positive than E_m, which had values between -36 and -60 mV, with a mean of -46 mV. This trend is reflected in figure 100, where the distributions of the two parameters are compared on the same axes. The two distributions are quite distinct, with only a very small area of overlap, between -32 and -40 mV, and a difference of 19 mV between the means. The E_K values calculated from the NIC-type ISM data were between -18 and -34 mV with a mean of -26 mV which fell in the modal class of the frequency histogram for this data (fig. 101). This data resembled that from LIX-type ISMs in E_K being consistently more positive than E_m in all cells studied, by an average of 19 mV. E_m values recorded by the refence barrels of NIC-type ISMs ranged from -36 to -54 mV with a mean of -45 mV which fell in the modal class of the frequency histogram for this data (fig. 101). The separation between the populations of E_K and E_m values is also illustrated in the same figure.

Thus, the intracellular K^+ activity data obtained from *Chilo* larval muscle cells using two types of K^+ ISM, based on LIX- and NIC-type K^+-sensors, were qualitatively similar. The mean values of a_K^i recorded using the two types of ISM (65 mM using LIX-type and 62 mM using NIC-type ISMs) were, however, signficantly different ($p < 0.05$, t-test). This implied that *Chilo*

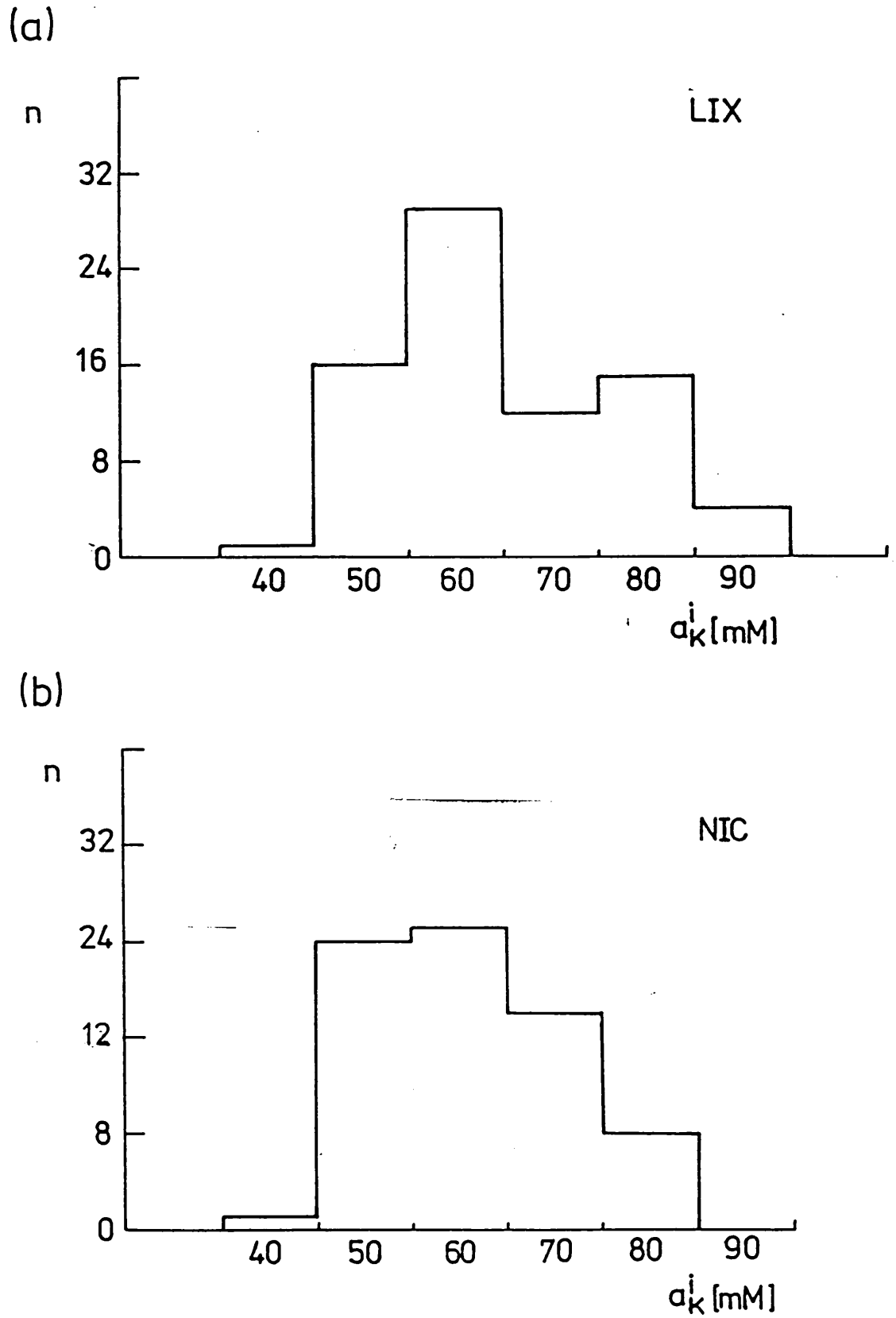


Fig. 99 Frequency histograms illustrating the distributions of a_K^i values measured in *Chilo* larvae using, a. LIX-type K^+-ISM's and b. NIC-type K^+-ISM's, drawn on the same scales for comparison.

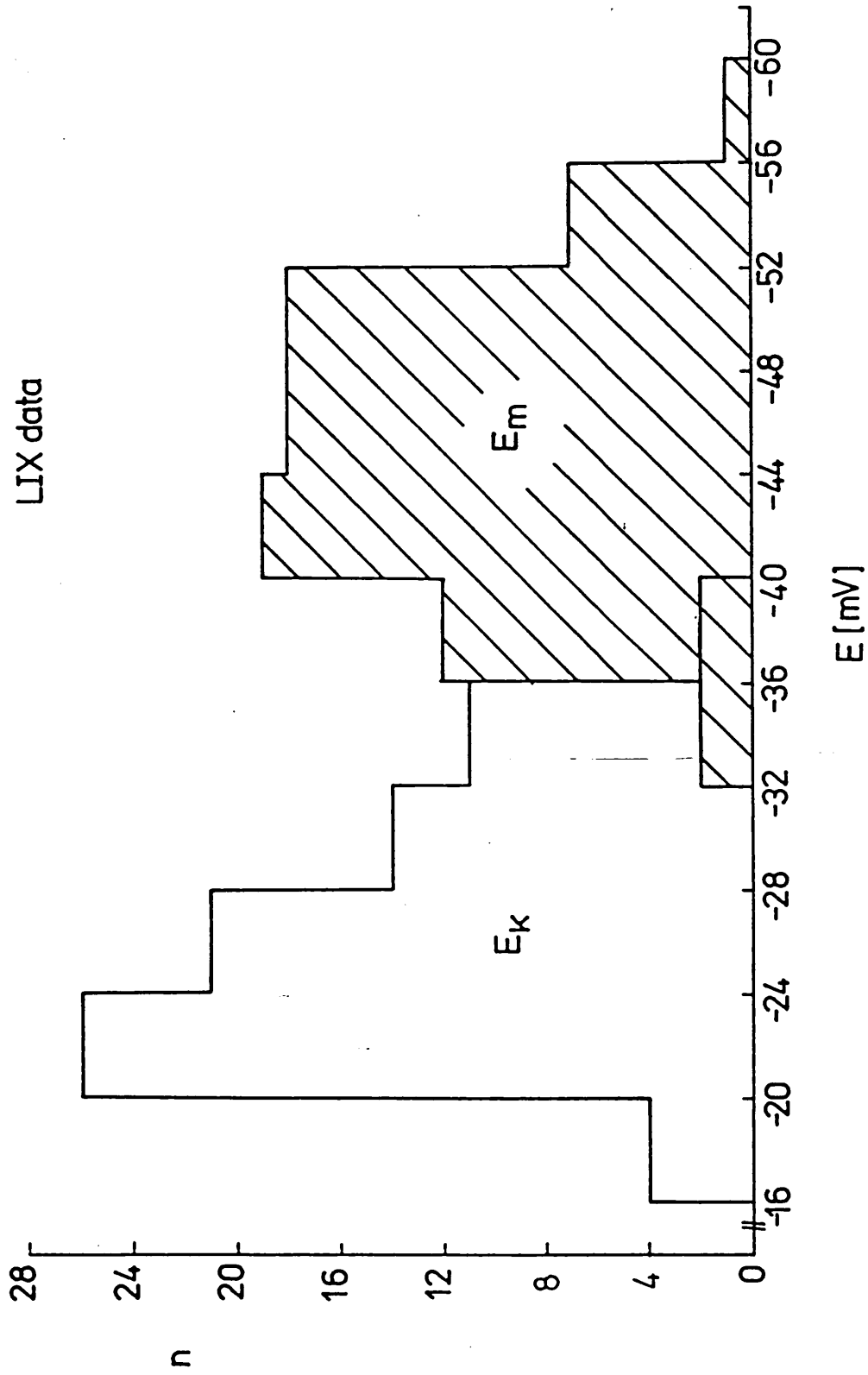


Fig. 100 Frequency histograms illustrating the distributions of E_K and E_m values measured in *Chilo* larvae using LIX-type K^+ ISM's, on the same abscissa for comparison.

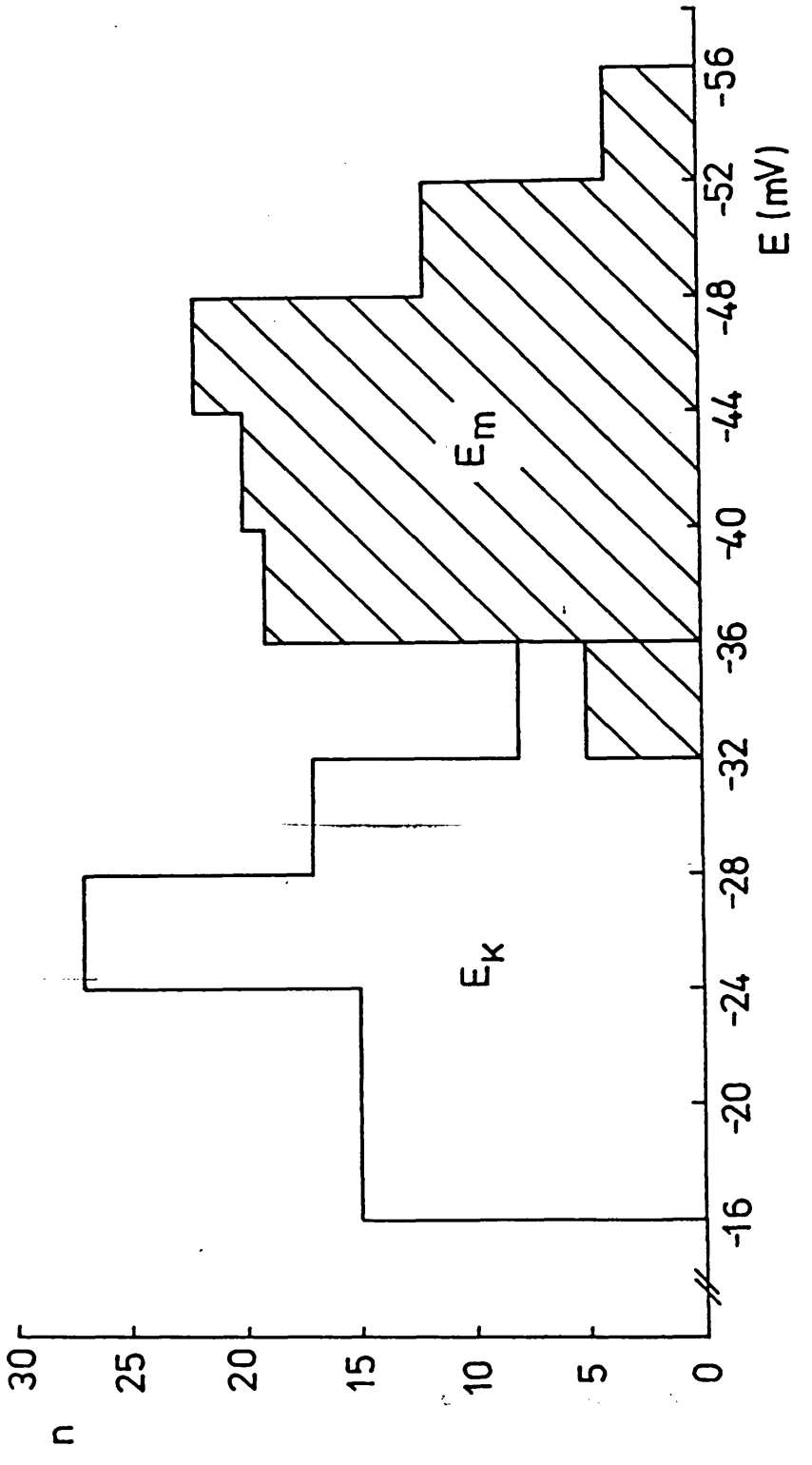


Fig. 101 Frequency histograms illustrating the distributions of E_K and E_m values measured in *Chilo* larvae using NIC-type K^+ ISM's, on the same abscissa for comparison.

larval muscle cells may contain a small amount of interferent to which the LIX responded, giving a slightly elevated value for apparent a_K^i (cf. *Calliphora* prepupae, section III.2.ii).

Values of E_K calculated from the above a_K^i data (from both types of K^+ ISM) were consistently more positive than E_m. There are two possible explanations for this observation: firstly, the high values of E_K may result from damage to the muscle cells during impalement allowing extracellular K^+ to enter the cell and elevate the intracellular K^+ activity; secondly, the fact that E_K is more positive than E_m may be a true reflection of the properties of the muscle cell membrane, suggesting that K^+ is not the only ion involved in resting membrane electrogenesis in *Chilo*. The former possibility was investigated by comparing the values of E_m measured using conventional microelectrodes (OMs) and K^+ ISMs, firstly in a given preparation, and secondly in the total population of cells investigated.

The E_m values measured in one preparation using a LIX-type K^+ ISM and an OM were very similar in both mean and distribution: E_m's measured using an ISM ranged from -40 to -45 mV with a mean of 43 mV, those measured using an OM were between -37 and -47 mV, with a mean of -42 mV (fig. 102 a,b). The total population of E_m values measured using K^+ ISMs (both LIX- and NIC-type) (fig. 103) also compared favourably with the total population recorded using OMs (fig. 96): values between -36 and -60 mV, with a mean of -45 mV were recorded using K^+ ISMs, cf. a range of -35 to -58 mV with a mean of -45 mV measured using OMs. This confirmed that K^+ ISMs do not cause significant damage to *Chilo* muscle cells, and that the high values of E_K calculated are therefore likely to reflect the true membrane properties. It was concluded that in this insect, K^+ is not the only ion involved in the maintenance of E_m. One or more ionic mechanisms, 'x', with equilibrium potential, E_x, more negative than E_m must also be involved. Possible candidates for this mechanism were Na^+, Cl^- and a metabolic pump, which were subsequently investigated.

V.3. Intracellular Na^+ activities

Measurements of intracellular Na^+ activities, a_{Na}^i, were made using ISMs based on the neutral ion carrier ETH 227 (Steiner *et al*, 1979). The behaviour of this type of ISM was found to be rather unstable in the high-Ca^{2+} lepidopteran saline used to bathe the *Chilo* preparation, however.

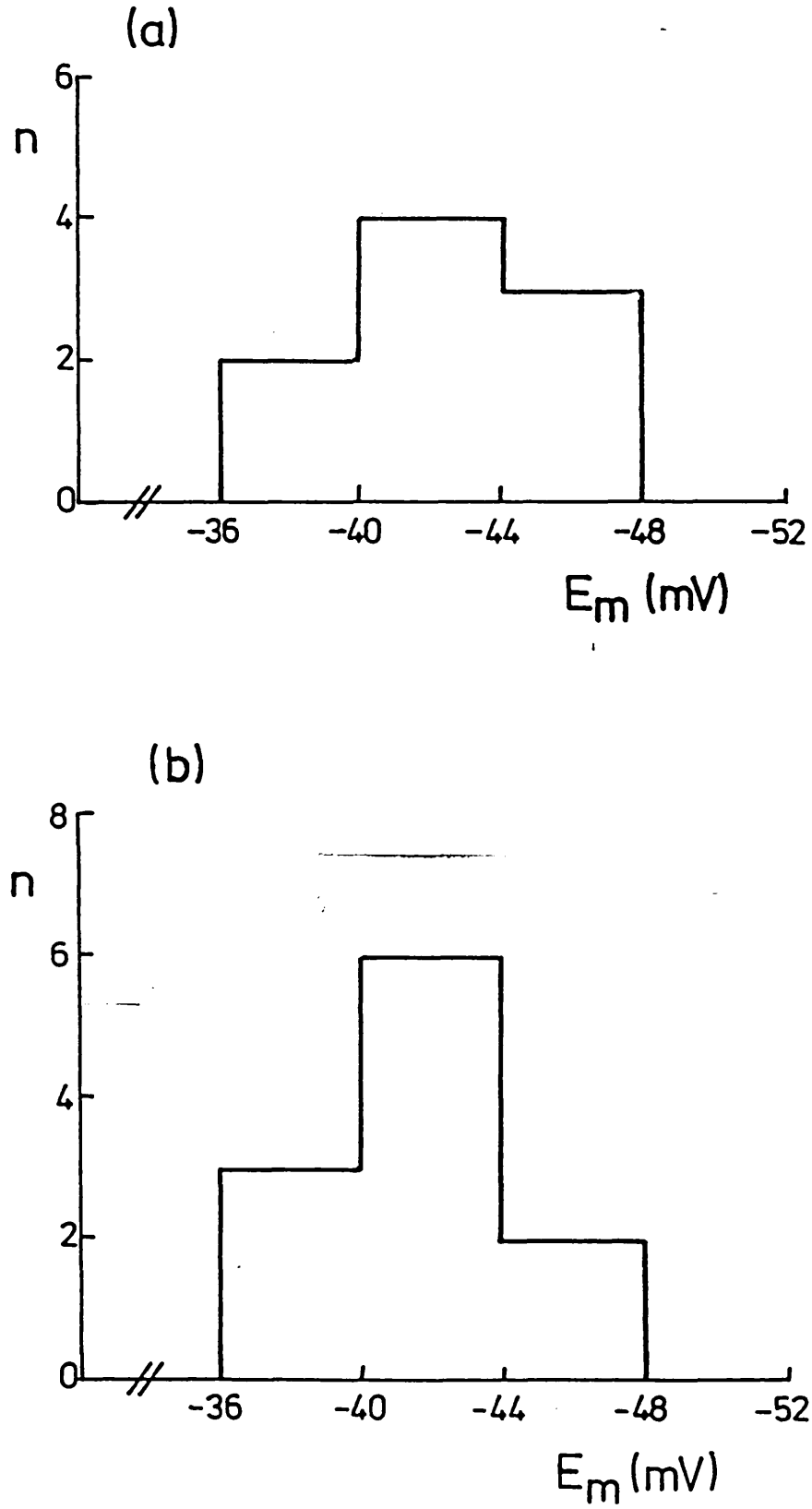


Fig. 102 Frequency histograms illustrating the distributions of E_m values measured in one *Chilo* larva, using, a. a conventional microeletrode and b. a K^+ ISM.

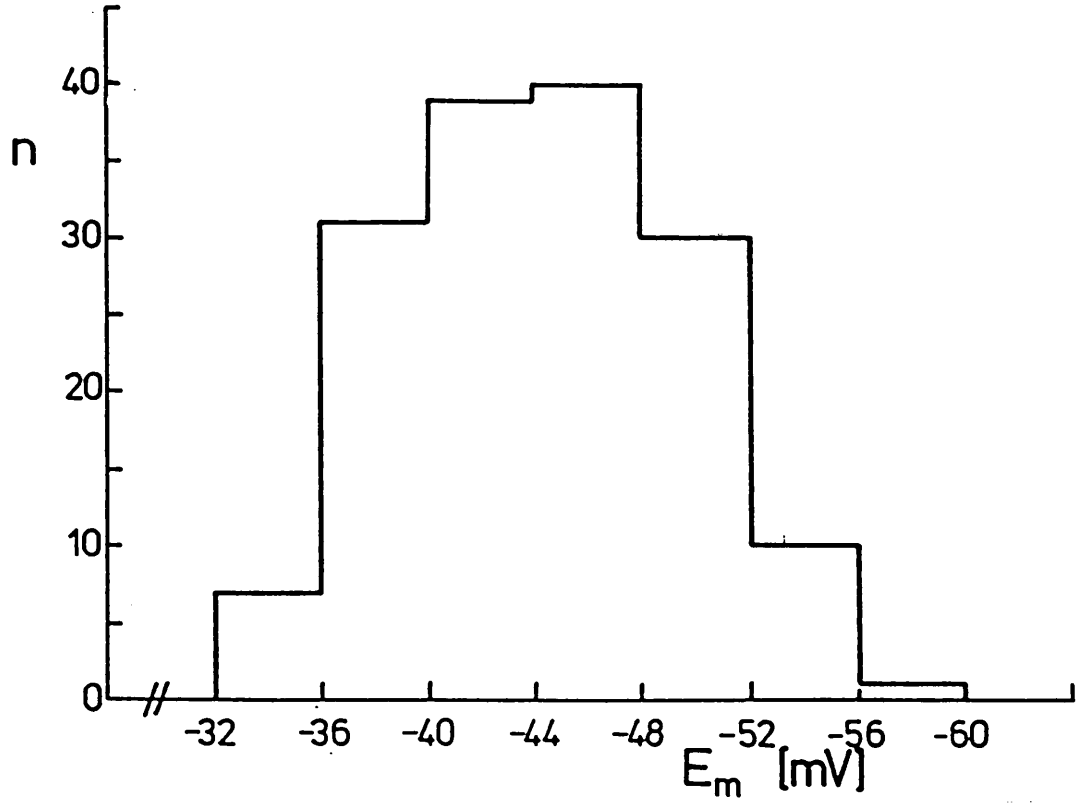


Fig. 103 Frequency histogram showing the distributions of E_m values measured in *Chilo* larvae using the two types of K^+ ISM.

The vast majority of impalements did not, therefore, obey the criteria for selection of results listed in section II.5. The results described below represent reliable impalements from only 13 cells (from 6 preparations). Such an impalement is shown in figure 104. The upper trace shows the intracellular Na^+ activity a_{Na}^i (here, 8 mM) and the lower, the membrane potential, E_m (-40 mV) of the cell, with steady values of each being maintained for four minutes, thus satisfying the criteria for selection of results. The data obtained from 13 cells is summarised in table 28 below.

Table 28 Intracellular Na^+ data from muscle cells of *Chilo* larvae
(Data from 13 cells, 6 preparations are given as mean ± SE)

a_{Na}^i :	12 ± 2 mM
E_{Na} :	-6 ± 4 mV
E_m :	-47 ± 2 mV
$E_{Na}-E_m$:	+41 ± 3 mV

The values of intracellular Na^+ activity, a_{Na}^i, recorded from *Chilo* larvae were between 4.6 and 29 mM, with a mean of 12.3 mM. The frequency histogram of these values (figure 105) shows an approximately normal distribution with the majority (92%) of values falling between 4.6 and 19 mM, and the mean close to the modal class.

The values for the sodium equilibrium potential, E_{Na}, calculated from the a_{Na}^i data had a normal distribution ranging from +15.9 to -30.5 mV with a mean of -6 mV (fig. 106). The mean fell in the modal class of the frequency histogram., E_{Na} was found to be consistently more positive than E_m, by an average of 41 mV. (E_m ranged from -39 to -60 mV with a mean of -47 mV). This is illustrated in figure 107, which shows frequency histograms for both E_{Na} and E_m on the same axes: the two populations do not overlap at any point.

In order to test that Na^+-ISMs did not damage cell membranes during impalements, the mean and range of E_m values recorded by the reference barrels of these ISMs were compared with those measured using conventional microelectrodes (fig. 96). There was found to be a close correspondence between the two sets of values: E_m's measured using Na^+ISMs were in the range -39 to -60 mV, with a mean of -47 mV; those recorded using OM's were between -36 and -60 mV with a mean of -45 mV. This confirmed that

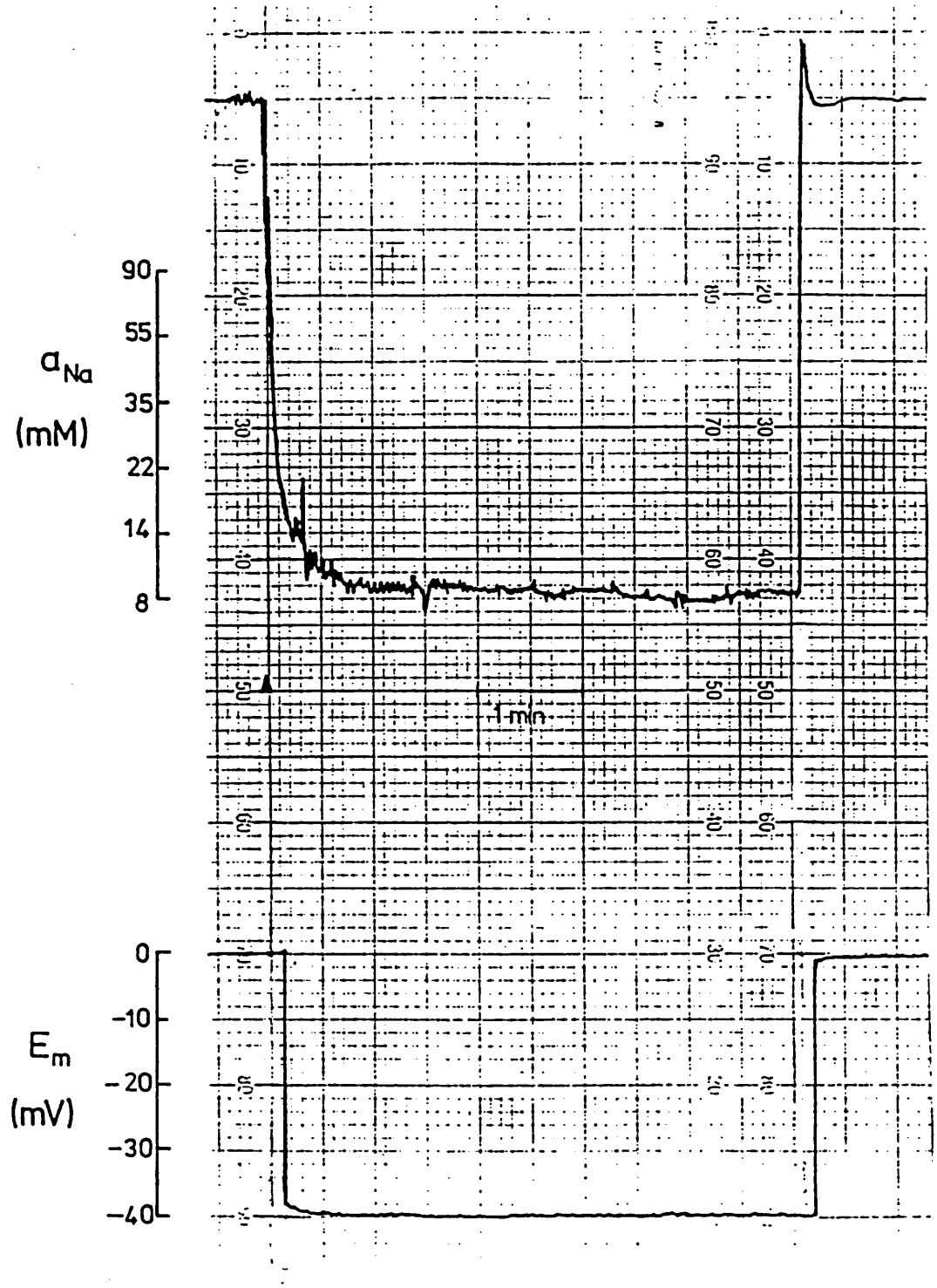


Fig. 104 Chart recording showing a typical impalement of a *Chilo* larval muscle cell with a Na^+ ISM.

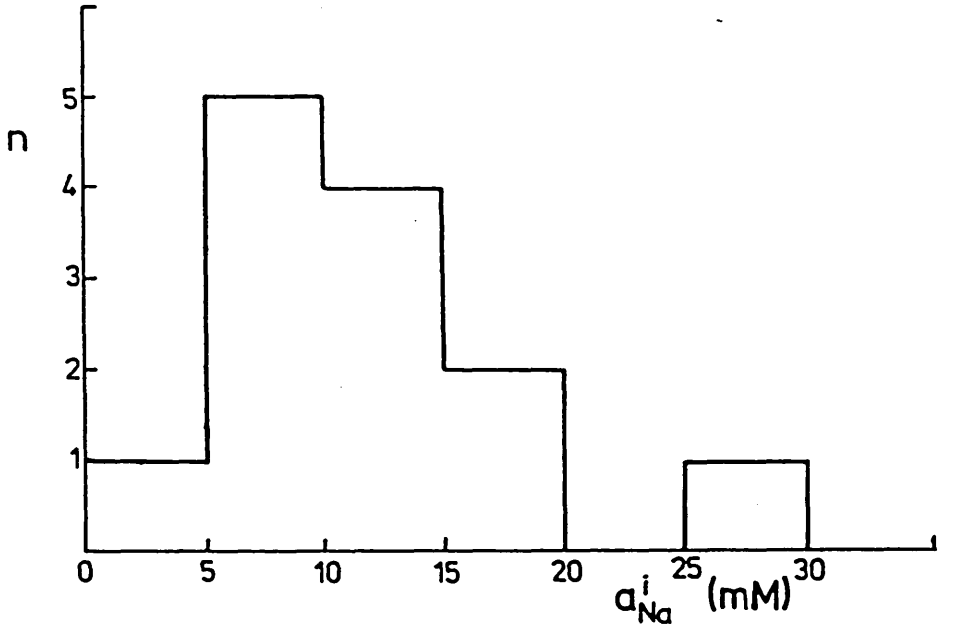


Fig. 105 Frequency histogram illustrating the distributions of a^i_{Na} values recorded in *Chilo* larvae.

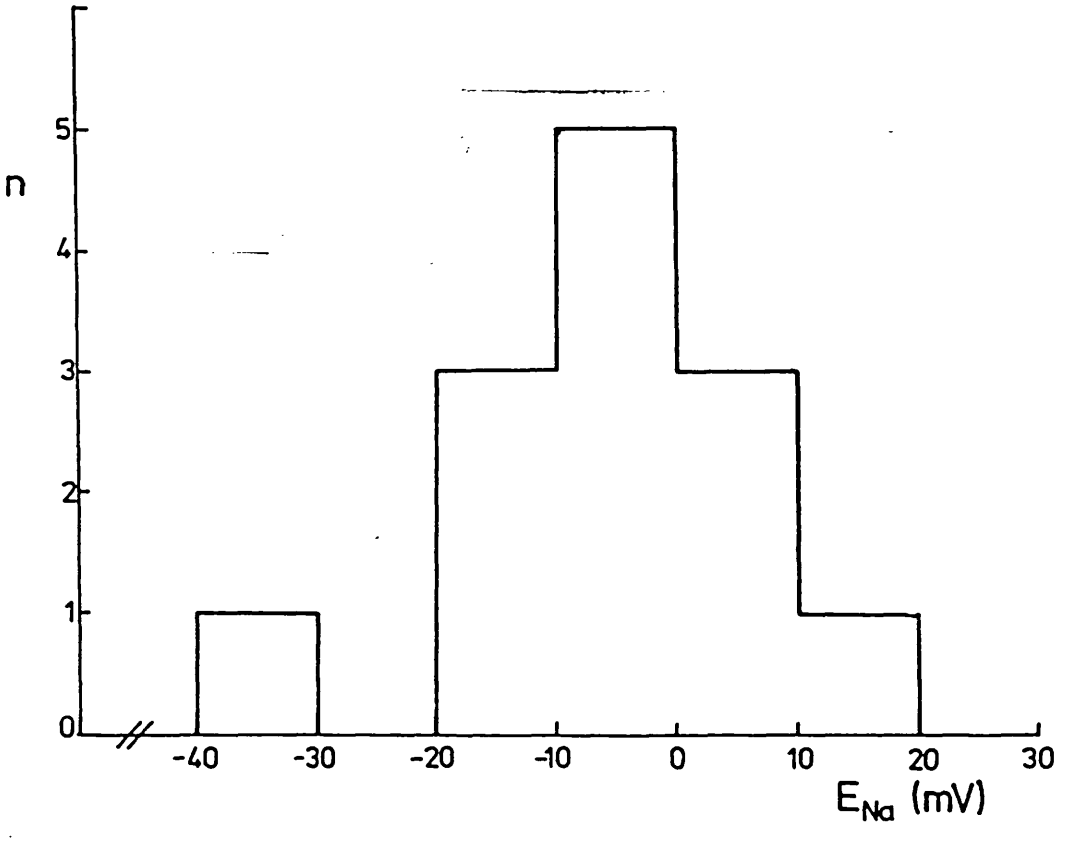


Fig. 106 Frequency histogram illustrating the distribution of E_{Na} values for *Chilo* larvae.

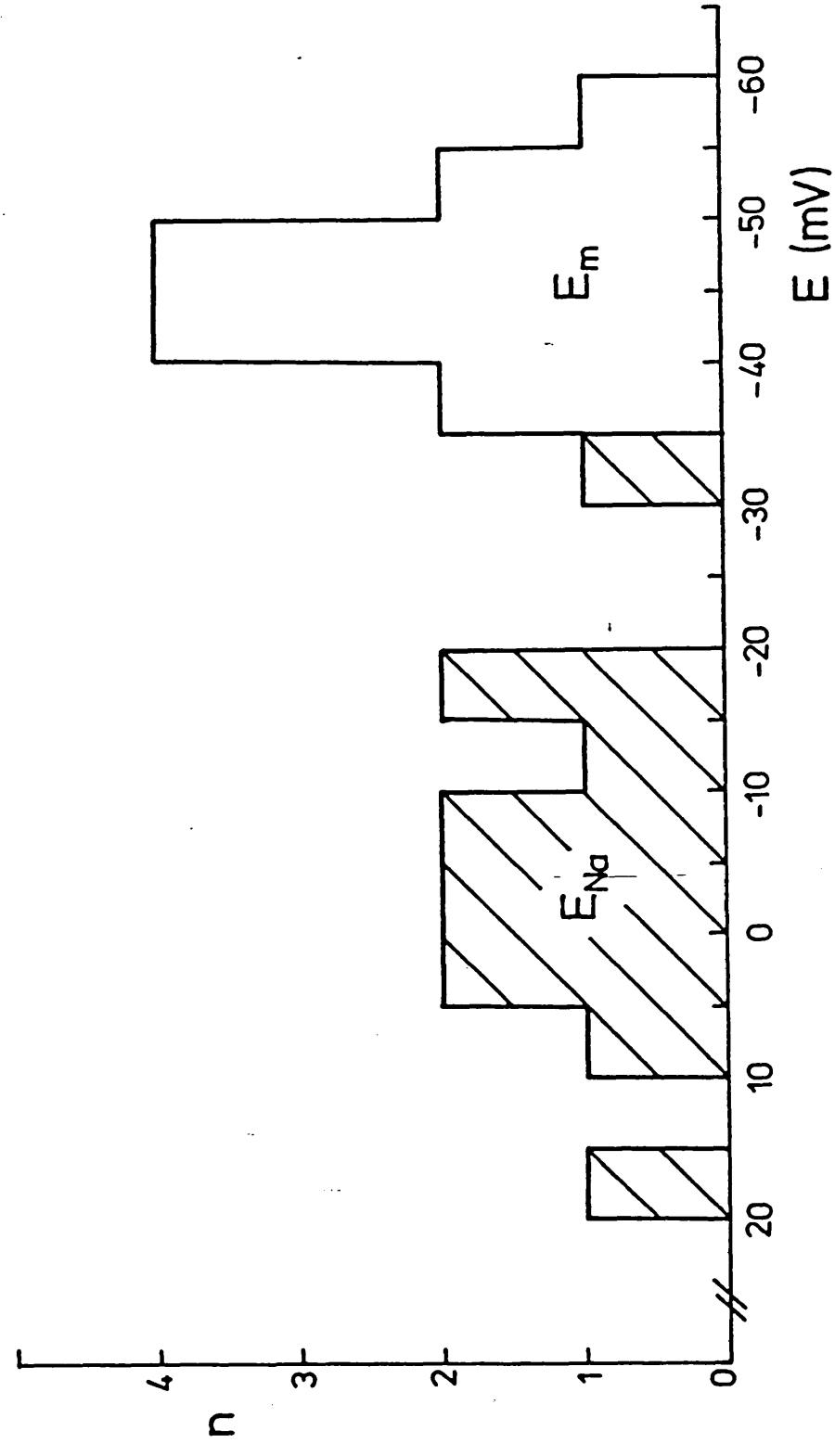


Fig. 107 Frequency histograms showing the distributions of E_{Na} and E_m values in *Chilo* larvae, on the same abscissa for comparison.

Na^+ ISMs had not inflicted damage on the muscle cells.

Thus, it was concluded from these measurements that whilst Na^+ may be involved to some extent in resting membrane electrogenesis, it is not the ion 'x' predicted at the end of the previous section to be involved in resting membrane electrogenesis in *Chilo*, since E_{Na} is not more negative than E_m, but more positive. Another candidate for the ion 'x' was Cl^-, which was investigated in the next section.

V.4. Intracellular Cl^- activities

Intracellular Cl^- activity measurements were made in muscle cells of *Chilo* larvae using double-barrelled Cl^- sensitive microelectrodes based on the improved Cl^- liquid ion exchanger (Corning 477913; Baumgarten, 1981). The reference barrels of these ISMs were filled with an organic reference liquid ion exchanger (RLIE, Thomas & Cohen, 1981). The latter had previously proved to be more suitable as a reference-barrel filling solution than the alternative mixture of KCl and K_2SO_4 (see section III.4.i) which shows a tendency to leak into impaled cells, thus artificially elevating the intracellular Cl^- activity sensed by the active barrel.

A typical impalement of a cell using a Cl^--ISM is shown in figure 108. The upper trace shows the Cl^--sensitive response of the active barrel, corresponding to an intracellular Cl^- activity of 8.2 mM, and the lower trace, the membrane potential of the cell (-50 mV). Both traces remained perfectly steady for more than 5 minutes, showing that the impalement was stable. The a_{Cl}^i value of 8.2 mM corresponds to a chloride equilibrium potential, E_{Cl}, of -53 mV, more negative than the E_m of -50mV. Similar data was obtained from a total of 92 cells from 9 preparations, giving the results listed in table 29 below.

Table 29 Intracellular Cl^- activity data from *Chilo* larvae. (Data from 92 cells, 9 preparations are given as mean ± SE)

a_{Cl}^i :	8 ± 0.2 mM
E_{Cl} :	-54 ± 1 mV
E_m :	-46 ± 0.5 mV
$E_{Cl}-E_m$:	-8 ± 0.4 mV

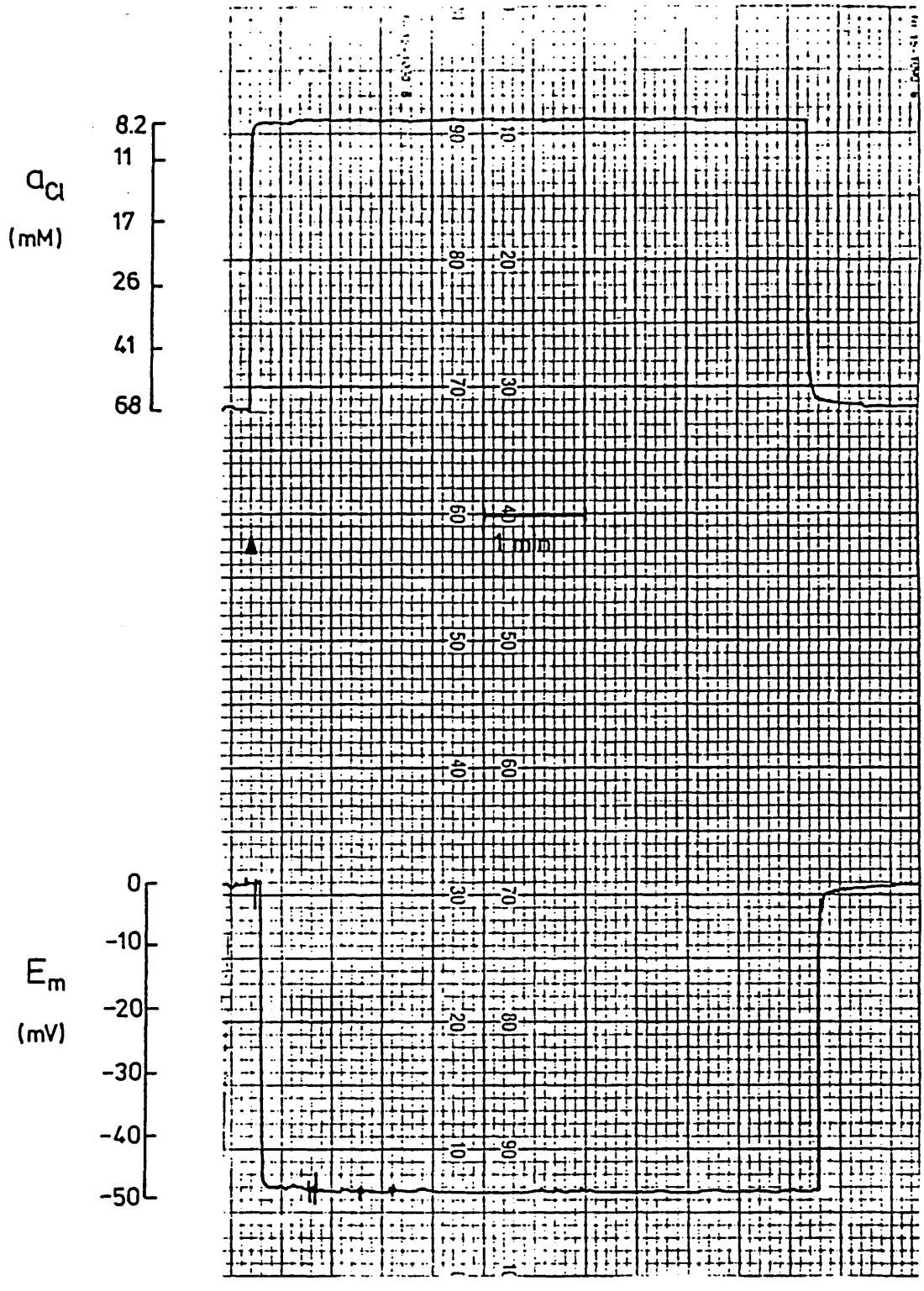


Fig. 108 Chart recording illustrating a typical impalement of a *Chilo* larval muscle cell with a Cl^--ISM.

The values for intracellular Cl^- activity, a_{Cl}^i, recorded ranged between 4.8 and 15 mM, with a mean of 8.2 mM. The frequency histogram of this data (figure 109) shows a somewhat asymmetrical distribution, with the majority (90%) of data points falling between 4.8 and 10.5 mM.

The chloride equilibrium potential values, E_{Cl}, calculated from the above a_{Cl}^i data were between -38 and -67 mV (mean, -54 mV) with a rather irregular but approximately normal distribution. E_{Cl} was consistently more negative than the membrane potential in all cells, by an average of 8 mV. (E_m values ranged between -36 and -55 mV, with an average of -46 mV). The distributions of E_m and E_{Cl} values are shown in frequency histograms (fig. 110 a,b). The fact that E_{Cl} was consistently more negative than E_m is better illustrated in figure 111, in which values of E_{Cl} from individual cells are plotted against the corresponding E_m value from the same cell. This result is not explicable in terms of membrane damage during impalements with ISM's for two reasons: (a) membrane damage is known to result in depolarisation of the E_m. Values of E_m recorded with ISM's were similar in both mean and distribution to those recorded with OM's (ranging from -36 to -55 mV with a mean of -46 mV cf. values of -36 to -60 mV, with a mean of -47 mV obtained with OM's). This confirmed that the ISMs did not damage the cell membranes during impalements; (b) if damage had occurred, it would have been expected to lead to an elevation in intracellular Cl^- activity levels, and hence to E_{Cl} values more positive than E_m.

Thus, these measurements of intracellular Cl^- activity in *Chilo* larvae indicate that Cl^- may play a role in resting membrane electrogenesis in this insect, since E_{Cl} does not equal E_m. Also, Cl^- is a likely candidate for the ion 'x' which contributes to E_m, as described at the end of section V.2, with its equilibrium potential more negative than E_m. This possibility is further investigated by a series of substitution experiments in section VI.5.

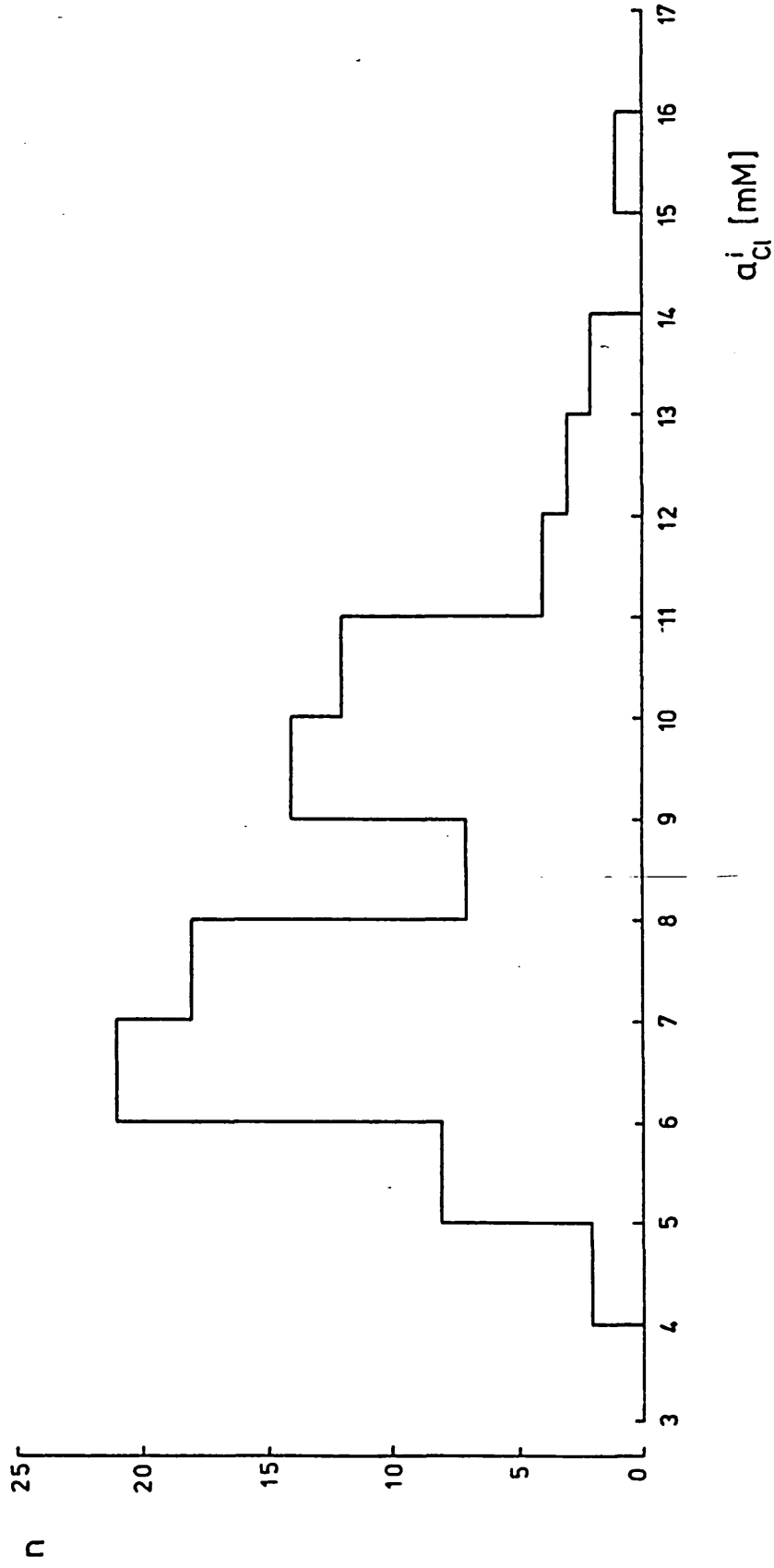


Fig. 109 Frequency histogram illustrating the distribution of a_{Cl}^{i} values in *Chilo* larvae.

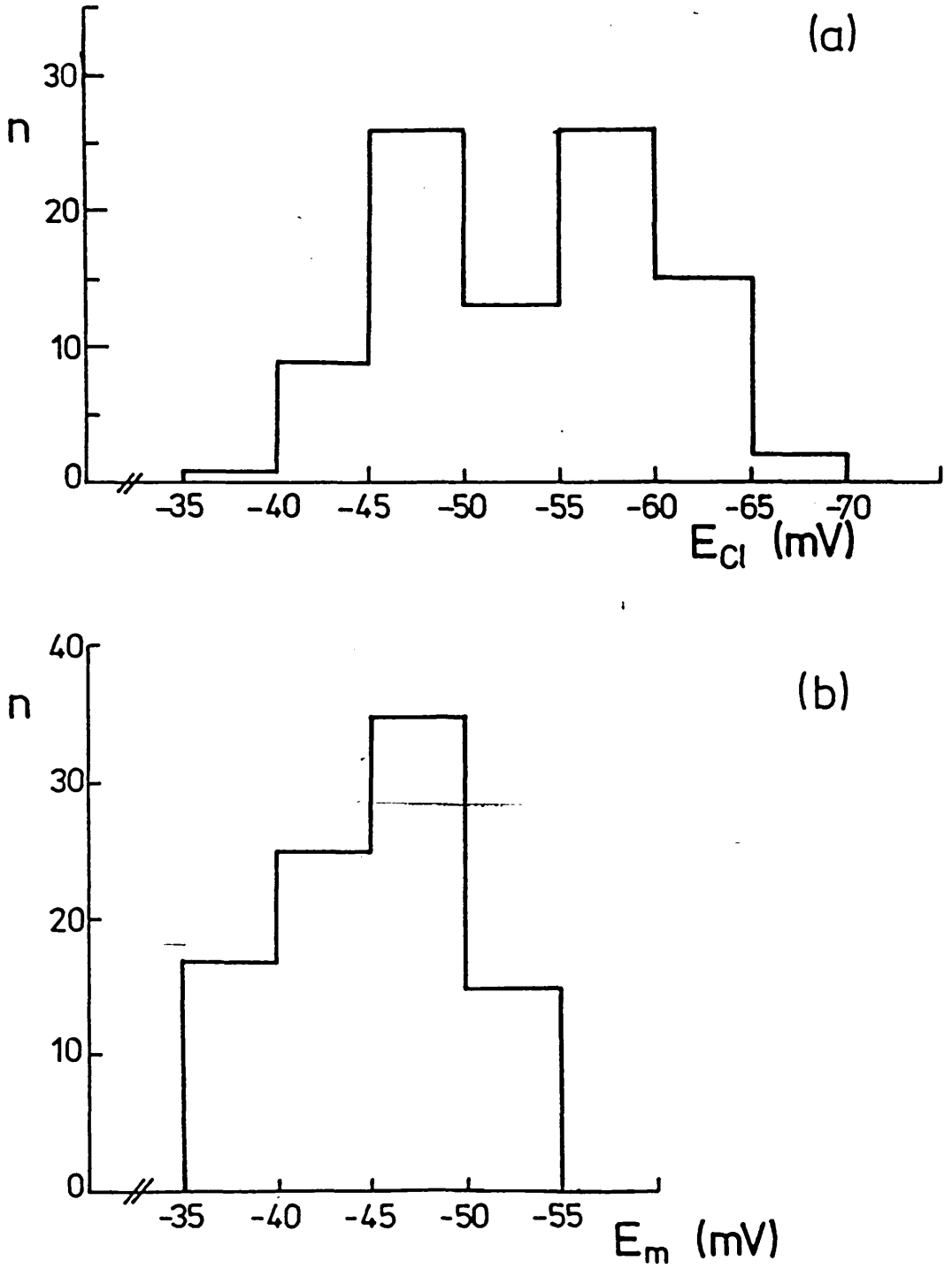


Fig. 110 Frequency histogram illustrating the distributions of, a. E_{Cl} values and b. E_m values in *Chilo* larvae.

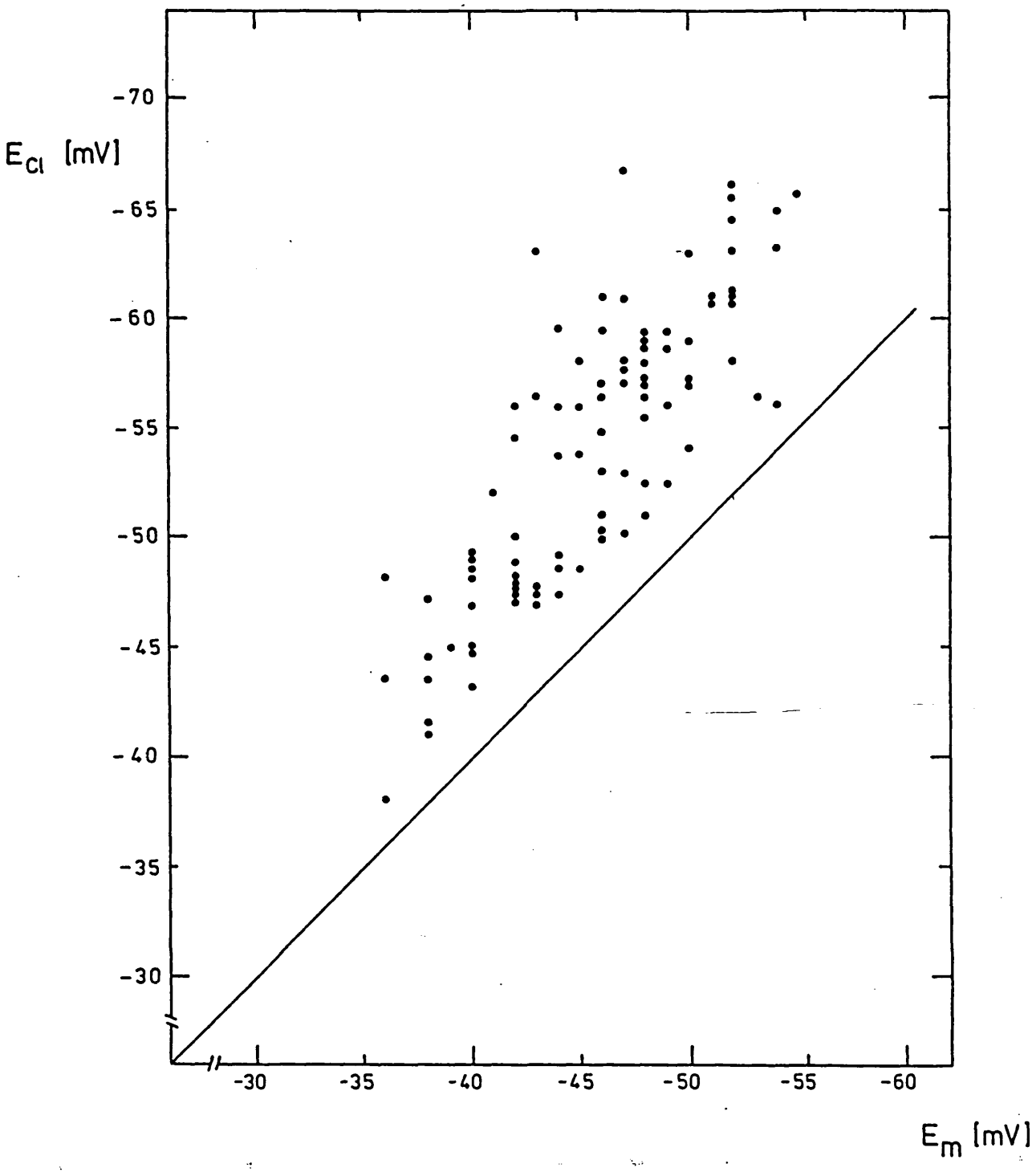


Fig. 111 Graph illustrating the relationship between E_{Cl} and E_m in *Chilo* larvae. The solid line denotes the equality $E_{Cl} = E_m$, showing that for all *Chilo* muscle cells, E_{Cl} was more negative than E_m.

VI. IONIC SUBSTITUTION EXPERIMENTS ON *CHILO* LARVAE

The haemolymph of Lepidoptera larvae is known to contain the inorganic ions K^+, Na^+, Mg^{2+} and Cl^-. The role of these ions in resting membrane electrogenesis in *Chilo* was therefore investigated by carrying out a series of ionic substitution experiments. All solutions used were based on Weevers' lepidopteran saline (appendix 2) and their compositions were as listed in appendices 3, 4, and 7. Ionic substitution experiments involved impaling a cell bathed in Normal saline and recording a steady membrane potential from it. Solutions containing a range of activities of the ion under investigation were substituted in and new, steady, E_m values recorded in each.

In addition to the roles of K^+, Na^+, Mg^{2+} and Cl^-, the possible contribution of an electrogenic, metabolic pump to E_m was investigated. Two types of experiment were performed: firstly classical cooling experiments, in which the temperature of the preparation was reduced, thus slowing down the chemical reactions of metabolism; and secondly the application of a specific Na^+-K^+ ATPase inhibitor, ouabain. The effect on E_m of these two procedures was assessed by impaling a cell with a conventional microelectrode at room temperature and recording a steady E_m. The preparation was then cooled or ouabain applied and new, steady, recordings of E_m obtained, and the reversibility of the effect tested by returning the cell to Normal Ringer at RT.

VI.1. Potassium substitution experiments

Previous ISM measurements of intracellular K^+ activities in *Chilo*, showed that in this insect the potassium equilibrium potential, E_K, is more positive than E_m in all cells. This implies that K^+ is not the only ion involved in generating E_m. In order to assess the size of the contribution of K^+ to E_m, substitution experiments were carried out in which the extracellular K^+ activity, a_K^o, was varied between 0.72 and 30.2 mM, using Na^+ as the substitute. The compositions of the solutions used are listed in appendix 3.

Figure 112 shows a chart recording of such an experiment. The cell was impaled with a conventional 2·5M KCl-filled microelectrode at the point marked by the arrowhead, and a steady E_m of -43 mV recorded. Solutions containing a range of K^+ activities were then substituted in and the cell allowed to equilibrate in each for at least 12 minutes, or until a completely

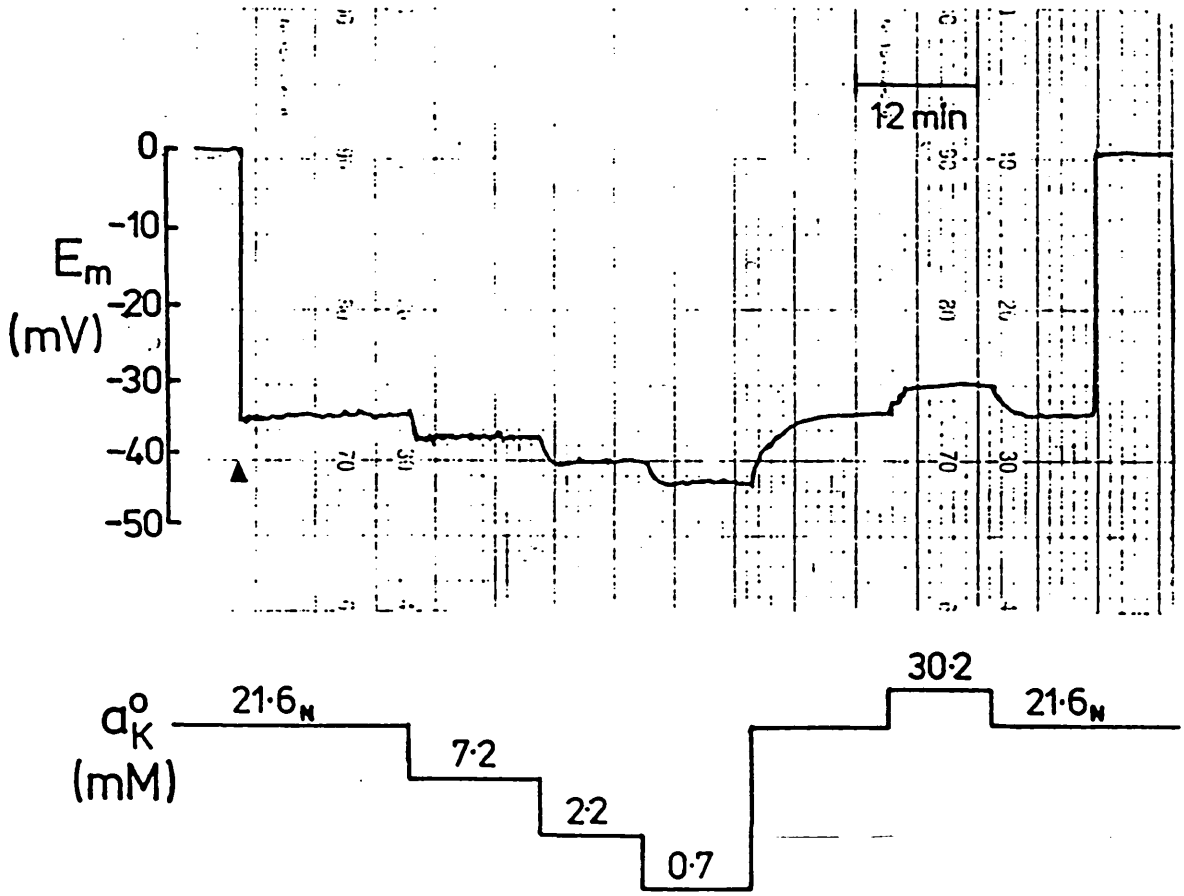


Fig. 112 Chart recording showing a K^+ substitution experiment on a *Chilo* larva. This illustrates the sustained effect on E_m of changing a_K^o.

steady new E_m was obtained. Similar data was obtained from a total of 8 cells, each from a different preparation, and are listed in table 30.

These results are represented graphically as mean E_m (± SE) against the logarithm of the extracellular K^+ activity, a_K^o, in figure 113. The points follow a curve rather than a straight line, with a maximum slope of 30 mV per tenfold change in a_K^o (for a_K^o values between 21.6 and 30.2 mM) and a minimum slope of 3 mV per tenfold change in a_K^o (for a_K^o values between 0.72 and 2.2 mM). This maximum slope of 30 mV is markedly different from the slope of 58 mV per tenfold change in a_K^o predicted by the Nernst equation for a cell membrane permeable only to K^+. This result is consistent with the fact that the potassium equilibrium potential, E_K, as calculated from the intracellular K^+ activity data for this insect, was not equal to E_m, but was consistently more positive than E_m in all cells studied (section V.2).

Table 30 Data from K^+ substitution experiments in *Chilo*

	Membrane potentials, E_m, (-mV) in various a_K^o's (mM)						
Cell no.	21.6_N	7.2	2.16	0.72	21.6_N	30.2	mMK^+
1	40	46	47	48	38	31	
2	43	46	48	50	44	39	
3	46	49	51	53	46	38	
4	44	52	58	60	44	38	
5	43	49	51	52	43	49	
6	35	38	41	43	35	30	
7	41	45	48	50	40	34	
8	40	44	47	48	41	35	
$\bar{x}$	41.5	46.1	48.9	50.5	41.4	36.8	
SE	1.2	1.5	1.7	1.7	1.3	2.1	

VI.2. Membrane resistance measurements

The results of K^+ substitution experiments (section VI.1) showed that the relationship between E_m and the logarithm of a_K^o was not linear, but followed a smooth curve (fig. 113). One possible explanation for the non-linearity of the membrane response to changes in a_K^o would be a change in the relative permeability of the muscle cell membrane to Na^+ and K^+ when the

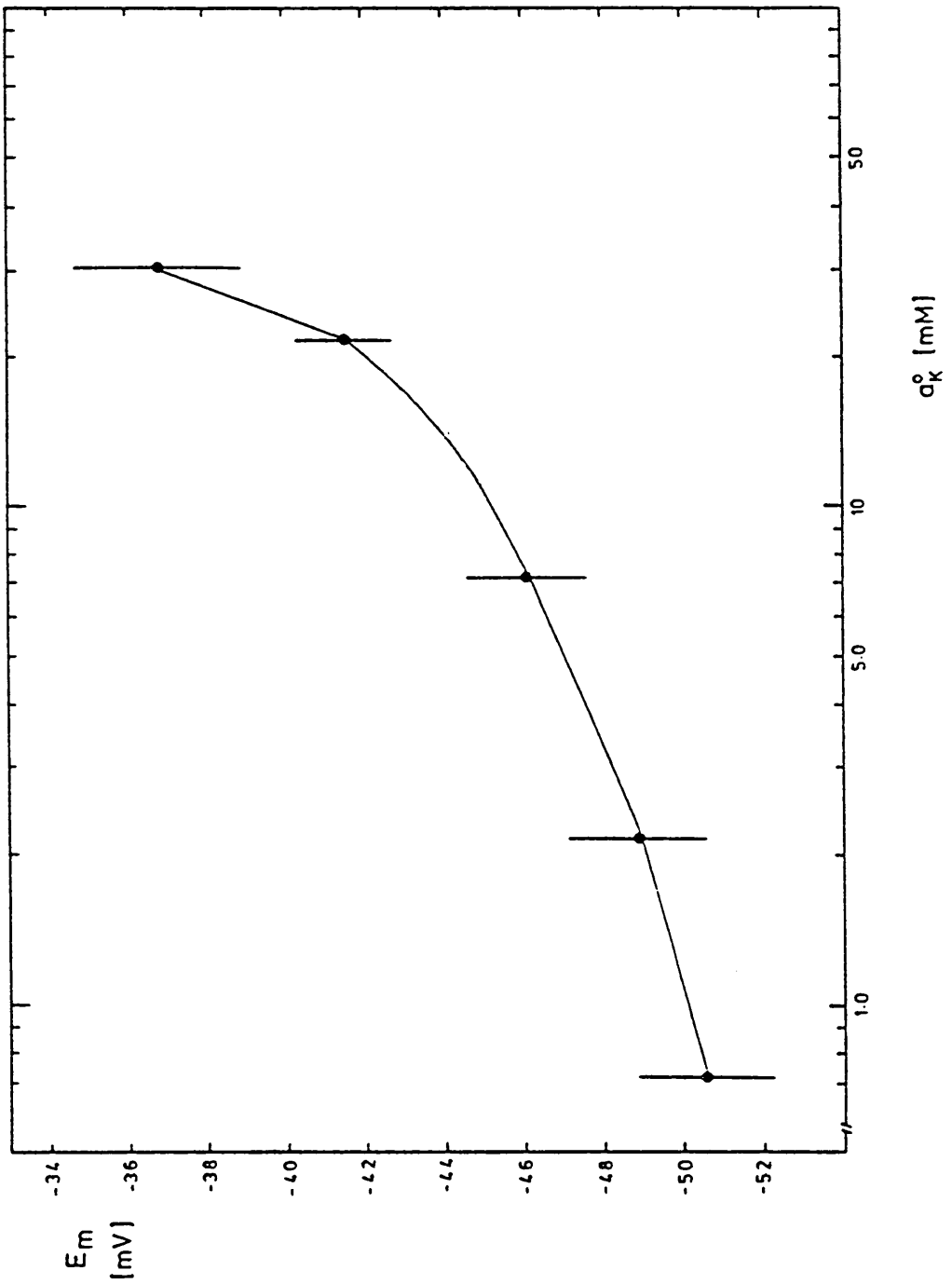


Fig. 113 Graph showing the relationship between E_m and the logarithm of a^o_K in *Chilo* larvae.

extracellular Na^+ activity, a^o_{Na}, was altered (cf. that in *Calliphora*, section IV.4.iii). In the K^+ substitution experiments described in section VI.1, Na^+ was used as the substitute, therefore high-K^+ solutions contained low Na^+ activities and low-K^+ solutions contained high Na^+ activities. Changes in membrane permeability might be expected to be reflected in changes in the resistance of the cell membrane. The following series of experiments was therefore carried out in which membrane resistance was monitored during a K^+ substitution experiment. Stimulating current pulses 7.5×10^{-9}A in size were applied continuously, allowing calculation of membrane resistance from Ohm's law. Measurements from 24 cells (4 preparations) gave an average value for membrane resistance of 4417 ± 310 KΩ (see appendix 14). In four of these cells, this response to the stimulating pulses was balanced using the bridge circuit facility on the amplifier, in order to make small subsequent resistance changes more obvious. Low-K^+ Ringer (0.72 mM K^+) was then substituted in, and any change in membrane resistance noted. The cell was returned to Normal Ringer (21.6 mM K^+) before being placed in high-K^+ Ringer (30.2 mM K^+) then finally returned to Normal Ringer. A typical recording of such an experiment is given in figure 114. This shows the decrease in membrane resistance typically observed in low K^+/high Na^+ solutions, and the increase observed in high K^+/low Na^+ solutions.

The results obtained from 4 cells, each from a different preparation, are given in table 31. It was found that in low K^+/high Na^+ Ringer, the membrane resistance decreased by an average of 37%, and in high K^+/low Na^+ Ringer, it increased by an average of 41%. These changes may be attributable to a number of mechanisms, which will be discussed in the final chapter.

VI.3. Sodium substitution experiments

Previous measurements of intracellular Na^+ activities in *Chilo* (section V. 3) showed that the sodium equilibrium potential, E_{Na} was not equal to E_m. This suggested that Na^+ might be involved in resting membrane electrogenesis, and to investigate this possiblity a series of Na^+ substitution experiments was carried out. Extracellular Na^+ activity, a^o_{Na} was varied between 0.9 and 8.6 mM, using Mg^{2+} as the substitute, the latter being an impermeant cation (see section VI.4). The composition of these solutions is given in appendix 7.

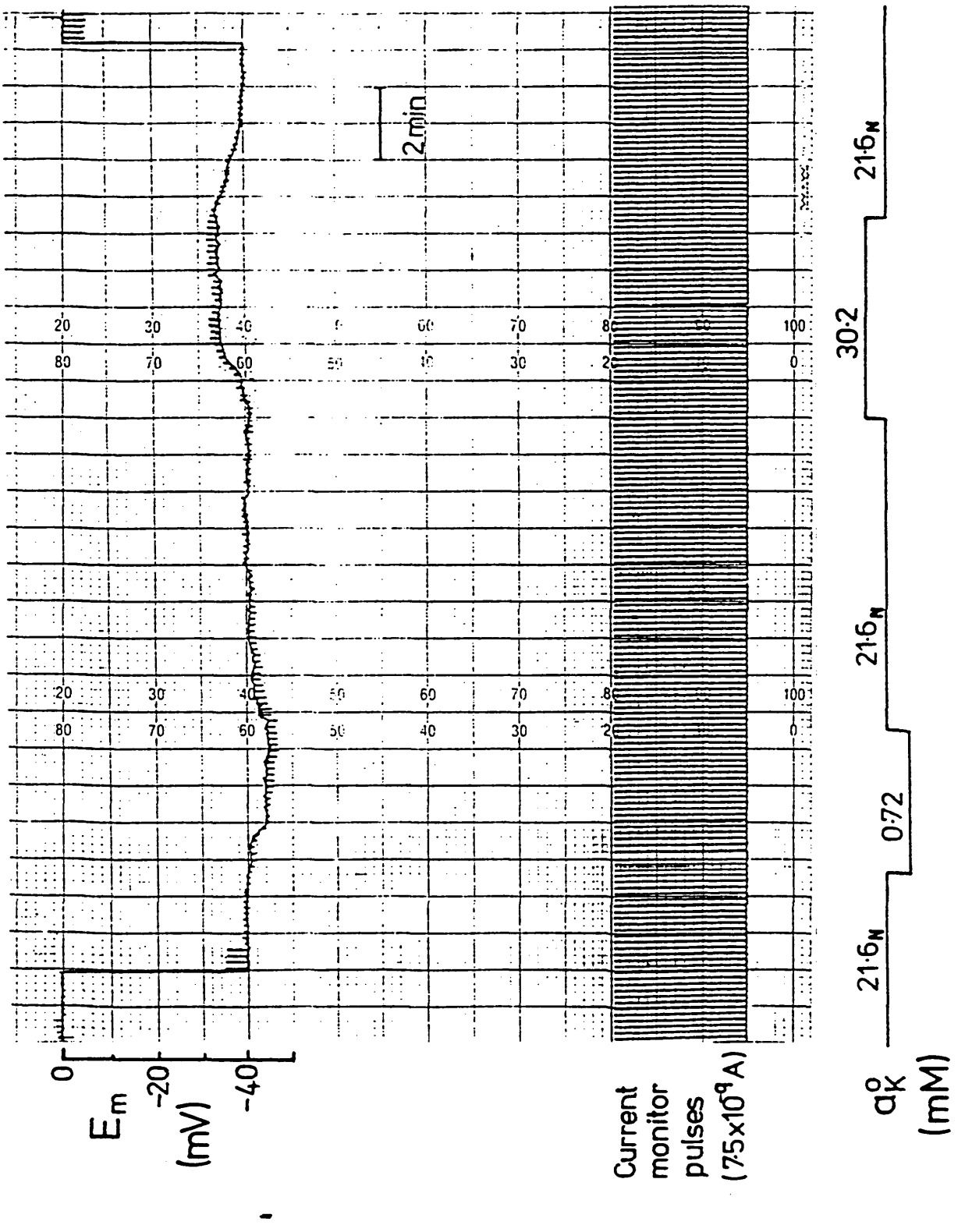


Fig. 114. Chart recording of a K^+ subtitution experiment on a *Chilo* larva during which membrane resistance was monitored by repeated application of constant-sized current pulses. It shows that membrane resistance increased when a^o_K was reduced/a^o_{Na} increased, and decreased when a^o_K was increased/a^o_{Na} reduced.

Table 31. Membrane resistance changes in *Chilo* during substitution experiments in which a^{o}_{K} and a^{o}_{Na} were varied simultaneously

Cell no.	Membrane resistance (kΩ)	Δ Membrane resistance (kΩ) in low K^+/high Na^+	Normal	high K^+/low Na^+
1	1667	- 667	0	+1333
2	3333	-1000	0	+1333
3	4000	-2667	0	+1333
4	3333	- 333	0	+ 333

Cell no.	Membrane resistance (kΩ)	Δ Membrane resistance (%) low K^+/high Na^+	Normal	high K^+/low Na^+
1	1667	-40%	0	+80%
2	3333	-30%	0	+40%
3	4000	-67%	0	+33%
4	3333	-10%	0	+10%
		———		———
	$\bar{x}$	-37% ± 23.7		+41% ±29.1

Table 32. Na^+ substitution data from *Chilo* larvae. (Data from 7 cells, 7 preparations.)

Cell no.	Extracellular Na^+ activity, a^{o}_{Na} (mM) 8.64	2.7	0.86	8.64
	Membrane potentials, E_m (-mV)			
1	45	46.5	48	45
2	47	49	50	48
3	40	41.5	42	40
4	37.5	38.5	39	37.5
5	39.5	41	41.5	40
6	50	51	52	49.5
7	50	51	51.5	49.5
$\bar{x}$	44.1	45.5	46.3	44.2
SE	2	1.9	2	1.9

Figure 115 shows a representative chart recording made during a Na^+ substitution experiment. The cell was impaled with a conventional microelectrode in Weevers' saline, giving a steady E_m of -50 mV. Solutions containing a_{Na}^o's of 2.7 and 0.9 mM were then introduced into the recording chamber as indicated beneath the membrane potential trace, and a new, steady E_m of -51 and -52 mV respectively obtained in each. Finally, the cell was returned to Normal saline to ensure that any change in E_m was reversible. (Only three substituion solutions were used to cover a decade change in a_{Na}^o because the response of the membrane to Na^+ was found to be very small and it would therefore not have been possible to record accurately the E_m changes resulting from finer adjustments in a_{Na}^o).

The results obtained from 7 cells (from 7 preparations) are listed in table 32. Data from each cell are plotted in figure 116 which shows the relationship between E_m and the logarithm of a_{Na}^o. This shows clearly that the muscle cell membrane in *Chilo* has a small but significant permeability to Na^+, with E_m changing consistently by some 2 mV in response to a tenfold change in a_{Na}^o. Na^+ is therefore involved to a small extent in generating E_m.

VI.4. Magnesium substitution experiments

These were carried out to determine whether Mg^{2+} contributed to E_m in *Chilo*, and involved the reduction of extracellular Mg^{2+} activity, a_{Mg}^o using glucose as a substitute, by a factor of ten from 13 to 1.3 mM (see appendix 7 for the composition of the solutions used) whilst monitoring E_m. A typical recording of such an experiment is shown in figure 117. This shows clearly that changing a_{Mg}^o had no effect on E_m. Similar data were obtained from 5 cells, each from a different preparation: any changes in E_m which did occur following the introduction of low-Mg^{2+} Ringer into the recording chamber were small ($\sim$ 1 mV), inconsistent in direction and irreversible.

Thus, it was concluded that Mg^{2+} is not involved in resting membrane electrogenesis in *Chilo*, since changing a_{Mg}^o had no effect on E_m.

VI.5. Chloride substitution experiments

Previous measurements of intracellular K^+ and Na^+ activities in *Chilo* (sections V.2 and V.3 respectively) showed that both the K^+ and Na^+

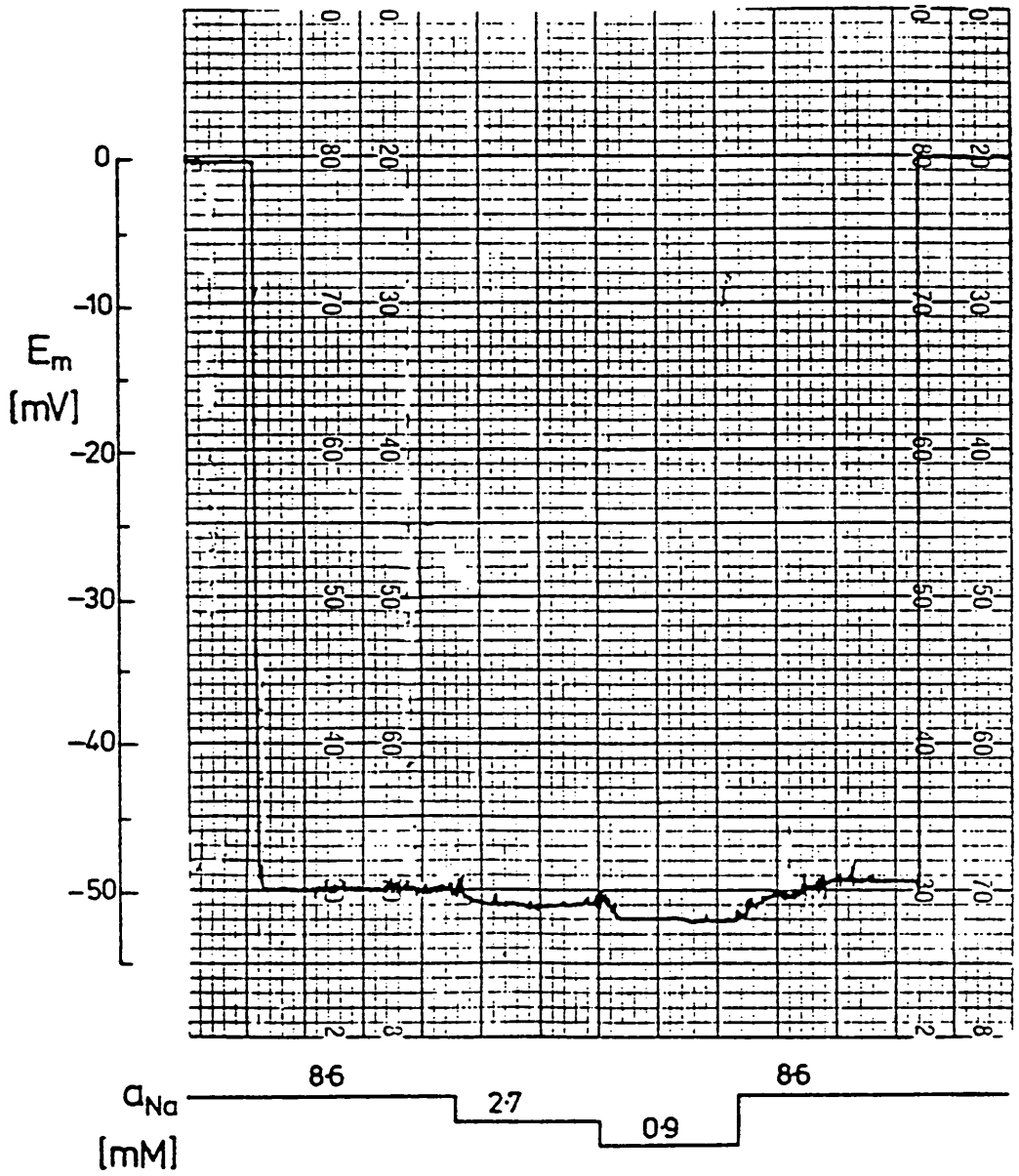


Fig. 115 Chart recording of a Na^+-substitution experiment on a *Chilo* larva, illustrating the small sustained effect on E_m of changing a_{Na}^o.

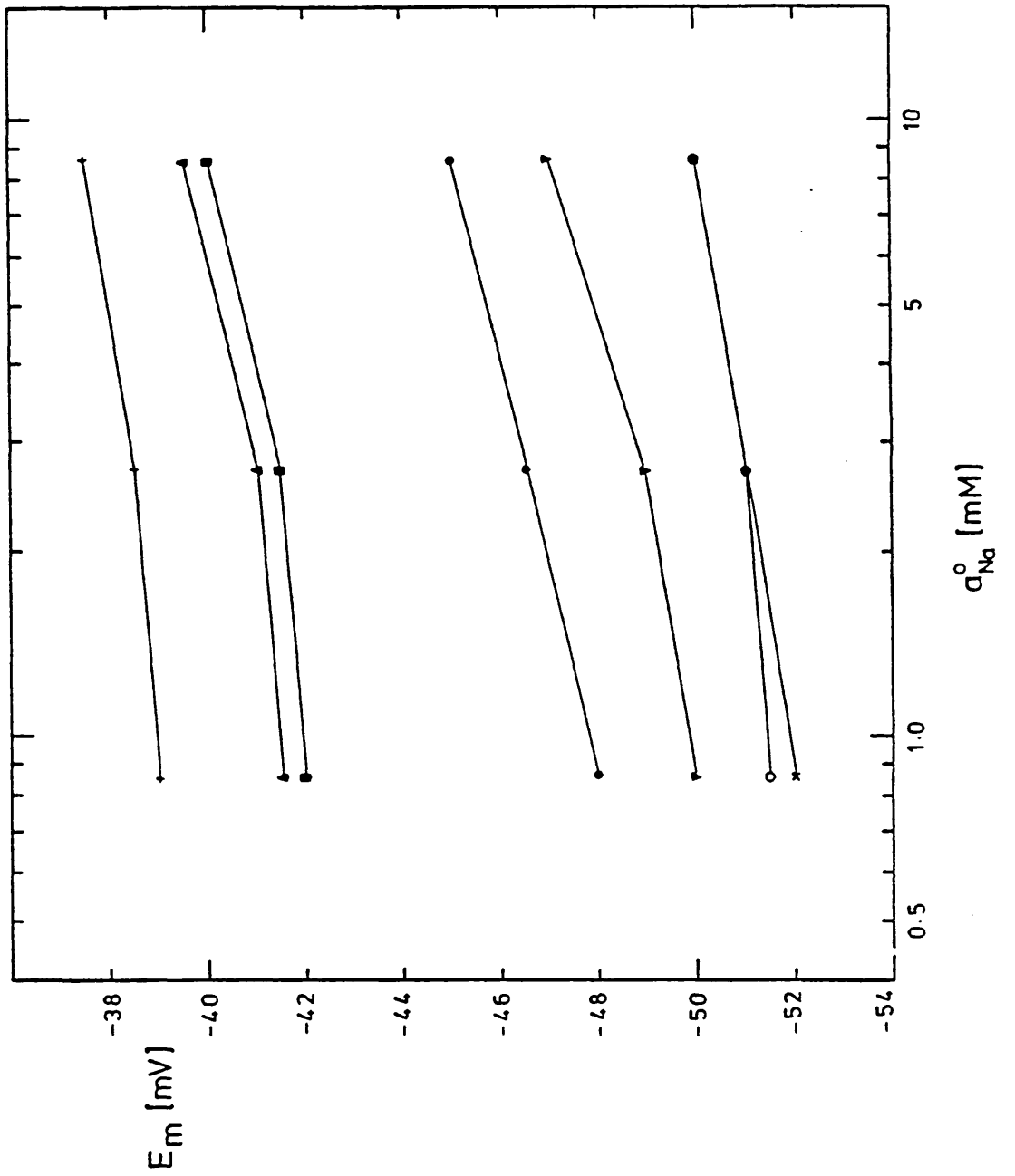


Fig. 116 Graph showing the relationship between E_m and the logarithm of a^o_{Na} in six *Chilo* muscle cells (each symbol represents a different cell). It illustrates the consistency of the effect of a^o_{Na} on E_m.

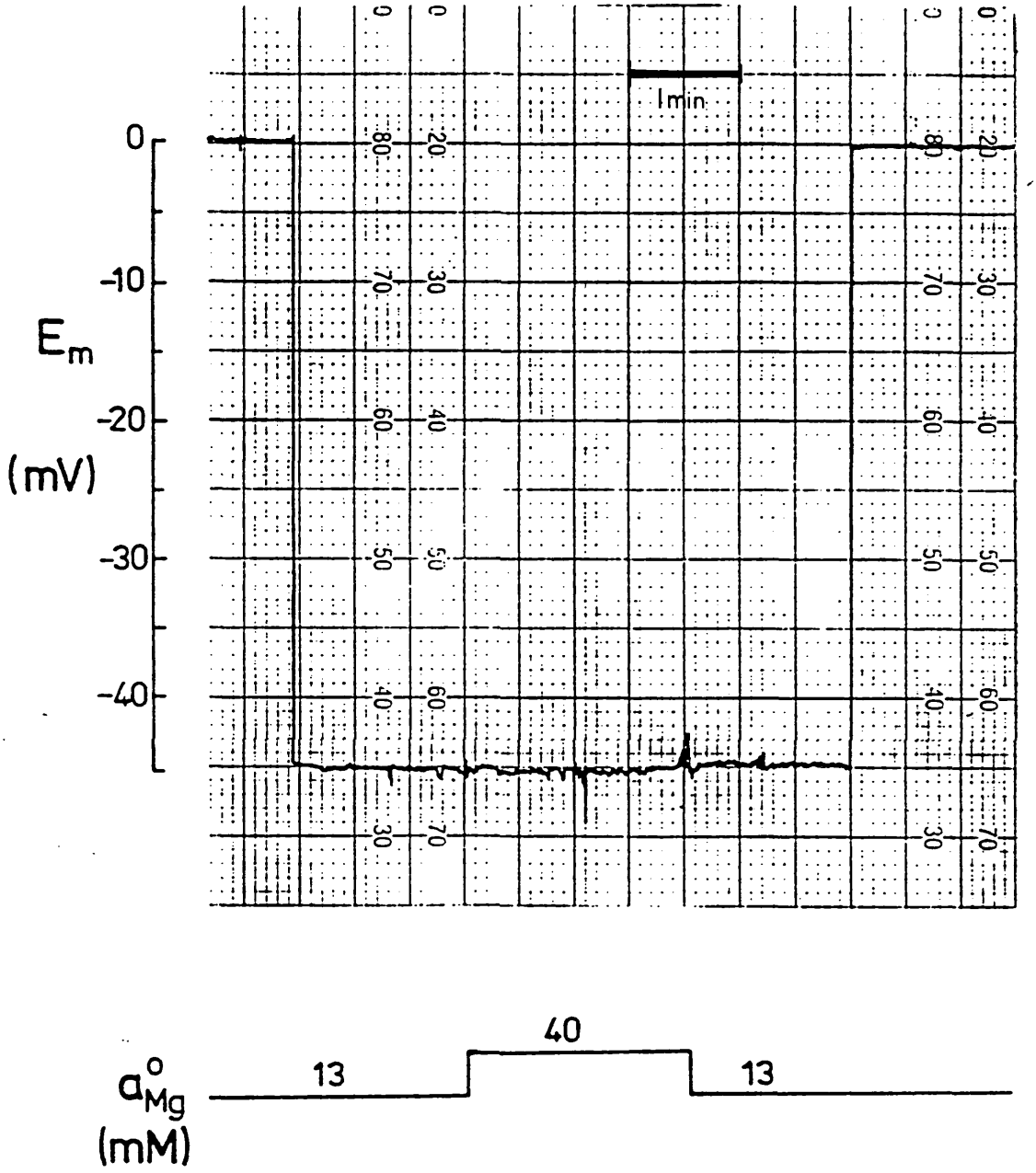


Fig. 117 Chart recording of a Mg^{2+}-substitution experiment on a *Chilo* larva, showing that changing a^o_{Mg} has no effect on E_m.

equilibrium potentials, E_K and E_{Na}, respectively, were consistently more positive than E_m. It was therefore concluded that another ion, 'x', with its equilibrium potential, E_x, more negative than E_m, must also be involved in the generation of E_m. Cl^- was a candidate for this ion, 'x', and measurements of intracellular Cl^- activities (section V.4) confirmed that the chloride equilibrium potential, E_{Cl}, was indeed more negative than the E_m. If Cl^- were involved in resting membrane electrogenesis, changing extracellular chloride activity, a_{Cl}^o, would be expected to lead to sustained alterations in E_m (cf. the transient effect on E_m of changing a_{Cl}^o when Cl^- is passively distributed across the cell membrane). In order to investigate this possibility, chloride substitution experiments were carried out in which a_{Cl}^o was varied one hundredfold from 0.7 to 67.7 mM Cl^-, using gluconate as a substitute. (The compositions of the solutions used are listed in appendix 4). A typical recording from such an experiment is shown in figure 118. Cells were impaled in the Ringer containing the lowest Cl^- activity (0.7 mM) and subsequently exposed to Ringers in order of increasing Cl^- activity. This was necessary because decreasing the a_{Cl}^o was found to cause depolarisation and hence contraction of the muscle cells, leading to expulsion of the microelectrode.

Cl^- substitution experiments of this type were carried out on a total of 7 cells from 7 preparations, and the data obtained is given in table 33. Thus, changes in a_{Cl}^o led to sustained alterations in E_m, indicating that Cl^- is involved in resting membrane electrogenesis in *Chilo*. The average E_m values are plotted against the logarithm of a_{Cl}^o in figure 119, showing a slightly curved line with a maximum slope of around 17 mV (between 23 and 67.7 mM Cl^-).

VI. 6. Electrogenic metabolic pumps

In order to investigate whether an electrogenic metabolic pump was involved in the maintenance of E_m in *Chilo*, two types of experiment were carried out: the preparation was cooled (to slow down the chemical reactions involved in metabolism), and since the Na pump is the most common type of electrogenic metabolic pump in active tissues, the metabolic blocker ouabain was applied (the latter is a cardiac glycoside which acts to prevent Na^+ extrusion).

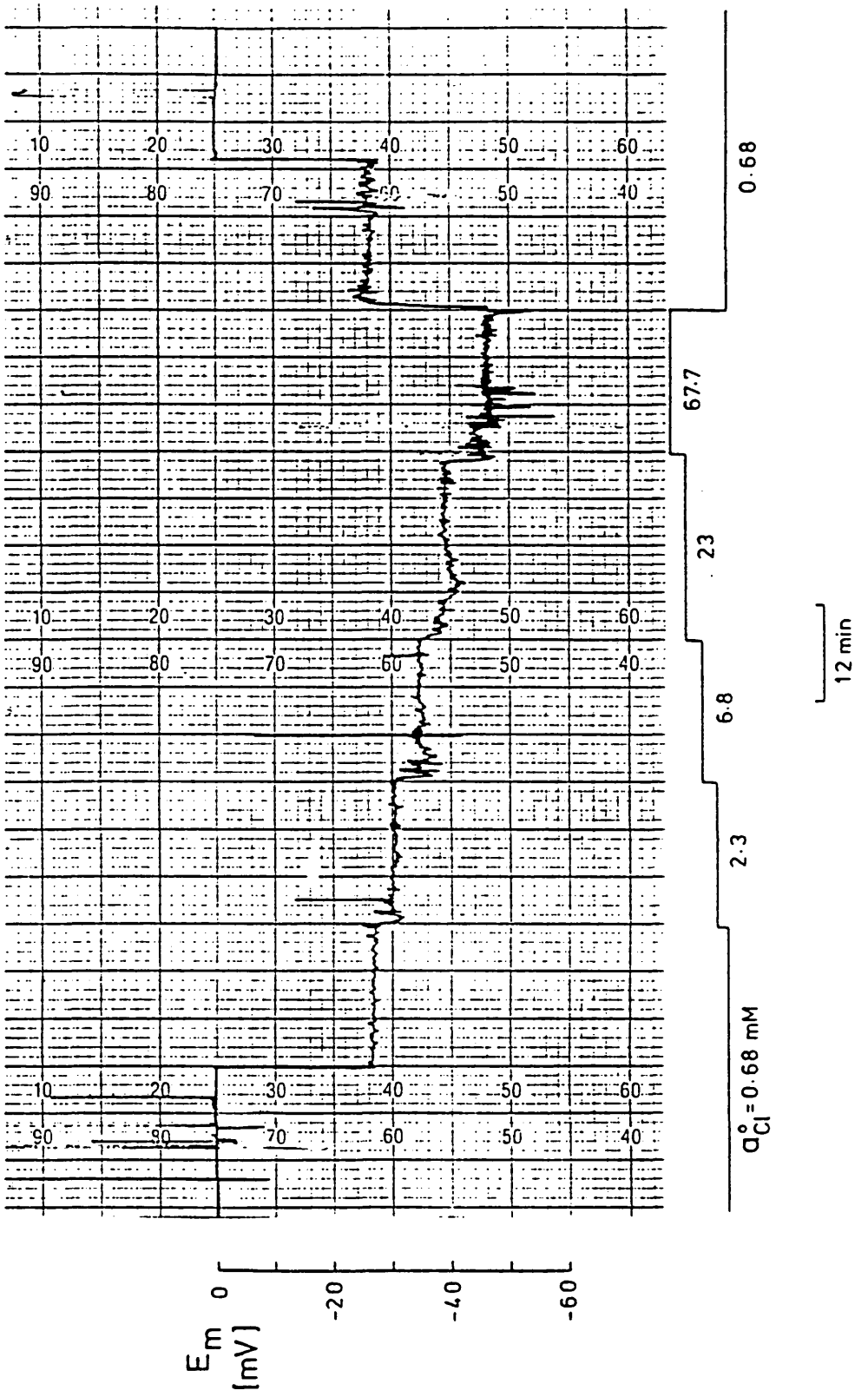


Fig. 118 Chart recording of a Cl^--substitution experiment on a *Chilo* larva, which illustrates the sustained effect on E_m of alterations in a^o_{Cl}.

Table 33. Cl^- substitution data from *Chilo* larvae. (Data from 7 cells, 7 preparations).

Cell no.	Extracellular Cl^- activity, a^o_{Cl} (mM) 0.7	2.3	6.8	23	68
	Membrane potentials, E_m (-mV)				
1	26	29.5	32	36	50
2	22	22	27	32	40
3	27	30	35	39	46
4	37	40	45	50	55
5	36	40	47	54	60
6	24.5	30	36	44	51
7	22	23.5	30	36	46
$\bar{x}$	27.8	30.7	36	41.6	49.7
SE	2.4	2.7	2.8	3	2.5

Table 34. Results from experiments on *Chilo* larvae to determine the effect of ouabain (1 mM) on the response of E_m to changes in a^o_K.

	no ouabain			with ouabain		
a^o_K(mM)	0.72	21.6_N	30.2	0.72	21.6_N	30.2
cell no.						
1	62	55	48	61	55	48
2	48	41	33	47	40	33
3	48	40	33	48	40	32
4	51	44	35	52	44	36
$\bar{x}$	52.3	45.0	37.3	52	44.8	37.3
SD	6.7	6.9	7.2	6.4	7.0	7.4

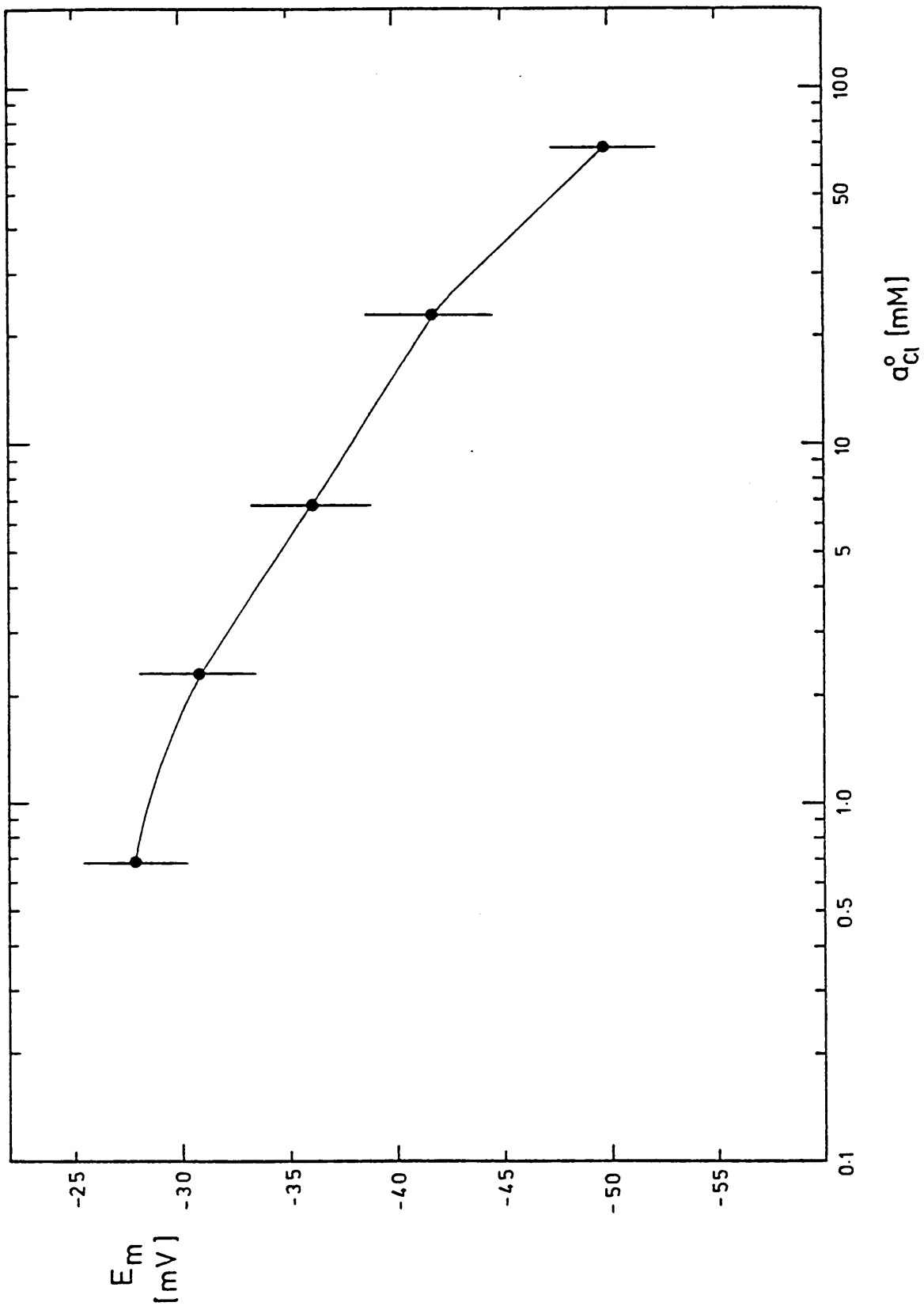


Fig. 119 Graph showing the relationship between E_m and the logarithm of a^o_{Cl} in *Chilo* larvae.

VI.6.i Cooling experiments

These were carried out on cells from which steady E_m recordings had been obtained, and involved the introduction of cooled Normal saline into the recording chamber whilst E_m was continuously monitored. Figure 120 shows a typical experiment, in which a cell was impaled in Normal saline at room temperature, (20°C) giving an E_m of -48 mV. Ice-cooled saline was then substituted in to reduce the temperature of the preparation to 6°C, which depolarised the membrane by 10 mV. Saline at RT was then re-introduced to test the reversibility of the effect, and the membrane quickly repolarised to its original level. This experiment was repeated on 7 cells from 7 preparations, and the average depolarisation in E_m following cooling by 14°C was 12 ± 2 mV (or 26 ± 3% of the initial E_m). (Appendix 15).

Thus, it can be concluded that, at rest, an electrogenic, metabolic pump operates to hyperpolarise the membrane. The exact contribution of this pump to E_m will be discussed in the final chapter.

VI.6.ii. Application of metabolic blocker

Experiments involving the application of the cardiac glycoside, ouabain, were designed firstly to determine whether an electrogenic metabolic pump contributes to the resting E_m of a cell, and secondly whether the activity of this pump varies when the cell is exposed to solutions containing a range of K^+ activities.

In the former type of experiment, a cell bathed in Normal Ringer was impaled and a steady E_m recorded. Normal Ringer containing ouabain was then substituted in (fig. 121). There was no effect on E_m. It is, however, known that K^+ competes with ouabain at its sites of action (Anstee & Bowler, 1979), and at a_K's such as that in Normal Ringer (21.6 mM) this may be the reason for its lack of effect. Alternatively the pump may only be active, for example, in low levels of a_K. In order to test this possibility, the K^+ substitution experiments described in section 6.I were repeated, with each solution containing 1 mM ouabain. The low-K^+ solutions contained a_K as low as 0.72 mM, which would not interfere with ouabain action. If a metabolic pump were responsible for the difference between the slope of the graph of E_m against the logarithm of a_K (a maximum of 30 mV/decade) and the theoretical slope of 58 mV/decade predicted by the Nernst equation, then a K^+ substitution

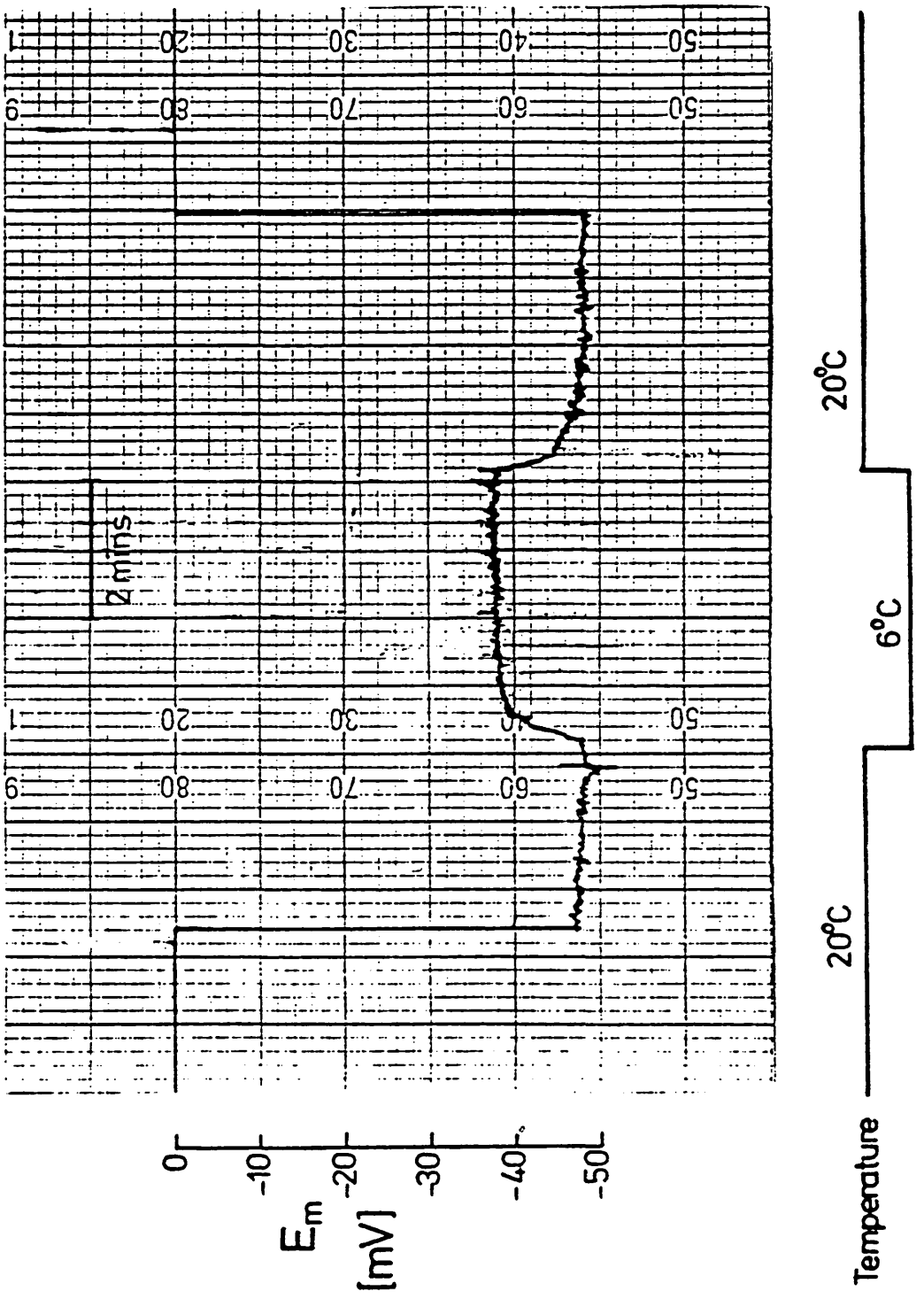


Fig. 120 Chart recording of an experiment in which a *Chilo* muscle cell was cooled by 14°C. It shows the sustained depolarisation in E_m which resulted.

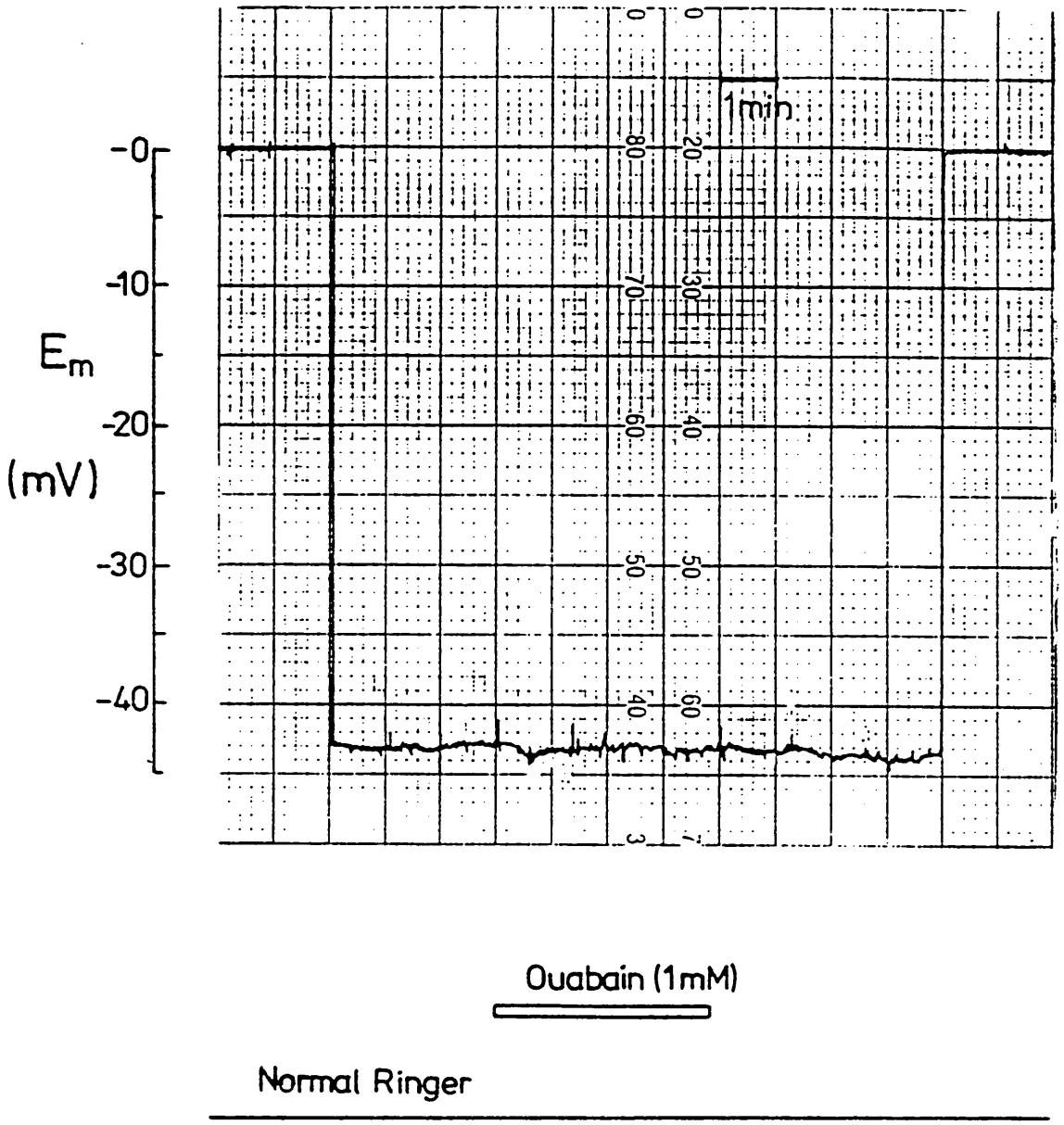


Fig. 121 Chart recording showing the lack of effect of ouabain on E_m in *Chila*.

experiment performed in the presence of ouabain should yield the theoretical 58 mV change in E_m per tenfold change in a_K^+.

Figure 122 shows such an experiment, in which the effect on E_m of three K^+ substitution solutions (with K^+ activities of 0.7, 21.6 (Normal saline) and 30.2 mM) was compared with the effect of the same solutions containing 1 mM ouabain in single cells. Each cell was impaled in Normal saline, and a steady E_m recorded. Normal saline containing ouabain was then substituted in and the cell allowed to equilibrate before returning it to Normal saline. The effect of low (0.72 mM) K^+ Ringer on E_m was then determined, and reversed by washing the cell in Normal saline. This procedure was then repeated using low K^+ Ringer containing 1 mM ouabain for comparison. Similarly for high (30.2 mM) K^+ Ringer, the effect of Ringer containing no ouabain was compared with that of Ringer plus 1 mM ouabain. The cell was returned to Normal saline to ensure that the effect was reversible prior to withdrawal of the microelectrode from the cell. Data were obtained from 4 cells, each from a different preparation, and are shown in table 34. This table shows that, on average, the difference between the alteration in the E_m in response to changes in a_K^+ in the presence and absence of ouabain was less than 1 mV. This is illustrated by figure 123, which shows the average E_m recorded in the three K^+ substitution solutions in the presence and absence of ouabain. There is clearly no signficant difference between the two sets of data.

Thus, whilst a temperature-sensitive hyperpolarising pump appears to be present in *Chilo* muscle cell membranes, it is insenstitive to ouabain. This result will be discussed in the last chapter.

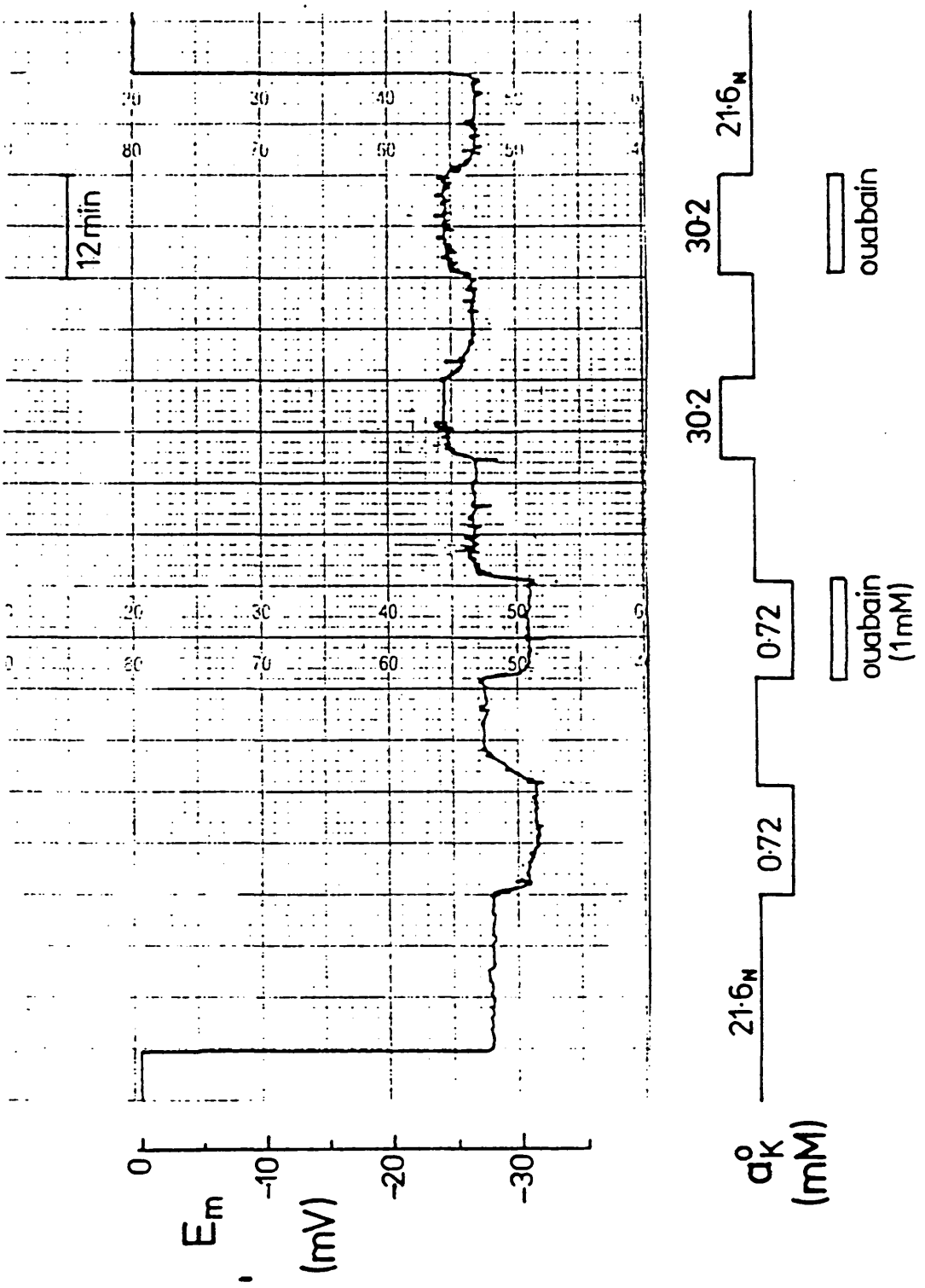


Fig. 122 Chart recording of a K^+ substitution experiment on a *Chilo* larva in which the effects of changing a_K in the presence and absence of ouabain were compared. It illustrates the fact that ouabain had no effect on the response of E_m to changes in a_K^o.

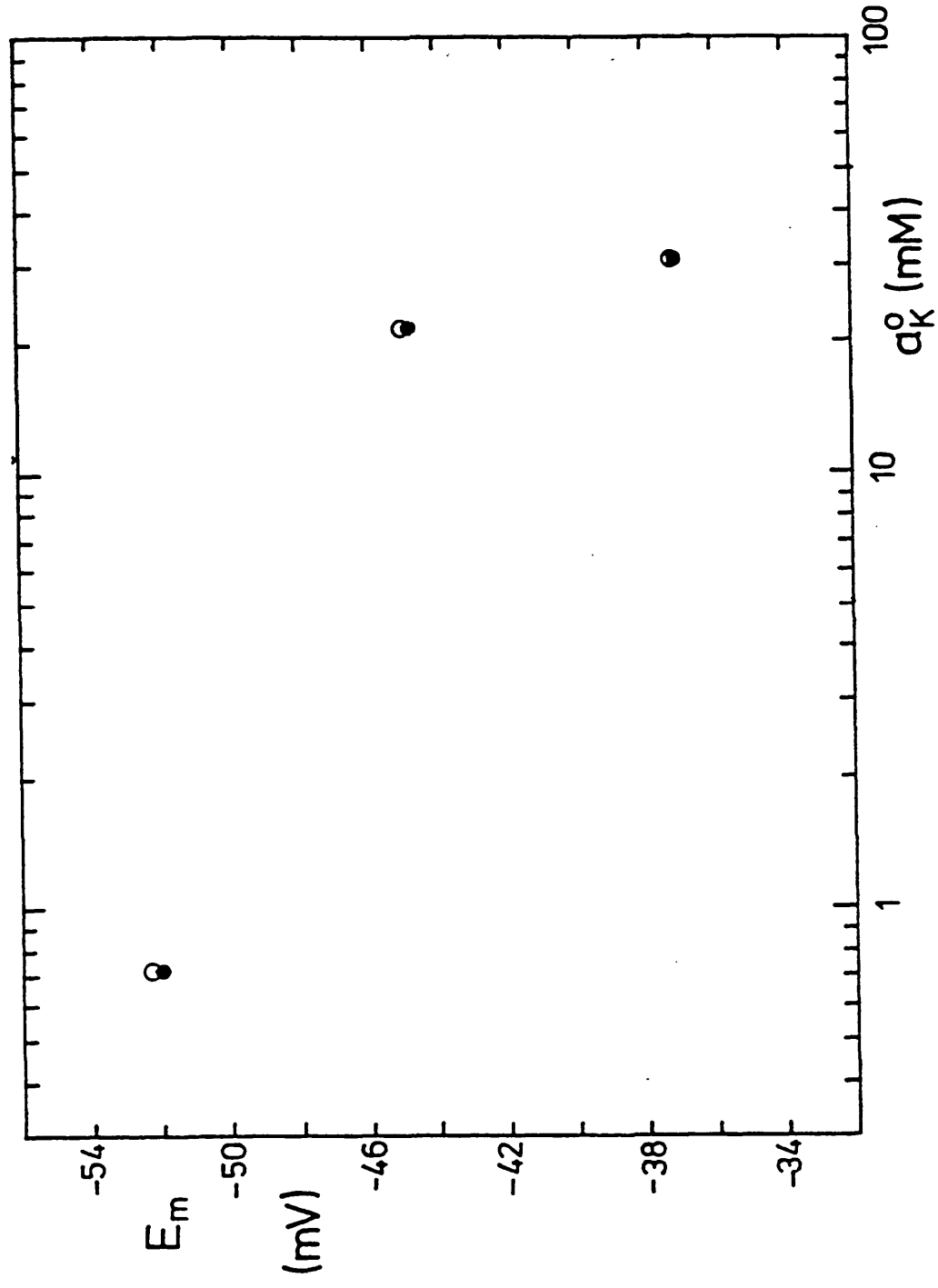


Fig. 123 Graph illustrating the relationship between E_m and the logarithm of a_K^o, in the presence (solid circles) and absence (hollow circles) of ouabain. The two curves are very similar.

VII DISCUSSION

VII.1. The ISM technique

The present study involved a comparative approach to the investigation of the mechanisms of resting membrane electrogenesis in body-wall muscle cells of larvae of two species of insect: the blowfly, *Calliphora erythrocephala* (Diptera) and the rice stem borer, *Chilo partellus* (Lepidoptera). A number of compatible microelectrode techniques were employed, with ion-sensitive microelectrodes being used for the first time in dipteran and larval lepidopteran muscle cells. The measurements thus obtained of the intracellular activities of K^+, Na^+ and Cl^- should respresent a substantial improvement upon the data available in the literature. All previous studies of insect muscle electrochemistry, except one (Rheuben, 1972: of adult *Antherea* (Lepidoptera) using LIX-type K^+ ISM's) relied exclusively on indirect estimates of the overall concentrations of intracellular ions eg. by flame photometry for K^+ and Na^+ (eg. Wood, 1957) and colorimetric diffusion or back-titration methods for estimating Cl^- (Gordon, 1952; Wigglesworth, 1938, respectively). The most physiologically relevant parameter for an ion is, however, its activity (ie. the proportion of the ions which are freely mobile and can therefore contribute to electrochemical phenomena, including the generation of membrane potentials) and not its total intracellular concentration. The latter, which measured indirectly as in the methods listed above, would represent the total amount of each ion present in the cell or extracellular medium, including that which is bound (eg. to proteins) and cannot therefore contribute to electrochemical potentials. One of the major advantages of ISM's is that they provide a direct measurement of the activity of each ion, and hence allow the accurate calculation of its equilibrium potential from the Nernst equation. A number of technical problems were, however, associated with the use of ISM's. These will now be discussed.

Selectivity of the liquid sensors

As already stated, certain problems were encountered with respect to the selectivities of the liquid ion-sensors for the primary ion over interfering ions, particularly in the case of liquid ion-exchangers (LIX's). In prepupal *Calliphora* cells, for example, LIX-type K^+ ISM's have a_K^i values on average 267 mM higher than those recorded using NIC-type K^+ ISM's. Thus, all measurements made with LIX-type K^+ ISM's were repeated using NIC-type K^+

ISM's known to be less prone to interference, and in all preparations, the a_K^i values recorded with LIX-type ISM's were significantly higher than those recorded with NIC-type ISM's.

An associated problem occurred in the use of Na^+ ISM's, which were based on a NIC that was poorly selective for Na^+ over Ca^{2+}. The behaviour of this type of ISM was found to be somewhat unstable in Rice's and Weevers' salines, which contain relatively high levels of Ca^{2+} (0.9 and 8 mM respectively). Calibration solutions for this type of ISM were therefore designed to include a constant background of interference, mimicking the intracellular medium as closely as possible, and containing very small amounts of Ca^{2+}. Intracellular levels of Na^+-sensitive potential recorded from the active barrel of the ISM were then referred directly to the calibration curve of the ISM, with no reference being made to the level of potential recorded when the ISM was bathed in Normal saline.

Leakage from the reference barrel

Leakage of salt solutions from the reference barrels of ISM's poses a problem in the measurement of intracellular ionic activities, tending to result in artificially high values being recorded. This source of error is normally countered by filling the reference barrel with the solution of a salt to which the ion sensor does not respond. Thus, leakage from the reference barrels of K^+ and Na^+ ISM's (filled with LiCl and KCl respectively) would have little effect upon the a_K^i or a_{Na}^i levels recorded, because of the high selectivities of K^+- and Na^+-sensors for the primary ion over secondary interfering ions such as Li^+ and K^+, respectively. Cl^-ISM's, however, are based on a rather unspecific anionic exchanger, and in this study problems were encountered when the reference barrels were filled with a mixture of KCl and K_2SO_4. Preliminary chart recordings of a_{Cl}^i in *Calliphora* larvae clearly showed that the level of apparent a_{Cl}^i continued to increase indefinitely, following the impalement of a cell with this type of ISM. This observation was attributed to the Cl^--exchanger responding to anions leaking from the reference barrel, and hence giving unstable readings and high values for apparanet a_{Cl}^i. The problem was solved by the use of Cl^--ISM's whose reference barrels were filled with an organic reference liquid ion-exchanger, RLIE (Thomas & Cohen, 1981). Any leakage from this type of reference barrel would have no effect on the active barrel of the ISM.

Tip potentials

Tip potentials constitute an inescapable problem with microelectrode recordings. They seem to arise from the presence of an aqueous salt solution inside the tip of a glass microelectrode, and therefore create a problem mainly in conventional microelectrodes and the reference barrels of double-barrelled ISMs. The main danger is that the tip potential of the microelectrode may change during the impalement of the cell, leading to erroneous measurements of E_m. There may also be a positive correlation between the tip potential of the microelectrode and the values of E_m recorded by that microelectrode, (Adrian, 1956). However, in the ISM's used in the present study, the differential potential recorded by the ion-sensitive barrel when the tip was immersed in an earthed solution of compositon identical to that of the back-filling solution was never more than 2 mV different from the theoretically predicted 0 mV reading. The same was observed by Vyskocil and Kriz (1972). The tip potentials associated with the reference barrels of the ISMs could only have been eliminated by increasing the tip sizes of the ISMs. This was undesirable, however, because it would have led to damage of the muscle cell membranes and leakage of filling solutions from the electrodes. The standard method of breaking the tips of electrodes to measure tip potentials was not performed in the present study, since it was found that the performance of an ISM (especially that of Na^+ ISM'S) often improved with time. ISM's were therefore kept for as long as possible without their tips being broken. Instead, the effect of the ISM tip potentials on the membrane potential (E_m) measurements was investigated by measuring E_m's in a given preparation independently using fine conventional microelectrodes filled with 2.5 M KCl. Good agreement was usually found between these two sets of values (eg. figs 51a, 55), which suggests that the tip potentials had been minimised sufficiently and/or kept constant so as not to have an adverse effect on the E_m measurements.

Further, investigations of the relationship betwen the E_m's measured using ISM's and the corresponding values of reference barrel resistances showed no correlation between these two parameters (fig. 124). This evidence provided further support for the claim that tip potentials in these ISMs had been sufficiently minimised and kept constant such that possible artefacts in the measurements of membrane potentials were eliminated.

Thus, ISM's were used to measure the intracellular activities of K^+, Na^+ and

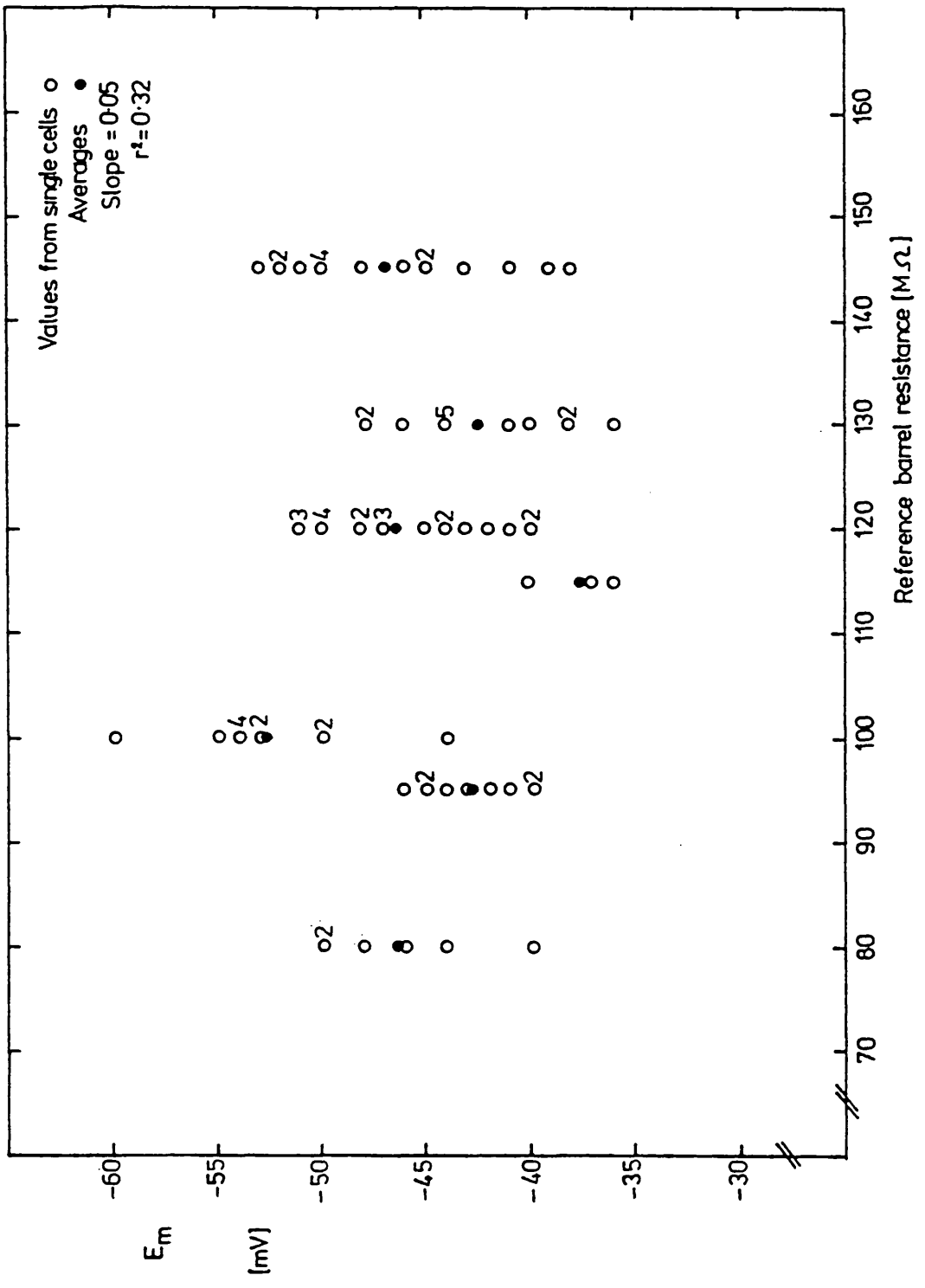


Fig. 124. Graph showing the relationship between the membrane potential (E_m) values recorded by an ISM and the tip resistance of the reference barrel. It indicates that there is no significant correlation between the two parameters (principle of least squares.)

Cl^- in *Calliphora* larvae and prepupae, and *Chilo* larvae. It was assumed that the activity coefficient, γ, had the same value in the intra- and extra-cellular medium, of 0.72 (CRC Handbook of Chemistry & Physics, 52nd ed. 1972). Thus values for the concentration of each ion can be calculated by dividing its activity by the γ value of 0.72.

VII.2. Ionic substitution experiments

Measurements of the intracellular activities of K^+, Na^+ and Cl^- gave equilibrium potentials for these ions which did not equal the average E_m, except for Cl^- in *Calliphora* larvae, where E_{Cl} was very close to E_m in all cells. The fact that the other equilibrium potentials were not equal to E_m suggested that each ion might be involved in generating E_m. Thus, in order to quantitatively assess the roles of K^+, Na^+ and Cl^- and, in *Chilo* alone, Mg^{2+}, ionic substitution experiments were carried out.

The present study has, however, highlighted a major reason to interpret the results of ionic substitution experiments with caution: the effects on the cell membrane of changing the extracellular activity of a particular ion may in some cases be complex, extending beyond the effect predicted by the Goldman-Hodgkin-Katz equation. This was noted with relation to Na^+ substitution experiments, where a reduction in extracellular Na^+ activity resulted in a transient hyperpolarisation in E_m, followed by a sustained depolarising phase. This contrasted with the sustained hyperpolarisation predicted by the Goldman-Hodgkin-Katz equation. In this case, the discrepancy between predicted and observed results was found to result from a secondary effect of Na^+ which caused a marked reduction in the permeability of the cell membrane to K^+ when exposed to low extracellular Na^+. Such permeability changes might be expected to be reflected in the resistance of the cell membrane, R_m, and it would therefore seem adviseable to monitor R_m during all substitution experiments in order to help identify when secondary effects may be occurring. Similarly the use of ionic pulsation experiments in which the response of the cell membrane to fixed-sized pulses of a particular ion is monitored in a variety of extracellular ionic media, could be very valuable in identifying more precisely any permeability changes which might be taking place. This type of procedure was employed in *Calliphora* prepupae to show that p_K was reduced when the cell was bathed in low Na^+ Ringer.

A further means by which the secondary effects of altering the extracellular activity of an ion may be mediated is by their action on various ionic pumping mechanisms which may operate under normal conditions in the cell membrane eg. the coupled Na^+-K^+ pump. Such action may be investigated by the application of specific metabolic inhibitors to the cell and monitoring the effect on E_m. This type of experiment was attempted on *Chilo* to determine whether the shallow slope of the graph of E_m against the logarithm of a_K^o in low levels of a_K^o might be caused by the activation of a depolarising pump under such conditions. Ouabain was applied to cells bathed in low-K^+ solutions, but was found to have no effect on E_m, which may indicate that the pump was present but was ouabain-insensitive, or that it was absent.

Ion-exchange mechanisms such as Na^+-Ca^{++}exchange may also be affected by changing the extracellular Na^+ activity, altering a_{Ca}^i and hence E_m (Bers & Ellis, 1981.)

Thus, altering the extacellular activities of a variety of ions may have secondary effects on the cell membrane which may obscure the simple effects resulting from changes in the equilibrium potential of the ion.

VII. 3. The model of resting membrane electrogenesis in body-wall muscle cells of *Calliphora* prepupae

The construction of a model to explain resting membrane electrogenesis in prepupal muscle cells based on the simplified Goldman-Hodgkin-Katz equation was described in chapter IV. The preliminary model proposed was based on several lines of evidence, including intracellular ionic activity measurements and ionic substitution experiments. Measurements of intracellular K^+ activity, a_K^i, indicated that K^+ was not the only ion involved in generating E_m, since E_K was consistently more negative than E_m. This was confirmed by a series of K^+ substituion experiments (using Na^+ as the substitute), which gave a maximum change in E_m of 32 mV per tenfold change in extracellular K^+ activity, a_K^o (cf. the 58 mV change predicted by the Nernst equation for a cell membrane permeable only to K^+). These results suggested that the cell membrane was permeable to another ion in addition to K^+, with its equilibrium potential more positive than E_m. Since Cl^- was known from the results of intracellular Cl^- activity measurements and Cl^- substitution experiments taken together, to be passively distributed, the most likely candidate for this ion was Na^+. The latter had, in fact, been used to substitute for K^+ in the K^+ substitution experiments, and it was therefore necessary to consider the E_m

changes observed during these experiments in relation to the alterations in both a^o_K and a^o_{Na}. If the cell membrane behaved according to the simplified Goldman-Hodgkin-Katz equation, a tenfold change in (a^o_K + α a^o_{Na}) would cause a 58 mV change in E_m, where α is the ratio of the partial permeability of the cell membrane for Na^+ to that for K^+ (P_{Na}/P_K). thus, a value for α of 0.086 was calculated by numerical substitution such that the above condition was met. This value was then substituted into the simplified Goldman-Hodgkin-Katz equation (equation 2), together with the values of a^o_K and a^o_{Na}, known from the composition of Normal Ringer (Appendix 1) to give the following model:

$$E_m = 58 \log\left[\frac{a^o_K + 0.086\ a^i_{Na}}{a^i_K + 0.086\ a^o_{Na}}\right]$$

$$= 76 - 58 \log\ (a^i_K + 0.086\ a^i_{Na})(mV)$$

This model predicted that the E_m of a cell could be explained in terms of the trans-membrane gradients of K^+ and Na^+.

Attempts to test this model by performing Na^+ substitution experiments to determine the effect of a^o_{Na} on E_m were only partially successful, however. When a^o_{Na} was reduced, the E_m hyperpolarised, as expected if Na^+ were involved in generating E_m. This initial hyperpolarisation was followed by an unexpected sustained depolarising phase, however. The latter coincided with an increase in membrane resistance (section IV.4.ii) and a marked reduction in p_K but no change in E_K (sections IV.4.iv and IV.4.ii respectively). Any change in p_K, without a corresponding change in p_{Na} would result in a change in the value of α, and hence lead to the invalidation of the above model. In view of the fact that p_K was known to change in low a^o_{Na}'s, separate α values were calculated for E_m data obtained in high-K^+ Ringers (where a^o_{Na} was lower than or equal to that in Normal Ringer) and in low-K^+ Ringers (where a^o_{Na} was higher than or equal to that in Normal Ringer). A value of 0.169 was obtained from data from high K^+/low Na^+ Ringers, and 0.036 for data from low K^+/high Na^+ Ringers. In order to test which of the three α values, 0.086 (from the total data), 0.169 (from high K^+/low Na^+ data) or 0.036 (from low K^+/high Na+ data) gave the best decription of the membrane properties, values of a^i_K, a^i_{Na} and E_m were measured in a number of cells (section IV.4.iv, appendix 12). Using these values of a^i_K and a^i_{Na} and each α in turn, values of E_m were predicted for each cell, and compared with the measured E_m of the cell. The most accurate prediction of E_m was provided by the α value calculated from the low K^+/high Na^+ E_m data,

Table 35. Relation between $[Na^+]_o$ and the resting potential in *Drosophila* larvae. (From Jan & Jan, 1976)

Expt.	External concentrations: Na^+	$Tris^+$	K^+	Cl^- (mM)	Ca^{2+}	Mg^{2+}	Sucrose	Relative ionic strength	Relative tonicity	Average resting potential (mV)	Predicted from eqn. (4) (mV)
1	127	1	2	142	1·8	4	36	1·0	1·0	−50 ± 5 (16)*	−43
2	102	26	2	142	1·8	4	56	1·0	1·0	−51 ± 4 (16)	−48
3	64	64	2	142	1·8	4	87	1·0	1·0	−59 ± 6 (16)	−59
4	26	102	2	142	1·8	4	118	1·0	1·0	−54 ± 8 (12)	−78
5	26	102	2	134	1·8	0	118	0·9	1·0	−59 ± 5 (20)	—
6	26	0	2	40	1·8	4	210	0·3	1·0	−57 ± 3 (24)	—
7	6	122	2	142	1·8	4	138	1·0	1·0	−54 ± 4 (14)	−99
8	6	122	2	134	1·8	0	138	0·9	1·0	−54 ± 5 (22)	—
9	6	0	2	20	1·8	- 4	242	0·2	1·0	−55 ± 2 (22)	—
10	0	0	2	99	45	4	155	1·0	1·0	−81 ± 4 (20)	−112
11	0	0	2	99	32	17	155	1·0	1·0	−88 ± 4 (20)	−112
12	0	0	2	99	19	30	155	1·0	1·0	−75 ± 5 (19)	−112
13	0	0	2	99	1·8	- 47	155	1·0	1·0	−56 ± 3 (20)	−112
14	128	0	2	142	5·8	0	36	1·0	1·0	−57 ± 3 (16)	−43
15	128	0	2	139	0·1	4	36	1·0	1·0	−40 ± 4 (17)	−43
16	128	0	2	142	0	5·8	36	1·0	1·0	−34 ± 4 (14)	−43

* The number in each parenthesis indicates the number of fibres studied in each experiment.

Table 36. Effect of sodium ion substitution on E_m in leech anterior neuropile glial cells. (From Walz & Schlue, 1982).

Na-substitute	*Na-substitute (mM)*	*Cl^- (mM)*	*SO_4^{2-} (mM)*	*Sucrose (mM)*	*$\triangle E_m \pm$ S.D. (mV)* *Hyperpolarization*	*Depolarization*
Sulphate-based saline						
Tris	160	3.6	82	—	−1.3 ± 1.1 (n = 6) →	+6.2 ± 3.0 (n = 9)
Li	115	3.6	59.5	76	−2.1 ± 1.6 (n = 11) →	+9.7 ± 2.0 (n = 7)
Chloride-based saline						
Tris	134	7.6				+4.8 ± 1.2 (n = 8)
Li	140	147.6			−4.0 ± 3.1 (n = 8) →	+9.0 ± 4.2 (n = 8)

In addition, all solutions contained 4 mM K, 1.8 mM Ca, 10 mM malic acid (buffer with Tris) and 11 mM glucose. In sodium-free solutions with Tris as sodium-substitute the pH was adjusted with HCl; in solutions with lithium as sodium-substitute the pH was brought to 7.4 with 1 M Tris solution. Osmolarity of all solutions was adjusted to 265 ± 10 m-osmole. Where hyperpolarization was followed by depolarization, the transition is indicated by an arrow.

0.036: the mean predicted E_m, -48 ± 1 mV, was equal to the mean measured E_m. The final model for resting membrane electrogenesis was therefore modified to include the α value of 0.036 to give the following:

$$E_m = 66.8 - 58 \log (a^i_K + 0.036\, a^i_{Na})$$

This model was finally tested by performing a series of substitution experiments in which a^o_K and a^o_{Na} were varied, whilst keeping (a^o_K + 0.036 and a^o_{Na}) x a^o_{Cl} constant. If the above model were correct, a tenfold change in (a^o_K + 0.036 a^o_{Na}) would be expected to give rise to a change in E_m of some 58 mV. Since Cl^- was known to be passively distributed, the changes in E_m resulting from changes in a^o_K and a^o_{Na} were expected to be rapid, which was the case. In addition, the slope of the graph of E_m against the logarithm of (a^o_K + 0.036 a^o_{Na}) was indeed close to 58 mV (fig. 94), providing conclusive evidence that the above model for resting membrane electrogenesis explains fully the ionic bases of the E_m.

A less detailed but broadly comparable investigation of resting membrane electrogenesis was carried out on *Drosophila melanogaster* (Diptera) larval body-wall muscles by Jan & Jan (1976). It was concluded that E_m was dependent upon the extracellular K^+ and Na^+ concentrations according to the Goldman-Hodgkin-Katz equation (p_{Na}/p_K = 0.23) with Cl^- distributed passively.

The major shortcoming of this work is the fact that the reversibility of the experiments performed was not tested during each experiment. This is particularly vital in experiments designed to determine the effects of extracellular K^+ and Na^+ , where the preparation was soaked for up to 50 minutes in each of 7 solutions. Each experiment could therefore last for several hours, during which time the condition of the cells could deteriorate and the E_m's depolarise irrespective of the extracellular K^+ and Na^+. The only test of the reversibility of the effect of extracellular K^+ and Na^+ was performed as a separate experiment. A preparation was bathed in Normal Ringer (2 mM K^+, 128 mM Na^+, 142 mM Cl^-) and the resting potential of a number of cells measured. It was then transferred to a Cl^--free solution containing 85 mM K^+, OmM Na^+ for 60 minutes. When returned to Normal Ringer, the E_m values recovered to only 80 to 90% of their original values at the start of the experiment within 10 minutes. This was taken as evidence that the effects of extracellular K^+ and Na^+ were completely reversible! A

second shortcoming of Jan & Jan's experiments is that they involved multiple impalements of the same population of cells. This may in itself have damaged the muscle cell membranes and hence depolarised E_m. This possibility was apparently not tested.

Jan & Jan (1976) made attempts to illustrate the dependence of E_m on $\{[K^+]_o + 0.23\ [Na^+]_o\}$ in two ways. Firstly, substitution experiments were carried out in which $\{[K^+]_o$ and $[Na^+]_o$ were varied, whilst keeping $\{[K^+]_o + 0.23\ [Na^+]_o\} \times [Cl^-]_o$ constant. If E_m did indeed depend on $\{[K^+]_o + 0.23\ [Na^+]_o\}$, then a graph of E_m against the logarithm of the latter would have had a slope of 58 mV per tenfold change in $\{[K^+]_o + 0.23\ [Na^+]_o\}$. The data points obtained, however, showed a marked deviation from a 58 mV slope (fig. 10) but were nevertheless taken as evidence that E_m was predicted correctly by the Goldman-Hodgkin-Katz equation with an α value of 0.23.

Secondly, Na^+ substitution experiments were carried out (using Tris as a substitute) to determine whether a reduction in $[Na^+]_o$ led to a hyperpolarisation in E_m as predicted by the α value of 0.23. The results obtained are listed in table 35. This data has been plotted in the form of a graph of E_m against the logarithm of $[Na^+]_o$ (fig. 125), which shows that E_m hyperpolarised when $[Na^+]_o$ was reduced. However, there is little correlation between the size of the hyperpolarisation and the amount by which $[Na^+]_o$ was reduced ($r^2 = -0.5$). The E_m values recorded in each $[Na^+]_o$ bore little relation to the E_m's predicted from the Goldman-Hodgkin-Katz equation using an α value of 0.23 (table 35). No mention was made of the time for which cells were allowed to equilibrate in each solution, which may have been crucial if the response of E_m to reduced $[Na^+]_o$ was similar to that of *Calliphora* muscles (ie. giving an initial hyperpolarisation followed by a depolarising phase). A far better experiment would have been to monitor E_m continuously during the substitution experiment, rather than repeatedly impale the same population of cells.

Jan & Jan (1976) estimated that the value of $\{[K^+]_i + 0.23\ [Na^+]_i\}$ was 173 mM. This is fairly close to the value of $\{[K^+]_i + 0.036\ [Na^+]_i\}$ of 160 mM calculated for *Calliphora* from the average measured values of a_K^i and a_{Na}^i by converting the latter to concentrations by division by 0.72. This agreement is not, however, inconsistent with Jan & Jan's value of α being incorrect, having been estimated from a series of crude experiments. The contribution

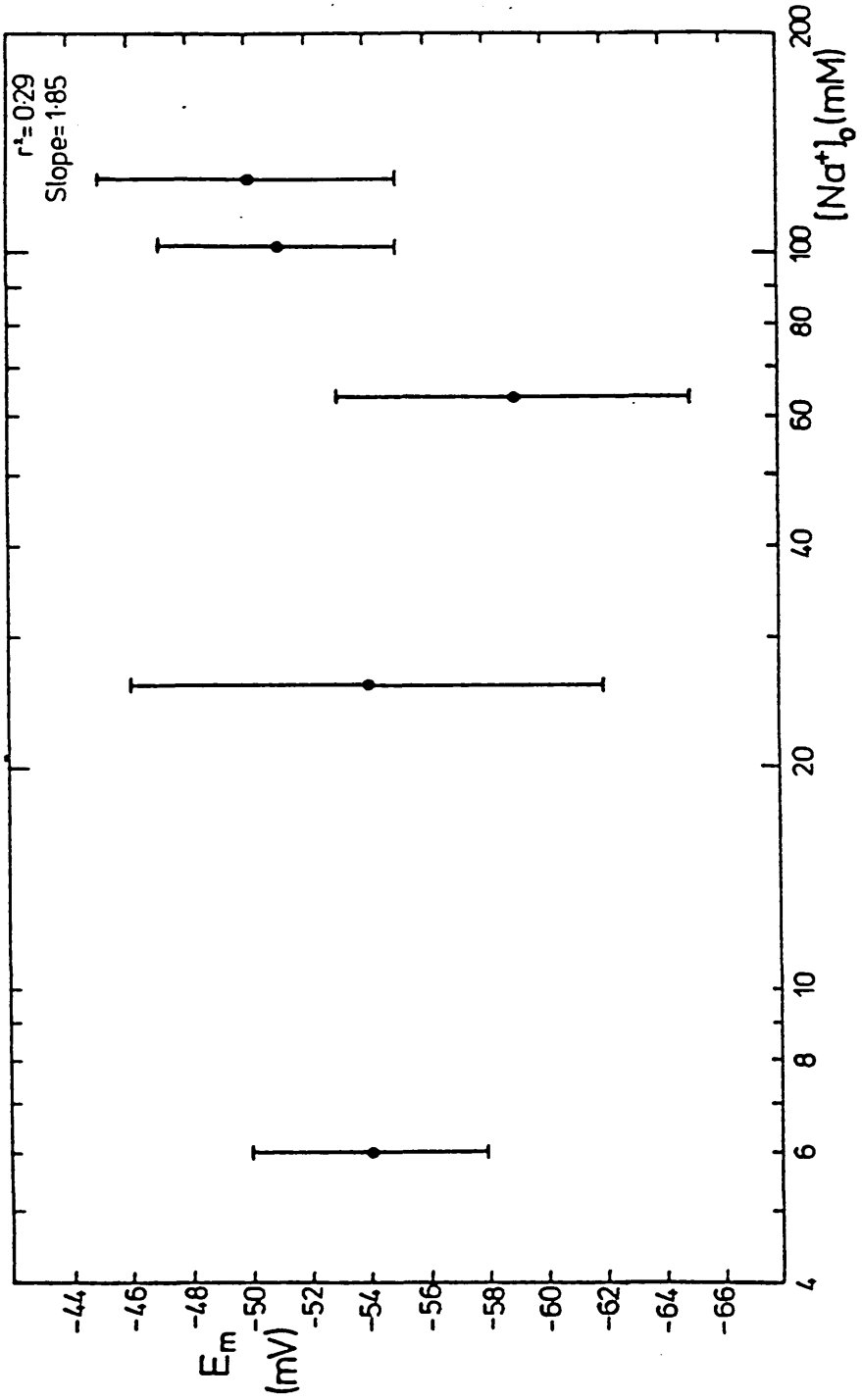


Fig. 125. Graph showing the relationship between E_m and the extracellular Na^+ concentraton in *Drosophila* (Data from Jan & Jan, 1976; see table35). It illustrates that there is little correlation between the two parameters. Bars represent standard deviations.

of 0.23 x $[Na^+]_i$ to the sum of $\{[K^+]_i + 0.23\ [Na^+]_i\}$ is very small compared to that of $[K^+]_i$, because in most systems $[K^+]_i$ is approximately ten times greater than $[Na^+]_i$.

A more detailed discussion of the roles of Cl^-, K^+ and Na^+ in resting membrane electrogenesis in *Calliphora* is presented in the following section.

VII.3.i. The role of Cl^- in generating E_m

Intracellular Cl^- activity, a^i_{Cl}, data for *Calliphora* larvae and prepupae was obtained using Cl^- ISM's based on the improved Corning Cl^--exchanger (477913; Baumgarten, 1981) with the reference barrel filled with an organic reference liquid ion exchanger (RLIE, Thomas & Cohen, 1981). The latter eliminated the possibility of anions leaking from the reference barrel into the cell. This data was presented in section III.4, and represents the first intracellular Cl^- activity data to be measured in Dipteran muscles. Average a^i_{Cl} values of 17 ± 1 mM and 40 ± 2 mM were obtained for larvae and prepupae respectively. In larvae, the E_{Cl} values calculated from this data were close to the E_m values: the average E_{Cl} (-53 ± 1 mV) was equal to the average E_m. In prepupae, however, E_{Cl} (-31 ± 1 mV) was consistently more positive than E_m (-50 ± 1 mV), by an average of 19 mV. Cl^- substitution experiments on the two preparations (section IV.1) indicated that Cl^- was passively distributed in each, confirming that the high apparent a^i_{Cl} value in prepupae was attributable to the presence of an interferent in the muscle cells. Thus, in parallel with the increase in the concentration of a cationic interferent during the 'development' from larva to prepupa (section III.2) an anionic interferent which was not present in sufficient quantities in larvae to affect a^i_{Cl} values, occurs in prepupae. Cl^- depletion experiments on prepupae showed that an apparent a^i_{Cl} of an average of 10 ± 1 mM remained in a cell following soaking of the cell in Cl^--free Ringer to deplete it of Cl^-, providing a measure of the amount of interferent present in the cell. Since the average E_m of the cells on which Cl^- depletion experiments were carried out was -50 ± 3 mV (Appendix 11), and Cl^- was known to be passively distributed, the true a^i_{Cl} would be expected to have an average value of 19 mM, corresponding to an E_{Cl} of -50 mV. When the cell was soaked in Cl^--free Ringer, this 19 mM Cl^- would be expected to move down its concentration gradient and out of the cell, leaving some 24 mM (43 - 19 mM) apparent a^i_{Cl} in the cell which would correspond to the activity of interferent present. The actual value of 10 ± 1 mM recorded was thus

considerably smaller than the expected value of 24 mM. There are two possible explanations for this: firstly, the ISM properties may change in the absence of Cl^-, giving a smaller response to the interferent when the cell was depleted of Cl^-; secondly, the interferent may leave the cell when it is soaked in Cl^--free Ringer, possibly via Cl^- channels.

The response of the cell membrane to lowered a_{Cl} was unexpected. Instead of the transient depolarisation predicted if Cl^- were distributed according to a Donnan equilibrium, a hyperpolarisation was observed. This contrasts with results obtained in other insects eg. *Schistocerca gregaria* (Lea & Usherwood, 1973), *Antherea polyphemus* (Rheuben, 1972), where a reduction in a_{Cl} caused a transient depolarisation in E_m, as predicted. *Calliphora* muscle cells also hyperpolarised in response to elevated a_{Cl}'s, as expected, and in agreement with data for other insects (Lea & Usherwood, 1973; Rheuben, 1972).

This hyperpolarisation of E_m in response to lowered a_{Cl} may be attributable to a number of mechanisms. Firstly, Cl^- is known to be involved in the regulation of intracellular pH, and a reduction in a_{Cl} might therefore change pH_i by affecting the Cl^- - HCO_3 exchange mechanism (Thomas, 1977). This might result in a hyperpolarisation of E_m. Secondly, lowering a_{Cl} may indeed lead to a very small depolarisation which may be sufficient to increase the permeability of the cell membrane to an ion such as K^+, thus causing E_m to hyperpolarise. This could occur via potential-sensitive, self-inactivating K^+ channels such as those found in *Drosophila* flight muscle (Salkoff & Wyman, 1983). Such channels would be activated immediately following the onset of the transient depolarising response to lowered a_{Cl} predicted from the Donnan equilibrium. This would result in the observed hyperpolarisation in E_m which would obscure the expected depolarisation. The E_m would then repolarise and return to its original resting level as the K^+ channels were inactivated, by which time Cl^- might already have re-established an equilibrium and have no further tendency to depolarise E_m.

However, as previously discussed, changes in a_{Cl} produced no sustained changes in E_m in either larvae or prepupae. It was therefore concluded that Cl^- was passively distributed in *Calliphora*, playing no part in resting membrane electrogenesis.

VII.3.ii. The role of K^+ in generating E_m

Intracellular K^+ activities, a_K^i's, were measured in larvae and prepupae using LIX-and NIC-type K^+ ISMs, (section III.2). This was the first such data to be obtained in Dipteran muscle. In larvae, the mean a_K^i value as measured by LIX-type ISM's was 129 ± 4 mM, by NIC-type ISM's, 102 ± 2 mM. In prepupae, the mean a_K^i measured using LIX-type ISM's was 382 ± 12 mM, and using NIC-type ISM's, 115 ± 3 mM. The E_K values calculated from these data were consistently more negative than E_m in all cells, by a minimum of 11 mV (larva, NIC-type ISM data) to a maximum of 41 mV (prepupa, LIX-type ISM data). The fact that E_K was not equal to E_m indicated that K^+ was not passively distributed across the cell membrane, but was likely to be involved in generating E_m. It also suggested that K^+ was not the only ion involved in resting membrane electrogenesis. The results of a series of K^+ substitution experiments in which Na^+ was used as the substitute, were consistent with these suggestions. The cell membrane depolarised in response to elevated levels of a_K^o, and hyperpolarised when a_K^o was reduced. The relationship between E_m and the logarithm of a_K^o was linear (correlation coefficient 0.995) with a slope of 28 mV per tenfold change in a_K^o. This was markedly shallower than the 58 mV per tenfold change in a_K^o predicted by the Nernst equation for a membrane permeable only to K^+, confirming that the membrane was likely to be permeable to one or more additional ions.

The depolarising response of the muscle cell membrane to elevated levels of a_K^o was used as an index of the permeability of the membrane to K^+ in a series of K^+ pulsation experiments (section IV.4.iv). The latter were designed to demonstrate any change in the membrane's permeability to K^+ occurring when the cell was exposed to low levels of a_{Na}^o. Each experiment involved the application of constant-sized pulses of high-K^+ (97.2 mM) Ringer to the cell and recording its response when bathed in Normal Ringer. Low Na^+ (a.25 mM) Ringer was then substituted in for the Normal Ringer. The size of the depolarising responses of the membrane to the pulses of high K^+ Ringer was found to decrease to an average of 4% of their initial size in Normal Ringer, when the cell was exposed to low a_{Na}^o. This indicated that the permeability of the cell membrane to K^+ was greatly reduced when the cell was bathed in low-Na^+ Ringer. The mechanism of this reduction in p_K is not clear. It has been shown that Dipteran muscle possesses three types of K^+ conductance mechanism (Salkoff & Wyman, 1983): 1. the classical delayed, rectifying K^+ conductance of the kind described in the squid giant

axon by Hodgkin and Huxley (1952); 2. a calcium-activated K^+ conductance, of the type found in snail neurones by Meech and Standen (1975); and 3. a fast transient K^+ conductance, whose time course could not explain the sustained depolarisation in E_m when the cell was exposed to low a^o_{Na}. Lowering a^o_{Na} would also not be expected to explain the delayed, rectifying K^+ conductance, and it has been shown that a^o_{Na} had no effect on this conductance in the squid giant axon (Hodgkin & Huxley, 1952). However, reducing a^o_{Na} might have an indirect effect on the Ca-activated K^+ conductance. Thus, in sheep heart Purkinje fibres, a reduction in a^o_{Na} causes a reduction in a^i_{Na} and a corresponding increase in $[Ca]_i$ (Bers & Ellis, 1982). A similar situation was reported in snail neurones (Partridge & Thomas, 1976). Such a rise in intracellular Ca^{2+} would be expected to activate the Ca^{2+}-dependent K^+ conductance, leading to an increase in p_K and a hyperpolarisation in E_m when a^o_{Na} was reduced, which is in fact observed. This scheme does not, however, explain the events seen in *Calliphora* muscle cells, where the transient hyperpolarisation in E_m which occurs when a^o_{Na} is reduced, is followed by a sustained depolarising phase. The depolarisation might, however, be explained if reducing a^o_{Na} led to a reduction in a^i_{Na} and hence via an unknown exchange mechanism to a <u>reduction</u> in intracellular Ca^{2+}. This would lower the Ca-dependent K^+-conductance, leading to a reduction in p_K and a corresponding depolarisation in E_m. Alternatively, the behaviour of *Calliphora* muscle cells may initially be similar to that of sheep heart Purkinje fibres, with a reduction of a^o_{Na} causing a drop in a^i_{Na} and hence an increase in a^i_{Ca} and a hyperpolarisation of E_m. When a^i_{Ca} reaches a certain level, it might be taken up by cellular organelles (Aidley, 1975) leading to a drop in a^i_{Ca} and a corresponding reduction in p_K and depolarisation in E_m. If a^i_{Ca} was thus reduced to a level lower than its original value, this could explain the net depolarisation in E_m to a level more positive than that initially recorded. The sequence of events occurring could be clarified further by monitoring a^i_{Na} and a^i_{Ca} during a low-Na^+ substitution experiment.

VII.3.iii <u>The role of Na^+ in generating E_m</u>

Measurements of intracellular K^+ activities in lavae and prepupae showed that the E_K was consistently more negative than E_m, implying that the cell membrane was permeable to one (or more) ions in addition to K^+, with equilibrium potentials more <u>positive</u> than E_m. Since Cl^- had been shown to be passively distributed, Na^+ was a likely candidate for such an ion.

Intracellular Na^+ activities were measured in both larvae and prepupae using NIC-based Na^+ ISM's. This was the first a^i_{Na} data to be obtained in insect muscle, and gave average values of 11 ± 1 and 7 ± 1 mM respectively. These corresponded to E_{Na} values of 65 ± 2 and 76 ± 2 mV, respectively, which were positive for all cells studied. The fact that E_{Na} was more positive than E_m and not equal to it was consistent with Na^+ being involved in generating E_m.

Attempts to determine quantitatively the role of Na^+ in resting membrane electrogenesis by performing Na^+ substitution experiments were complicated by the fact that the effects of changing a^o_{Na} on the cell membrane were not simple. Secondary effects were also found to occur eg. the permeability of the cell membrane to K^+ was reduced when the cell was exposed to low-Na^+ Ringer. This was thought to explain the observation that following the initial hyperpolarisation of 2 to 7 mV which resulted from reducing a^o_{Na} (an effect consistent with Na^+ being involved in the maintenance of E_m), a depolarisation of E_m occurred, to levels 2 to 8 mV more positive than its original value. This delayed depolarisation could be explained qualitatively, as follows: if the permeability of the cell membrane to K^+ was reduced in low a^o_{Na}, the E_m would tend to move away from E_K, which is more negative than E_m, and hence to depolarise.

Further evidence for the involvement of Na^+ in generating E_m in *Calliphora* was obtained from a series of substitution experiments, designed to test the model for resting membrane electrogenesis. These involved varying a^o_K and a^o_{Na} whilst keeping $(a^o_K + 0.036\ a^o_{Na}) \times a^o_{Cl}$ constant, and a tenfold change in $(a^o_K + 0.036\ a^o_{Na})$ was found to give a change in E_m close to 58 mV as expected if the model fully accounted for the ionic bases of E_m. The test solutions in these experiments were constructed such that only relatively small changes in a^o_{Na} occurred (from 124.6 to 88.6 mM ie. by 29% cf. the change from 124.6 to 1.25 mM ie. of 99% in the Na^+ substituion experiments). Thus, the E_m gave sustained responses to all solutions, with no transient hyperpolarisations /depolarisations of the type recorded in conventional Na^+ substitution experiments. The responses of the E_m to changes in solutions in which $(a^o_K + 0.036\ a^o_{Na}) \times a^o_{Cl}$ was kept constant were much faster than those in conventional K^+ substitution experiments, occurring within a few minutes, as opposed to several tens of minutes in K^+ substitution experiments. This confirms the conclusions from Cl^- substitution experiments that Cl^- is passively distributed in this preparation. Since the slope of the

graph of E_m against the logarithm of (a_K^o + 0.036 a_{Na}^o) was very close to 58 mV, this confirmed that the p_{Na}/p_K or α value of 0.036 was correct. This value is markedly larger than the α of 0.01 calculated for frog skeletal muscle fibres (Hodgkin & Horowicz, 1959).

As previously noted, Jan & Jan (1976) predicted that Na^+ was involved in generating in E_m in *Drosophila* (section VII.3). Their model for resting membrane electrogenesis did not, however, stand up to experimental testing. When Na^+ substitution experiments were performed, E_m did hyperpolarise in response to reduced extracellular Na^+ activity, but there was little correlation between E_m and a_{Na}^o (fig.125). This lack of correlation was not explained, but it was suggested that the muscle membrane may have been unstable, sealing poorly after microelectrode penetration, especially when the fibre was hyperpolarised by reducing a_{Na}^o. It is more likely that the E_m's of *Drosophila* muscle cells behave similarly in low a_{Na}^o's to those of *Calliphora* cells, with an initial hyperpolarisation being followed by a depolarisation, and that the E_m values recorded in *Drosophila* were obtained during different stages of this response.

Results comparable to those obtained in *Calliphora* were reported from Na^+ substitution experiments on leech neuropile glial cells (Walz & Schlue, 1982). Na^+ was replaced by Tris and Li^+, giving the results shown in table 36. In most experiments, E_m hyperpolarised, by a maximum of -4 mV in a chloride-based saline and a maximum of -2.1 mV in sulphate-based saline with Li^+ as the Na^+ substitute. The initial hyperpolarisation was usually followed by a depolarisation, and in some experiments E_m depolarised as soon as Na^+ was removed from the saline bathing the cell. This result was not explained.

VII.3.iv. Other mechanisms

In *Calliphora*, the model based on the simplified Goldman-Hodgkin-Katz equation fully accounts for the resting E_m in terms of the trans-membrane K^+ and Na^+ gradients. This, however, does not rule out the possiblity that additional mechanisms may contribute to E_m. Such mechanisms include pH, Ca^{2+}, Mg^{2+} and an electrogenic, metabolic pump, none of which were investigated.

The effect of pH is difficult to assess, since changing pH may affect a range

of cellular mechanisms and hence have secondary effects on E_m. In *Drosophila* larvae, E_m was found not to be very sensitive to changes in pH between 6.8 and 7.3, altering by only 2-3 mV in this range. (Jan & Jan, 1976). Increasing $[Ca^{2+}]_o$ in the same preparation caused a hyperpolarisation in E_m, of some 26 mV when $[Ca^{2+}]_o$ was raised from 1.8 to 45 mM. This was attributed to the cell membrane forming improved seals around the microelectrode in elevated levels of $[Ca^{2+}]_o$ (Jan & Jan, 1976; Stefani & Steinbach, 1969). It is, however, possible that Ca^{2+} may have secondary effects on E_m. Increasing $[Mg^{2+}]_o$ from 4 to 47 mM gave an average hyperpolarisation of only 2 mV in *Drosophila*, indicating a low permeability to Mg^{2+}.

A Na^+/K^+ pump is certain to be present in the muscle cell membrane in *Calliphora*, maintaining the trans-membrane Na^+ and K^+ gradients. It is not known whether this pump contributes directly to resting membrane electrogenesis. If it does, its involvement must be minor, since E_m can be explained quantitatively by the model based on the Goldman-Hodgkin-Katz equation. There are no reports on an electrogenic pump in Diptera.

VII.4. Developmental changes in intracellular ionic activities in *Calliphora*

Changes were observed in the intracellular activities of certain ions and interferents in *Calliphora* as the insect developed from the larval to prepupal stages. It should be noted, however, that the muscle cells investigated in the present study, the ventral longitudinal body-wall muscles 6A and 7A, do not persist in the adult fly but are broken down during metamorphosis (Crossley, 1965, 1968). The changes in intracellular ionic activities occurring as the insect passes from larval to prepupal stages may therefore be interpreted as being due to the gradual deterioration of the cell prior to cell death.

(i) Cl^-, Na^+ and K^+

Cl^- was passively distributed across the cell membrane in both larvae and prepupae and since there was no consistent change in E_m during development, the average a^i_{Cl} would be expected to remain approximately constant at the level of 17 ± 1 mM found in larvae. It was not, however, possible to verify this, because an interferent present in prepupal muscle cells led to artificially elevated a^i_{Cl} values being recorded, giving an average apparent

a^i_{Cl} of 40 ± 2 mM. Thus, whilst in larvae, the average E_{Cl} was equal to the average E_m, at -53 ± 1 mV, in prepupae E_{Cl} (-31 ± 1 mV) was consistently more positive than E_m (-50 ± 1 mV), by an average of 19 mV.

Measurements of intracellular K^+ activities were made in both larvae and prepupae of *Calliphora* using two types of K^+-ISM's: one based on the Corning K^+-exchanger, LIX, (Code 477317) and the second on a valinomycin-based neutral ion carrier, NIC (Oehme & Simon, 1976). The results obtained have been presented in chapter III. The mean value of intracellular K^+ activity, a^i_K, in larvae measured with LIX-type ISM's was 129 ± 4 mM, and with NIC-type ISM's, 102 ± 2 mM. That in prepupae measured with LIX-type ISMs was 382 ± 12 mM, and with NIC-type ISM's, 115 ± 3 mM.

Intracellular Na^+ activity measurements were made in larvae and prepupae using neutral ion carrier based ISMs (ETH 227, Steiner *et al*, 1979). These results were presented in chapter III. The mean intracellular Na^+ activity, a^i_{Na}, value recorded in larvae was 11 ± 1 mM; in prepupae it was 7 ± 1 mM.

It was concluded from the a^i_K data that there is an increase both in a^i_K (from 102 to 115 mM) and in the concentration of an interferent to which the K^+ LIX responds, in *Calliphora* muscle cells during the 'development' from larva to prepupa. The former may reflect an increase in the activity of a Na^+/K^+ pumping mechanism.

This increase in a^i_K from 102 to 115 mM as the insect passes from larva to prepupa is consistent with data obtained concerning changes in nuclear K^+ activity and total nuclear K^+ content in salivary glands of *Chironomus tetans* (Wuhrmann *et al*, 1979). These two parameters were measured using valinomycin-based double-barrelled K^+ ISM's and flameless atomic absorption spectrometry, respectively. The K^+ activity increased by a factor of 2.6 (from 25 ± 10 to 64 ± 15 mM) and the total K^+, by a factor of 1.5 (from 12 ± 2 to 18 ± 3 mM) as oligopausing larvae developed into prepupae.

In addition to the 'developmental' increase in a^i_K from 102 to 115 mM, a corresponding decrease in a^i_{Na} was observed: from an average of 11 mM in larvae to 7 mM in prepupae (fig. 126a). This is consistent with the earlier suggestion that the developmental increase in a^i_K might be due to the

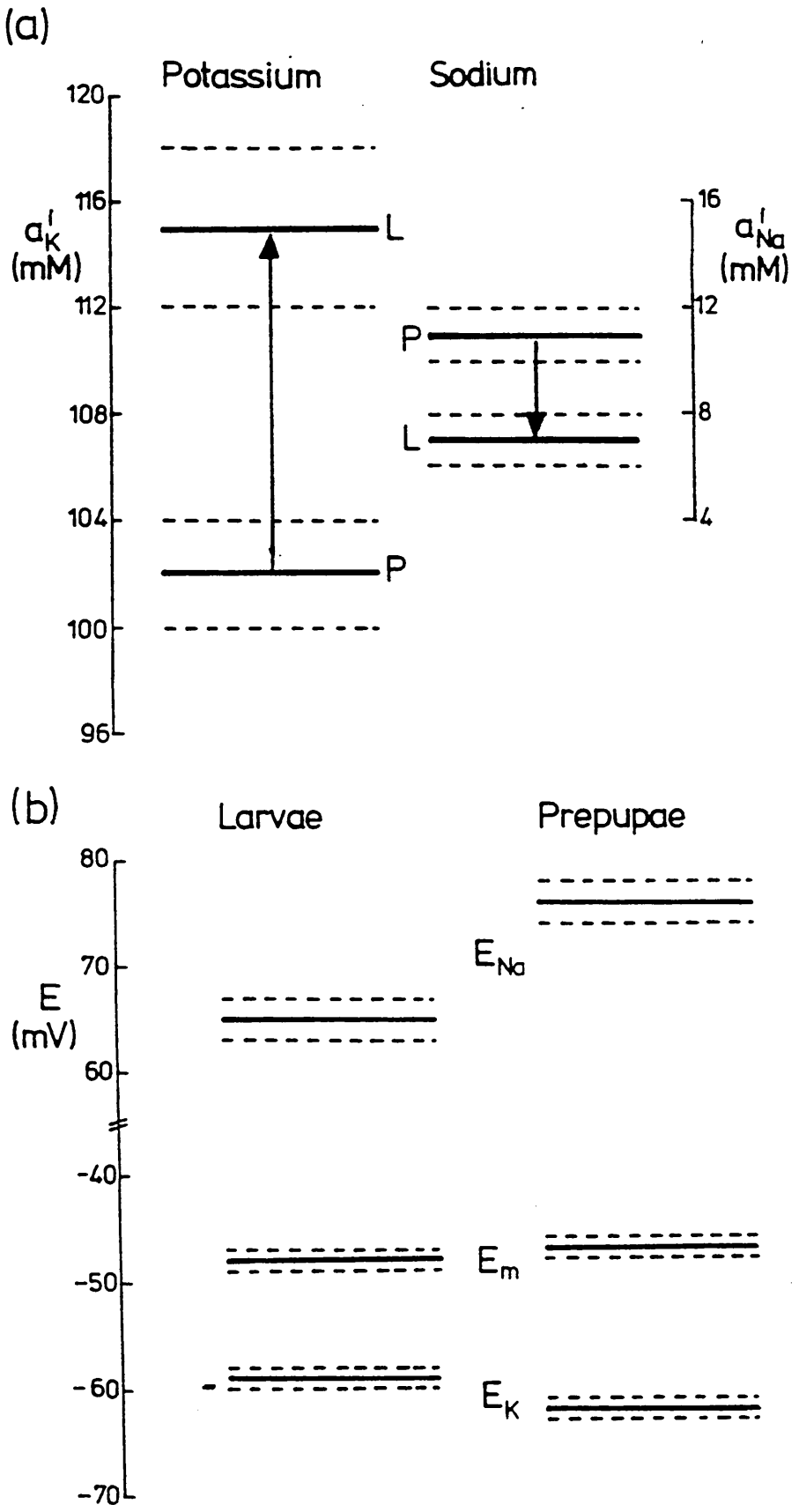


Fig. 126. Schematic diagrams showing a. the increase in a_K^i and reduction in a_{Na}^i which occurs as *Calliphora* develops from the larval (L) to the prepupal (P) stage, and (b) the relative positions of E_{Na}, E_m and E_K on a potential scale in larval and prepupal (Mean values are shown as solid lines, S.E's as dashed lines).

increased activity of a Na^+/K^+ exchange mechanism. Such a mechanism might be expected to have a coupling ratio of 3 Na^+: 2 K^+. The observed ratio was, however, close to 3 Na^+ : 1 K^+ (0.36 : 0.11). This may indicate that the acceptance of data from only a small number of cells which gave totally steady impalements has led to the developmental change in a^i_{Na} being overestimated.

Comparable developmental increases in a^i_K and decreases in a^i_{Na} have been reported in mouse skeletal muscle (Wood & Wareham, 1984) and chick ventricular muscle (Pozzard & Sheu, 1980). In mouse skeletal muscle, the E_m is low at birth, increasing from -50.4 ± 0.8 mV at 8 days to -71.2 ± 1.1 mV at 30 days (cf. *Calliphora*, where there is no consistent difference between E_m in larvae and prepupae). The a^i_K also increased rapidly with age, from 82.5 ± 1.4 mM at 8 days to 109.1 ± 4.2 mM at 18 days (measurements were made using NIC-based K^+ ISMs). The E_K calculated from this data was always greater than the recorded E_m. This discrepancy was greatest (26.9 ± 0.85 mV) at 8 days and least at 30 days (12.7 ± 0.65 mV). This contrasts with the situation in *Calliphora*, where the difference between E_m and E_K increases with development (fig. 126 b). It was concluded that in mouse skeletal muscle, rises in a^i_K in developing muscle fibres do not fully account for observed increases in E_m. An associated decrease in a^i_{Na} was thought likely to make a significant contribution: a^i_{Na} fell from 30 mM in 8 day-old mice to around 8 mM in adult fibres.

In chick ventricular muscle E_m hyperpolarised from -65.4 ± 1.1 at 4 days to -75.8 ± 0.6 at 18 days. An increase in a^i_K was also observed, from 71.3 ± 1.9 mM at 4 days to 89.9 ± 1.1 mM at 18 days. In agreement with the situation in mouse skeletal muscle the difference between E_m and E_K decreased with development. In addition, a^i_{Na} was found to decrease from 12.5 ± 0.4 mM in 4 day-old chicks to 7.0 ± 0.3 mM in 18 day-old individuals. It was concluded that in this preparation, the hyperpolarisation of E_m could be explained by a rise in a^i_K and fall in a^i_{Na}, as if the Na-K exchange pump became more active. (In fact, Klein, (1963) and Sperelakis (1972) found increases in the specific activity of isolated membrane Na-K ATPase with development of the chick heart, which tends to confirm the latter suggestion).

Thus, in these two preparations, developmental increases in a^i_K and decreases in a^i_{Na} similar to those in *Calliphora* have been found. In both

chick ventricular muscle and mouse skeletal muscle, however, E_m hyperpolarises and thus the difference between E_m and E_K decreases, with development. This contrasts with the situation in *Calliphora*, where there is no consistent difference between the average E_m's recorded in larvae and prepupae, and as a result the E_m/E_K difference increases with development. The fact that the E_m remains constant during development is consistent with the contribution of Na^+ to E_m being larger in *Calliphora* than in chick or mouse muscle. (The latter are both vertebrates and might therefore be expected to have α values similar to the value of 0.01 found in frog muscle (Hodgkin & Horowicz, 1959) cf. the α of 0.036 calculated for *Calliphora*). Thus, in *Calliphora*, the increasing contribution of K^+ to E_m during development would balance the decreasing contribution of Na^+, with the result that E_m remained approximately constant. In contrast, in chick and mouse muscle, the increase in a_K^i during development would tend to hyperpolarise E_m, whilst the reduction in a_{Na}^i would have relatively little effect, explaining the observed hyperpolarisation in E_m.

ii. Interferents

The activities of at least two interferents increase as *Calliphora* develops from larva to prepupa. One is anionic, interfering with the Cl^--exchanger, and the second, cationic, interfering with the K^+-exchanger. The former is apparently absent in larvae, or present at low enough activities to have little effect on a_{Cl}^i measurements, but occurs in significant quantities in prepupal cells and accounts for the difference between the expected a_{Cl}^i of around 17 mM and the observed value of 40 mM. Its identity is not known. The latter is present in the muscle cells of both larvae and prepupae, but is more abundant in prepupae. It accounts for the discrepancy between the mean a_K^i values recorded in the two preparations using LIX-and NIC-type K^+ISM's: in larvae the a_K^i obtained with LIX-type ISM's was some 27 mM higher than that recorded with NIC-type ISM's; in prepupae the a_K^i measured with LIX-type ISM's was around 267 mM higher than that obtained with NIC-type ISM's. The nature of this interferent is not clear, but it is known that the LIX is highly sensitive to the presence of certain organic compounds such as quaternary amines, responding around three hundred times more strongly to these than to K^+ (fig. 4). Thus, the presence of an extremely small amount of such a compound in a cell would explain the high values of apparent K^+ activity recorded from prepupal cells in particular (Oehme & Simon, 1976). Compounds such as polyamines are well known to accumulate in dying tissues

(Carnicero *et al*, 1982) and would be likely to interfere with the K^+ LIX. Alternative candidates for the interferent are carnitine, an imine, which tends to be abundant in active tissues, and choline, which may occur in the free state in cells eg. as phosphatidyl choline (Bridges, 1972 ; Morley & Schachter, 1961.)

VII.5. Mechanisms of resting membrane electrogenesis in body-wall muscle cells of *Chilo* larvae

Larvae of *Chilo*, the rice stem borer, are phytophagous, and as a result, their haemolymph contains low levels of Na^+, and high levels of K^+, Mg^{2+} and Ca^{2+}. The main reason for studying *Chilo* was for comparison with data from *Calliphora* larvae, which are carrion feeders whose haemolymph contains low K^+, Mg^{2+} and Ca^{2+}, and high Na^+ levels. Such differences in haemolymph composition might be expected to be reflected in differences in the muscle electrochemistries of the two species of insect. Thus, the roles of K^+, Na^+ and Cl^- in resting membrane electrogenesis were investigated by measuring their intracellular activities and performing substitution experiments, and the role of Mg^{2+} was investigated by substitution experiments alone.

VII.5.i. The role of K^+

Intracellular K^+ activities were measured in *Chilo* larvae using both LIX- and, for the first time in Lepidoptera, NIC-type K^+ ISMs. The two types of K^+ ISM gave average a_K^i values of 65 ± 1 and 62 ± 1 mM, respectively (section V.1). These values were significantly different ($p < 0.05$, Student's t-test) suggesting that *Chilo* muscle cells contain a small amount of interferent to which the LIX responds, giving somewhat elevated values for apparent a_K^i. The E_K values calculated from this a_K^i data were consistently more positive than E_m, by an average of 19 mV for both LIX- and NIC-type ISM data. (E_K had an average value of -27 ± 1 and -26 ± 1 mV, and E_m, an average value of -46 ± 1 and -45 ± 1 mV as measured using LIX- and NIC-type ISM's respectively).

These results are broadly in agreement with other data available for skeletal muscle in the Lepidoptera (Table 37), eg. in *Sphinx ligustri* the $[K^+]_i$, as measured by flame photometry, was 84.4 ± 7 mM which corresponded to an average E_K of -13.3 mV, 29 mV more positive than the measured E_m of -44.5 ± 2.2 mV (Huddart, 1966a) $[K^+]_i$ measured in the same preparation

Species	$[K^+]_i$ (mM)	$[K^+]_o$ (mM)	E_K (mV)	E_m (mV)	Method	Reference
Sphinx ligustri	84.4 ± 7.0	49.8 ± 1.3	-13.3	-44.5 ± 2.2	FP	Huddart (1966a)
" "	110.3 ± 2.5	22.7 ± 1.4	-39.8	-59.8 ± 0.9	AAS	Wareham *et al* (1975)
Antherea polyphemus	78.9 ± 5.1	41.0 ± 1.7	-16.5	-48.2 ± 1.4	FP	Huddart (1966a)
" "	152.5	50	-28.4	-49.6	LIX	Rheuben (1972)
Bombyx mori	97.7 ± 8.7	41.3 ± 1.2	-21.7	-48.1 ± 1.4	FP	Huddart (1966a)
Actias selene	115.6 ± 5.2	47.2 ± 1.5	-22.6	-46.4 ± 1.3	FP	Huddart (1966a)
Chilo partellus	90.3 ± 1	30	-27	-46.0 ± 1.0	LIX	Present study
	86.1 ± 1	30	-26	-45.0 ± 1.0	NIC	" "

FP - Flame photometry

AAS - atomic absorption spectrophotometry

LIX - LIX-type K^+ ISM

NIC - NIC-type K^+ ISM

Table 37. A comparison between $[K^+]_i$ data available for five species of Lepidoptera

using an atomic spectrophotometer gave a value of 110 mM, and an E_K of -40 mV, 20 mV more positive than E_m, (Wareham *et al*, 1975). The difference between the $[K^+]_i$ values measured using the two techniques (84.4 mM by flame photometry; 110 mM by atomic spectrophotometry) may reflect either real differences betwen the two cultures of *Sphinx* used in the two different laboratories, or the presence of an interferent in the muscle cells, to which the atomic spectrophotometer responds more than the flame photometer. Similarly the difference between the E_m values recorded by the two authors (an average of -44.5 mV by Huddart (1966a) cf. an average of -60 mV by Wareham *et al* (1974)) might be attributable to real differences between the two *Sphinx* cultures, but is more likely to reflect that the preparations used by Wareham *et al* were healthier or that the cells were damaged less during microelectrode impalements than those used by Huddart.

In *Actias selene*, the $[K^+]_i$ value of 115.6 ± 5.2 mM measured by flame photometry was of the same order of magnitude as those obtained in *Sphinx*. This corresponded to an E_K of -21 mV, which was 25.4 mV more positive than the average E_m of -46.4 ± 1.3 mV (Huddart, 1966 a,b). In *Antherea polyphemus*, a_K^i has been measured using both flame photometry (Huddart, 1966 b) and LIX-type K^+ ISMs (Rheuben, 1972). The former technique gave an average a_K^i of 78.9 mM, the latter, an a_K^i of 109.8 mM. Both these values corresponded to E_K values more positive than E_m: for the flame photometry data by 32 mV, and for the ISM data by 21.2 mV (table 37).

Thus, the values for $[K^+]_i$ measured in three species of Lepidoptera, *Sphinx*, *Actias* and *Antherea*, using flame photometry were 84.4, 115.6 and 78.9 mM, respectively (table 37). These values were comparable with the $[K^+]_i$ values measured in *Chilo* using LIX- and NIC-type K^+ ISM's : 90.3 and 86.1 mM respectively (calculated from the a_K^i data by dividing a_K^i by the activity coefficient, γ, of 0.72). The fact that the results obtained by flame photometry were comparable to those measured with ISM's suggest that K^+ is not significantly bound in Lepidoptera muscle cells. This would need to be confirmed, however, by measurements of a_K^i in *Sphinx*, *Actias* and *Antherea* using NIC-type K^+-ISM's. A comparison between the $[K^+]_i$ values measured in *Antherea* using flame photometry and LIX-type K^+ ISM's (78.9 and 152.5 mM respectively) suggests that *Antherea* muscle cells contain an interferent to which the K^+-exchanger responded. The true $[K^+]_i$ would be expected to be somewhat <u>smaller</u> than the value estimated by flame photometry, since the latter technique is known to suffer from interference by

cations other than K^+, and to measure bound as well as 'active' ions. The fact that the apparent $[K^+]_i$ measured by Rheuben (1972) was some 30 mM higher than that estimated by Huddart (1966) is thus most likely to have been due to interference. Candidates for this interferent include quaternary ammonium ions eg. acetyl choline or carnitine, to which the LIX is known to be very responsive (Oehme & Simon, 1976). In *Chilo* the presence of a small amount of such an interferent resulted in the average a_K^i recorded by LIX-type K^+ ISM's being some 3 mM higher than that recorded with NIC-type ISM's.

The K^+ substitution experiments carried out on *Chilo* to obtain a quantitative assessment of the role of K^+ in generating E_m showed that E_m hyperpolarised from its normal resting level in a_K^o's lower than that in Normal Ringer, and depolarised when a_K^o was increased above that in Normal Ringer (section VI.1). The relationship between E_m and the logarithm of a_K^o was not, however, linear, but followed a smooth curve with a maximum slope of 30 mV per tenfold change in a_K^o (in the a_K^o range 21.6 to 30.2 mM). This is also in agreement with published data on Lepidoptera: in all species studied, the relationship between E_m and the logarithm of a_K^o was curved and not linear eg. in *Bombyx mori* (fig. 15 A), *Sphinx ligustri* (fig. 15 B), *Actias selene* (fig. 15 V) (Huddart, 1966a), *Philosamia cynthia* (fig. 17) (Piek, 1975). Piek (1975) noted that this relationship showed a marked deviation at $[K^+]_o$'s close to that found in the Normal Ringer for the insect, but did not satisfactorily explain this trend.

Thus, the relationship between E_m and the logarithm of a_K^o in *Chilo* was not linear. A possible explanation for this would have been a change in the relative permeability of the cell membrane to K^+ and Na^+ when exposed to altered levels of extracellular Na^+, comparable to that observed in *Calliphora* (section IV.4.iii). If such a change occured, it might be reflected as a change in membrane resistance. In conjunction with the full K^+ substitution experiments, a series of 3-step K^+ substitution experiments was therefore performed in which membrane resistance was monitored (section VI.2). These experiments showed that, when exposed to low K^+/high Na^+ saline, the membrane resistance decreased by an average of 37% from its resting level of 4417 ± 310 kΩ; in high K^+/low Na^+ saline, membrane resistance increased by an average of 41% from its resting level in Normal saline. Thus, it is likely that the p_{Na}/p_K ratio for the cell membrane changed when a_{Na}^o and a_K^o were varied, accounting for the non-linearity of

the relationship between E_m and the logarithm of a^o_K.

VII.5.ii. The role of Na^+

The fact that E_K was consistently more positive than E_m in *Chilo* suggested that the muscle cell membrane was permeable to at least one ion other than K^+ with its equilibrium potential more negative than E_m. Huddart (1966) stated that in *Sphinx*, E_{Na} (as calculated from $[Na^+]$ data measured using flame photometry) was as negative as E_m, both parameters having values close to -44 mV. In order to investigate whether E_{Na} might also be as negative or more negative than E_m in *Chilo*, measurements of intracellular Na^+ activity, a^i_{Na}, were made in this insect using NIC-based Na^+ ISM's (section V.2).

The average a^i_{Na} recorded was 12 ± 2 mM, which is greater than the a^o_{Na} (8.6 mM) in the Normal saline for the insect. This corresponded to an average E_{Na} of -6 ± 4 mV, which was more positive than E_m by an average of 41 mV. The difference between this and the situation in *Sphinx* may be a genuine species difference, or may reflect the fact that flame photometry measures bound Na^+ as well as 'active' ions, and therefore gave high $[Na^+]_i$ values and correspondingly negative E_{Na} values. The range of E_{Na} values obtained in *Chilo* was surprisingly wide, including both negative and positive values (-30.5 to + 15.9 mV). E_{Na} was, however, more positive than E_m in all cells studied, indicating that whilst Na^+ might be involved in generating E_m, it is not the ion mentioned above with its equilibrium potential more negative then E_m.

Thus, the average a^i_{Na} recorded in *Chilo* was 12 mM, which corresponds to a concentration of 16.7 mM. This figure is of the same order of magnitude as $[Na^+]_i$ values recorded in other species of Lepidoptera using flame photometry (table 38): 20.7 ± 1.6 mM (*Sphinx ligustri*), 5.0 ± 0.7 mM (*Antherea polyphemus*), 12.4 ± 1.2 mM (*Bombyx mori*) and 16.0 ± 2.2 mM (*Actias selene*) (Huddart, 1966a). The fact that similar values for $[Na^+]_i$ were obtained using both flame photometry and Na^+-ISMs suggests that in the Lepidoptera, intracelluar Na^+ is not significantly bound. The relatively small discrepancies between the values are likely to be attributable to species differences. The E_{Na} values obtained for *Chilo* had an average of -6 ± 4 mV, somewhat less negative than the E_{Na}'s obtained for the above four species: -44 mV (*Sphinx*), -10.5 mV (*Antherea*), -14.2 mV (*Actias*) and -8

Species	$[Na^+]_i$ (mM)	$[Na^+]_o$ (mM)	E_{Na} (mV)	E_m (mV)	Method	Reference
Sphinx ligustri	20.7 ± 1.6	3.6 ± 0.3	-44.0	-44.5 ± 2.2	FP	Huddart (1966a)
Antherea polyphemus	5.0 ± 0.7	3.3 ± 0.3	-10.5	-48.2 ± 1.4	FP	" "
Bombyx mori	12.4 ± 1.2	9.0 ± 0.5	-8.0	-48.1 ± 1.4	FP	" "
Actias selene	16.0 ± 2.2	9.1 ± 0.5	-14.2	-46.4 ± 1.3	FP	" "
Chilo partellus	16.7 ± 1	12	-6 ± 4	-47.0 ± 2.0	NIC	Present study

FP - Flame photometry

NIC - NIC-type Na^+ ISM

Table 38. A comparison between $[Na^+]_i$ data available for five species of Lepidoptera

mV (*Bombyx*). In all species, however, E_{Na} was more positive than E_m.

In all Lepidoptera studied, the $[Na^+]_i$ was greater than $[Na^+]_o$. In *Chilo* the ratio of $[Na^+]o$ to $[Na^+]_i$ was 0.72; in *Sphinx*, its value was 0.174; in *Antherea*, 0.66; in *Actias*, 0.726 and *Bombyx*, 0.568. This property appears to be unique to Lepidoptera, and is almost certainly a reflection of the unusual composition of the haemolymph.

The Na^+ substitution experiments carried out on *Chilo* to determine quantitatively the extent of the involvement of Na^+ in generating E_m, showed that E_m hyperpolarised from its resting level when a^o_{Na} was reduced, and depolarised when a^o_{Na} was increased (section VI.3). The sizes of these responses were, however, extremely small (some 2 mV per tenfold change in a^o_{Na}, fig. 115), indicating that the cell membrane has a small but significant permeability to Na^+, with around 3% of E_m being generated by Na^+.

This result is consistent with data for *Antherea* (Rheuben, 1972), where a tenfold increase in $[Na^+]_o$ caused a depolarisation of 4.6 mV in E_m, from which it was concluded that the resting muscle membrane was slightly permeable to Na^+.

VII.5.iii. The role of Cl^-

Measurements of intracellular K^+ and Na^+ activities (sections V.2 and V.3 respectively) showed that both E_K and E_{Na} were consistently more positive than E_m. This implied that the cell membrane must be permeable to at least one ion in addition to K^+ and Na^+ with its equilibrium potential more negative than E_m. In order to investigate whether Cl^- might be this ion, intracellular Cl^- activities, a^i_{Cl}'s, were measured using LIX-based ISMs with RLIE-filled reference barrels.

An average a^i_{Cl} value of 8 ± 0.2 mM was obtained, which corresponded to a $[Cl^-]_i$ of 11.1 mM and to an average E_{Cl} value of -54 ± 1 mV. The latter was consistently more negative than E_m, by an average of 8 ± 0.4 mV, suggesting that Cl^- is not passively distributed in this insect .

The fact that E_{Cl} is more negative than E_m in *Chilo* contrasts with data available for the Lepidoptera, in which $[Cl^-]$ was estimated by back titration (Huddart, 1966a). $[Cl^-]$'s were measured using this technique in *Sphinx*,

Antherea, *Actias* and *Bombyx* (Table 39).

Table 39. $[Cl^-]$ data from five Lepidoptera species (Data from Huddart, 1966a, and the present study).

Species	$[Cl^-]_i$ (mM)	$[Cl^-]_o$ (mM)	E_{Cl} (mV)	E_m (mV)
Sphinx ligustri	14.5 ± 1.9	61.3 ± 2.8	-36.3	-44.5 ± 2.2
Antherea polyphemus	15.0 ± 1.4	67.5 ± 3.0	-37.9	-48.2 ± 1.4
Actias selene	14.0 ± 1.4	75.0 ± 3.3	-42.5	-46.4 ± 1.3
Bombyx mori	13.3 ± 1.3	68.2 ± 3.2	-41.2	-48.1 ± 1.4
Chilo partellus	11.1 ± 0.2	67.7	-54 ± 1	-46.0 ± 1.4

Thus, E_{Cl} was more positive than E_m in all four species, by 8.2, 10.3, 3.9 and 6.9 mV in *Sphinx*, *Antherea*, *Actias* and *Bombyx* respectively. The fact that E_{Cl} was more negative than E_m in *Chilo*, but more positive than E_m in the other four species of Lepidoptera might reflect true species differences. It is more likely, however, that a proportion of the intracellular Cl^- was bound in all species. The titration method of estimating $[Cl^-]_i$ would measure both bound and 'active' Cl^-, giving unrealistically high values of E_{Cl}. This would also explain the fact that the $[Cl^-]_i$ values measured in *Sphinx*, *Antherea*, *Bombyx* and *Actias* using this technique were all higher than that measured in *Chilo* using Cl^- ISM's.

In order to determine whether Cl^- was actively involved in resting membrane electrogenesis in *Chilo*, a series of Cl^- substitution experiments was carried out (section VI.5). Changes in a_{Cl}^{δ} were found to lead to sustained changes in E_m, confirming that Cl^- was indeed involved in the maintenance of E_m. The relationship between E_m and the logarithm of a_{Cl}^{δ} was a somewhat curved line, with a maximum slope of 17 mV at high levels of a_{Cl}^{δ} (fig. 118). This result is in agreement with the situation in *Sphinx*, where a tenfold change in a_{Cl}^{δ} gave rise to a sustained change of around 8 mV in E_m (Huddart, 1967). Similar results were obtained in the same insect by Wareham *et al*, who reported that removal of all extracellular Cl^- caused a depolarisation of around 19 mV in E_m. Since addition of ouabain also led to a 19 mV depolarisation after the apparently arbitrary time interval of 150 minutes, the Cl^--induced depolarisation was proposed to be an effect on the active component of the E_m. There appears to be little logical basis for this

proposition except that both experiments gave exactly 19 mV depolarisation, and it seems more likely that the contributions of Cl^- and a metabolic mechanism are unrelated.

In *Antherea*, alterations in a_{Cl} caused only transient changes in E_m (Rheuben, 1972). In Rheuben's study, methane-sulphonate was used to substitute for Cl^-. No mention was made of any tests to determine whether it was a truly impermeant anion, and no raw data is shown.

In conclusion, in *Chilo*, Cl^- is actively involved in resting membrane electrogenesis, contributing some 29% (17 mV out of a possible 58 mV) to E_m.

VII.5.iv. The role of a metabolic mechanism in generating E_m

It was found that in *Chilo*, the contributions of K^+ (a maximum of 30 mV/tenfold change), Na^+ (2 mV/tenfold change) and Cl^- (a maximum of 17 mV/tenfold change) accounted for a total change in E_m of 49 mV out of a possible 58 mV ie: 84% of the expected change of 58 mV if all the factors affecting E_m had been identified and their contributions evaluated. A further mechanism which might have been involved in resting membrane electrogenesis was an electrogenic metabolic pump. In order to determine whether such a mechanism occurred in *Chilo*, two types of experiment were carried out: firstly, the preparation was cooled (section VI.6.i) and secondly, the Na^+-K^+ pump inhibitor ouabain was applied (section VI.6.ii) and the effect on E_m monitored.

The cooling experiments constituted an unspecific investigation of the presence of an active mechanism by generally slowing down the chemical reactions involved in metabolism. A depolarisation of 12 ± 2 mV was observed when the preparation was cooled by 14°C, representing a change of 26 ± 3% of the initial resting E_m. If all or part of E_m consisted of a diffusion potential, the amount by which a change in temperature would affect E_m would be predicted by the 'T' term in the Nernst equation. This would however, be a relatively small effect: some 1.4 mV depolarisation for a 14°C decrease in temperature (appendix 16). Thus, the average depolarisation of 12 mV which occurred when the preparation was cooled by 14°C could not be attributed solely to the effect of temperature on the equilibrium potential for each ion. It was therefore concluded that, at rest,

a hyperpolarising pump is active in the cell membrane. The exact size of the contribution of this pump to E_m cannot be assessed accurately from this experiment, however, since there is no evidence that further cooling of the preparation would not lead to further depolarisation of E_m. It can only be stated that a pump contributed a minimum of 11 mV to E_m at rest. This result is consistent with the situation in *Antherea* muscles, where a 9°C decrease in temperature depolarised E_m by 6 mV (Rheuben, 1972). In *Antherea*, a 10°C reduction in temperature also gave rise to an average increase in effective membrane resistance of 71 ± 45%, which was explained as follows. The small potential change, together with the large increase in resistance were taken to suggest that two processes with nearly equal but opposing potential effects were responding to temperature simultaneously. If cooling decreased the amount of current generated by an active transport system, a smaller potential would be produced; however, since the resistance increased simultaneously, the smaller amount of current would be able to produce almost as large a voltage drop as before, hence the small change in E_m with temperature. The increase in resistance may be attributable to a reduction in the coupling coefficient between electrically coupled cells, such as that observed in the crayfish lateral giant axon when temperature is reduced (Payton *et al*, 1969).

A more specific investigation of the nature of the hyperpolarising pump apparently present in *Chilo* was attempted by the application of ouabain to muscle cells. Ouabain is a cardiac glycoside which inhibits the membrane-bound Na^+-K^+ ATPase. 1 mM ouabain, however, had no effect on E_m. This is in accordance with results obtained in *Antherea* muscles, where ouabain produced no change in E_m (Rheuben, 1972). A similar situation has been reported in a variety of insect tissues, particularly epithelial tissues, reviewed by Anstee and Bowler (1979). The lack of effect of ouabain on some insect muscle may perhaps reflect that the Na^+-K^+ pump plays little part in generating E_m, or that the Na^+-K^+ ATPase is inaccessible to topically applied ouabain. The high concentration of ouabain used in this study (1 mM) was however, intended to maximise the effect of the chemical on the cell. In contrast with the situation in *Chilo*, however, in *Sphinx*, Wareham *et al* (1975) reported that application of 0.5 mM ouabain gave a depolarisation in E_m of some 19 mV, illustrating that an active contribution to E_m was made by the Na^+-K^+ pump in this insect.

The majority of metabolic inhibition studies on other insect preparations

involved the use of unspecific inhibitors such as DNP (eg. Huddart & Wood, 1966) or sodium cyanide (eg. Wareham *et al*, 1974). Results from such experiments should be interpreted with extreme caution, because these chemicals simply kill any preparation to which they are applied, by completely preventing cellular metabolism. The fact that E_m depolarises when DNP is applied therefore provides little information about the mechanisms of resting membrane electrogenesis.

Thus, in *Chilo* an active, ouabain-insensitive mechanism contributes some 24% (11 mV out of a total of 45 mV) of the resting E_m. This situation is similar to that in *Antherea* (Rheuben, 1972), but contrasts with data available for *Sphinx*, where the active mechanism is ouabain-sensitive (Wareham *et al*, 1974).

VII.5.v. Other mechanisms

In *Chilo*, it has been possible to account for the resting E_m in terms of the contributions of K^+, Na^+, Cl^- and an electrogenic pump, with an error of only 10%. However, this does not exclude the possibility that additional mechanisms make some contribution to E_m. Such mechanisms include pH and Ca^{2+}, and these were not investigated. In *Antherea*, an increase in pH from 7 to 8 gave rise to a hyperpolarisation of E_m by some 30 mV (Rheuben, 1972). Such experiments provide only limited information, however, since pH may affect E_m indirectly via its action on a wide range of cellular processes eg. conductances, enzymic reactions. *Antherea* muscle fibres were found not to be appreciably permeable to Ca^{2+}, and it is therefore likely that this ion would not contribute significantly to E_m in *Chilo*. Rheuben (1972) also investigated the role of NH_4^+ in generating E_m in *Antherea*, but concluded that it was not involved. This was somewhat surprising since pH had a marked effect on E_m, and changing $[NH_4^+]_o$ would also alter pH_i.

VII.6. A comparison between the muscle electrochemistries of *Calliphora* and *Chilo*

i. Haemolymph ion levels

As previously stated, these two insects were selected for this comparative study because of their different feeding habits and correspondingly different haemolymph ion contents. *Calliphora* larvae are carrion feeders cultured on

rotting liver (although it should be noted that neither final instar, (wandering stage) nor prepupae, feed and as such, have haemolymph which contains a high level of Na^+ and low levels of K^+, Mg^{2+} and Ca^{2+}. In contrast, *Chilo* larvae are phytophagous, feeding on rice plants in the wild and cultured on an artificial medium. As a result, their haemolymph contains a low level of K^+ and high levels of Na^+, Mg^{2+} and Ca^{2+}. (Florkin & Jeuniaux, 1974).

The muscle electrochemistries of the two species are compared in the following section, which highlights differences in the contributions of the major inorganic ions K^+, Na^+ and Cl^- to resting membrane electrogenesis. These are almost certainly related to the differences in haemolymph ion levels in the two species.

ii. Membrane potentials

The levels of membrane potential recorded in the two species were comparable and are summarised in table 40, below.

Table 40. Summary of E_m data for *Calliphora* and *Chilo*

	Mean E_m (mV)	Range of values (mV)
Calliphora larvae	-48 ± 1	-33 to -63
Calliphora prepupae	-47 ± 1	-35 to -62
Chilo larvae	-45 ± 1	-35 to -59

Thus, whilst various ionic and metabolic mechanisms may contribute to E_m to different extents in the two species, the overall potential generated across the cell membrane is similar in each preparation.

iii. The role of K^+

The involvement of K^+ in resting membrane electrogenesis is clearly different in *Calliphora* and *Chilo*. The intracellular K^+ data obtained from each of the three preparations using NIC-type K^+ ISM's are summarised in table 41, below.

Table 41 Intracellular K^+ data measured using NIC-type K^+ ISM's in *Calliphora* and *Chilo*. (Data from a minimum of 77 cells from 8 preparations, given as mean ± SE.)

	Calliphora larvae	*Calliphora* prepupae	*Chilo* larvae
a_K^i (mM) :	102 ± 2	115 ± 3	62 ± 1
E_K (mV) :	-59 ± 1	-62 ± 1	-26 ± 1
E_m (mV) :	-47 ± 1	-47 ± 1	-45 ± 1
E_K-E_m (mV):	-11 ± 1	-15 ± 1	+19 ± 1

Thus, in *Calliphora* and *Chilo* the average E_m's are very similar. In *Calliphora*, E_K was consistently more negative than E_m, whilst in *Chilo*, E_K was consistently more positive than E_m, indicating that in neither insect is K^+ the only ion involved in generating E_m. Since the E_m's in the two species are so similar, the fact that in one species, E_K is more negative than E_m, whilst in the other it is more positive, reflects differences in the ratio of a_K^o to a_K^i. In *Calliphora* larvae, this ratio has a value of 0.1 (calculated using the a_K in Normal saline, 9.7 mM); in prepupae, its value is 0.08; in *Chilo*, the ratio is 0.35 (calculated using the a_K in Normal Saline, 21.6 mM). Thus in both *Calliphora* preparations, there is around 10 times as much K^+ inside the cell as outside; in *Chilo*, there is only around 3 times as much K^+ inside the cell as outside.

K^+ substitution experiments to assess quantitatively the contribution of K^+ to E_m showed that the relationship between E_m and the logarithm of a_K^o in *Calliphora* prepupae was linear, with a slope of 32 mV per tenfold change in a_K^o; in *Chilo* larvae, the relationship followed a smooth curve, with a maximum slope of 30 mV per tenfold change in a_K^o. These slopes are both significantly shallower than the 58 mV/tenfold change in a_K^o predicted by the Nernst equation for a membrane permeable only to K^+. This confirmed the conclusion from the fact that E_K was not equal to E_m in either insect, that K^+ was not the only ion involved in resting mebrane electrogenesis.

The fact that a_K^i measurements made in the two species with LIX-type ISMs were repeated with NIC-type ISM's revealed the presence of one or more interferents to which the LIX responded, in both species. This is illustrated by data from larvae of the two species, listed in table 42, below.

Table 42 Intracellular K^+ data from *Calliphora* and *Chilo* measured using LIX- and NIC-type ISMs (Data from an minimum of 77 cells, 7 preparations, given as mean ± SE.)

	Calliphora larvae		*Chilo* larvae	
	LIX	NIC	LIX	NIC
a_K^i (mM) :	129 ± 4	102 ± 2	65 ± 1	62 ± 1
E_K (mV) :	-64 ± 1	-59 ± 1	-27 ± 1	-26 ± 1
E_m (mV) :	-46 ± 1	-47 ± 1	-46 ± 1	-45 ± 1
E_K-E_m (mV)	-18 ± 1	-11 ± 1	+19 ± 1	+19 ± 1

Thus the average a_K^i value recorded by LIX-type K^+ ISMs was 27 mM higher than that measured by NIC-type ISMs in *Calliphora* larvae, and 3 mM higher than that measured by NIC-type ISMs in *Chilo* larvae. Thus, both species contain one or more interferents to which the Corning K^+ exchanger (code 477317) responded, giving elevated values of apparent intracellular K^+ activity. The nature of these interferents is uncertain, but it is known that the LIX is particularly responsive to quaternary ammonium ions eg. acetyl choline, carnitine, which may be present intracellularly.

iv. The role of Na^+

The intracellular Na^+ data measured in *Calliphora* and *Chilo* is summarised in table 43, below.

Table 43. Summary of intracellular Na^+ activity data in *Calliphora* and *Chilo*. (Data from a minimum of 13 cells, 6 preparations, given as mean ± SE.)

	Calliphora larvae	*Calliphora* prepupae	*Chilo* larvae
a_{Na}^i(mM) :	11 ± 1	7 ± 1	12 ± 2
E_{Na} (mV) :	65 ± 2	76 ± 2	-6 ± 4
E_m (mV) :	-48 ± 1	-46 ± 1	-47 ± 2
E_K-E_m (mV):	113	124	41

Thus, whilst the a_{Na}^i values measured in the three preparations were similar in magnitude, the corresponding E_{Na} values were markedly different, because

of the ionic differences in the haemolymph. In *Calliphora*, E_{Na} values were consistently positive, (in the range 41.5 to 83.6 mV), which contrasted with the situation in *Chilo*, where both positive and negative E_{Na}'s were recorded (range -30.5 to +15.9 mV). In both species, however, E_{Na} was consistently more positive than E_m, suggesting that Na^+ was not passively distributed but might be involved in generating E_m.

This suggestion was confirmed by Na^+ substitution experiments on *Calliphora* prepupae and *Chilo* larvae. In *Calliphora*, the p_{Na}/p_K ratio for the cell membrane had a value of 0.036. Altering the extracellular Na^+ activity, a^o_{Na}, was, however, found to have unexpected secondary effects on E_m. A hundredfold reduction in a^o_{Na} resulted in a transient hyperpolarisation of 2 to 7 mV, followed by a sustained depolarisation to levels 2 to 8 mV more positive than the original resting E_m. The hyperpolarisation was consistent with Na^+ being involved in generating E_m: it was concluded that the depolarisation might result from the reduction in p_K which occurred when the cell was exposed to low a^o_{Na}. In *Chilo*, the muscle membrane also had a small but significant permeability to Na^+, with E_m changing in a sustained, reversible manner by some 2 mV (3.5%) per tenfold change in a^o_{Na}.

V. The role of Cl^-

Intracellular Cl^- activity data from *Calliphora* and *Chilo* measured using LIX-type ISMs with RLIE-filled reference barrels is summarised in table 44, below

Table 44. Summary of intracellular Cl^- activity data for *Calliphora* and *Chilo* (Data from a minimum of 35 cells, 5 preparations, given as mean ± SE.)

	Calliphora larvae	*Calliphora* prepupae	*Chilo* larvae
a^i_{Cl} (mM) :	17 ± 1	40 ± 2	8 ± 1
E_{Cl} (mV) :	-53 ± 1	-31 ± 1	-54 ± 1
E_m (mV) :	-53 ± 1	-50 ± 1	-46 ± 1
E_K-E_m (mV):	0 ± 0.3	+19 ± 1	-8 ± 1

Thus, in *Calliphora* larvae, E_{Cl} was on average equal to E_m, indicating that

Cl^- was passively distributed. This was confirmed by a series of Cl^- substitution experiments, in which varying a^o_{Cl} was found to cause only transient changes in E_m.

In *Calliphora* prepupae, the apparent a^i_{Cl} was some 23 mM higher on average than that of larvae, giving a correspondingly more positive E_{Cl}. This was found to be due to the presence of an anionic interferent to which the Cl^--exchanger responded, since Cl^- substitution experiments showed that Cl^- was passively distributed, as in larvae.

In *Chilo*, however, E_{Cl} was consistently more negative than E_m, a result which was not explicable in terms of interference, suggesting that Cl^- was not passively distributed in this insect. Cl^- substitution experiments confirmed that Cl^- was indeed involved in resting membrane electrogenesis, since E_m changed by up to 17 mV (29.3%) per tenfold change in a^o_{Cl}.

Thus, probably the most significant difference between the muscle electrochemistries of *Calliphora* and *Chilo* was that in *Calliphora*, Cl^- was passively distributed across the cell membrane, whereas in *Chilo*, Cl^- was actively involved in generating E_m.

vi. Membrane resistances

The resting membrane resistance R_m, of *Calliphora* prepupal muscle was on average 46 times smaller than that of *Chilo* larvae: 96 ± 9 KΩ as opposed to 4417 ± 310 KΩ in *Chilo*. The fact that R_m is so much higher in *Chilo* than in *Calliphora* may reflect either (a) that the true R_m's of the two species are similar, but the input resistance in *Chilo* cells is higher because the cells are electrically coupled to a lesser extent than those of *Calliphora*; or (b) that muscle cells in *Chilo* and *Calliphora* are coupled to a similar extent, and R_m in *Chilo* has a truly high value which allows a large E_m to be generated from a given pump current. Coupling coefficients between insect muscle cells range from less than 0.1 in *Drosophila* larvae (Diptera) (Jan & Jan, 1976), to 0.21 in pharate adult *Manduca* (Lepidoptera) (Schwartz, 1981) and 0.37 in *Calliphora* larvae (Hardie, 1978). Thus, there is no evidence for coupling coefficients being lower in Lepidoptera than in Diptera, as suggested in (a) above. It is therefore most likely that possibility (b) is correct: that *Chilo* and *Calliphora* muscles are coupled to similar degrees, with R_m in *Chilo* having a truly high value.

Parallel experiments were carried out on the two species in which the membrane resistance, R_m, was monitored during an experiment in which low Na^+/high K^+ Ringer was substituted in for Normal Ringer in the recording chamber. The results of these experiments are summarised in table 45, below.

Table 45. Summary of changes in membrane resistance in *Calliphora* prepupae and *Chilo* larvae during a low-Na^+/high K^+ substitution experiment. (Data from a minimum of 4 cells, 4 preparations, given as mean ± SE.)

	R_m in Normal Ringer (KΩ)	R_m in low Na^+/ high K^+ Ringer (KΩ)	% increase in R_m in low Na^+/ high K^+
Calliphora	96 ± 9	121 ± 10	26
Chilo	3083 ± 995	4166 ± 518	41

This increase in membrane resistance in *Calliphora* was attributed to a decrease in the p_K of the cell membrane when exposed to low-Na^+ Ringer. A similar mechanism might be operating in *Chilo* muscles, although this possibility was not tested.

vii Electrogenic pump(s)

The resting E_m of *Calliphora* prepupae was found to be fully accounted for by a model based on the Goldman-Hodgkin-Katz equation, taking into account only the trans-membrane gradients of K^+ and Na^+, with a value of 0.036 for α (p_{Na}/p_K). In *Chilo*, however, the situation was more complex, with K^+, Na^+, Cl^- and a metabolic pump all contributing to E_m. The extent to which each mechanism is involved in generating E_m is summarised in table 46, below.

Table 46. The contributions of various mechanisms to E_m in *Chilo*

	Maximum change in E_m per tenfold change in a_X^o (% of 58 mV)
K^+	52
Na^+	3.5
Cl^-	29.3
Total % Contribution by Ka^+, Na^+ and Cl^-	84.8

Thus, the contributions of the ionic conductance mechanisms to E_m in *Chilo* add up to some 85% of E_m. It would therefore be predicted that an electrogenic pump might contribute the remaining 15%. Cooling the cell would hence be expected to give rise to a maximum depolarisation of some 7 mV (ie. 15% of 45 mV, the mean E_m recorded in *Chilo*). In fact, a 14°C reduction in temperature caused an average depolarisation of 12 ± 2 mV, 1.4 mV of which could be accounted for by the effect of temperature on the equilibrium potentials of K^+, Na^+ and Cl^- (appendix 16). The average observed depolarisation attributable to the metabolic pump was therefore some 3.6 mV larger than predicted.

Thus, an error of some 9% was made in this attempt to account fully for the E_m of *Chilo* muscle cells in terms of the contributions of K^+, Na^+, Cl^- and an electrogenic, metabolic pump. This may be due to the fact that the roles of the inorganic ions were assessed from the <u>maximum</u> response of the cell membrane to changes in their extracellular activities. It may also reflect that additional mechanisms which were not investigated, may contribute to E_m in this insect eg. Ca^{2+}, pH.

APPENDIX 1

The pH of all solutions used in this study was 7.

Rice's Saline (Finlayson & Osborne, 1970)

	Conc (mM)	g/l
NaCl	173	10
KCl	13.5	1
$MgCl_2$	1	0.2
$NaHCO_3$	1.2	0.1
NaH_2PO_4	0.8	0.1
$CaCl_2$	0.9	0.13
Glucose	55.5	10

Osmolarity 402 mOsm

APPENDIX 2

Modified Weever's Lepidopteran Saline (Weevers, 1966)

	Conc. (mM)	g/l
NaCl	12	0.7
KCl	30	2.24
$MgCl_2$	18	1.71
$NaHCO_3$	1.5	0.13
NaH_2PO_4	1.5	0.23
$CaCl_2$	8	1.18
Glucose	117 Chilo	21.1

Osmolarity 280 mOsm

APPENDIX 3: Solutions used to calibrate K^+ ISMs

Calliphora = K^+ calibrating solutions / K^+ substitution solutions

The term 'N' (see solution number 4) is used in this and subsequent appendices to identify Normal Ringer.

The activity coefficient for K^+ is 0.72 in these solutions (CRC Handbook of Chemistry & Physics, Ed Robert C Weast, Pub. Chemical Rubber Co.)

Solution number	a_K (mM)	[KCl] (mM)	[NaCl] (mM)
1	0.97	1.35	185.2
2	2.16	3	183.5
3	5.04	7	179.5
4_N	9.72	13.5	173
5	21.6	30	156.5
6	50.4	70	116.5
7	97.2	135	51.5

All solutions also contained $MgCl_2$ (1mM), $NaHCO_3$ (1.2mM), NaH_2PO_4 (0.8mM), $CaCl_2$ (0.9mM), D-Glucose (55.5mM).

Solution number	a_K (mM)	[KCl] (mM)	[NaCl] (mM)
1	0.97	1.35	185.2
2	3.6	5	181.5
3_N	9.7	13.5	173
4	36	50	136.5
5	97.2	135	51.5

All solutions also contained $MgCl_2$ (1mM), $NaHCO_3$ (1.2mM), NaH_2PO_4 (0.8mM), $CaCl_2$ (0.9mM), D-Glucose (55.5mM).

Both series of solutions cover the same range of a_K's: the upper one was used to calibrate K^+ ISM's, the lower one for K^+ substitution experiments.

Caterpillar K^+-ISM calibrating solutions / K^+ substitution solutions

Solution number	a_K (mM)	[KCl] (mM)	[NaCl] (mM)
1	0.72	1	41
2	2.2	3	39
3	7.2	10	32
4_N	21.6	30	12
5	30.2	40	0
6	43.2	60	0

In solutions 1 - 5: $MgCl_2$ (18mM), $NaHCO_3$ (1.5mM), NaH_2PO_4 (1.5mM), $CaCl_2$ (8mM), D-Glucose (117mM).

Solution 6 contained no $MgCl_2$, but was otherwise similar to solutions 1 to 5.

APPENDIX 4: SOLUTIONS USED TO CALIBRATE CL^-:ISM'S

Calliphora: Calibration solutions for $C\ell^-$ ISMs/$C\ell^-$substitution solutions

Solution	a_{Cl} (mM)	[NaCl] (mM)	[Na gluconate] (mM)	$CaCl_2$ (mM)
1_N	137	173	0	0.9
2	70	80	93	4.5
3	41.2	40	133	4.5
4	24.9	17.5	155.7	4.5
5	18.2	7.8	164.9	4.5

All solutions also contained KCl (13.5mM), $MgCl_2$ (1mM), $NaHCO_3$ (1.2mM), $NaH_2PO_4^-$ (0.8mM), Glucose (55.5mM). Extra Ca^{2+} was added to solutions 2-5 to compensate for the fact that gluconate is known to sequester Ca^{2+} (Kenyon & Gibbons, 1977; Vaughan-Jones, 1979).

Chilo Cl^-;ISM calibrating solutions / Cl^--substitution solutions

Solution number	a_{Cl} (mM)	[KCl] (mM)	[NaCl] (mM)	[$MgCl_2$] (mM)	[$CaCl_2$] (mM)	[K gl] (mM)	[Na gl] (mM)	[Mg gl] (mM)	[Ca gl] (mM)
1	0.68	0.94	0	0	0	29.1	12	36	80
2	2.3	3.2	0	0	0	26.8	12	36	80
3	6.8	9.4	0	0	0	20.6	12	36	80
4	23	30	1.9	0	0	0	10.1	36	80
5N	67.7	30	12	36	8	0	0	0	0

(gl = gluconate)

All solutions also contained $NaHCO_3$ (1.5mM), NaH_2PO_4 (1.5mM) and glucose (117 mM).

APPENDIX 5: Solutions used to calibrate Na^+-ISMs.

Calliphora: Calibration solutions for Na^+-ISMs

Solution number	Activity coefficient for Na^+, γ	a_{Na} (mM)	[NaCl] (mM)
1	0.748	1.0	1.4
2	0.747	3.7	4.9
3	0.744	10.3	13.9
4	0.734	35.7	48.6
5	0.715	99.3	138.9

Each solution also contained KCl (152.8 mM), $MgCl_2$ (2.8 mM), $CaCl_2$ (0.014 mM) and HEPES (2.8 mM).

Chilo: Calibration solutions for Na^+-ISMs

Solution number	Activity coefficient for Na^+, γ	a_{Na} (mM)	[NaCl] (mM)
1	0.782	1.1	1.4
2	0.781	3.8	4.9
3	0.773	10.7	13.9
4	0.754	36.6	48.6
5	0.731	101.5	138.9

Each solution also contained KCl (86.1 mM), $MgCl_2$ (2.8 mM), $CaCl_2$ (0.014 mM) and HEPES (2.8 mM).

APPENDIX 6: Additional solutions used for ionic substitution experiments on *Calliphora*

Cl^- - free Ringer

	Concentration (mM)
Sodium gluconate	173
Potassium gluconate	13.5
Hemi-magnesium gluconate	2
Hemi-calcium gluconate	9
$NaHCO_3$	1.2
NaH_2PO_4	0.8
D-Glucose	55.5

Low-Cl^- (1.7mM) Ringer

	Concentration (mM)
NaCl	1.7
Sodium gluconate	171.3
Potassium gluconate	13.5
Hemi-magnesium gluconate	2
Hemi-calcium gluconate	9
$NaHCO_3$	1.2
NaH_2PO_4	0.8
D-Glucose	55.5

Calliphora: K^+ substitution solutions with $[a_K^o + 0.036\ a_{Na}^o] \times a_{Cl}^o$ constant

Solution number	$[a_K^o + 0.036\ a_{Na}^o]$ (mM)	[KCl] (mM)	[NaCl] (mM)	Total [Glucose] (mM)
1	12.9	11	194	18.5
2_N	14.2	13.5	173	55.5
3	15.5	16	153.6	89.3
4	17.2	19	134.5	121.5
5	18.3	21	123	140.5

All solutions also contained $MgCl_2$ (1mM), $NaHCO_3$ (1.2mM), NaH_2PO_4 (0.8mM), $CaCl_2$ (0.9mM).

These solutions were constructed such that a pair of simultaneous equations was satisfied:

1. $[a_K^o + 0.036\ a_{Na}^o] \times a_{Cl}^o$ = constant (1946 mM^2)

2. $Cl_{KCl} + Cl_{NaCl} \leq Cl_{Total(Normal)}$

where Cl_{KCl} is the Cl^- present as KCl; Cl_{NaCl} the Cl^- present as NaCl; Cl_{Total} the Cl^- content of Normal Ringer.

Calliphora Na^+ substitution solutions

All solutions were based on Rice's saline, i.e.; in addition to NaCl and the Na^+ substitute, all solutions contained KCl (13.5 mM), $MgCl_2$ (1mM), $NaHCO_3$ (1.2mM), NaH_2PO_4 (0.8mM), $CaCl_2$ (0.9 mM) and D-Glucose (55.5mM).

Solution number	a_{Na} (mM)	[NaCl] (mM)	Substitute	Total [Glucose] (mM)
1	1.25	1.73	Choline chloride	171.3
2	1.25	1.73	Glucose	342.5
3	1.25	1.73	Tetramethyl ammonium chloride	171.3
4	1.25	1.73	Magnesium chloride	85.6
5_N	124.6	173	-	-

APPENDIX 7: Additional solutions used for ionic substitution experiments on Chilo

Chilo: Na^+-substitution solutions

Solution number	a_{Na} (mM)	[NaCl] (mM)	$[MgCl_2]$ (mM)	[Glucose] (mM)
1_N	8.64	12.0	0	0
2	2.7	3.75	4.1	4.1
3	0.86	1.2	5.4	5.4

In addition, all solutions contained KCl (30mM), $MgCl_2$ (18mM), $NaHCO_3$ (1.5mM), NaH_2PO_4 (1.5mM), Glucose (117mM), $CaCl_2$ (8mM).

Chilo: Mg^{2+}-substitution solutions

Solution number	a_{Mg} (mM)	[$MgCl_2$] (mM)	[Mg gluconate] (mM)	[Glucose] (mM)
1	1.3	1.8	32.4	117
2N	13	18	-	117
3	40	55.5	-	42

In addition, all solutions contained KCl (30mM), NaCl (12mM), $NaHCO_3$ (1.5mM), NaH_2PO_4 (1.5mM), $CaCl_2$ (8mM).

APPENDIX 8: Intracellular K^+ activity data:

Calliphora larvae : LIX-type K^+ ISM data

E_m (-mV)	V_K (-mV)	a_K^i (mM)	E_K (-mV)	$E_K - E_m$ (-mV)
63	69	200	76.2	13.2
44	54	114	62.0	18.0
47	56	124	64.1	17.1
52	64	170	72.1	20.1
38	52	110	61.1	23.1
42	59	150	68.9	26.9
41	57	140	67.2	26.2
44	55	130	65.3	21.3
44	59	150	68.9	24.9
44	55	130	65.3	21.3
56	59	155	69.8	13.8
50	57	140	67.2	17.2
47	57	140	67.2	20.2
52	55	130	65.3	13.3
49	59	150	68.9	19.9
49	55	130	65.3	16.3
40	59	150	68.9	28.9
51	59	150	68.9	17.9
65	55	130	65.3	0.3
40	51	105	59.9	19.9
36	57	145	68.1	32.1
40	46	86	54.9	14.9
41	43	72	50.4	9.4
40	45	80	53.1	13.1
43	47	87	55.2	12.2
43	47	90	56.1	13.1
41	47	90	56.1	15.1
34	46	83	54.0	20.0
31	49	100	58.7	27.7
44	44	74	51.1	7.1
47	55	125	64.3	17.3
47	65	190	74.9	27.9
52	68	210	77.4	25.4
54	56	125	64.3	10.3
33	40	61	46.3	13.3
65	59	140	67.2	2.2
44	56	125	64.3	20.3
43	55	115	62.2	19.2
47	60	145	68.1	21.1
47	60	150	68.9	21.9
44	58	140	67.2	23.2
48	58	140	67.2	19.2
56	62	170	72.1	16.1
58	68	220	78.6	20.6
50	60	150	68.9	18.9
43	56	125	64.3	21.3
44	55	120	63.3	19.3

E_m (-mV)	V_K (-mV)	a_K^i (mM)	E_K (-mV)	$E_K - E_m$ (-mV)
44	55	120	63.3	19.3
52	60	125	64.3	12.3
62	66	160	70.6	8.6
55	63	140	67.2	12.2
53	58	120	63.3	10.3
54	63	140	67.2	13.2
49	60	130	65.3	16.3
56	63	140	67.2	27.5
55	60	130	65.3	10.3
51	61	135	66.3	15.3
39	42	80	53.1	14.1
60	63	215	78.0	18.0
52	55	160	70.6	18.6
44	51	134	66.1	22.1
42	52	127	64.7	22.7
55	59	188	74.6	19.6
48	50	117	62.7	14.7
44	52	127	64.7	20.7
43	56	105	59.9	16.9
34	50	80	53.1	19.1
44	52	88	55.5	11.5
36	57	113	61.8	25.8
37	56	105	59.9	22.9
46	57	113	61.8	15.8
38	59	113	61.8	23.8
50	63	134	66.1	16.1
46	62	128	64.9	18.9
45	66	150	68.9	23.9
42	60	118	62.9	20.9
36	56	104	59.7	23.7
35	57	108	60.7	25.7
34	56	104	59.7	25.7
36	55	100	58.7	22.7

Calliphora larvae: NIC-type K^+ ISM data

E_m (-mV)	V_K (-mV)	a_K^i (mM)	E_K (-mV)	$E_K - E_m$ (-mV)
55	64	140	67.2	12.2
58	66	150	68.9	10.9
46	63	132	65.7	19.7
44	59	113	61.8	17.8
54	63	132	65.7	11.7
50	60	120	63.3	13.3
50	61	123	63.9	13.9
48	60	120	63.3	15.3
44	61	123	63.9	19.9
42	62	130	65.3	23.3
48	62	130	65.3	17.3
40	57	97	57.9	17.9
41	56	94	57.2	16.2
43	56	94	57.2	14.2
44	56	94	57.2	13.2
47	58	100	58.7	11.7
48	64	130	65.3	17.3
44	63	123	63.9	19.9
45	56	92	56.6	11.6
44	58	100	58.7	14.7
47	58	100	58.7	11.7
47	60	110	61.1	14.1
46	58	100	58.7	12.7
45	60	110	61.1	16.1
46	64	149	67.2	21.2
50	50	110	61.1	11.1
52	62	127	64.7	12.7
49	59	112	61.6	12.6
49	60	117	62.6	13.6
46	56	190	58.7	12.7
48	62	127	64.7	16.7
48	58	110	61.1	13.1
47	60	117	62.6	15.6
48	60	117	62.6	14.6
48	64	140	67.2	19.2
44	61	120	63.3	19.3
47	66	150	68.9	21.9
46	54	80	53.1	7.1
44	51	70	48.7	5.7
44	52	72	50.4	6.4
46	52	72	50.4	4.4
49	54	80	53.1	4.1
49	55	82	53.7	4.7
48	50	68	49.0	1.0
48	58	92	56.6	8.6
52	56	84	54.3	2.3
46	49	66	48.2	2.2
48	55	82	53.7	5.7

E_m (-mV)	V_K (-mV)	a_K^i (mM)	E_K (-mV)	$E_K - E_m$ (-mV)
53	56	84	54.3	1.3
49	53	75	51.5	2.5
50	54	80	53.1	3.1
48	50	68	49.0	1.0
48	52	72	50.4	2.4
43	50	68	49.0	6.0
46	50	68	49.0	3.0
49	52	72	50.4	1.4
48	52	72	50.4	2.4
52	54	80	53.1	1.1
46	54	80	53.1	7.1
52	56	78	52.4	0.4
46	60	92	56.6	10.6
48	52	66	48.2	0.2
44	56	78	52.5	3.5
46	53	70	49.7	3.7
46	50	62	46.7	0.7
54	59	88	55.5	1.5
55	57	110	61.1	6.1
57	56	107	60.4	3.4
52	54	100	58.7	6.7
54	55	103	59.5	5.5
52	54	100	58.7	6.7
45	46	71	50.1	5.1
43	54	100	58.7	15.7
53	57	110	61.1	8.1
49	56	107	60.4	11.4
38	51	86	54.9	16.9
42	53	94	57.2	15.2
41	48	76	51.8	10.8
45	53	92	56.6	11.6
44	53	92	56.6	12.6
46	54	96	57.7	11.7
44	53	92	56.6	12.6
39	54	96	57.7	18.7
50	63	134	66.1	16.1
52	68	165	71.3	19.3
50	62	130	65.3	15.3
40	68	165	71.3	31.3
54	68	165	71.3	17.3
45	60	120	63.3	18.3
43	60	120	63.3	20.3
42	56	100	58.7	16.7
50	66	150	68.9	18.9
47	56	100	58.7	11.7
38	55	97	57.9	19.9
49	63	134	66.1	17.1
57	63	123	63.9	6.9
52	60	110	61.1	9.1
48	56	94	57.2	9.2
46	56	94	57.2	11.2

E_m (-mV)	V_K (-mV)	a_K^i (mM)	E_K (-mV)	$E_K - E_m$ (-mV)
48	54	87	55.2	7.2
53	62	120	63.3	10.3
53	61	113	61.8	8.8
46	54	87	55.2	9.2
45	54	87	55.2	10.2
45	53	83	54.0	9.0
46	53	83	54.0	8.0
43	53	83	54.0	11.0
48	63	124	64.1	16.1
53	63	124	64.1	11.1
49	52	80	53.1	4.1
45	54	87	55.2	10.2
48	54	87	55.2	7.2
45	56	94	57.2	12.2
45	54	87	55.2	10.2
40	50	74	51.1	11.1

Calliphora prepupae: LIX-type K^+ ISM data

E_m (-mV)	V_K (-mV)	a_K^i (mM)	E_K (-mV)	$E_K - E_m$ (-mV)
60	88	500	99.3	39.3
59	80	290	85.5	26.5
69	97	580	103.0	34.0
60	87	380	92.3	32.3
46	81	300	86.4	40.4
41	80	290	85.5	44.5
55	84	340	89.5	34.5
47	96	560	102.1	55.1
54	97	580	103.0	49.0
53	90	440	96.0	43.0
58	84	340	89.5	31.5
50	87	380	92.3	42.3
66	92	470	97.7	31.7
41	879	380	92.3	26.3
68	95	540	101.2	33.2
60	87	390	93.0	33.0
46	76	255	82.3	36.3
43	72	208	77.2	34.2
43	75	235	80.2	37.2
46	70	190	74.9	28.9
51	82	320	88.0	37.0
32	74	230	79.7	47.7
37	80	290	85.5	48.5
43	76	255	82.3	39.3
46	75	235	80.2	34.2
43	64	150	68.9	25.9
44	76	255	82.3	38.3
38	71	200	76.2	38.2
34	70	190	74.9	40.9
54	102	660	106.2	52.2
40	92	440	96.0	56.0
39	92	4409	96.0	57.0
44	97	540	101.2	57.2
45	98	560	102.1	57.1
48	105	760	109.8	61.8
37	96	520	100.2	63.2
39	92	440	96.0	57.0
50	76	230	79.7	29.7
47	93	460	97.2	50.2
71	83	300	86.4	15.4
55	71	184	74.1	19.1
47	87	360	91.0	44.5
53	91	420	113.6	60.6
51	92	440	96.0	45.0
52	92	440	96.0	44.0
48	94	490	98.7	50.7
59	87	360	91.0	32.0
58	99	385	92.7	34.7
53	101	640	105.5	52.5
40	91	420	94.9	54.9

E_m (-mV)	V_K (-mV)	a_K^i (mM)	E_K (-mV)	$E_K - E_m$ (-mV)
38	86	340	89.5	51.5
39	85	330	88.8	49.8
42	82	290	85.5	45.5
50	81	280	84.7	34.7
47	85	330	88.8	41.8
46	84	320	88.0	42.0
46	88	370	91.7	45.7
51	87	360	91.0	40.0
47	88	370	91.7	44.7
45	92	420	94.9	49.9
49	89	390	93.0	44.0
50	87	370	91.7	41.7
48	90	400	93.6	45.6
52	87	370	91.7	39.7
59	85	330	88.8	29.8
55	85	330	88.8	33.8
52	85	330	88.8	36.8
46	82	290	85.5	39.5
52	83	300	86.4	34.4
49	76	226	79.3	30.3
55	82	290	85.5	30.5
54	86	340	89.5	45.5
56	83	300	86.4	30.4
58	87	370	91.7	33.7
58	86	340	89.5	31.5
53	86	340	89.5	36.5
56	86	340	89.5	33.5
51	82	290	85.5	34.5
55	82	290	85.5	30.5
57	86	340	89.5	32.5
48	71	183	73.9	25.9
59	86	340	89.5	30.5
50	94	480	98.2	48.2
47	97	545	101.4	54.4
41	92	440	96.0	55.0
54	95	500	99.3	45.3
48	97	545	101.4	53.4
54	96	520	100.2	46.2
54	98	570	102.6	48.6
47	93	460	97.2	50.2
49	92	440	96.0	47.0
47	94	480	98.2	51.2
47	92	440	96.0	49.0
43	92	440	96.0	56.0
44	100	620	104.7	60.7
43	87	370	91.7	48.7

Calliphora prepupae: NIC-type K^+ ISM data

E_m (-mV)	V_K (-mV)	a_K^i (mM)	E_K (-mV)	$E_K - E_m$ (-mV)
52	58	92	56.6	4.6
54	60	100	58.7	4.6
50	57	90	56.1	6.1
51	56	84	54.3	3.3
47	55	82	53.7	6.7
44	62	108	60.7	16.7
38	56	85	54.6	16.6
44	62	108	60.7	16.7
46	65	130	65.3	19.3
50	62	116	62.5	12.5
42	62	116	62.5	20.5
41	62	116	62.5	21.5
44	63	121	63.5	19.5
47	63	121	63.5	16.5
35	58	100	58.7	23.7
51	66	140	67.2	16.2
34	58	100	58.7	24.7
48	62	116	62.5	14.5
66	69	154	69.6	3.6
47	64	128	64.9	17.9
59	60	110	61.1	2.1
63	60	110	61.1	1.9
41	50	72	50.4	9.4
46	60	110	61.1	15.1
44	61	112	61.6	17.6
36	53	80	53.1	17.1
50	67	142	67.5	17.5
50	66	140	67.2	17.2
47	60	110	61.1	14.1
48	66	140	67.2	19.2
47	62	117	62.7	15.7
46	54	90	56.1	10.1
54	57	100	58.7	4.7
49	57	100	58.7	9.7
50	54	90	56.1	6.1
48	55	94	57.1	9.1
46	52	82	53.7	7.7
47	55	94	57.1	10.1
43	62	122	63.7	20.7
37	50	90	56.1	19.1
45	60	112	61.6	16.6
46	56	97	57.9	11.9
56	69	147	68.4	12.4
51	68	140	67.2	16.2
35	51	72	50.4	15.4
45	60	102	59.2	14.2
42	60	120	63.3	21.3
59	74	210	77.4	18.4

E_m (-mV)	V_K (-mV)	a_K^i (mM)	E_K (-mV)	$E_K - E_m$ (-mV)
44	63	134	66.1	22.1
55	68	165	71.3	16.3
46	64	140	67.2	21.2
40	56	100	58.7	18.7
50	67	158	70.2	20.2
44	64	140	67.2	23.2
44	62	130	65.3	21.3
46	46	93	56.9	10.9
40	61	113	61.8	21.8
44	51	79	51.8	7.8
50	58	100	58.7	8.7
42	62	120	63.3	21.3
35	48	68	49.0	14.0
43	60	112	61.6	18.6
49	66	143	67.7	18.7
47	58	104	59.7	12.7
48	58	104	59.7	11.7
50	59	110	61.1	11.1
48	60	113	61.8	13.8
50	61	118	62.9	12.9
54	66	144	67.9	13.9
48	59	110	61.1	13.1
47	59	110	61.1	14.1
46	61	119	63.1	17.1
39	65	140	67.2	28.2
49	70	170	72.1	23.1
44	56	97	57.9	13.9
51	62	122	63.7	12.7
45	61	118	62.9	17.9
52	62	122	63.7	11.9
43	58	103	59.5	16.5
45	59	110	61.1	16.1
44	56	97	57.9	13.9
47	64	132	65.7	18.7
56	72	182	73.8	17.8
49	60	130	65.3	16.3
45	60	130	65.3	20.3

Chilo larvae: LIX-type K^+ ISM data

E_m (-mV)	V_K (-mV)	a_K^i (mM)	E_K (-mV)	$E_K - E_m$ (-mV)
50	33	76	31.7	+18.3
44	26	60	25.7	18.3
50	28	64	27.4	22.6
46	27	62	26.6	19.4
40	26	60	25.7	14.3
48	33	78	32.3	15.7
44	32	76	31.7	12.3
44	35	85	34.5	9.5
48	30	70	29.6	18.4
46	33	78	32.3	13.7
44	34	82	33.6	10.4
48	38	96	37.6	10.4
36	32	76	31.7	4.3
38	29	67	28.5	9.5
44	34	82	33.6	10.4
44	33	78	32.3	11.7
40	34	82	33.6	6.4
38	36	88	35.4	2.6
41	31	72	30.3	10.7
40	22	49	20.6	19.4
44	22	49	20.6	23.4
42	23	51	21.6	20.4
44	24	54	23.1	20.9
47	26	58	24.9	22.1
50	26	58	24.9	25.1
43	26	58	24.9	18.1
45	27	60	25.7	19.3
47	27	60	25.7	21.3
47	25	56	24.0	23.0
41	24	54	23.1	17.9
51	29	64	27.4	23.6
48	27	60	25.7	22.3
51	26	58	24.9	26.1
40	24	54	23.1	16.9
51	26	58	24.9	26.1
50	26	58	24.9	25.1
50	26	58	24.9	25.1
50	28	72	30.3	19.7
48	30	68	28.9	19.1
51	30	74	31.0	20.0
52	32	80	33.0	19.0
50	33	83	33.9	16.1
50	28	66	28.1	21.9
38	26	62	26.6	11.4
50	31	77	32.0	18.0
43	33	83	33.9	9.1
52	32	80	33.0	19.0
53	34	87	35.1	17.9
48	30	74	31.0	17.0
50	34	87	35.1	14.9

E_m (-mV)	V_K (-mV)	a_K^i (mM)	E_K (-mV)	$E_K - E_m$ (-mV)
41	26	62	26.6	14.4
45	29	70	29.6	15.4
39	29	70	29.6	9.4
45	36	94	37.0	8.0
46	28	66	28.1	17.9
43	26	58	24.9	18.1
44	27	60	25.7	18.3
45	24	54	23.1	21.9
40	23	52	22.1	17.9
46	25	56	24.0	22.0
45	27	60	25.7	19.3
42	22	50	21.1	20.9
40	21	48	20.1	19.9
41	25	56	24.0	17.0
36	24	54	23.1	12.9
37	18	43	17.3	19.7
40	23	51	21.6	18.4
53	26	58	24.9	28.1
60	27	60	25.7	34.3
54	29	65	27.8	26.2
54	26	58	24.9	29.1
55	23	51	21.6	33.4
53	30	68	28.9	24.1
54	24	54	23.1	30.9
50	26	58	24.9	25.1
50	29	65	27.8	22.2
44	24	54	23,1	20.9
54	28	62	26.6	27.4

Chilo larvae: NIC-type K^+ ISM data

E_m (-mV)	V_K (-mV)	a_K^i (mM)	E_K (-mV)	$E_K - E_m$ (-mV)
39	28	69	29.3	9.7
40	28	69	29.3	10.7
42	30	75	31.4	10.6
40	30	75	31.4	8.6
42	27	66	28.1	13.9
40	28	69	29.3	10.7
46	32	80	33.0	13.0
40	30	75	31.4	8.6
43	30	75	31.4	11.6
39	30	75	31.4	7.6
40	22	53	22.6	17.4
40	21	50	21.1	18.9
39	20	48	20.1	18.9
40	20	48	20.1	19.9
43	20	48	20.1	22.9
42	21	50	21.1	20.9

E_m (-mV)	V_K (-mV)	a_K^i (mM)	E_K (-mV)	$E_K - E_m$ (-mV)
41	28	62	26.6	14.4
41	24	54	23.1	17.9
41	27	62	26.6	14.4
40	22	49	20.6	19.4
37	24	54	23.1	13.9
40	24	54	23.1	16.9
52	26	54	23.1	28.9
53	32	66	28.1	24.9
48	23	48	20.1	27.9
51	24	50	21.1	29.9
51	24	50	21.1	29.9
38	22	47	19.6	18.4
44	22	47	19.6	24.4
47	24	50	21.1	25.9
40	20	44	17.9	22.1
40	22	48	20.1	19.9
46	25	53	22.6	23.4
51	22	48	20.1	30.9
46	21	46	19.0	27.0
42	22	48	20.1	21.9
43	20	45	18.5	24.5
46	28	60	25.7	20.3
44	21	46	19.0	25.0
54	29	61	26.2	27.8
53	26	56	24.0	29.0
48	26	56	24.0	24.0
51	30	65	27.8	23.2
48	31	68	28.9	19.1
50	30	65	27.8	22.2
44	28	60	25.7	18.3
45	30	65	27.8	17.2
46	30	65	27.8	18.2
41	29	63	27.0	14.0
40	30	65	27.8	12.2
41	28	60	25.7	15.3
44	32	70	29.6	14.4
40	30	65	27.8	12.2
46	28	60	25.7	20.3
44	29	63	27.0	17.0
49	30	65	27.8	21.2
36	28	60	25.7	10.3
42	28	60	25.7	16.3
48	30	65	27.8	20.2
46	28	60	25.7	20.3
46	30	65	27.8	18.2
44	28	60	25.7	18.3
44	29	63	27.0	17.0
54	31	82	33.6	20.4
50	30	80	33.0	17.0
48	26	66	28.1	22.6

E_m (-mV)	V_K (-mV)	a_K^i (mM)	E_K (-mV)	$E_K - E_m$ (-mV)
51	31	82	33.6	17.4
52	30	80	33.0	19.0
48	28	73	30.7	17.3
49	30	80	33.0	16.0
48	32	80	33.0	15.0
46	29	92	30.3	15.7
48	30	75	31.4	16.6
48	29	72	30.3	17.7
46	28	69	29.3	16.7
45	30	75	31.4	13.6
50	32	80	33.0	17.0

APPENDIX 9

Intracellular Na^+ data: Calliphora Larvae (Na^+ NIC)

E_m (-mV)	V_{Na} (-mV)	a_{Na}^i (mM)	E_{Na} (-mV)	$E_{Na}-E_m$ (-mV)
44	38	14.4	54.3	98.3
42	45	10.0	63.5	105.5
41	54	4.5	83.6	124.6
48	42	11.8	59.4	107.4
44	54	4.5	83.6	127.6
45	47	9.0	66.2	111.2
52	39	13.7	55.6	107.6
49	40	13.0	56.9	105.9
48	28	24.0	41.5	89.5
48	44	10.4	62.5	110.5
47	38	20.2	45.8	92.8
51	50	10.0	63.5	114.5
46	42	16.2	51.4	97.4
48	50	10.0	63.5	111.5
49	52	8.8	66.8	115.8
48	45	13.8	55.4	103.4
51	44	14.6	54.0	105.0
50	46	13.0	56.9	106.9
47	46	13.0	56.9	103.9
52	58	5.3	79.5	131.5
52	56	6.6	74.0	126.0
52	56	6.6	74.0	126.0
52	54	8.0	69.2	121.2
46	59	7.4	71.1	117.1
44	62	6.0	76.4	120.4
46	58	7.8	73.7	119.7
46	57	8.4	71.8	117.8
48	57	8.4	71.8	119.8
46	55	9.6	68.4	114.4
44	54	10.0	67.4	111.4

Intracellular Na^+ data: Calliphora prepupae (Na^+ NIC)

E_m (-mV)	V_{Na} (-mV)	a_{Na}^i (mM)	E_{Na} (-mV)	$E_{Na}-E_m$ (-mV)
46	57	5.4	79.1	125.1
42	58	4.9	83.1	125.1
44	54	7.0	72.5	116.5
44	53	7.6	70.4	114.4
45	53	7.6	70.4	115.4
46	60	3.6	89.3	135.3
48	59	4.3	84.8	132.8
47	62	2.9	94.7	141.7
49	44	13.2	56.5	105.5
49	45	12.6	57.7	106.7
46	49	9.8	64.0	110.0
46	50	9.0	66.2	112.2
40	59	4.4	84.2	124.2
38	58	4.8	82.0	120.0
47	49	9.8	64.0	111.0
48	54	6.6	74.0	122.0
44	57	5.3	79.5	123.5
48	50	9.0	66.2	114.2
46	52	7.8	69.8	115.8
46	50	9.0	66.2	112.2
47	52	8.4	67.9	114.9
44	49	10.6	62.1	106.1
48	46	12.7	57.5	105.5
46	53	7.8	69.8	115.8
47	48	11.2	60.7	107.7
46	48	11.2	60.7	106.7
46	46	12.7	57.5	103.5
42	49	10.6	62.1	104.1
44	49	9.8	64.0	108.0
44	42	15.0	53.3	97.3
46	46	12.0	58.9	104.9
44	52	7.8	69.8	113.8
41	58	4.7	82.5	123.5
46	58	4.7	82.5	128.5
40	56	5.6	78.1	118.1
46	58	1.6	109.7	155.7
48	59	1.2	116.9	164.9
48	53	6.2	75.6	123.6
49	59	1.2	116.9	165.9
46	48	1.7	108.1	154.1
48	44	3.4	90.7	138.7
48	44	3.4	90.7	138.7
47	41	5.2	80.0	127.0

Intracellular Na^+ data: Chilo larvae

E_m (-mV)	V_{Na} (-mV)	a_{Na}^i (mM)	E_{Na} (-mV)	$E_{Na}-E_m$ (-mV)
48	49	11.0	-6.1	41.9
55	52	7.4	3.9	58.9
40	52	8.0	1.9	41.9
52	60	4.6	15.9	67.9
43	49	10.3	-4.4	38.6
42	46	12.2	-8.7	33.3
39	54	6.7	6.4	45.4
60	28	29.0	-30.5	29.4
46	37	19.0	-19.8	26.2
45	50	9.3	-1.9	43.1
50	36	19.0	-19.9	30.1
46	40	15.0	-13.9	32.1
43	50	9.0	-1.0	42.0

APPENDIX 10 Intracellular Cl^- activity data:

Calliphora larvae

E_m (-mV)	V_{Cl} (-mV)	a_{Cl}^i (mM)	E_{Cl} (-mV)	$E_{Cl}-E_m$ (-mV)
51	50	19.0	49.7	1.3
55	51	18.3	50.7	4.3
50	50	19.0	49.7	0.3
48	48	20.8	47.5	0.5
50	51	18.6	50.3	-0.3
54	54	16.3	53.6	0.4
56	56	15.2	55.4	0.6
48	53	18.2	50.8	-2.8
54	52	19.0	49.8	4.2
41	43	27.0	40.9	0.1
40	42	28.0	49.0	0.0
46	48	22.0	46.1	-0.1
49	50	20.6	47.7	1.3
44	46	24.0	43.9	0.1
41	43	27.0	40.9	0.1
44	48	22.2	45.8	-1.8
52	52	15.2	55.4	-3.4
54	50	16.4	53.5	0.5
53	47	19.0	49.8	3.2
50	46	20.0	48.5	1.5
52	45	23.0	48.0	4.0
58	50	16.4	53.5	4.5
58	57	13.2	58.9	-0.9
49	47	20.3	48.1	0.9
58	58	12.7	59.9	-1.9
57	56	14.0	57.5	-0.5
54	50	17.0	52.6	1.4
57	55	14.4	56.7	0.3
60	60	13.0	59.3	0.7
59	54	13.0	59.3	-0.3
54	54	16.3	53.6	0.4
60	60	13.0	59.3	0.7
56	60	13.0	59.3	-3.3
58	59	13.4	58.5	-0.5
58	58	14.0	57.5	0.5
57	58	14.0	57.5	-0.5
56	56	15.0	55.7	0.3
56	58	14.0	57.5	-1.5
52	53	17.0	52.6	-0.6
52	56	15.0	55.7	-3.7
55	57	14.4	56.7	-1.7
58	60	13.0	59.3	-1.3
56	56	15.0	55.7	-1.7
52	53	17.0	52.6	-0.6
53	54	16.3	53.6	-0.6

54	54	16.3	53.6	0.4
51	50	18.8	50.1	0.9
51	52	18.2	50.8	0.2
52	53	17.0	52.6	-0.6
48	49	19.7	48.9	0.9

Intracellular Cl^- activity data: Calliphora prepupae

E_m (-mV)	V_{Cl} (-mV)	a_{Cl}^i (mM)	E_{Cl} (-mV)	$E_{Cl}-E_m$ (-mV)
50	24	53.0	23.9	26.1
56	31	40.0	31.0	25.0
57	32	39.0	31.7	25.3
56	34	36.0	33.7	22.3
52	40	30.0	38.3	13.7
48	38	32.0	36.6	11.4
48	41	28.6	39.5	8.5
46	40	30.0	38.3	7.7
48	40	30.0	38.3	9.7
49	41	28.6	39.5	9.5
48	40	30.0	38.3	9.7
42	40	30.0	38.3	3.7
38	36	34.7	34.6	3.4
46	38	32.0	36.6	9.4
48	36	35.0	34.4	13.6
50	39	31.0	37.4	12.6
38	26	51.0	24.9	13.1
42	37	33.3	35.6	6.4
45	34	37.0	33.0	12.0
42	35	36.0	33.7	8.3
57	30	43.5	28.9	28.1
58	30	43.5	28.9	29.1
56	31	42.0	29.8	26.2
58	25	52.0	24.4	33.6
56	31	41.5	30.0	26.0
55	29	45.0	28.0	27.0
53	30	43.5	28.9	24.1
51	31	41.5	30.0	21.0
49	26	50.5	25.1	23.9
50	25	52.5	24.2	25.8
50	26	50.5	25.1	24.9
50	26	50.5	25.1	24.9
52	30	42.0	29.8	22.2
45	27	48.5	26.2	18.8
49	19	66.0	18.4	30.6

E_m (-mV)	V_{Cl} (-mV)	a_{Cl}^i (mM)	E_{Cl} (-mV)	$E_{Cl}-E_m$ (-mV)
42	40	10.5	46.9	4.9
40	42	9.8	48.7	8.7
42	42	9.8	48.7	6.7
40	37	12.2	43.2	3.2
38	36	13.0	41.6	3.6
40	38	11.5	44.7	4.7
38	35	13.3	41.0	3.0
54	54	5.5	63.2	9.2
44	49	7.3	56.1	12.1
45	48	7.3	56.1	11.1
49	50	6.6	58.6	9.6
49	48	7.3	56.1	7.1
46	47	7.7	54.8	8.8
47	57	4.8	66.7	19.7
44	46	8.0	53.8	9.8
45	46	8.0	52.8	8.8
50	49	7.0	57.1	7.1
47	49	7.0	57.1	10.1
43	48	7.2	56.4	13.4
46	49	7.0	57.1	11.1
48	50	6.6	58.6	10.6
49	51	6.4	59.4	10.4
38	40	10.4	47.2	9.2
48	50	6.6	58.6	10.6
36	41	10.0	48.2	12.2
48	48	7.2	56.4	8.4
40	42	9.6	49.2	9.2
43	49	10.3	47.4	4.4
39	38	11.3	45.1	6.1
46	43	9.2	50.3	4.3
42	40	10.3	47.4	5.4
40	42	9.6	49.2	9.2
44	42	9.6	49.2	5.2
44	40	10.3	47.4	3.4
46	43	9.2	50.3	4.3
38	37	12.0	43.6	5.6
36	37	12.0	43.6	7.6
42	40	10.3	47.4	5.4
47	43	9.2	50.3	3.3
43	40	10.3	47.4	4.4
40	38	11.3	45.1	5.1
42	41	10.0	48.2	6.2

Intracellular Cl^- activity data: Chilo larvae

E_m (-mV)	V_{Cl} (-mV)	a_{Cl}^i (mM)	E_{Cl} (-mV)	$E_{Cl}-E_m$ (-mV)
43	42	10.5	46.9	3.9
54	50	7.5	55.4	1.4
53	51	7.2	56.4	3.4
36	34	15.0	38.0	2.0
48	50	7.5	55.4	7.4
54	59	5.1	65.1	11.1
40	44	9.7	48.9	8.9
47	48	8.2	53.2	6.2
46	51	7.2	56.4	10.4
52	58	5.2	64.6	12.6
50	53	6.6	58.6	8.6
43	50	5.5	63.2	20.2
46	48	6.0	61.0	15.0
48	47	6.4	59.4	11.4
45	46	6.8	57.9	12.9
42	44	7.4	55.8	13.8
47	48	6.0	61.0	14.0
44	47	6.4	59.4	15.4
48	46	6.8	57.9	9.9
52	52	5.0	65.6	13.6
52	46	6.8	57.9	5.9
55	52	5.0	65.6	10.6
51	48	6.0	61.0	10.0
52	50	5.5	63.2	10.2
46	44	8.2	53.2	7.2
48	42	9.0	50.8	2.8
48	47	7.0	57.2	9.2
52	50	6.0	61.0	9.0
52	50	6.0	61.0	9.0
52	55	4.9	66.1	14.1
47	48	6.8	57.9	10.9
46	42	9.0	50.8	4.8
50	52	5.6	62.8	12.8
50	47	7.0	57.2	7.2
41	43	8.6	52.0	11.0
42	45	7.8	54.4	12.4
46	49	6.4	59.4	13.4
48	47	7.0	57.2	9.2
47	48	6.8	57.9	10.9
50	44	8.0	53.8	3.8
52	50	6.0	61.0	9.0
40	40	10.5	46.9	6.9
51	52	6.0	61.0	10.0
38	38	11.5	44.7	6.7
48	45	8.4	52.6	4.6
49	45	8.4	52.6	3.6
45	42	9.8	48.7	3.7
44	42	9.8	48.7	4.7
42	41	10.2	47.7	5.7
42	43	9.3	50.0	8.0

Appendix 11 Data from Cl^- depletion experiments on *Calliphora* prepupae

	E_m (mV)	(1) (mM)	(2) (mM)	(3) (mM)	(4) (mV)	(5) (mM)	(6) (mM)
	-44	52	14.5	37.5	-32.6	23.9	13.6
	-60	24	10.4	13.6	-58.2	12.7	0.9
	-54	60	7	53	-23.9	16.1	36.9
	-44	52	10	42	-29.8	23.9	18.1
	-42	41	12	29	-39.1	25.9	3.1
	-52	44	6	38	-32.2	17.4	20.6
	-54	25	7	18	-51.1	16.1	1.1
$\bar{x}$	-50	42.6	9.6	33	-38.1	19.4	13.5
SE	2.5	5.2	1.2	5.2	4.7	1.9	5.0

Columns (1) a^i_{Cl} values recorded when the cells were bathed in Normal Ringer.

(2) a^i_{Cl} values recorded when cells were bathed in Cl^--free Ringer.

(3) Difference between a^i_{Cl} values recorded in Normal Ringer and those recorded from the same cells in Cl^--free Ringer. This column represents the 'true' a^i_{Cl} values.

(4) E_{Cl} values calculated from column 3 a^i_{Cl} data.

(5) a^i_{Cl} values predicted if Cl^- were passively distributed (calculated such that E_{Cl} is equal to the measured E_m for each cell).

(6) Difference between the a^i_{Cl} values for each cell (column 3) and the a^i_{Cl}'s expected if Cl^- were passively distributed (column 5).

Appendix 12 Measurements of a^i_K and a^i_{Na} from the same preparations *Calliphora* prepupae

Cell number	a^i_K (mM)	a^i_{Na} (mM)	E^m (mV)	Predicted E_ms α=0.086 (mV)	α=0.03565 (mV)	α=.1685 (mV)
(1)	74	8.8	45	32.7	41.7	21.0
(2)	82	6.8	47	35.2	44.3	23.5
(3)	74	12.6	47	32.8	41.8	21.2
(4)	78	4.6	47	33.9	43.0	22.1
(5)	88	2.8	48	36.8	46.0	25.0
(6)	98	2.8	46	39.6	48.7	27.7
(7)	86	10	47	36.5	45.5	24.8
(8)	110	5.4	50	42.5	51.6	30.7
(9)	83	9.6	47	35.6	44.6	23.9
(10)	78	11.2	49	34.1	43.1	22.4
(11)	82	10	47	35.3	44.3	23.6
(12)	120	15.6	54	44.9	53.9	33.2
(13)	140	28	49	48.9	57.9	37.4
(14)	98	20	48	39.9	48.9	28.4
(15)	110	20	52	42.8	51.8	31.3
(16)	113	26	49	43.6	52.5	32.1
(17)	94	20	44	38.9	47.8	27.4
(18)	140	21	50	48.8	57.8	37.2
Mean	97.1	13.1	48.1	39	48.2	27.4
±SE	4.9	1.8	±0.6	±1.2	±1.2	±1.2

Predicted E_ms were calculated from the modified G-H-K equation

$$E_m = 58 \log \frac{[a^o_K + \alpha\, a^o_{Na}]}{[a^i_K + \alpha\, a_{Na}]}$$

For $\alpha = 0.086$, $E_m = 76 - 58 \log [a_K^i + 0.086\, a_{Na}^i]$

$\alpha = 0.03565$, $E_m = 66.8 - 58 \log [a_K^i + 0.03565\, a_{Na}^i]$

$\alpha = 0.1685$, $E_m = 87.9 - 58 \log [a_K^i + 0.1685\, a_{Na}^i]$

Appendix 13 Solutions for experiments on *Calliphora* prepupae in which $[a_K^o + 0.036\ a_{Na}^o]$ was varied whilst keeping $[a_K + 0.036\ a_{Na}^o] \times a_{Cl}^o$ constant

Solution number	$[a_K + 0.036\ a_{Na}^o]$ (mM)	[KCl] (mM)	[NaCl] (mM)	Total [Glucose] (mM)
(1)	12.9	11	194	18.5
$(2)_N$	14.2	13.5	173	55.5
(3)	15.5	16	153.6	89.3
(4)	17.2	19	134.5	121.5
(5)	18.3	21	123	140.5

All solutions also contained $MgCl_2$ (1 mM), $NaHCO_3$ (1.2 mM), NaH_2PO_4 (0.8 mM), $CaCl_2$ (0.9 mM)

These solutions were constructed such that a pair of simultaneous equations was satisfied:

1. $[a_K^o + 0.036\ a_{Na}^o] \times a_{Cl}^o$ = constant (1946 mM^2)

2. $Cl_{KCl} + Cl_{NaCl} \leq Cl_{Total(Normal)}$

   where Cl_{KCl} is the Cl^- present as KCl; Cl_{NaCl} the Cl^- present as NaCl; Cl_{Total} the Cl^- content of Normal Ringer.

Appendix 14 Membrane resistance measurements in *Chilo* muscle fibres

Cell number	Membrane resistance (kΩ)	Cell no.	Membrane resistance (kΩ)
(1)	7333	(13)	4000
(2)	5333	(14)	6667
(3)	5333	(15)	4000
(4)	4000	(16)	4667
(5)	4000	(17)	6667
(6)	2667	(18)	1667
(7)	3000	(19)	4333
(8)	5333	(20)	3333
(9)	3667	(21)	5333
(10)	3333	(22)	4000
(11)	2667	(23)	4667
(12)	7333	(24)	2667

Appendix 15 Effect of low temperatures on E_m.

Cell No.	E_m (mV) at R.T (20°)	E_m (mV) at 6°C	Depolarisation of E_m at 6°C	% depolarisation
(1)	-43	-34	9	21
(2)	-36	-27	9	25
(3)	-50	-40	10	20
(4)	-48	-38	10	21
(5)	-50	-30	20	40
(6)	-44	-34	10	23
(7)	-44	-30	14	32
Mean	-45 mV	-33.3	11.7 mV	26%
SE	1.9	1.8	1.5	2.8

Appendix 16 The effect of temperature on the ionic conductance mechanisms involved in generating E_m in *Chilo*

The effect of temperature on ionic conductance mechanisms is incorporated into the Nernst equation in the 'T' term:

$$E_x = \frac{RT}{z_x F} \ln \left[\frac{a_x^o}{a_x^i}\right]$$

where R, the universal gas constant has a value of
8.314 joules/degree/mole;
T is the Absolute temperature;
F is the Faraday constant (96,500 coulombs/mole);
a_x^o and a_x^i are the intra- and extracellular activities of the ion 'x';
z_x is the valency of the ion 'x'
and E_x is the equilibrium potential for the ion 'x'.

Thus, for the 14°C reduction in temperature which occurred in cooling experiments on *Chilo*, the equilibrium potentials for K^+, Na^+ and Cl^- would be expected tochange by a factor of:

$$\frac{8.314 \times 14}{96{,}500} \quad \text{ie. } 1.21 \text{ mV}$$

relative to the value of RT/F at 20°C, which is 25 mV. The changes in the equilibrium potentials of K^+, Na^+ and Cl^-, E_K, E_{Na} and E_{Cl} respectively, and hence the change in E_m expected when the temperature is reduced by 14°C could therefore be calculated as follows:

$$\frac{30}{58} E_K \times \frac{1.21}{25} = 0.65 \text{ mV}$$

$$\frac{17}{58} E_{Cl} \times \frac{1.21}{25} = 0.77 \text{ mV}$$

$$\frac{2}{58} E_{Na} \times \frac{1.21}{25} = 0.01 \text{ mV}$$

Total predicted change in E_m 1.43 mV

Thus, E_m would be expected to change by some 1.4 mV per 14°C change in temperature if it were generated exclusively by ionic conductance mechanisms.

The fact that, on average, E_m changed by 12 ± 2 mV provides evidence for the presence of an electrogenic, metabolic pump.

Adrian, R H (1956). The effect of internal and external potassium concentration on the E_m of frog muscle. J. Physiol. 133, 631-658.

Anderson, C R & Stevens, C F (1973). Voltage clamp analysis of ACh produced end-plate current fluctuations at the frog neuromuscular junction.
J. Physiol. 235, 655-692.

Anderson, C R , Cull-Candy, S G, & Miledi, R (1978). Glutamate current noise: post-synaptic channel kinetics investigated under voltage clamp. J. Physiol 282, 219-242.

Anwyl, R (1977). Permeability of the post-synaptic membrane of an excitatory glutamate synapse to sodium and potassium. J. Physiol 273, 367-388.

Anstee, J H and Bowler, K (1979). Review: Ouabain-sensitivity of insect epithelial tissues. Comp. Biochem. Physiol 62A, 763-9.

Ammann, D, Lanter, F, Steiner, R A, Schulthess, P, Shijo Y, & Simon, W. (1981). Neutral carrier based hydrogen ion selective microelectrode for extra- and intracellular studies. Analytical Chemistry, 53, 2267.

Armstrong, W McD, Wojtkowski, W & Bixenman, W R (1977). A new solid-state microelectrode for measuring intracellular Cl^- activities. Biochim. biophys. Acta, 465, 165-170.

Ascher, P, Kunze, D & Neild, T O (1976). Chloride distribution in *Aplysia* neurones. J. Physiol, 256, 441-464.

Baumgarten, C M (1981). An improved liquid ion exchanger for chloride ion-selective microelectrodes. Am. J. Physiol 241 (Cell Physiol. 10): C 258-C263.

Beranek, R & Miller, P L (1968). The action of iontophoretically-applied glutamate on insect fibres. J. exp. Biol. 49: 83-93.

Bers, D M & Ellis, D (1982). Intracellular calcium and sodium activity in sheep heart Purkinje fibres: effect of changes of external sodium and intracellular pH. Pflugers Archiv 393, 171-178.

Bishop, C A & O'Shea, M (1982). Neuropeptide proctolin: immunocytochemical mapping of neurons in the CNS of the cockroach. J. comp Neurology, 207, 223-238.

Bolton, T B & Vaughan-Jones, R D (1977). Continuous direct measurement of intracellular chloride and pH in frog skeletal muscle. J Physiol 270, 801-833.

Boron, W F, McCormick, W C & Roos, A (1981). pH regulation in barnacle muscle fibres: dependence on extracellular sodium and

bicarbonate. Am. J Physiol 240 (Cell Physiol.9): C80-C89.

Bridges, R G (1972) Choline metabolism in insects. Adv. Insect Physiol. 9, 51-110.

Brown, B E (1975). Proctolin: a peptide transmitter candidate in insects. Life Sci. 17: 1241-1252.

Brown, H M & Owen, J D (1979). Micro ion-selective electrodes for intracellular ions. Ion-Selective Electrode Rev. 1. 145-186.

Buchan, P B & Evans, P D (1980). Use of an operational amplifier signal differentiator reveals that octopamine increases the rate of development of neurally evoked tension in insect muscle. J. exp. Biol. 85, 349-352.

Buck, J B (1953). Review of insect haemolymph compositions. In Insect Physiology (K D Roeder, ed) Chapter 6. Wiley, New York.

Callec, J-J (1974). Synaptic transmission in the central nervous system of insects. In Treherne, J E (ed) Insect neurobiology. North-Holland Biomedical Press/American Elsevier, Amsterdam & New York p.119-178.

Carnicero, H H, Englard, S & Seifter, S (1982). Carnitine uptake and fatty acid utilisation by diploid cells ageing in culture. Archiv. Biochem. Biophys. 215, 78-88.

Coles, J.A & Tsacopoulos, M (1979). K^+ activity in photoreceptors, glial cells and extracellular space in the drone retina: changes during photostimulation. J.Physiol 290, 525-549.

Collett, J I (1976). Some features of the regulation of the free amino acids in adult *Calliphora erythrocephala*. J Insect Physiol. 22, 1395-1403.

Cook, B J & Holman, G M (1979). The pharmacology of insect visceral muscle. Comp. Biochem. Physiol. 64C: 183-190.

Crossley, A C (1965). Transformations in the abdominal muscles of the blue blowfly, *Calliphora erythrocephala* (Meig) during metamorphosis. J. Embryol. Morph. 14, 89-110.

Crossley, A C (1968). Fine structure and breakdown of intersegmental muscles during metamorphosis of the blowfly. J. Insect Physiol, 14, 1389-1407.

Cull-Candy, S G & Miledi, R (1981). Junctional and extra-junctional membrane channels activated by GABA in locust muscle fibres. Proc. R. Soc. Lond. B. . 211, 527-535.

Cull-Candy, S G , Miledi, R and Parker, I (1981). Single glutamate-activated channels recorded from locust muscle fibres with perfused

patch clamp electrodes. J. Physiol. 321, 195-210.

Cull-Candy, S G & Usherwood, P N R (1973). Two populations of L-glutamate receptors on locust muscle fibres. Nature 246, 62-64.

Dipolo, R, Requeuna, J, Brinley, F J, Mullins, L J, Scarpa, A, & Tiffert, T (1976). Ionised Ca^{2+} concentrations in squid axons. J. gen. Physiol. 67, 433-467.

Eisenmann, G (1967). Theory of membrane electrode potentials. Chapter I in "Ion-selective electrodes" ed. R A Durst, NBC Spec. Publ. 314, U.S Gov. Printing Off, Washington DC.

Eisenmann, G. (1976) (ed). Glass electrodes for hydrogen and other cations. Marcel Dekker, New York.

Eisenmann, G, Bates, R G, Mattock, G & Friedman, S M (1966). The Glass Electrode. Interscience, New York.

Evans, P D & O'Shea, M (1977). The identification of an octopaminergic neurone which modulates neuromuscular transmission in the locust. Nature 270, 257-259.

Evans, P D & O'Shea, M (1978). The identification of an octopaminergic neurone and the modulation of a myogenic rhythm in the locust. J. Exp. Biol. 73, 235-260.

Evans, P D & Siegler, M V S (1982). Octopamine-mediated relaxation of maintained and catch tension in locust skeletal muscle. J. Physiol. 324. 99-112.

Finlayson, L H & Osborne, M P. (1970). Electrical activity of neurohaemal tissue in the stick insect, *Carausius morosus*. J. Insect Physiol. 16, 791-800.

Florkin, M & Jeuniaux, C. (1974). Haemolymph: Composition. In Physiology of Insecta (Ed. Rockstein) 3, 109-152.

Fozzard, H A & Sheu, S-S. (1980). Intracellular potassium and sodium activities of chick ventricular muscle during embryonic development. J. Physiol. 306, 579-586.

Funck, R J, Morf, W E, Schulthess, P, Ammann, D & Simon, W. (1982). Bicarbonate-sensitive liquid membrane electrodes based on neutral carriers for H^+ ions. Anal. chem. 54, 423-429.

Goldman, D E (1943). Potential, impedance and rectification in membrane. J. gen. Physiol. 27, 37-60.

Gordon, H T (1952). Colorimetric microdiffusion estimation of chloride. Analyt. Chem. 24, 857-862.

Gerschenfeld, H M (1973). Chemical transmission in invertebrate central nervous systems and neuromuscular junctions. Physiol. Rev. 531, 1-119

Gration, K A F, Clark, R B & Usherwood, P N R. (1979). Denervation in insect muscle: A comparative study of the changes in L-glutamate sensitivity on locust retractor unguis and extensor tibiae muscle. Neuropharmacology 18, 201-208.

Green, R & Giebisch, G. (1974). Some problems with the antimony microelectrode. In Ion-Selective Microelectrodes. Berman, H J & Herbert, N C, eds. Plenum Pr., New York 43-52.

Guggi, M, Oehme, M, Pretsch, E & Simon, W. (1976) A Na^+-selective neutral carrier which induces a K^+ discrimination in PVC-liquid membrane electrodes. Helv. Chim. Acta. 58, 2417.

Hardie, J (1976). Motor innervation of the supercontracting longitudinal ventro-lateral muscles of the blowfly larva. J. Insect Physiol. 22, 661-668

Hardie, J (1978). Electrotonic coupling between supercontracting body-wall muscle fibres and their attachment morphology in the blowfly larva. J. Insect Physiol. 24, 647-655.

Harrow, I D, David, J A & Sattelle, D B (1982). Acetylcholine receptors of identified insect neurons. In Neuropharmacology of Insects. (Ciba Foundation Symposium 88) pp. 12-31. London: Pitman.

Harrow, I D & Sattelle, D B (1983). Acetylcholine receptors on the cell body membrane of giant interneurone 2 in the cockroach, *Periplaneta americana*. J. exp. Biol. 105, 339-350.

Hinke, J A M (1959). Glass microelectrodes for measuring intracellular Na^+ and K^+ activities. Nature 184, 1257-1258.

Hodgkin, A L & Horowicz, P. (1959) The influence of potassium and chloride ions on the membrane potential of single muscle fibres. J. Physiol. 148, 127-160.

Hodgkin, A L & Huxley, A F (1952). Currents carried by sodium and potassium ions through the membrane of the giant axon of *Loligo*. J. Physiol. 116, 449-472.

Hodgkin, A L & Katz, B (1949). The influence of sodium ions on the electrical activity of the giant axon of the squid. J. Physiol Lond. 108, 37-77.

Hodgkin, A L & Keynes, R D (1956). Experiments on the injection of substances into squid giant axons by means of a microsyringe. J. Physiol, 131, 592-616.

Horackova, M & Vassort, G (1979). Sodium-calcium exchange in regulation of cardiac contractility. J.gen. Physiol. 73, 403-424.

Hoyle, G (1953). Potassium ions and insect nerve muscle. J. exp. Biol. 30, 121-135.

Hoyle, G (1955). The effect of some common cations on neuromuscular transmission in insects. J. Physiol. 127, 90-103.

Hoyle, G (1975). Evidence that insect dorsal unpaired median (DUM) neurones are octopaminergic. J. Exp. Zool 193, 425-431.

Hoyle, G & Barker, D L (1975). Synthesis of octopamine by insect dorsal median unpaired neurones. J. exp. Zool. 193, 433-439.

Huddart, H (1966a). Ionic composition of haemolymph and myoplasm in the Lepidoptera in relation to their membrane potentials. Archs. int. Biochem. Physiol., 74, 603-613.

Huddart, H (1966b). The effect of K^+ on resting and action potentials in Lepidopteran muscle. Comp. Biochem. Physiol. 18, 131-140.

Huddart, H (1967). Effect of Cl^- on moth skeletal muscle fibres. Comp. Biochem. Physiol. 20, 355-359.

Huddart, H, & Wood, D W. (1966). The effect of DNP on the resting potential and ionic content of some insect skeletal muscle fibres. Comp. Biochem. Physiol 18, 681-688.

Irving, S N & Miller, T A (1980a). Aspartate and glutamate as possible transmitters at the 'slow' and 'fast' neuromuscular junctions of the body wall muscles of *Musca* larvae. J. comp. Physiol. 135, 299-314.

Irving, S N & Miller, T A (1980b). Ionic differences in 'fast' and 'slow' neuromuscular transmission in body wall muscles of *Musca domestica* larvae. J. Comp. Physiol. 135, 291-298.

Irving, S N & Miller, T A (1980c) Octopamine and proctolin mimic spontaneous membrane depolarisations in *Lucilia* larvae. Experientia 36, 566-567.

Jan, L Y & Jan, Y N. (1976) Properties of the larval neuromuscular junction in *Drosophila melanogaster*. J. Physiol. 262, 189-214.

Katz, B & Miledi, R. (1973). The characteristics of "end-plate noise" produced by different polarising drugs. J. Physiol. 230, 707-717.

Kenyon, J L & Gibbons, W R. (1977). Effects of low-chloride solutions on action potentials of sheep cardiac Purkinje fibres. J. gen. Physiol. 70, 635-660.

Kotera K, Satake N, Honda M & Fujimoto M (1979). The measurement of intracellular sodium activities in the bullfrog by means of double-barrelled sodium LIX microelectrodes. Memb. Biochem. 2, 323-338.

Kuramoto, T & Haber, B. (1981)$^{+}$ liquid ion exchange electrode system: Responses to drugs and neurotransmitters. J. Neuroscience Research 6, 37-48.

Laming, P J (1982). Ph.D. Thesis (University of London).

Laming, P J & Djamgoz, M B A (1983). A comparison of the selectivities of microelectrodes incorporating the Orion and Corning liquid ion exchangers for potassium over sodium. J. Neuroscience Methods, 8,. 399-402.

Lanter, F, Erne, D, Ammann, D & Simon, W (1980). Neutral carrier based ion-selective electrode for intracellular magnesium studies. Analytical Chemistry 52, 2400.

Lea, T J & Usherwood, P N R (1973). Effect of ibotenic acid on chloride permeability of insect muscle fibres. Comp. gen. Pharmacol. 4, 351-363.

Lettau, J, Foster, W A, Harker, J E & Treherne, J E. (1977). Diel changes in K^{+} activity in the haemolymph of the cockroach, *Leucophaea maderae*. J. exp. Biol. 71, 171-186.

Levenbook, L & Hollis, V W (1961). Organic acids in insects - I. citric acid. J. Insect Physiol. 6, 52-61.

Marban, E, Rink, T J, Tsien, R W & Tsien, R Y. (1980). Free Ca in heart muscle at rest and during contraction measured with a Ca^{2+}-sensitive microelectrode. Nature 286, 845-850.

Mathers, D A & Usherwood, P N R (1976). Concanavalin A blocks desensitisation of glutamate receptors on insect muscle fibres. Nature (Lond) 259, 409-411.

Mathers, D A & Usherwood, P N R (1978a). Effects of concanavalin A on junctional and extra-junctional L-glutamate receptors on locust skeletal muscle fibres. Comp. Biochem. Physiol. 59.C, 151-155.

Mathers, D A & Usherwood, P N R (1978b). The sensitivity of locust skeletal muscle fibres to L-glutamate following denervation and injury. Comp. Biochem. Physiol. 60C. 7-10.

Meech, R W & Standen, N B (1975). Potassium activation in *Helix aspersa* neurones under voltage clamp: a component mediated by Calcium

influx. J. Physiol. 249, 211-239.

Morf, W E, Ammann, D, Bissing, R, Prestch, E & Simon, W (1979). In "Progress in macrocyclic chemistry", Eds. R M Izatt & J J Christensen. Vol 1, Wiley, N.Y, 1-61.

Neher, E, Sakmann, B, Steinbach, J H. (1978). The extracellular patch clamp: a method for resolving currents through individual open channels in biological membranes. Pflugers Arch. 375, 219-228.

Neild, T O & Thomas, R C (1973). New design for a Cl^--sensitive microelectrode. J. Physiol. 231, 7-8P.

Nikolsky, B P (1937). A theory of the glass electrode. Zh. Fiz. Khim. 10, 495-503.

O'Doherty, J, Garcia-Diaz, J F & Armstrong, W McD. (1979). Sodium-sensitive LIX microelectrodes for intracellular measurements. Science 203, 1349-1351.

Oehme, M, Kessler, M & Simon W. (1976). Neutral carrier Ca^{2+} microelectrode. Chimia 30, No. 3.

Oehme, M & Simon W (1976). Microelectrode for potassium ions based on a neutral carrier and comparison of its characteristics with a cation exchanger sensor. Analytica. Chimica. Acta. 86, 21-25.

O'Shea, M. & Adams, M E, (1981). Pentapeptide (Proctolin) associated with an identified neuron. Science 213, 567-569.

O'Shea, M & Evans, P D. (1979). Potentiation of neuromuscular transmission by an octopaminergic neurone in the locust. J. exp. Biol. 79, 169-190.

Partridge, L D, & Thomas, R C (1976). The effects of lithium and sodium on the potassium conductance of snail neurones. J. Physiol. 254, 551-563.

Patlak, J B, Gration, K A F, Usherwood, P N R (1979). Single glutamate-activated channels in locust muscle. Nature (Lond). 278, 643-645.

Payton, B W, Bennett, M V L & Pappas, G D (1969). Temperature-dependence of resistance at an electrotonic synapse. Science, 165, 594-597.

Piek, T (1975). Ionic and Electrical properties. Chapter 5 in "Insect Muscle" (Ed. P N R Usherwood) Academic Press.

Pitman, R M (1971). Transmitter substances in insects: a review. Comp gen. Pharmacol. 2, 347-371.

Prescott, D J Hildebrand, J G Sanes, J R & Jewett, S. (1977). Biochemical and developmental studies of acetylcholine metabolism in the

central nervous system of the moth, *Manduca sexta*. Comp Biochem. Physiol, 56C: 77-84.

Rheuben, M.B.(1972). The resting potential of moth muscle fibre. J. Physiol. 225, 529-554.

Rink T J & Tsien R (1980). Ca^{2+}-selective microelectrodes with bevelled sub-micron tips containing poly (vinyl-chloride)-gelled neutral ligand sensor. J. Physiol. 308, 5-6P.

Russell J M & Boron W F (1979). Intracellular pH regulation in squid giant axons. Biol. Bull. 157, 392.

Salkoff, L. & Wyman, R (1983). Ion channels in *Drosophila* muscle. Trends in Neurosciences 6, 128-133.

Sanes, J R & Hildebrand, J G (1976). Acetylcholine and its metabolic enzymes in developing antennal lobes of the moth, *Manduca sexta*. Dev. Biol. 52, 105-120.

Sanes J R, Prescott D J & Hildebrand J G (1977). Cholinergic neurochemical development of normal and deafferented antennal lobes during metamorphosis of the moth, *Manduca sexta*. Brain Res. 119, 389-402.

Sattelle D B (1977). Cholinergic synaptic transmission in invertebrate central nervous systems. Trans. Biochem. Soc. 5, 849-852.

Sattelle D B (1980). Acetylcholine receptors of insects. Adv. Insect Physiol. 15, 215-315.

Saunders, J H & Brown H M (1977). Liquid and solid state Cl^--sensitive microelectrodes: characteristics and application to a_{Cl}^i in *Balanus* photoreceptors. J. gen. Physiol. 70, 507-530.

Schwartz, L M (1981). Transegmental electrical coupling between adjacent intersegmental muscles in the tobacco hawkmoth (*Manduca sexta*). J. Insect Physiol. 27, 727-733.

Starratt A N (1979). Proctolin, an insect neuropeptide.Trends in Neurosciences 2, 15-17.

Stefani E & Steinbach A B (1969). Resting potential and electrical properties of frog slow muscle fibres. Effects of different external solutions. J Physiol. 203, 383-401.

Steiner, R A, Oehme M, Ammann D & Simon W. (1979). Neutral carrier Na^+ ion-selective microelectrode for intracellular studies. Analytical Chemistry 51, 351.

Stobbart R H & Shaw J (1964). Salt and water balance excretion. In the Physiology of Insecta (M Rockstein, ed.) Vol. III. pp. 189-258. Academic Press, London & New York.

Sutcliffe D W (1963). The chemical composition of haemolymph in insects and some other arthropods, in relation to their phylogeny. Comp. Biochem. Physiol 9, 121-135.

Thomas R C (1969). Membrane current and intracellular $\overset{\text{sodium}}{\wedge}$ changes in a snail neurone during extrusion of injected Na^+. J. Physiol. 201, 495-514.

Thomas R C (1976). Construction and properties of recessed-tip microelectrodes for sodium and chloride ions and pH. In "Ion and Enzyme Electrodes in Biology and Medicine". Ed. M Kessler *et al*, Urban and Schwarzenberg, Munich, 141-148.

Thomas R C (1977). The role of bicarbonate, chloride and sodium ions in the regulation of intracellular pH in snail neurones. J. Physiol. Lond. 273, 317-338.

Thomas R C & Cohen J C (1981). A liquid ion-exchanger alternative to KCl for filling intracellular reference microelectrodes. Pflugers Arch. 390, 96-98.

Thomas R C, Simon W and Oehme M (1975). Lithium accumulation by snail neurones measured with a new Li^+-sensitive microelectrode. Nature, Lond. 258, 754-756.

Tobias J M (1948). Potassium, sodium and water interchange in the irritable tissues and haemolymph of an omnivorous insect, *Periplaneta americana*. J. Cell. Comp. Physiol. 31, 125-142.

Tsien R Y (1980). Liquid sensors for ion-selective microelectrodes. Trends Neurosci. 3. 219-220.

Usherwood P N R (1967a). Insect neuromuscular mechanisms. Am. Zoologist, 7, 553-582.

Usherwood P N R (1967b). Permeability of insect muscle fibres to potassium and chloride ions. J. Physiol. 191, 29-30P.

Usherwood P N R (1969a). Electrochemistry of insect muscle. Adv. Ins. Physiol 6, 205-278.

Usherwood P N R (1969b). Glutamate sensitivity of denervated insect muscle fibres. Nature 223, 411-413.

Usherwood P N R (1981). Amino acid gated ion channels in locust muscle membrane. Adv. Physiol. Sci. 22, 191-203.

Usherwood P N R & Cull-Candy S G (1975). Pharmacology of somatic nerve-muscle synapses. In "Insect Muscle" (Ed. Usherwood) Ch. 4. pp 207-251. Academic Press, London, New York, San Francisco.

Usherwood, P N R & Grundfest H (1965). Peripheral inhibition in skeletal muscle of insects. J. Neurophysiol. 28, 497-518.

Usherwood P N R & Machili P (1966). Chemical transmission at insect excitatory synapses. Nature 210, 643-646.

Usherwood P N R & Machili P (1968). Pharmacological properties of excitatory neuromuscular synapses in the locust. J. exp. Biol. 49, 341-361.

Vyskocil F & Kriz N (1972). Modifications of single and double-barrel potassium-specific microelectrodes for physiological experiments. Pflugers Arch. 337, 265-276.

Walker J L (1971). Ion-specific liquid ion-exchanger microelectrodes. Anal. Chem. 43, 89-92A.

Walz, W & Schlue W R (1982). External ions and membrane potential of leech neuropile glial cells. Brain Research, 239, 119-138.

Ward K M & Wareham A C (1984). Changes in intrafibre Na^+ and K^+ activity of mouse skeletal muscle during development. J. Physiol. (In press).

Wareham A C, Duncan C J & Bowler K (1974). The resting potential of cockroach muscle membrane. Comp. Biochem. Physiol. 48A 765-797.

Wareham A C, Duncan C J & Bowler K (1975). The resting potential of the muscle membrane of moths (*Sphinx ligustri*). Comp. Biochem. Physiol. [A] 52A, 295-298.

Wigglesworth V B (1938). A modification of the Volhard back titration for estimation of chloride. Biochem. J. 31, 1719-1727.

Wood D W (1957). The effect of ions upon neuromuscular transmission in a herbivorous insect (*Carausius morosus*). J. Physiol. 138, 119-139.

Wood D W (1963). The Na^+ and K^+ composition of some insect skeletal muscle fibres in relation to their membrane potentials. Comp. Biochem. Physiol. 9, 151-159.

Wuhrmann P, Ineichen H, Riesen-Willi U & Lezzi M. (1979). Change in nuclear potassium electrochemical activity and puffing of K^+-sensitive salivary chromosome regions during *Chironomus* development. Proc. Natl. Acad. Sci. USA 76, 806-808.

Wyatt G R (1961). The biochemistry of insect haemolymph. A Rev. Ent. 6, 75-102.

Additional References

Aidley, D.J.(1975) Excitation-contraction coupling and mechanical properties. In 'Insect Muscle' (Ed. P.N.R. Usherwood) Academic Press, New York and London.

Ashcroft, F.M.(1982) Electrical properties of insect muscle. In Membrane Physiology of Invertebrates (Ed. R.B. Poderta) Marcel Dekker Inc. , New York & Basel.

Belton, P.& Grundfest, H.(1962) Potassium activation and potassium spikes in muscle fibres of mealworm larvae, Tenebrio molitor. Am.J.Physiol.203, 588-594.

Bers, D.M.& Ellis, D.(1981) Changes in intracellular calcium and sodium activities in sheep heart Purkinje fibres measured with ion-selective microelectrodes. J.Physiol. 310, 73-74P.

Campbell, A.K.(1983) Intracellular calcium: Its Universal Role as Regulator. 204pp (John Wiley and Sons, New York.)

Colhoun, E.H.(1963) The Physiological significance of acetylcholine in insects and observation upon other pharmacologically active substances. Adv. Insect Physiol. 1, 1-46.

Djamgoz, M.B.A.& Laming, P.J.(1981) Intracellular measurement of ionic activity. Trends in Neurosciences 4, 280-283.

Gilbert, L.I.(1967) Lipid metabolism and function in insects. Adv. Insect Physiol 4, 69-211.

Hair, M.L.& Hertl, W.(1973) Reactivity of borosilica surface hydroxylgroups. J.Phys.Chem. 77, 1965-1969.

Lederer, W.J., Spindler, A.J. & Eisner, D.A.(1979) Thick slurry bevelling. A new technique for bevelling extremely fine microelectrodes and micropipettes. Pflügers Arch. 381, 287-288.

Magazanik, L.G. & Vyskocil, F.(1979) Spontaneous junctional currents in Drosophila muscle fibres: Effects of temperature, membrane potential and ethanol. Experientia 35 : 213.

Morf, W.E. & Simon, W.(1978) Ion-selective electrodes based on neutral carriers. In 'Ion-selective electrodes in analytical chemistry' (Ed. Henry Freiser) Plenum Press.

Morley, J. & Schachter, M.(1961) Identification of acetylcholine in the silk gland of the caterpillar of Arctia caja. J.Physiol, 157, 1-2P.

Vaughan-Jones, R.D.(1979) Non-passive chloride distribution in mammalian heart muscle: microelectrode measurement of the intracellular chloride activity. J.Physiol. 295, 83-109.

Weevers, R.de.G.(1966) A Lepidopteran Saline: effects of inorganic cation concentrations on sensory, reflex and motor responses in a herviborous insect. J.exp.Biol. 44, 163-175.

Acknowledgements

Financial support for this project was provided by a Science and Engineering Research Council CASE studentship, in which I.C.I. (Plant Protection Division) was the collaborating body. I would particularly like to thank Dr M B A Djamgoz for his unfailing enthusiasm in supervising the work and my parents for their encouragement.

The technical staff of the department of Pure and Applied Biology have also been most helpful, particularly Mr J Harmer and Mr D Hopkins (construction and maintenance of apparatus and instrumentation), Mr D Batt (supply of maggots) and Mr S Stammers (photography).

My thanks are also due to Drs S Irving (I.C.I. Plant Protection Division) and J Hardie for general help and useful discussions, to Dr Irving for supplying caterpillars, and to Professor W R Schlue (University of Dusseldorf) for helpful suggestions. I am also grateful to Professor C K Govind (University of Toronto) for providing an excellent incentive to complete this thesis, by inviting me to spend the summer at Woods Hole; and to Mrs S Wright for typing the thesis at extremely short notice. Finally, I must thank Colin, Simon and most of all Hugh, for moral support and outings.

[*From the Proceedings of the Physiological Society*, 16–18 *June* 1983
Journal of Physiology, **343**, 30–31*P*]

Intracellular potassium activities of blowfly larval muscle cells

By Jill Dawson and M. B. A. Djamgoz. *Department of Pure and Applied Biology, Imperial College, London SW7 2BB*

The longitudinal body wall muscle cells 6A and 7A (Crossley, 1965; Hardie, 1976), found on either side of the ventral midline of *Calliphora erythrocephala* larvae and prepupae were studied. The muscle cells of the latter lose their contractibility, whilst appearing to retain their electrochemical responsiveness. The intracellular potassium activities (a_K^i's) and membrane potentials (E_m's) of these cells were measured simultaneously using double-barrelled K^+-sensitive micro-electrodes (K^+-ISM's) employing either the Corning ion-exchanger 477317, LIX (Djamgoz & Laming, 1981), or the valinomycin-based neutral ion carrier, NIC (Wuhrmann, Ineichen, Riesen-Willi & Lezzi, 1979, modified from Oehme & Simon, 1976). The preparations were bathed in Rice's saline (Finlayson & Osborne, 1970). Stable impalements were obtained from a minimum of eighty cells from seven preparations for each insect.

The results obtained are summarized in Table 1, in which all values are given as means ± S.E.'s.

Table 1. Intracellular potassium activities (a_K^i's) and potassium equilibrium potentials (E_K's) of blowfly larval and prepupal muscle cells

	Larvae		Prepupae	
	LIX	NIC	LIX	NIC
a_K^i (mM)	129±4	102±2	382±12	115±3
E_K (mV)	−64±1	−59±1	−91±1	−62±1
E_m (mV)	−46±1	−47±1	−50±1	−47±1
E_K-E_m (mV)	−18±1	−11±1	−42±1	−15±1

These results suggest that in both larvae and prepupae an interfering ion is present. The latter is probably an organic ion to which the NIC-type K^+-ISM is unlikely to be sensitive. If so, E_K is more negative than E_m. The apparent rise in a_K^i during development may reflect an increase in the activity of a K^+-pumping mechanism.

Jill Dawson holds an S.E.R.C. CASE studentship in association with ICI Ltd. We thank Dr Jonathan Coles for a gift supply of the neutral K^+ carrier ligand.

REFERENCES

Crossley, A. C. (1965). *J. Embryol. exp. Morph.* **14**, 89–110.
Djamgoz, M. B. A. & Laming, P. J. (1981). *Trends Neurosci* **4**, 280–283.
Finlayson, L. H. & Osborne, M. P. (1970). *J. Insect Physiol.* **16**, 791–800.
Hardie, J. (1976). *J. Insect Physiol.* **22**, 661–668.
Oehme, M. & Simon, W. (1976). *Analytica chim. Acta* **86**, 21–25.
Wuhrmann, P., Ineichen, H., Riesen-Willi, U. & Lezzi, M. (1979). *Proc. natn. Acad. Sci. U.S.A.* **76**, 806–808.

[*From the Proceedings of the Physiological Society*, 24–25 *February* 1984
Journal of Physiology, **351**, 36*P*]

Intracellular potassium activities of the muscle cells of a Lepidopteran larva

By Jill Dawson and M. B. A. Djamgoz. *Department of Pure & Applied Biology, Imperial College, London SW7 2BB*

Previous measurements of the intracellular potassium activities (a_K^i's) of the body wall muscles of a dipteran larva showed that the potassium equilibrium potential (E_K) is consistently more negative than the resting membrane potential (E_m) (Dawson & Djamgoz, 1983). Since Lepidoptera are known to have markedly different haemolymph ionic contents from Diptera (Usherwood, 1969), these parameters have therefore been measured in *Chilo partellus* for comparison. a_K^i's and E_m's of the ventral longitudinal body wall muscle cells of the larvae of this insect were measured simultaneously using double-barrelled K^+-sensitive microelectrodes (K^+-ISM's) employing either the Corning ion-exchanger 477317, LIX, or a valinomycin-based neutral ion carrier, NIC (Oehme & Simon, 1976). The preparations were bathed in a Lepidopteran saline (Weevers, 1966). Data were obtained from 78 cells (7 preparations) with LIX-, and 77 cells (8 preparations) with NIC-type K^+-ISM's and are summarized in Table 1.

Table 1. Intracellular potassium activities (a_K^i's), potassium equilibrium potentials (E_K's) and resting membrane potentials (E_m's) of *Chilo* larval muscle cells, measured using LIX- and NIC-type K^+-ISM's. All values are given as means ± S.E.'s

	a_K^i (mM)	E_K (mV)	E_m (mV)	$E_K - E_m$ (mV)
LIX	65 ± 1	−27 ± 1	−46 ± 1	19 ± 1
NIC	62 ± 1	−27 ± 1	−45 ± 1	19 ± 1

Thus, the two K^+-ISM's give very similar results, the slight difference between the measured a_K^i values, possibly reflecting the fact that LIX-type K^+-ISM's are more prone to interference than the NIC-type (Oehme & Simon, 1976).

The main conclusion is that E_K is more *positive* than E_m (the opposite to the situation in Diptera) thereby suggesting that the resting membrane potential must also be driven by at least one other ionic mechanism with its equilibrium potential more *negative* than E_m. A similar conclusion was reached by Rheuben (1972), working on adult *Antherea* muscle fibres.

Jill Dawson holds an S.E.R.C. CASE studentship with I.C.I. Ltd. We thank Drs J. Hardie and S. Irving for many useful discussions.

REFERENCES

Dawson, J. & Djamgoz, M. B. A. (1983). *J. Physiol.* **343**, 30–31*P*.
Oehme, M. & Simon, W. (1976). *Analytica chim. Acta* **86**, 21–25.
Rheuben, M. B. (1972). *J. Physiol.* **225**, 529–554.
Usherwood, P. N. R. (1969). *Adv. Ins. Physiol.* **6**, 205–279.
Weevers, R. de G. (1966). *J. exp. Biol.* **44**, 163–175.

The contribution of potassium ions to membrane electrogenesis in body-wall muscle cells of blowfly larvae

By Jill Dawson and M. B. A. Djamgoz (introduced by K. H. Ruddock). *Department of Pure and Applied Biology, Imperial College, London SW7 2BB*

Previous measurements of intracellular potassium activity (a_K^i) in *Calliphora erythrocephala* prepupae showed that the potassium equilibrium potential (E_K) is consistently more negative than the resting membrane potential, E_m (Dawson & Djamgoz, 1983). This indicates that K^+ is not the only ion involved in generating E_m.

In order to assess the size of the contribution of K^+ to E_m, a series of K^+ substitution experiments was performed. Preparations were bathed in Rice's saline (Finlayson & Osborne, 1970), and ventral longitudinal body-wall muscle cells found within the bands 6A and 7A (Crossley, 1965; Hardie, 1976) were impaled with conventional micro-electrodes, filled with 2·5 M-KCl. After a steady E_m value was recorded from a given cell, a series of salines containing varying K^+ activities (a_K^o's) in the range 0·97–97 mM (using Na^+ as the substitute) were applied to the preparation. During each full substitution series, the preparation was returned to the 'normal' saline twice to check that the same E_m values were recorded. Full data sets were obtained from ten cells, each from a different preparation, and the mean E_m value in each solution calculated. The relationship between E_m and log a_K^o was linear (correlation coefficient 99·49 %) but had a slope of only 30 mV. this agrees with our earlier conclusion that potassium ions could only be responsible for generating part of E_m.

If the changes in the extracellular sodium activity (a_{Na}^o) were weighted and also taken into account, however, then the data points, i.e. the relationship between E_m and log ($a_K^o + \alpha a_{Na}^o$), could be fitted by a straight line of slope 58 mV (correlation coefficient 93·7 %). This relationship is essentially the one given by the Goldman–Hodgkin–Katz equation (Hodgkin & Katz, 1949), assuming that the membrane is permeable to both K^+ and Na^+, and that the Na^+:K^+ permeability ratio (α) has a value of 0·086.

Thus, the resting membranes of blowfly larval muscle cells may have a finite permeability to Na^+, and the generation of the resting potential can be explained by weighted contributions from the K^+ and Na^+ gradients, similar to the situation in *Drosophila* larval muscles (Jan & Jan, 1976).

Jill Dawson is the recipient of an SERC-ICI Plc CASE studentship.

REFERENCES

Crossley, A. C. (1965). *J. Embryol. exp. Morph.* **14**, 89–110.
Dawson, J. & Djamgoz, M. B. A. (1983). *J. Physiol.* **343**, 30–31*P*.
Hardie, J. (1976). *J. Insect Physiol.* **22**, 661–668.
Hodgkin, A. L. & Katz, B. (1949). *J. Physiol.* **108**, 37–77.
Finlayson, L. H. & Osborne, M. P. (1970). *J. Insect Physiol.* **16**, 791–800.
Jan, L. Y. & Jan, Y. N. (1976). *J. Physiol.* **262**, 189–214.

Distribution of chloride ions in the body-wall muscle cells of insect larvae: a comparison between Diptera and Lepidoptera

By Jill Dawson and M. B. A. Djamgoz (introduced by G. L. Kidd). *Department of Pure and Applied Biology, Imperial College, London SW7 2BB*

Measurements of intracellular K^+ activities in single body-wall muscle cells of *Calliphora erythrocephala* larvae and prepupae (Diptera) and *Chilo partellus* larvae (Lepidoptera) have shown that K^+ is not the only ion involved in generating the membrane potential, E_m, in these insects (Dawson & Djamgoz, 1983, 1984). In order to determine whether Cl^- might also be involved, two types of experiment were carried out: (1) intracellular Cl^- activities (a^i_{Cl}'s) and E_m's were measured in the three preparations using double-barrelled Cl^--sensitive micro-electrodes (ISM's); (2) the effect of varying the extracellular chloride activity (a^o_{Cl}) on E_m was investigated using gluconate as the Cl^- substitute.

The active barrel of each ISM was based on the improved Corning chloride ion-exchanger (Corning 477913; Baumgarten, 1981), and the reference barrel filled with an organic reference liquid ion-exchanger (Thomas & Cohen, 1981). *Calliphora* preparations were bathed in Rice's saline (Finlayson & Osborne, 1970) and *Chilo* preparations in Weevers' saline (Weevers, 1966). Using measured a^i_{Cl} values, the chloride equilibrium potential, E_{Cl}, was calculated for each cell from the Nernst equation. The results are summarized in Table 1.

Table 1. Intracellular Cl^- activity data for *Calliphora* larvae and prepupae and *Chilo* larvae. All data are given as means ± S.E.'s; $n = 35$ minimum

	a^i_{Cl} (mM)	E_{Cl} (mV)	E_m (mV)	$E_{Cl}-E_m$ (mV)
Calliphora larvae	17±1	−53±1	−53±1	0·1±0·3
Calliphora prepupae	40±2	−31±1	−50±1	19±1
Chilo larvae	8±1	−54±1	−46±1	−8±1

Thus, in *Calliphora* larvae, $E_{Cl} \simeq E_m$, indicating that Cl^- may be passively distributed in this insect. This conclusion was supported further by Cl^--substitution experiments, in which changing a^o_{Cl} had only a transient effect on E_m. In *Calliphora* prepupae, although E_{Cl} appears to be more positive than E_m, changes in a^o_{Cl} produced no sustained alteration in E_m. Taken together, these observations suggest that Cl^- is passively distributed across the cell membrane and that the apparently high value of a^i_{Cl} recorded is probably due to the presence of an interfering ion. In contrast, in *Chilo* larvae, E_{Cl} is consistently more negative than E_m, a result which cannot be explained by interference. Cl-substitution experiments confirmed that Cl^- is involved in resting membrane electrogenesis in this insect: a tenfold reduction in a^o_{Cl} gave a sustained membrane depolarization of around 14 mV.

Jill Dawson acknowledges financial support from I.C.I. plc.

REFERENCES

Baumgarten, C. M. (1983). *Am. J. Physiol.* **241**, C258–263.
Dawson, J. & Djamgoz, M. B. A. (1983). *J. Physiol.* **343**, 30–31*P*.
Dawson, J. & Djamgoz, M. B. A. (1984). *J. Physiol.*, Proc. (Imperial College meeting).
Finlayson, L. H. & Osborne, M. P. (1970). *J. Insect Physiol.* **16**, 791–800.
Thomas, R. C. & Cohen, C. J. (1981). *Pflügers Arch.* **390**, 96–98.
Weevers, R. de G. (1966). *J. exp. Biol.* **44**, 163–175.